

Analytical Methods and Thermodynamic Frameworks for Efficient Biocatalytic Nucleoside Synthesis via Nucleoside Phosphorylases

vorgelegt von

M.Sc.

Felix Kaspar

ORCID: 0000-0001-6391-043X

an der Fakultät III – Prozesswissenschaften
der Technischen Universität Berlin
zur Erlangung des akademischen Grades

Doktor der Naturwissenschaften

- Dr. rer. nat. -

genehmigte Dissertation

Promotionsausschuss:

Vorsitzender: Prof. Dr. Roland Lauster

Gutachter: Prof. Dr. Peter Neubauer

Gutachter: Prof. Dr. Jens Kurreck

Gutachter: Prof. Dr. Frank Hollmann

Tag der wissenschaftlichen Aussprache: 15.04.2021

Berlin 2021

*The pursuit of truth and beauty
is a sphere of activity in which we are permitted
to remain children all our lives.*

Albert Einstein

Abstract

Nucleosides and nucleoside analogs are indispensable biomolecules which serve as building blocks of DNA and RNA, pharmaceuticals and molecular biology tools. Sparked by the demand for synthetic access to these compounds, a variety of approaches for nucleoside synthesis has been developed. Among these, biocatalytic nucleoside synthesis via nucleoside phosphorylases promises a solution to the long-standing selectivity challenges encountered during established chemical approaches. These enzymes enable direct access to nucleosides from their corresponding free nucleobases in a one-pot fashion under mild aqueous conditions. However, the admission of this methodology to the standard repertoire for nucleoside synthesis has been slow, despite the wealth of examples of nucleoside phosphorylase-catalyzed transglycosylations in the literature. This is likely due to a lack of predictability of biocatalytic nucleoside transglycosylations as well as an insufficient arsenal of high-throughput methodologies for the characterization of the respective enzymes and their transformations.

To close this gap, this thesis presents analytical methods and thermodynamic frameworks for the characterization and optimization of nucleoside phosphorylase-catalyzed reactions. First, a comprehensive route efficiency assessment of *N*-glycosylation methods for nucleoside synthesis reveals the bottlenecks of current synthetic approaches and highlights the importance of developing concise and efficient biocatalytic routes. To facilitate this cause, a UV-based high-throughput method for reaction monitoring is described which relies on deconvolution of highly overlapping absorption spectra. With this assay at hand, the equilibrium thermodynamics of nucleoside phosphorolysis were explored systematically, establishing the tight thermodynamic control of this reaction system and providing a range of temperature-dependent equilibrium constants. Building on this foundation, an analytical approach to the monitoring of the hydrolytic decay of UV-inactive pentose-1-phosphates through UV spectroscopy is presented which employs apparent equilibrium shifts via LeChatelier's principle. Furthermore, the transfer of these thermodynamic principles to transglycosylation reactions provided guidelines and mathematical tools for the yield prediction and optimization in synthetically relevant applications. These were demonstrated via the biocatalytic preparation of synthetically challenging selenium-containing pyrimidine nucleosides in a proof-of-concept study. Lastly, a hyperthermostable enzyme is described which performs phosphorolysis and transglycosylation reactions in cosolvent-heavy and near-boiling media, enabling increased substrate loading compared to common nucleoside transglycosylations.

Collectively, the results and thermodynamic insights disclosed in this thesis enable the prediction and optimization of yields in nucleoside phosphorolysis and transglycosylation reactions, paving the way for efficient nucleoside synthesis via biocatalytic one-pot processes.

Zusammenfassung

Nukleoside und Nukleosidanaloga sind wichtige Biomoleküle, die als Bausteine von DNA und RNA, Pharmazeutika und molekularbiologische Werkzeuge dienen. Der breite Bedarf an diesen Molekülen hat die Entwicklung einer Vielzahl von synthetischen Ansätzen angetrieben. Unter diesen ist die biokatalytische Nukleosidsynthese durch Nukleosidphosphorylasen besonders vielversprechend, da diese eine Lösung für die bestehenden Selektivitätsprobleme etablierter chemischer Methoden bietet. Diese Enzyme ermöglichen direkten synthetischen Zugang zu Nukleosiden, ausgehend von den zugehörigen freien Nukleobasen unter milden wässrigen Bedingungen. Trotz der wachsenden Zahl an Literaturbeispielen für Transglykosylierungsreaktionen mit Nukleosidphosphorylasen, geschieht die Aufnahme dieser Methodik in das Standardrepertoire für Nukleosidsynthesen jedoch nur sehr langsam. Dies begründet sich wahrscheinlich in der mangelnden Vorhersehbarkeit der Ausbeuten in biokatalytischen Transglykosylierungen, sowie dem limitierten Arsenal an Hochdurchsatzmethoden zur Charakterisierung der entsprechenden Enzyme und ihrer Reaktionen.

Um diese Lücke zu schließen, präsentiert diese Arbeit analytische Methoden und einen thermodynamischen Rahmen zur Charakterisierung und Optimierung von Nukleosidphosphorylase-katalysierten Reaktionen. Zunächst werden Engpässe und Limitationen von bekannten Methoden zur Nukleosidsynthese mittels einer Effizienzanalyse beleuchtet, was die Notwendigkeit der Entwicklung von effizienten biokatalytischen Ansätzen aufzeigt. Um dieses Unterfangen zu ermöglichen, wird darauffolgend eine UV-basierte Hochdurchsatzmethode zum Reaktionsmonitoring von Nukleosidphosphorolyse-Reaktionen präsentiert, die auf Dekonvolution von stark überlappenden Absorptionsspektren beruht. Mittels dieser Methode wurde die Gleichgewichtsthermodynamik von Nukleosidphosphorolyse-Reaktionen untersucht, wodurch die thermodynamische Reaktionskontrolle in diesem System etabliert werden konnte. Aufbauend auf diesen Erkenntnissen wurde ferner ein analytischer Ansatz zur UV-spektroskopischen Beobachtung der Hydrolyse von UV-inaktiven Pentose-1-phosphaten entwickelt, welcher sich Gleichgewichtsverschiebungen nach dem Prinzip von LeChatelier bedient. Der Transfer dieser thermodynamischen Erkenntnisse auf Nukleosidtransglykosylierungen ergab Richtlinien und mathematische Werkzeuge zur Vorhersage und Optimierung der Ausbeuten in diesen synthetisch relevanten Reaktionen. Diese wurden anschließend anhand der Präparation von synthetisch anspruchsvollen Selen-modifizierten Pyrimidinnukleosiden in einer Proof-of-concept Studie demonstriert. Zuletzt wird eine hyperthermostabile Nukleosidphosphorylase beschrieben, welche in Kosolvens-lastigen und fast kochenden Medien stabil und katalytisch aktiv ist, wodurch eine höhere Substratlöslichkeit verglichen mit gängigen Nukleosidtransglykosylierungen ermöglicht wird.

Zusammenfassend erlauben die Ergebnisse dieser Arbeit die Vorhersage und Optimierung von Ausbeuten in Nukleosidphosphorolyse und -transglykosylierungen, was die effiziente Synthese von Nukleosiden in biokatalytischen Eintopfreaktionen ermöglicht.

Acknowledgements

My friends and family hold a special place in my heart, but that shall not be the topic of this page, for this is a thanks to the scientific world.

First, I need to thank Peter Neubauer for welcoming me to his group, being a never-ending source of constructive feedback and optimism and making my PhD studies in Berlin possible in the first place. Thanks for the constant support, quick proofreading and acceptance of unconventional ideas. In the same breath, my thanks go to Anke Wagner (now Kurreck) for being the best supervisor I could have asked for. Thanks for supporting my scientific adventures, tolerating my various submarine projects and most of all for raising the absolutely crazy idea of doing a PhD inside a year. The Covid-19 pandemic pushed all our plans back a little, but I am happy about the way it all turned out (also, Covid, I thank you for nothing). I also need to thank both Anke and Peter for being very accepting of my unconventional way of writing and scientific storytelling. In more than one way, thanks for granting me the freedom to pursue true curiosity-driven science.

There are too many people to thank who contributed to my life in the Neubauer lab, my scientific upbringing and my various projects in one way or another. I need to thank Rhia for being incredibly supportive and often lending me her sharp eye (and teaching me chemistry all the way back in Brisbane), Annie for crazy ideas and lots of inspiration (and an amazing cover design!), Irmgard, Brigitte, Thomas and Sabine for keeping the institute in working condition (there would be no biotechnology in the Ackerstraße without you), Robert for being an amazing mentor to me when I first joined the institute and teaching me the ways of open science (I would choose to work together with you again any day!), Caroline, Sarah and Julia for support with all things cloning and expression (living things are not my strong suit...), Katja for her immense experimental effort with the selenium-modified nucleosides (and her great resilience!), Sarah for routinely lending a helping hand (and generally being a great person), Darian for pursuing our kinetic projects with exceptional curiosity (that work is not in this thesis, but it's soon to see the light of day), Amin for not giving up on his enzymes (more cool stories in progress!), Rita for sharing her modelling and protein structural expertise with me (*even* more cool stories!), Carmen for challenging our view of insoluble enzymes (and the pleasant smell of fragrant tea in the office), Isabel and Saskia for semi-serious feedback during all phases of various projects (and the never-ending lunchtime comedy) and like half the people above for all their valuable feedback and user experiences which helped our UV-based assay become the versatile method it is now (I believe we've found just about every possible source of error messages and all ways to screw up a measurement).

My thanks also go to my thesis committee, Jens Kurreck, Frank Hollmann and Roland Lauster, for dedicating their time and effort to reading and improving this work. I am also indebted to Anett Schallmeyer for her continued support and first introducing me to the fascinating and diverse field of biocatalysis. Further, I need to thank Uwe Hohm for being an inspirational teacher during my first university semesters (way back then...) and equipping me with an appreciation for physical chemistry.

Last but most certainly not least, I need to thank Kerstin for being my most critical proofreader and supplier of baked goods.

Table of Contents

Abstract	I
Zusammenfassung	II
Acknowledgements	III
Table of Contents	IV
List of Publications	VI
1 Introduction	1
2 Scientific Background	3
2.1 Nucleosides and Nucleoside Analogs	3
2.2 Synthesis of Nucleosides	5
2.3 Environmental Concerns in Nucleoside Synthesis	7
2.4 Nucleoside Phosphorylases	8
2.5 Biocatalytic Nucleoside Synthesis Via Nucleoside Phosphorylases	11
3 Research Hypotheses	12
4 Results and Discussion	13
4.1 Efficiency Assessment of Nucleoside Synthesis Approaches	14
4.2 A Spectral Unmixing-Based Method for Reaction Monitoring	18
4.3 Equilibrium Thermodynamics of Nucleoside Phosphorolysis	21
4.4 Equilibrium Shifts for the Kinetic Analysis of Sugar Phosphate Hydrolysis	23
4.5 Yield Optimization of Nucleoside Transglycosylations	25
4.6 Synthesis of Selenium-Modified Pyrimidine Nucleosides	28
4.7 A Hyperthermostable Enzyme for Reactions Under Harsh Conditions	30
5 Conclusions and Outlook	32
6 References	34
7 Ten Theses	50
8 Publications	51

List of Publications

This thesis is based on the following publications which have appeared either i) as publications in peer-reviewed journals and/or ii) as preprints on the open access preprint server *ChemRxiv* and are, at the time of this writing, under consideration by peer reviewed journals. They are ordered non-chronologically according to their topic and role in the work presented in this thesis. The full texts and author contributions¹ are available at the end of this thesis. As a commitment to open science, all publications which are part of this work are freely available as open access texts from the publishers (or as open access preprints) and accompanied by an externally hosted supplementary material containing all raw and calculated data presented in the items across the individual works as well as supplementary software and additional data such as reference spectra and workflow recommendations. The externally hosted supplementary information is available from the data sharing website zenodo.org via the digital online identifiers listed below.

denotes an equal contribution of these authors

Paper I

Kaspar, F.; Stone, M.R.L.; Neubauer, P.; Wagner, A. Route efficiency assessment and review of the synthesis of β -nucleosides via *N*-glycosylation of nucleobases. *Green Chem.* **2020**, accepted article, <https://doi.org/10.1039/D0GC02665D>, open access preprint at <https://doi.org/10.26434/chemrxiv.12753413.v1>.

The external supplementary material is available at <https://doi.org/10.5281/zenodo.4265828>.

Paper II

Kaspar, F.; Giessmann, R.T.; Westarp, S.; Hellendahl, K.F.; Krausch, N.; Thiele, I.; Walczak, M.C.; Neubauer, P.; Wagner, A. Spectral Unmixing-Based Reaction Monitoring of Transformations Between Nucleosides and Nucleobases. *ChemBioChem* **2020**, *21*, 2604, <https://doi.org/10.1002/cbic.202000204>.

The external supplementary material is available at <https://doi.org/10.5281/zenodo.3723806>.

Paper III

Kaspar, F.;[#] Giessmann, R.T.;[#] Neubauer, P.; Wagner, A.; Gimpel, M. Thermodynamic Reaction Control of Nucleoside Phosphorolysis. *Adv. Synth. Catal.* **2020**, *362*, 867–876, <https://doi.org/10.1002/adsc.201901230>.

The external supplementary material is available at <https://doi.org/10.5281/zenodo.3568858>.

Paper IV

Kaspar, F.; Neubauer, P.; Kurreck, A. Kinetic Analysis of the Hydrolysis of Pentose-1-Phosphates through Apparent Nucleoside Phosphorolysis Equilibrium Shifts. *ChemPhysChem* **2020**, accepted article, <https://doi.org/10.1002/cphc.202000901>.

The external supplementary material is available at <https://doi.org/10.5281/zenodo.4088390>.

Paper V

Kaspar, F.,[#] Giessmann, R.T.,[#] Hellendahl, K.F.; Neubauer, P.; Wagner, A.; Gimpel, M. General Principles of Yield Optimization of Nucleoside Phosphorylase-Catalyzed Transglycosylations. *ChemBioChem* **2020**, 21, 1428–1432, <https://doi.org/10.1002/cbic.201900740>.

The external supplementary material is available at <https://doi.org/10.5281/zenodo.3565561>.

Paper VI (preprint)

Hellendahl K.F.,[#] Kaspar, F.,[#] Zhou, X.; Yang, Z.; Huang, Z.; Neubauer, P.; Kurreck, A. Biocatalytic Synthesis of 2-Seleno Pyrimidine Nucleosides via Transglycosylation. *ChemRxiv* **2020**, preprint at <https://doi.org/10.26434/chemrxiv.13318202.v1>.

The external supplementary material is available at <https://doi.org/10.5281/zenodo.4302198>.

Paper VII

Kaspar, F.; Neubauer, P.; Wagner, A. The Peculiar Case of the Hyperthermostable Pyrimidine Nucleoside Phosphorylase from *Thermus thermophilus*. *ChemBioChem* **2020**, accepted article, <https://doi.org/10.1002/cbic.202000679>.

The external supplementary material is available at <https://doi.org/10.5281/zenodo.4043929>.

1 Introduction

Nucleosides are truly central biomolecules. Much of today's progress in the biological sciences and medicinal chemistry depends on nucleosides and nucleoside analogs serving as molecular probes, raw materials for oligonucleotide synthesis and pharmaceuticals for the treatment of various cancers and viral infections. However, nucleoside analogs are notoriously hard to access using traditional synthetic chemistry. In fact, the current lack of straightforward and robust methodologies for the synthesis and diversification of nucleosides and their analogs stems not from a lack of desire but rather from the difficulty to prepare these compounds in a selective and efficient manner. The main obstacles to this end are presented by the low nucleophilicity of nucleobases (complicating direct *N*-glycosylation) as well as the density of functional groups on the sugar moiety (complicating regio-, chemo- and diastereoselectivity of all transformations). To address these challenges, a variety of creative approaches have been devised to prepare nucleosides from their corresponding nucleobases which are comparably easy to access. Nonetheless, these approaches typically require lengthy routes of more than six synthetic steps as well as considerable purification effort throughout the route.

Biocatalytic nucleoside synthesis employing nucleoside phosphorylases represents an attractive alternative to bypass the challenges plaguing conventional nucleoside synthesis. These enzymes perform the reversible phosphorolysis of nucleosides to their corresponding nucleobases and pentose-1-phosphates. Synthetically, they can be used in (trans)glycosylation approaches to furnish nucleosides directly from their free nucleobases with perfect selectivity. This considerably shortens the synthetic process down to a single step which can be done under mild aqueous conditions without the need for toxic or otherwise harmful reagents.

However, the acceptance of nucleoside phosphorylases into the repertoire of nucleoside chemists has been slow, presumably due to a limited understanding and lack of predictability of these biocatalysts and their reactions. For one, the choice of the right enzyme and substrate for maximum phosphorolysis and transglycosylation conversions had remained difficult and, secondly, the thermodynamics of these reaction systems had not yet been systematically analyzed, making it challenging to rationally engineer efficient bioprocesses. Thirdly, physicochemical frameworks for the prediction and optimization of yields in such coupled equilibrium reactions were missing. Additionally, versatile analytical tools for the high-throughput characterization of nucleoside phosphorylases and their reactions had not yet been developed, limiting the analysis of these processes to time-consuming HPLC analysis. Besides that, the prejudice of enzymes having a narrow substrate scope and being limited to low temperatures and fully aqueous reaction conditions is likely still deeply rooted in synthetic organic chemistry, ultimately hindering the admission of biocatalytic methodologies to the toolkit of synthetic chemists.

To address these obstacles, this thesis presents analytical methods and thermodynamic frameworks for the characterization and optimization of biocatalytic nucleoside synthesis processes employing nucleoside phosphorylases. In the first chapter, the state of the art is established by highlighting the significance of nucleosides and nucleoside analogs, expanding on the synthesis of nucleosides as well as some associated environmental concerns and introducing nucleoside phosphorylases along with a brief history of their discovery and applications. The following chapters present and discuss the

research hypotheses which laid the foundation for the work presented in this thesis. A route efficiency assessment of the synthesis of nucleosides via *N*-glycosylation reveals the current bottlenecks hindering the available synthetic options and sets the stage for the improvement of biocatalytic approaches bearing significant potential. To aid this cause, the development of a UV-based high-throughput analytical method is presented which employs spectral unmixing of highly overlapping absorption spectra for reaction monitoring. This ultimately proved central to the following systematic exploration of the thermodynamics of nucleoside phosphorolysis as well as the characterization of the stability of pentose-1-phosphate intermediates. Building on these fundamental insights, the transfer of these methodologies to the characterization of transglycosylation reactions is described. Their straightforward optimization via principles of thermodynamic control is presented and further demonstrated by synthetic applications. This thesis closes with an interesting case of enzymatic thermostability and cosolvent tolerance, refuting the stereotype that enzymes always have a narrow working space.

2 Scientific Background

2.1 Nucleosides and Nucleoside Analogs

All life on earth builds on nucleosides. Linked together by phosphate ester bridges, nucleosides are central components of DNA and RNA, enabling the storage of information in the genomes of all known living organisms. Triphosphates of nucleosides, known as nucleotides, serve as essential cellular energy transfer and storage systems, empowering the cellular machinery to perform a spectrum of vital enzymatic reactions ranging from simple functional group interconversions to the synthesis of proteins, genomes and whole new cells. This machinery further depends on a range of other nucleoside-based compounds such as flavin or nicotinamide dinucleotides, both of which enable enzymatic oxidations and reductions central to the primary and secondary metabolism. Simply put, nucleoside-based compounds enable life on earth as we know it.

Structurally, nucleosides are composed of a functionalized *N*-heterocyclic base and a ribose-based sugar moiety. The natural nucleosides carry the nucleobases adenine (**1**), guanine (**2**), cytosine (**3**), thymine (**4**) and uracil (**5**, Chart 1) representing either a purine (**1** and **2**) or a pyrimidine scaffold (**3–5**). While genomic information is stored as stable DNA featuring a 2'-deoxyribosyl backbone and the corresponding nucleosides **1a–4a**, transcribed (transient) information is contained in RNA featuring uracil instead of thymine and the more labile ribosyl-based backbone of **1b–3b** and **5b**. Interestingly, the names of these nucleosides and nucleobases date back to the early days of biochemistry and reflect the fundamental nature of these compounds. All nucleosides are termed according to their nucleobases and share the *-ine* suffix, descriptive of the fact that they contain nitrogen atoms, with the purine nucleosides additionally hinting at the presence of a sugar moiety via the *-ose* suffix (e.g. aden-*os*-ine). Named after their origins of discovery, the nucleobase cytosine¹ was found as a vital part of cells (from the Greek *zyto-*, meaning cell),² adenine was first isolated from ox pancreas (from the Greek *aden-*, meaning gland),³ thymine from thymus glands⁴ and guanine, infamously, from guano (commonly known as bird droppings).⁵ Only uracil deviates from this rule as its name originates from Behrend's early syntheses of pyrimidine and purine nucleobases,⁶ during which he mentioned a demethylated analogue of thymine and "arbitrarily termed it uracil",¹¹ presumably due to its partial structural resemblance to uric acid, which in turn had been known as a constituent of urine since before the dawn of systematic scientific literature records.⁷

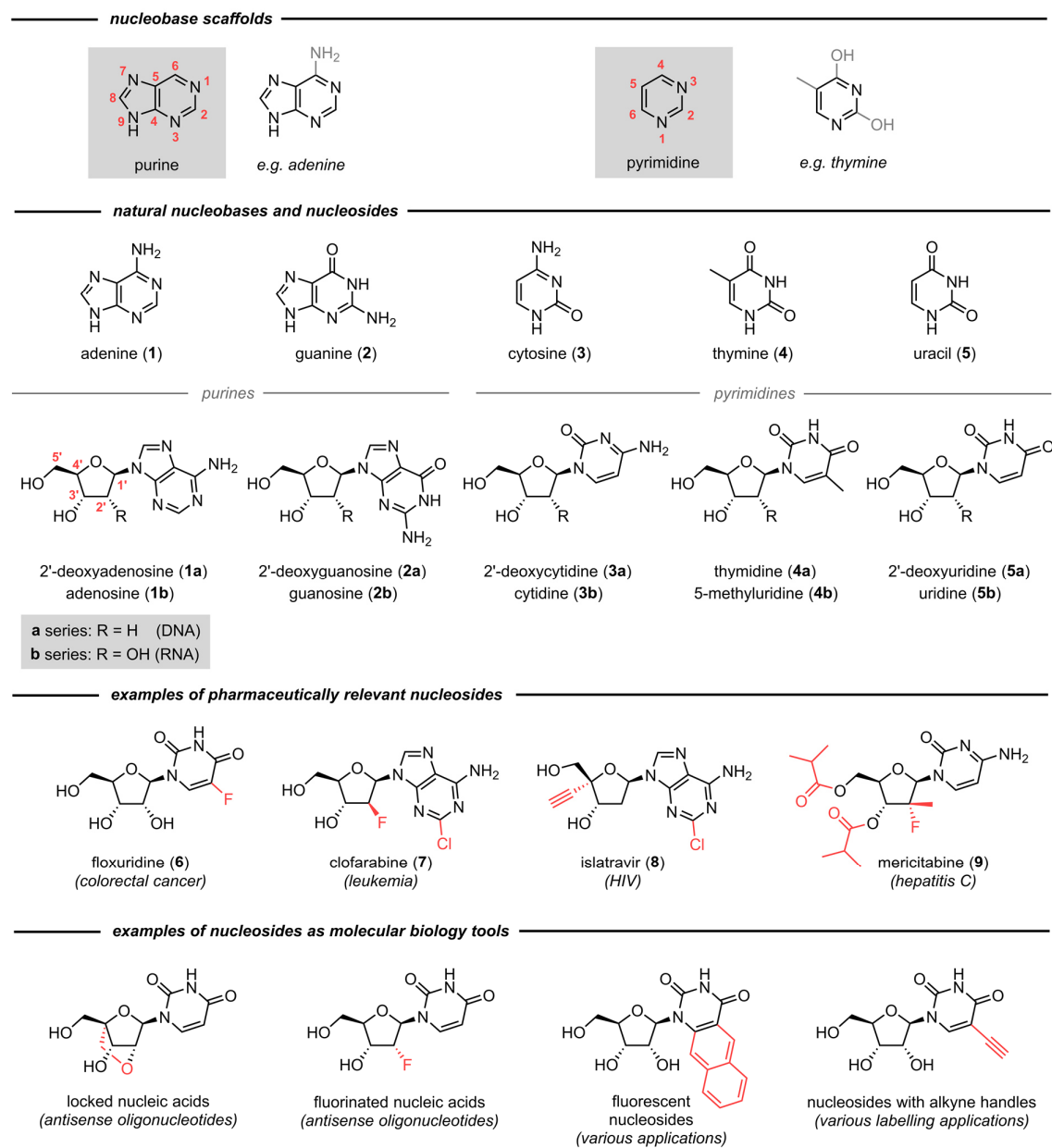
Inspired by the central role of natural nucleosides in cellular processes, an astounding variety of modified nucleosides has been designed and prepared to fulfill, extend or influence a range of biological functions. Predestined by the vital role of nucleosides in cell replication, analogs of these compounds often serve as entry points for the development of anticancer and antiviral interventions. In fact, nucleoside analogs currently represent approximately one fourth of all approved small molecule pharmaceuticals for cancer treatments.^{8–12} These comprise heavily modified scaffolds such as mericitabine (**9**) bearing only distant resemblance to their natural counterparts, as well as

¹ which is a bit of a misnomer since it contains no sugar moiety

¹¹ translated from German: "welche ich willkürlich mit dem Namen Uracil belege"

compounds such as floxuridine (**6**), clofarabine (**7**) or islatravir (**8**), which only feature a few key substitutions. Despite their structural diversity, nucleoside analogs for cancer and antiviral treatments are united by the core principles of their modes of action relying on DNA replication inhibition in fast-replicating cells typical of cancerous or virus-infected tissues.^{9,10,13,14} Other nucleoside analogs serve a spectrum of functions as molecular biology tools. For instance, locked^{15,16} or fluorinated¹⁷ nucleic acids can be employed as thermally stable DNA or RNA labelling probes and nucleoside analogs bearing a conjugated fluorophore are used as markers and fluorescent probes.¹⁸ Alkynes like 5-ethynyluridine enable further straightforward diversification of oligonucleotides, granting access to the study of RNA synthesis or visualization of cellular localization via click chemistry-based conjugation of fluorophores.^{19,20} Collectively, these examples showcase the power of nucleoside analogs which play an integral role in nearly all areas of modern life science.

Chart 1.



2.2 Synthesis of Nucleosides

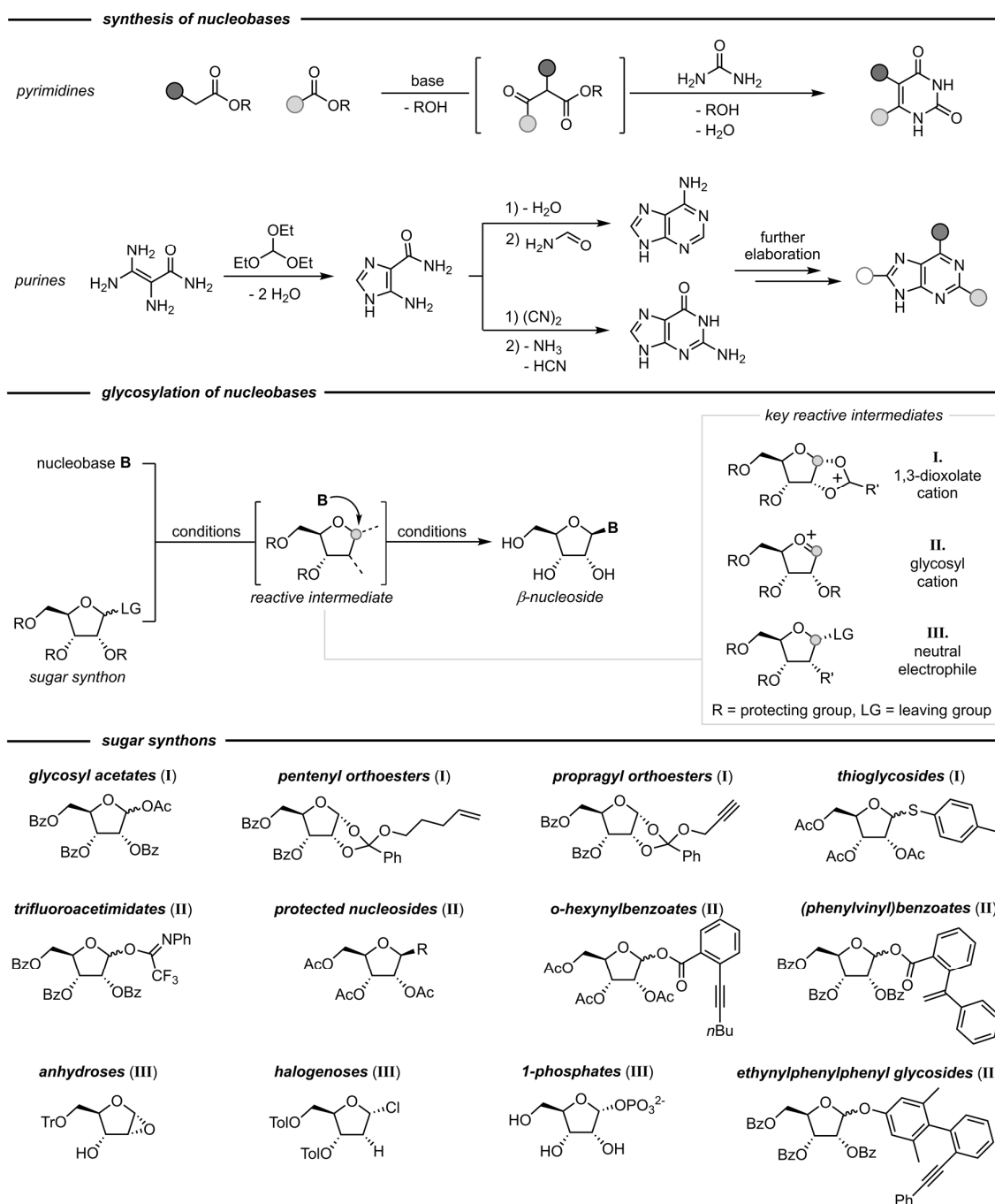
Driven by the demand for nucleosides and nucleoside analogs in nearly all areas of life science, a variety of synthetic approaches to nucleosides has been developed, with early reports dating back more than six decades.²¹ Synthetic access to heterocyclic nucleobases with various substitutions is rather straightforward through a number of condensation reactions (Scheme 1, top),^{22–28} while the corresponding nucleosides require the addition of a sugar moiety to said bases via *N*-glycosylation, which is a much more challenging task. Indeed, the synthesis of many nucleobases has already been accomplished in the late 1800s⁶ (not considering prebiotic nucleobase/nucleoside synthesis, of course, which is currently a hot topic of its own)^{29–36} whereas nucleoside synthesis through glycosylation continues to be an active research area in present days.^{37–41} This thesis focuses on the synthesis of ribosyl and 2'-deoxyribosyl nucleosides, whose synthesis via *N*-glycosylation has attracted by far the most research interest due to these scaffolds representing the bulk of nucleoside analogs used. Nucleosides featuring other sugar moieties require entirely different synthetic approaches such as starting from natural nucleosides to install substitutions via elaboration of the existing scaffold,^{42–44} preparation of modified sugar synthons from carbohydrates from the chiral pool⁴⁵ or even *de novo* synthesis.^{46–48} All these approaches necessitate complicated and often lengthy routes of their own and shall not be the focal point of this thesis.

The main obstacles for (2'-deoxy)ribosyl nucleoside synthesis via *N*-glycosylation are presented by the low nucleophilicity of nucleobases and the density of preexisting functional groups on both the nucleobase and the sugar scaffold. These issues serve to complicate a direct nucleophilic attack of a nucleobase at the anomeric center of a sugar moiety to yield the corresponding nucleoside. The low nucleophilicity of nucleobases typically requires activation of the base either by silylation or deprotonation, often in the presence of rather harsh reaction conditions to overcome the sluggish reactivity of these compounds. This generally creates problems with regio-, chemo- and diastereoselectivity as both nucleobases and ribosyl-based sugars present a density of functional groups with nearly every carbon center bearing at least one heteroatom. As such, common undesired byproducts of glycosylation approaches are the hard-to-separate α -anomer of the target nucleoside (bearing the wrong^{III} C1' configuration), the N7 regioisomer of purine nucleosides (bearing a glycosylation at the wrong ring nitrogen) or glycosylation products arising from nucleophilic attack of other functional groups. To overcome these challenges, a variety of approaches has been developed to facilitate selective and high-yielding *N*-glycosylation of nucleobases to grant synthetic access to β -nucleosides.^{37–39,49–69}

Despite their differences, all methods for *N*-glycosylation of nucleobases stand united in relying on nucleophilic attack of a nucleobase on an activated glycosyl intermediate (Scheme 1, center). To this end, one of three possible key intermediates is generated from a corresponding sugar synthon to enable selective nucleophilic attack at the anomeric position. These include i) a 1,3-dioxolane cation

^{III} “Wrong” is always a matter of perspective, of course. It is herein assumed that natural nucleosides or close analogs thereof are sought after, which are β -anomers of pyrimidine (N1-glycosylation) or purine nucleosides (N9-glycosylation).

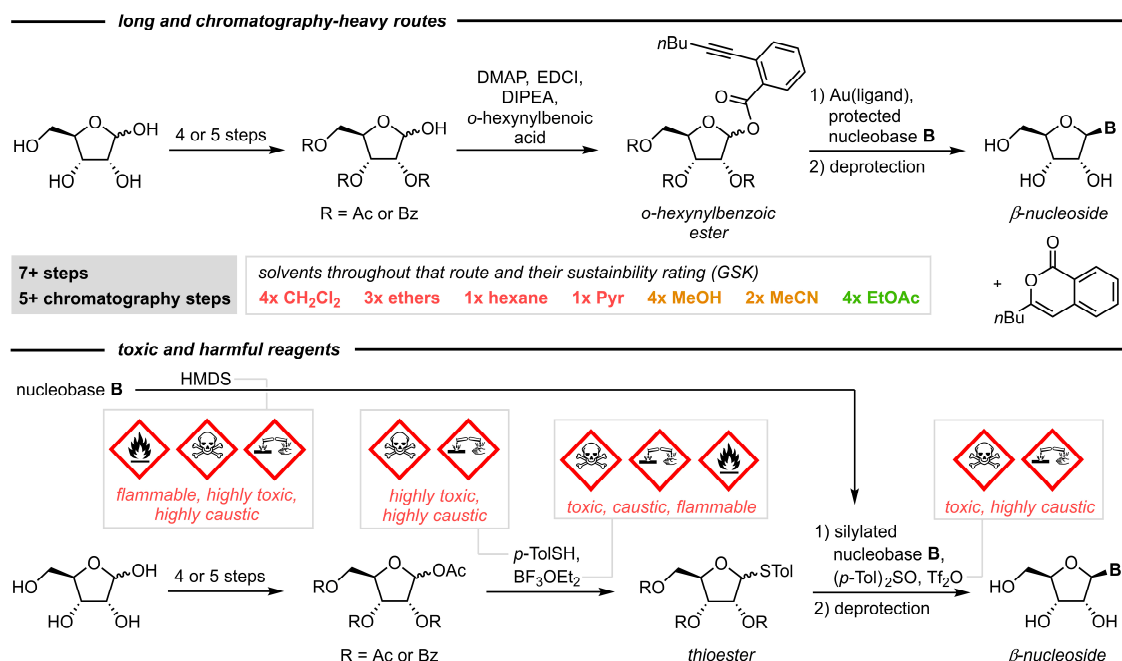
formed via recruitment of the adjacent protecting group, ii) a highly reactive glycosylation cation generated by sequestration of a leaving group and charge delocalization across the ring oxygen and iii) an intermediate bearing a good leaving group at the anomeric center which can be replaced by classic S_N2 -type substitution to give a β -nucleoside. These intermediates can be accessed directly from an assortment of sugar synthons (Scheme 1, bottom), which in turn need to be prepared from (deoxy)ribose by installation of protecting and leaving groups in up to 7 steps.



Scheme 1. Synthesis of nucleobases and *N*-glycosylation to access the corresponding β -nucleosides. Adapted in part from ⁷⁰.

2.3 Environmental Concerns in Nucleoside Synthesis

Although a variety of glycosylation methods for nucleoside synthesis is available from the literature, many of these come with significant drawbacks and environmental concerns. Since the preparation of the highly functionalized scaffolds of nucleosides presents a range of issues regarding the selectivity of glycosylation approaches, elaborate protecting group schemes are typically employed. As such, all hydroxyl groups across common sugar synthons are generally decorated with acetyl or benzoyl groups (Scheme 1). This not only requires reaction steps for installation and removal of these protecting groups, but also significantly contributes to lower atom economies and high waste accumulation.^{71–73} Furthermore, the low reactivity of nucleobases requires i) activation of the anomeric position of sugar synthons as well as ii) methods to suppress or prevent the competing reattack of anomeric leaving groups, which could otherwise hinder a productive attack by the nucleobase.^{21,37,54,74} To this end, a spectrum of tactics has been employed to sequester the anomeric leaving group, such as iodine-mediated cyclization of a pentenyl scaffold⁵⁴ or gold-catalyzed formation of isocoumarins from *ortho*-hexynylbenzoic acids (Scheme 2).³⁷ This, however, necessitates lengthy routes to install these leaving groups, making the preparation of suitable sugar synthons for nucleobase glycosylation a considerable investment of time, money and labor.²¹ Moreover, purification effort throughout these multistep routes routinely amounts to substantial solvent use, with common chromatography solvents such as hexane or dichloromethane raising additional environmental concerns (Scheme 2, top).^{75–77} From a practical perspective, almost all glycosylation approaches employ anhydrous conditions and several toxic, flammable and/or otherwise harmful reagents, including fluorinated Lewis acids or harsh silylating agents such as those employed by approaches relying on thioglycosides,⁵⁸ making traditional nucleoside synthesis an unattractive endeavor for the wet lab chemist (Scheme 2, bottom). Therefore, efficient biocatalytic methods that bypass these obstacles are highly desirable and promise selective nucleobase glycosylation under mild aqueous conditions (please see below).



Scheme 2. Environmental and safety concerns in nucleoside synthesis.^{37,58,75}

2.4 Nucleoside Phosphorylases

Nucleoside phosphorylases are enzymes which present solutions to the selectivity challenges encountered in chemical nucleoside synthesis.^{IV} In nature, these enzymes play an integral role in the central metabolism across all kingdoms of life by channeling ribosyl units in salvage pathways.^{78–80} Their discovery dates to a 1945 report by Kalckar⁸¹ who observed that an enzyme obtained from rat liver shows phosphorolytic activity with inosine. Having established that nucleoside phosphorylases perform the reversible phosphorolysis of nucleosides to yield the corresponding nucleobase and a pentose-1-phosphate (Scheme 3, top), the following works by Kalckar,⁸² Friedkin^{83–85} and others^{86,87} explored the synthesis of ribose- and 2-deoxyribose-1-phosphate (**10a** and **10b**) as well as their use in the reverse reaction to obtain a different nucleoside via glycosylation. Consequently, these early works already provided a wealth of information, including the mode of reactivity, thermodynamic investigations and preparative examples. Much of the subsequent reports on nucleoside phosphorylases focused on the kinetics of the reaction and provided kinetic constants as well as deep mechanistic insights.^{78,88–104} The acceleration of structural biology powered by X-ray crystallography yielded a series of structures of nucleoside phosphorylases following the late 1990s, further contributing to a mechanistic understanding on the molecular level.^{105–116} In recent years, nucleoside phosphorylases regained attention as biocatalysts for the synthesis of nucleosides via transglycosylation which might offer a more sustainable alternative to traditional nucleoside synthesis.^{41,117–130}

Commonly, nucleoside phosphorylases are divided into pyrimidine and purine nucleoside phosphorylases, based on their substrate preference.¹³¹ This functional characterization largely overlaps with the structural classification since pyrimidine nucleoside phosphorylases mainly form S-shaped dimers with active sites located in the solvent-exposed pockets of the monomers, while purine nucleoside phosphorylases are predominantly functional as hexamers with inter-monomer active sites (Figure 1).¹³² The exception to this rule is presented by uridine phosphorylases which belong to the family of purine nucleoside phosphorylases from a structural standpoint but perform the phosphorolysis of a pyrimidine nucleoside.^{92,97,99,115,133} In both families of enzymes, substrate binding and catalysis follow a similar scheme. Hydrogen bonds between active site residues and the nucleobase heteroatoms as well as interactions with the 5'-OH group position the nucleoside substrate in a productive pose to the nucleophilic phosphate. The latter, in turn, is bound through interactions with histidine or arginine residues in a polar pocket of the active site (Figure 1). Catalysis in these enzymes is then achieved via dissipation of the increased electron density in the nucleobase in the transition state as the phosphate attacks at the anomeric center, displacing the nucleobase (Scheme 3, bottom). Although the exact reaction mechanisms are still a topic of debate, there is increasing consensus that the transformations performed by purine nucleoside phosphorylases have more S_N1-character while pyrimidine nucleoside phosphorylase-catalyzed reactions proceed in a more concerted fashion according to a S_N2-type substitution.^{91,92,94,134–142} In either case, the reaction products pentose-1-phosphate and the nucleobase are generated in the active site and released into the bulk solvent where protonation steps reestablish the charge of both species according to the ambient pH

^{IV} Nucleoside deoxyribosyltransferases catalyze a similar reaction,^{206,207} but with a very limited substrate scope.

(Scheme 3, center).^{92,94,143} The substrate spectra of both classes of enzymes are rather relaxed and largely limited by the H-bonding substituents needed for productive substrate binding.^{122,144} For instance, nucleoside phosphorylases have been reported to convert a range of modified nucleosides, including pyrimidines with substitutions in the 5- and 6-position of the nucleobase,^{41,120,145} purines with various substitutions in the 2- and 6- position,¹²⁶ arabinosyl nucleosides,^{128,146} fluorinated^{121,146,147} or aminated¹⁴⁸ nucleosides as well as selenium- or sulfur-containing nucleosides.¹⁴⁹ Combined with the discovery and classification of a spectrum of highly thermostable members of the family,^{122,127,128,144,150} these examples showcase the versatility and potential of nucleoside phosphorylases for biocatalytic applications.

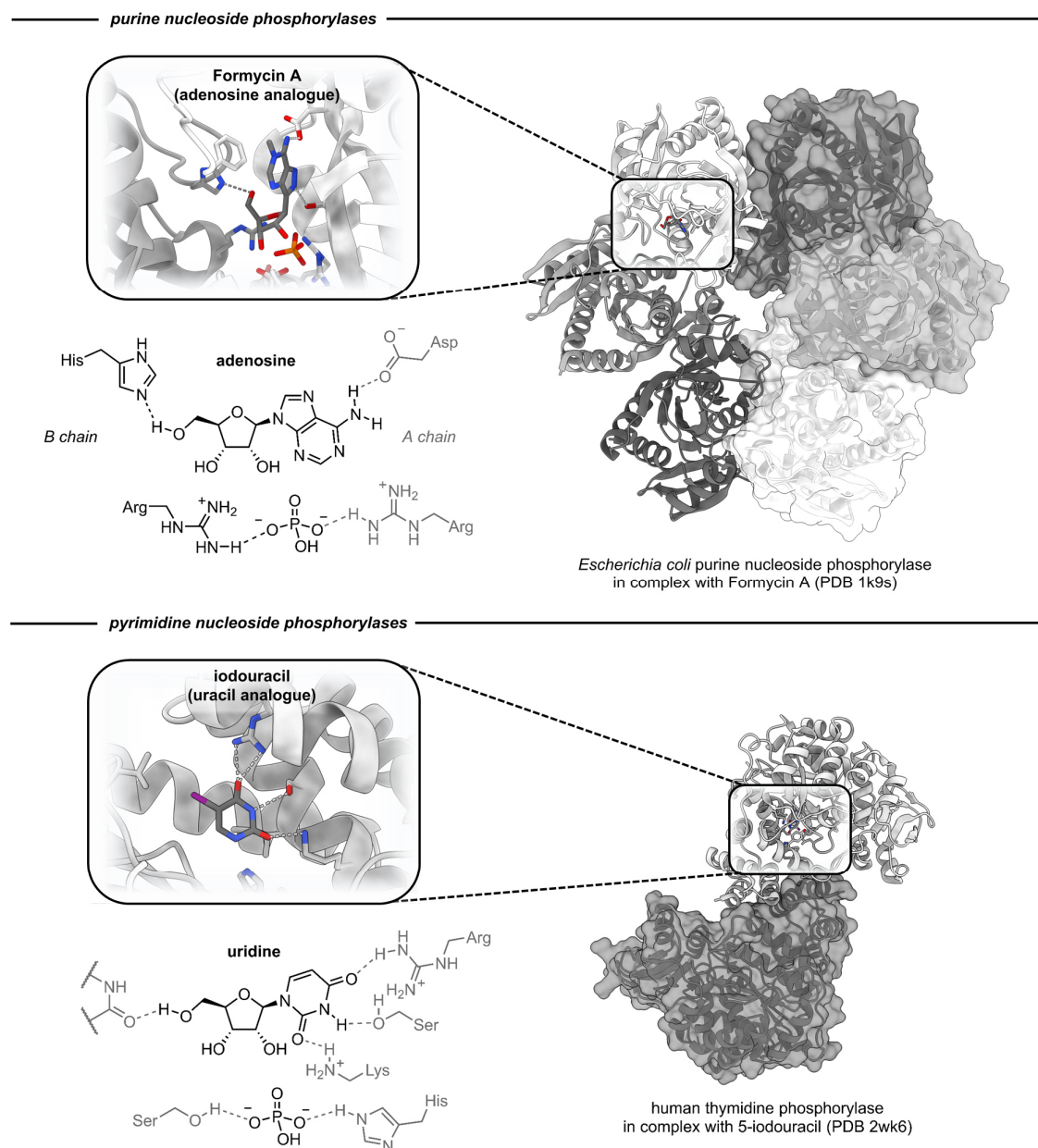
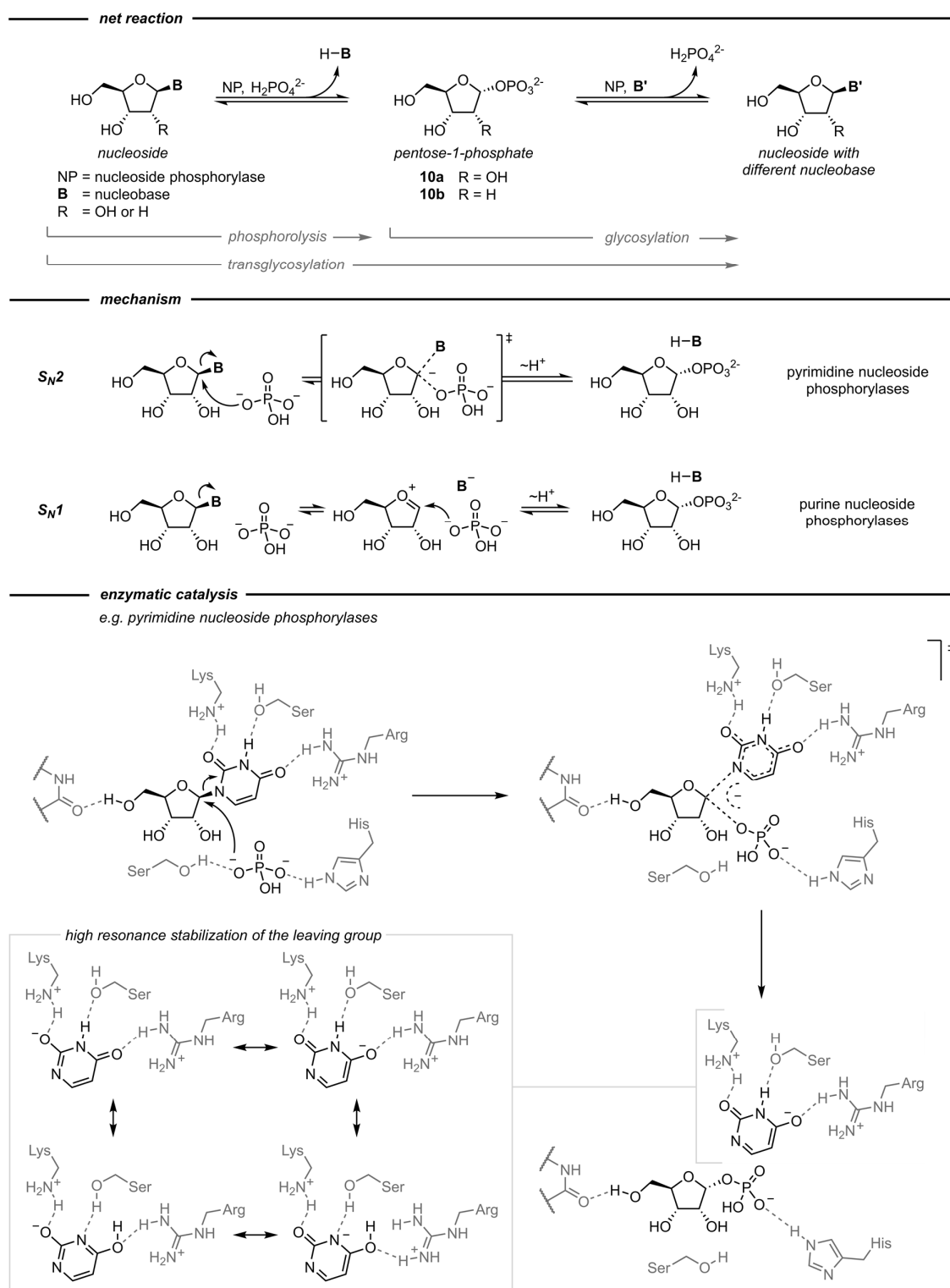


Figure 1. Crystal structures of nucleoside phosphorylases revealing the modes of substrate binding.^{113,116} Thymidine phosphorylases are structural homologues of non-specific pyrimidine nucleoside phosphorylases. Charges of amino acid residues are shown for pH 9.



Scheme 3. Nucleoside phosphorylase-catalyzed reactions. The reactions performed by pyrimidine and purine nucleoside phosphorylases exhibit both S_N1 and S_N2 character and may not be as defined as shown in this scheme. Charges of amino acid residues are shown for pH 9. For clarity, only selected resonance structures of the stabilized negatively charged pyrimidine nucleobase are shown. These only provide a snapshot of the possible and plausible resonance structures one could imagine. Likewise, participation of the ring oxygen in the transition state was omitted for clarity.

2.5 Biocatalytic Nucleoside Synthesis Via Nucleoside Phosphorylases

Owing to their outstanding selectivity in glycosylation reactions, nucleoside phosphorylases have been applied to the synthesis of various nucleosides. Although the early examples of nucleoside phosphorylase-catalyzed nucleoside synthesis^{82,84} were largely curiosity-based, these enzymes have reattracted attention as biocatalysts for preparative applications over the past decade.^{119,122–124,126,129} By offering perfect chemo-, regio- and diastereoselectivity in *N*-glycosylation reactions, they effectively bypass the main obstacles troubling established nucleoside synthesis approaches and shorten the respective synthesis down to a single step. Furthermore, aqueous conditions obviate the need for the excessive use of organic solvents, greatly reducing the potential environmental impact of many nucleoside syntheses. Additionally, these biocatalytic reactions are appealing from a practical perspective since they do not require any protecting groups or hazardous reagents and are operationally simple. For these reasons, nucleoside phosphorylases are currently under development in industry and academia to achieve more sustainable nucleoside synthesis by supplementing and augmenting existing methods.^{28,151,152}

In preparative applications, nucleoside phosphorylases are commonly employed as transglycosylation catalysts (Scheme 3, top). Therefore, a starting nucleoside, typically naturally occurring uridine (**5b**) or thymidine (**4a**), is subjected to enzymatic phosphorolysis, liberating the corresponding nucleobase and a pentose-1-phosphate.¹³¹ The latter then serves as a sugar synthon in a reverse phosphorolysis (glycosylation) with a different nucleobase to furnish the target nucleoside bearing the desired nucleobase. Depending on the starting and the product nucleoside, either one or two nucleoside phosphorylases are required to yield a pyrimidine or purine nucleoside of interest. Herein, inorganic phosphate only plays a catalytic role since it is consumed in the first step but liberated again in the second step. Formally, such a transglycosylation reaction sequence equals the direct glycosylation of a nucleobase with the sugar moiety of a sacrificial nucleoside.

Despite the numerous advantages offered by nucleoside phosphorylase-based nucleoside synthesis, the admission of this methodology to the toolkit of organic chemists has been slow. For instance, the low water solubility of many nucleobases generally restricts the substrate loading in transglycosylation reactions to the low millimolar range, which is several orders of magnitude lower than the desired substrate titers in industrial applications.^{71,153,154} Additionally, the equilibrium nature of nucleoside phosphorolysis (and in extension transglycosylation) has so far not been systematically investigated and only selected examples of equilibrium constants for this transformation can be found in the literature.^{89,97,99,104,117,125,155–158} Furthermore, the choice of the right enzyme(s) as well as reaction conditions has remained elusive and reliable physicochemical frameworks for the optimization of conversions in these reactions are missing. Ultimately, these obstacles hinder the design of efficient biocatalytic processes using nucleoside phosphorylases and prevent the introduction of these enzymes into the standard repertoire for nucleoside synthesis.

3 Research Hypotheses

Given the limited understanding of nucleoside phosphorylase-catalyzed (trans)glycosylations and their potential in organic synthesis, the following research hypotheses were central to the work presented in this thesis.

- H1 Biocatalytic nucleoside synthesis is more efficient and sustainable than nucleoside synthesis via traditional chemical routes.**
- H2 Deconvolution of overlapping UV absorption spectra can provide a means for quick and cheap reaction monitoring of enzymatic nucleoside phosphorolysis and glycosylation reactions.**
- H3 Nucleoside phosphorolysis is a reversible endothermic reaction with a substrate-specific equilibrium constant.**
- H4 The thermodynamic reaction control of nucleoside phosphorolysis can be leveraged to observe the hydrolysis of pentose-1-phosphates via apparent equilibrium shifts.**
- H5 The thermodynamic reaction control of nucleoside phosphorolysis enables a systematic prediction of transglycosylation yields.**
- H6 Equilibrium thermodynamics can be employed to rationally improve the yields of hard-to-access nucleosides such as selenium-modified pyrimidines in transglycosylation reactions.**
- H7 Thermostable nucleoside phosphorylases enable reactions under harsh conditions facilitating increased substrate loading.**

4 Results and Discussion

Prompted by the demand for methods to access nucleosides and their analogs, a variety of synthetic approaches has been developed. Among these, biocatalytic nucleoside synthesis catalyzed by nucleoside phosphorylases has recently attracted renewed interest. This thesis presents analytical tools and thermodynamic frameworks for the characterization and optimization of nucleoside phosphorolysis and (trans)glycosylation reactions. To this end, each chapter is built around a central research hypothesis and a publication in a peer-reviewed journal. Consequently, the following chapters are only condensates. The points raised for each topic are discussed in more detail in the full texts of the respective publications, which are available at the end of this thesis. Although key findings of these works are summarized and put into context in the following chapters, the reader is encouraged to view the full texts for deeper insights, additional figures and technical details. In many cases, these publications are further supported by electronic supplementary materials comprised of further experimental details, additional data, calculations or supplementary resources such as reference spectra or calculation tools. These are available from the data sharing platform zenodo.org via the digital online identifiers provided in the List of Publications.

4.1 Efficiency Assessment of Nucleoside Synthesis Approaches

The identification of bottlenecks and obstacles encountered in the pursuit of efficient (biocatalytic) nucleoside synthesis was fundamental to the work presented in this thesis. All chemical approaches to nucleoside synthesis published so far require protected sugar synthons and overall routes of varying length. Since these routes also vary greatly in their synthetic strategy, yields as well as the conditions used, it becomes rather challenging to compare different approaches in terms of their overall efficiency or sustainability. Although biocatalytic nucleoside synthesis was often praised as the greener or more environmentally friendly method, there was no set of benchmarks which would have allowed a substantiation of this claim. Furthermore, there is a growing consensus that biocatalytic approaches are often, but certainly not always, more efficient than their chemical competitors.¹⁵³ This led to the formulation of the first research hypothesis:

H1 Biocatalytic nucleoside synthesis is more efficient and sustainable than nucleoside synthesis via traditional chemical routes.

This hypothesis was examined through an analysis of the environmental factor (E-factor) of methods for nucleoside synthesis by *N*-glycosylation. The E-factor^{71,72} is a mass-based metric to express the amount of waste generated for a (hypothetical) kilogram of product as

$$\text{E-factor} = \frac{m_{\text{waste}}}{m_{\text{product}}} \quad (1)$$

where waste includes all materials in a process that are not the product. To generate a level playing field for all methods, the E-factor was calculated over the entire route required for that method. This *route E-factor* therefore includes materials over a number of steps and allows a comparison of vastly different methods on the basis of the amount of waste they produced to access a given product. The required data about material usage was extracted directly from the experimental sections of the publications describing the use of the respective method. Although some quantities frequently had to be estimated since literature reports across different journals contained insufficient data (e.g. regarding the amount of solvent use or workup materials), literature precedents^{153,159} as well as experimental data⁷⁷ on the matter allowed a realistic estimation of the missing data.

Paper I presents a route efficiency assessment of all published methods for the *N*-glycosylation of nucleobases to access β -nucleosides. This analysis includes 80 route E-factor, covering up to 11 total steps, from 12 different glycosylation methods. All glycosylation approaches, including nucleoside phosphorylase-catalyzed transglycosylations, share some fundamental synthetic strategies regarding the use of an activated glycosyl species primed for nucleophilic attack. Nonetheless, the respective routes differed vastly and so did their route E-factors. The syntheses covered in this analysis have E-factors of 165–42,499 with most methods scoring between 5,000 and 10,000. Considering that E-factors for several different types of transformations in industrial settings are generally in the range of 100 per step,^{160,161} these E-factors for nucleobase glycosylation routes are almost shockingly high. Furthermore, no single method consistently delivered lower E-factors than its competitors. This apparent lack of efficiency in a sense of resource usage¹⁶² demanded a search for the pitfalls of

nucleoside synthesis as well as the identification of approaches or strategies that worked particularly well, given that a few syntheses did achieve comparably low route E-factors.

The most important factors for the route E-factors of glycosylation methods were the length of the route and the overall yield. While the yield in the key glycosylation step is commonly regarded as a key metric in the literature, it showed no correlation with the cumulative E-factor of the respective method. In contrast, total yield correlated negatively with the E-factor so that the routes with >80% total yield had among the lowest E-factors. Similarly, shorter routes tended to have lower E-factors as the lower boundary for the possible E-factor appeared to increase nearly linearly over the number of steps. As such, all single-step routes had lower E-factors than the best-performing route featuring nine steps, highlighting the importance of route design and step economy. Although both findings may be somewhat intuitive since i) high-yielding routes should generally fare better than very low-yielding ones and ii) the potential for waste accumulation is a lot higher in longer routes than in shorter ones, there are several interesting outliers to these rules in the dataset. For instance, Downey *et al.*'s anhydrose-based glycosylation method⁵⁹ offered some of the lowest E-factors, with only around 30% glycosylation yield and 20% total yield. This was achieved by running a short route of only two steps and employing an efficient protecting group installation as well an *in situ* deprotection strategy, both of which contributed to lower solvent use compared to other routes. On the other end of the spectrum, the Lewis acid-catalyzed transglycosylation from cytidine to adenosine by Azuma and Isono⁶³ offered 71% total yield, but an E-factor of over 13,000 which is well above average in this dataset. In this case, route length (four steps) and excessive solvent usage outweighed the favorable yield, demonstrating that a suitable compromise between total yield and route length is a balancing act. Together, these data reveal that shorter *N*-glycosylation routes typically outperform longer ones in terms of their E-factor, even when the shorter routes heavily sacrifice yield. Nonetheless, a low step count alone does not guarantee a low E-factor as there are several two-step routes in the dataset with high E-factors of 20,000–40,000. Clearly, shorter routes have the potential to be a lot more efficient than longer ones, but there appear to be factors rooted in reaction design which offset the route length and tremendously contribute to waste production.

Irrespective of the type of glycosylation method, solvent usage was the main contributor to the overall E-factor of the route (Figure 2). Although nucleobases and nucleosides are generally poorly soluble in most solvents, the bulk of this solvent must be attributed to chromatographic purification steps. As **paper I** highlights, the number of chromatography steps linearly correlates with the overall E-factor of the route. As such, the methods which include zero or one chromatography step displayed the lowest E-factors by far. This reiterates the importance of route length since purification of intermediates accounts for most of the E-factor of routes with more than two steps. Admittedly, some form of chromatography is probably unavoidable in nucleoside synthesis to achieve a sufficient purity of the product, but it appears that limiting chromatography steps throughout a synthetic route should be a central aim for “greener” nucleoside synthesis.

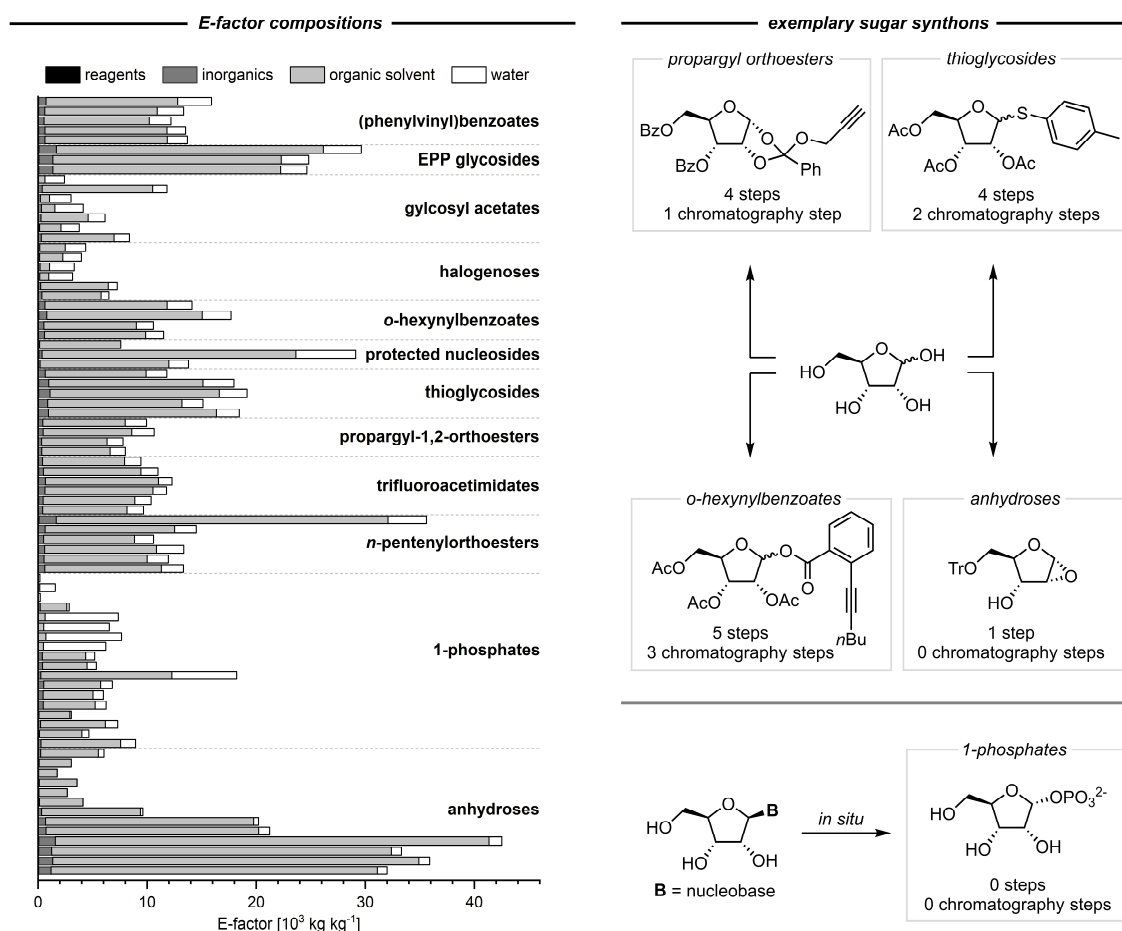


Figure 2. E-factor composition of *N*-glycosylation routes and exemplary sugar synthons. Adapted in part from ⁷⁰.

So where does that put biocatalytic nucleoside synthesis in terms of its efficiency? Nucleoside phosphorylase-catalyzed transglycosylations shine by offering a concise single-step route by generating a pentose-1-phosphate *in situ* followed by glycosylation of a nucleobase, directly yielding the target nucleoside. Additionally, their perfect selectivity ensures exclusive generation of the nucleoside of interest, avoiding unwanted byproducts such as α -nucleosides or hard-to-separate regioisomers. So far, however, the poor solubility of nucleobases in aqueous solution restricts most biocatalytic nucleoside syntheses to working concentrations of 1–5 mM. Therefore, contaminated water presents a significant source of waste in these processes (Figure 2). The chromatographic purifications required to remove the residual (unreacted) donor nucleoside can further contribute to solvent waste. Moreover, the equilibrium nature of nucleoside transglycosylations limits the maximum yields in these reactions such that most transglycosylation achieve only around 50% total yield. For these reasons, biocatalytic nucleoside synthesis is currently on par with many of its chemical competitors in terms of their E-factors. One may argue that the E-factor only gives limited insights into the wastefulness or sustainability of a process or reaction and that the kind of waste generated by biocatalytic approaches is “greener” than that of many chemical syntheses. Both arguments are

certainly valid. The E-factor completely ignores the *kind* of waste that is generated and biocatalytic processes yield primarily water and buffer substances as byproducts. Nonetheless, any kind of waste requires downstream processing and remediation, which can be especially energy-intensive in the case of water. Consequently, it appears that biocatalytic approaches to nucleoside synthesis are currently not significantly more sustainable than chemical methods, but they certainly hold great potential.

Based on the insights gained by this E-factor analysis, there are several obstacles that need to be addressed to move towards “greener” nucleoside synthesis. Future work should seek to develop more concise routes which avoid chromatographic purifications and unnecessary protecting group transformations. To this end, instead of focusing on maximizing glycosylation yield, the development of heterogenous processes or one-pot reactions is more likely to bear fruit. Biocatalytic approaches should aim to reduce solvent use by applying higher substrate loadings and overcome the equilibrium constraints imposed in transglycosylation reactions.

Paper I further presents a systematic review of all glycosylation methods for nucleobases in addition to a more in-depth discussion of the above points.

4.2 A Spectral Unmixing-Based Method for Reaction Monitoring

The optimization of nucleoside phosphorylase-catalyzed transglycosylations as well as the characterization of the respective enzymes demanded the development of an efficient analytical tool for versatile high-throughput experimentation. Previous work in the field had largely relied on time-consuming HPLC-based detection of nucleosides and nucleobases from reaction mixtures with only some spectroscopy-based methods for the analysis of nucleoside phosphorolysis reactions being available from the literature. For instance, the fluorescence of 4-thiopyrimidines,¹²⁵ 8-azapurines,^{163–165} tricyclic nucleosides^{163,166,167} or guanine⁹⁸ has been exploited for spectroscopic reaction monitoring. For UV absorption-based reaction monitoring, coupling of the reaction of interest with the oxidation of hypoxanthine to uric acid¹⁶⁸ or with colorimetric phosphate detection¹⁶⁹ as well as single-wavelength detection approaches for uridine, thymidine or guanosine^{118,170,171} were already available. However, these spectroscopic methods are generally highly specific and can only be applied to selected nucleoside-nucleobase pairs, limiting the chemical space that can be investigated. Many of these approaches also rely on subtle changes in the extinction at a specific wavelength, making these methods prone to pipetting or readout errors. Moreover, the compatibility of these approaches with varying reaction conditions, including temperature, pH and cosolvents, is limited. Consequently, a versatile method for robust spectroscopy-based reaction monitoring of transformations between nucleosides and nucleobases was missing. Building on previous work by Wittenburg,¹⁷² Fox¹⁷³ and Shugar,¹⁷⁴ Giessmann and Krausch *et al.* recently developed a UV spectroscopy-based method for the monitoring of thymidine phosphorolysis which employed a spectral shift of thymine under alkaline conditions.¹⁷⁵ Following work by me and Giessmann *et al.* further demonstrated that this deprotonation-driven spectral shift of nucleobases can be extended to all natural nucleoside-nucleobase pairs and be used for reaction monitoring via deconvolution of the resulting spectra.¹⁷⁶ The natural continuation of this work was guided by the second research hypothesis:

H2 Deconvolution of overlapping UV absorption spectra can provide a means for quick and cheap reaction monitoring of enzymatic nucleoside phosphorolysis and glycosylation reactions.

Therefore, **paper II** presents a robust and versatile UV-based method for reaction monitoring of (enzymatic) transformations between nucleosides and nucleobases via spectral deconvolution. To this end, an extended spectrum of established substrates, examples of applications deviating from previously reported protocols as well as recommendations regarding common problems encountered with spectral unmixing-based monitoring are addressed.

The fundamental principle of this approach builds on pioneering work by Fox and Shugar in the 1950s,¹⁷⁴ who demonstrated that, under alkaline conditions, nucleobases have different UV absorption spectra than their corresponding nucleosides. Wittenburg later substantiated these findings and established that this effect is rooted in the protonation-dependent tautomeric equilibrium of nucleobases.¹⁷² Indeed, *N*1-substitution of pyrimidines (e.g. with a ribosyl moiety) changes the electronic characteristics of the nucleobase. The free base readily tautomerizes to an aromatic structure upon deprotonation which goes along with a significant shift of its absorption spectrum to

higher wavelengths (Figure 3). In contrast, the substituted base (i.e. the nucleoside) shows almost no spectral difference between neutral or alkaline conditions (Figure 3, bottom). This effect can be exploited for reaction monitoring to obtain absorption spectra which can easily be differentiated.

My previous work with Giessmann¹⁷⁶ had described a Python-based tool for the deconvolution of overlapping absorption spectra which relied on fitting of reference spectra to an experimental spectra. Therein, normalization to the isosbestic point of base cleavage (Figure 3) minimized errors from changing signal intensities, as only spectral shape is considered for analysis. The work presented in **paper II** extends this method to a total of 38 established substrates, including all natural nucleosides, a range of modified nucleosides such as halogenated and alkynylated species as well as 5'-mononucleotides. While a standard protocol involving alkaline quenching in aqueous NaOH (pH 13) proved robust and applicable to various nucleosides, adjusted sample treatment protocols had to be developed for some outliers such as dihalogenated purine nucleosides. For these cases, quenching in an organic solvent such as methanol or isopropanol followed by a more subtle pH shift via a glycine-buffered system provided suitable and reproducible absorption spectra.

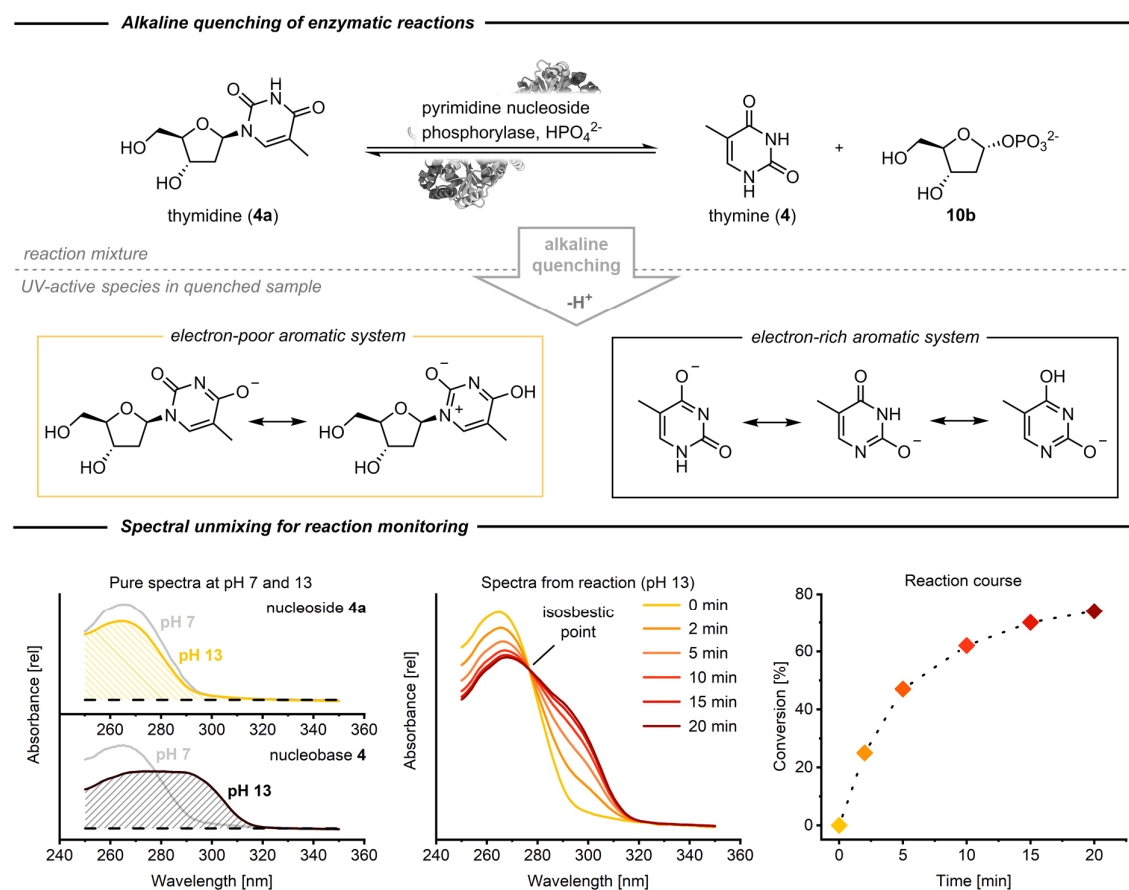


Figure 3. Spectral unmixing for reaction monitoring of transformations between nucleosides and nucleobases. Adapted in part from ¹⁷⁷.

Furthermore, a number of common problems surrounding background absorption were resolved. Along with atypical absorption of the multiwell plate, background signals from proteins and other reaction components are often encountered, depending on the application. In most cases, appropriate background spectra can resolve the issue, but some settings (e.g. involving UV-active cosolvents) may require a narrowing of the wavelength range for consideration.

Ultimately, the unparalleled versatility and substrate spectrum of reaction monitoring via spectral deconvolution as well as its robustness to background signals make it a highly valuable addition to the analytical repertoire for nucleoside phosphorylase-catalyzed reactions. Since this method is approximately 20 times faster per sample than conventional HPLC, while being more than 5 times cheaper and offering comparable accuracy, it has become the analytical method of choice for the experimental work presented in this thesis. Given that the underlying principle should enable a transfer of this methodology to nearly any nucleoside-nucleobase pair which fulfills the prerequisites of being i) UV-active, with an isosbestic point of base cleavage, and ii) sufficiently stable in alkaline solution, it should be expected that this approach will find applications beyond the ones explored so far. Lastly, this methodology is not restricted to nucleosides and will be valuable for a wealth of other (enzymatic) reaction systems where a substrate and a product of a transformation have highly overlapping but not identical UV absorption spectra.

Paper II additionally lists the spectral characteristics of all established substrates and provides workflow recommendations for reaction quenching and data handling.

4.3 Equilibrium Thermodynamics of Nucleoside Phosphorolysis

Biocatalytic nucleoside transglycosylations involve a nucleoside phosphorolysis as well as a reverse phosphorolysis (commonly termed glycosylation), which are coupled *in situ* to furnish a nucleoside of interest via formal glycosylation of a nucleobase. This requires a given reversibility of the reaction, such that it can proceed to some extent in both directions. Therefore, the individual nucleoside phosphorolysis steps must be a thermodynamically controlled equilibrium reaction. Indeed, for selected nucleosides, including adenosine (**1b**), uridine (**5b**) and inosine, equilibrium constants of phosphorolysis have been reported in the literature.^{81,97,99,117,125,156,178,179} However, this had not been recognized as a general characteristic of nucleoside phosphorolysis reactions, as indicated by the fact that efforts including enzyme discovery,^{127,130} enzyme immobilization¹⁸⁰ or enzyme engineering^{181,182} have recently been employed to increase conversions in biocatalytic nucleoside phosphorolysis reactions. This incomplete understanding of the equilibrium nature of this reaction system led to the formulation of the third research hypothesis:

H3 Nucleoside phosphorolysis is a reversible endothermic reaction with a substrate-specific equilibrium constant.

This hypothesis was probed with various phosphorolysis experiments enabled by the spectral unmixing-based method described in **paper II**, revealing a systematic and characteristic behavior of pyrimidine and purine nucleosides in phosphorolysis reactions.

Paper III confirms the equilibrium nature of nucleoside phosphorolysis and presents equilibrium constants for 24 nucleosides as well as thermodynamic data regarding the temperature-dependence of these substrate-specific constants. In a first set of experiments building on previous work,^{127,175,176} the model substrate uridine (**5b**) was subjected to phosphorolysis by five different pyrimidine nucleoside phosphorylases in the presence of 5 equivalents of phosphate (with respect to the nucleoside). All reactions showed incomplete conversion of the nucleoside to the corresponding nucleobase, stopping short at 55.5% conversion under these conditions (Figure 4). This observation was not due to concentration effects of the enzyme or due to enzyme inactivation, as experiments with increased enzyme loading or enzyme spiking after reaction completion gave identical conversions (Figure 4). With different amounts of phosphate, varying equilibrium conversions were observed, which were all consistent with an equilibrium constant of phosphorolysis of 0.15. This unambiguously confirmed that the phosphorolysis of **5b** is a thermodynamically controlled equilibrium reaction. Interestingly, related pyrimidine nucleosides, including the 2'-deoxy analog **5a** or the fluorinated analogs of **5a** and **5b**, behaved almost identically with comparable equilibrium constants of 0.14–0.20. Notably, enzyme-independent equilibrium behavior was also observed for all purine nucleosides tested, but with much lower equilibrium constants of 0.01–0.02. This was further confirmed with phosphorolysis experiments at different temperatures, which revealed that i) the equilibrium constant of nucleoside phosphorolysis is a temperature-dependent characteristic with a highly substrate-dependent entropy contribution and ii) purine nucleosides have much higher Gibbs energies of phosphorolysis than pyrimidine nucleosides. As such, almost all equilibrium constants of nucleoside phosphorolysis increased with temperature in an Arrhenius fashion with the purines generally giving

much lower conversions under identical conditions than pyrimidines, consistent with their respective thermodynamic properties.

Thus, **paper III** reveals a range of equilibrium constants giving insights into the thermodynamics of nucleoside phosphorolysis and represents the first systematic characterization of this reaction system. While the practical significance of the temperature-dependence of nucleoside phosphorolysis may arguably be limited, the characteristic thermodynamic properties of pyrimidine and purine nucleosides as well as the spectrum of equilibrium constants reported in this publication laid the foundation for the following works presented in **papers IV–VII**.

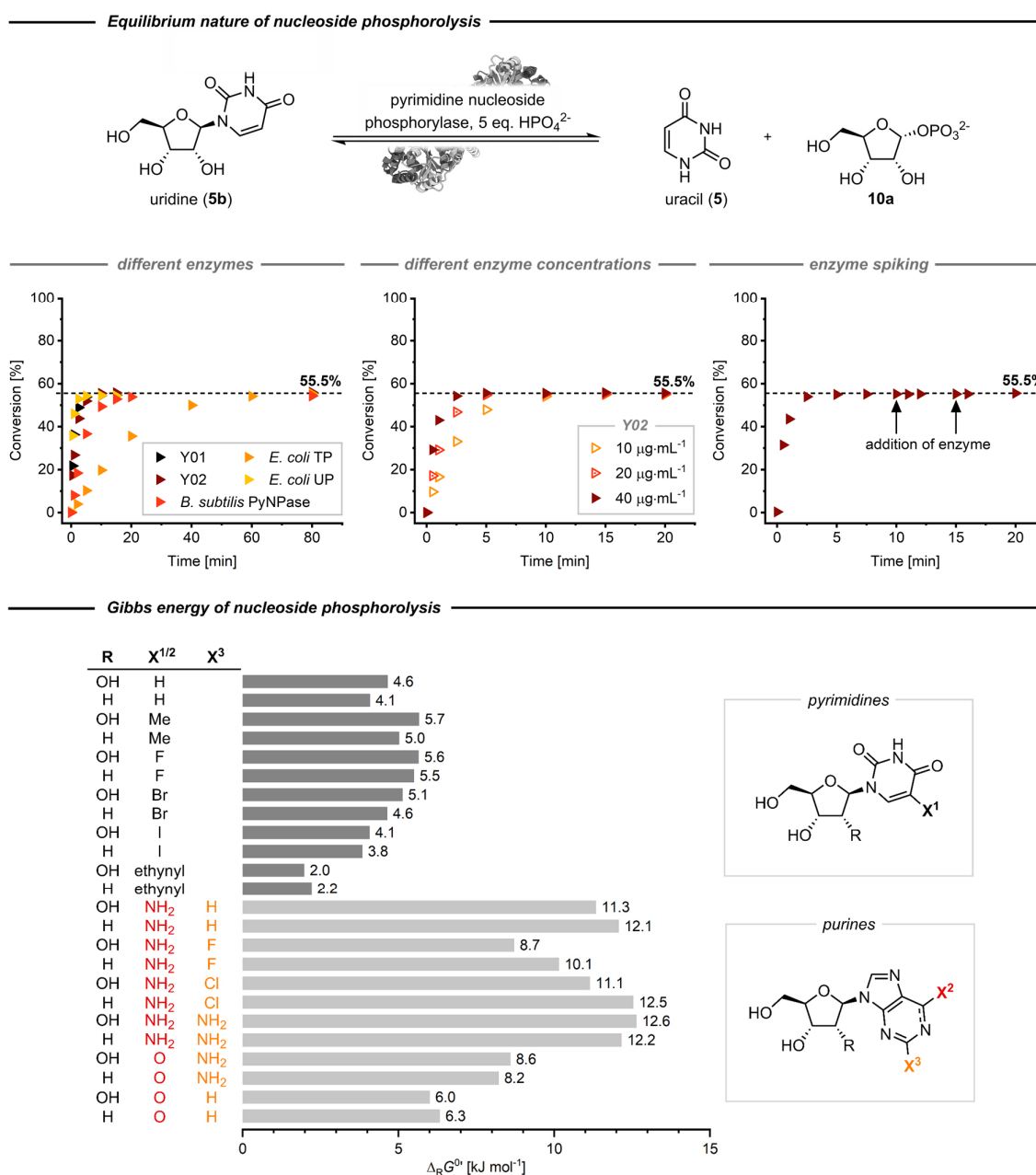


Figure 4. Thermodynamic control of nucleoside phosphorolysis. Adapted in part from ¹⁸³.

4.4 Equilibrium Shifts for the Kinetic Analysis of Sugar Phosphate Hydrolysis

With a good understanding of the equilibrium nature of nucleoside phosphorolysis, these reaction systems are predictable and can easily be manipulated through the choice of reaction conditions. However, some applications involving 2'-deoxy nucleosides tend to show more conversion of the nucleoside to the nucleobase over time than expected for their equilibrium constant. This often manifests itself in a slow increase of the apparent conversion after an initial establishment of an equilibrium state. Since this effect is highly pH- and temperature-dependent, it was easily ascribed to the decay of the pentose-1-phosphate product **10b**, which is known to be prone to hydrolysis under acidic conditions.¹²¹ Nonetheless, synthetic applications require an understanding of the stability of these sugar phosphate intermediates, which necessitated an investigation into the hydrolysis of these compounds.¹⁸⁴ The elusive nature of these UV-inactive molecules and the lack of high-throughput methodologies for the detection and quantification of pentose-1-phosphates prompted the formulation of the fourth research hypothesis:

H4 The thermodynamic reaction control of nucleoside phosphorolysis can be leveraged to observe the hydrolysis of pentose-1-phosphates via apparent equilibrium shifts.

For this method, spectral unmixing was employed to detect slight changes of the apparent equilibrium conversion in nucleoside phosphorolysis reactions. With the law of mass action and the mass balances of all reactants, this information could be leveraged to assess the hydrolysis of pentose-1-phosphates in a discontinuous manner by uncoupling the phosphorolysis and hydrolysis processes.

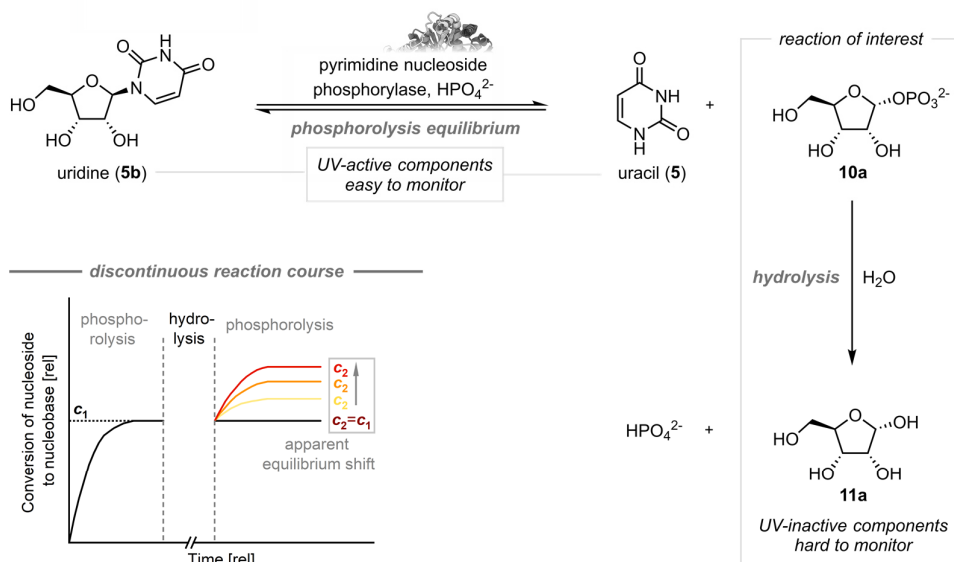
Therefore, **paper IV** presents a UV spectroscopy-based method for the quantification and kinetic analysis of the hydrolysis of UV-inactive pentose-1-phosphates. This flashlight approach exploits the tight thermodynamic control of nucleoside phosphorolysis via the observation of deviations from an established equilibrium following LeChatelier's principle (Figure 5, top). To this end, a nucleoside phosphorolysis reaction in equilibrium can be subjected to hydrolyzing conditions after termination of the enzymatic reaction, which leads to (partial) hydrolysis of the initially generated sugar phosphate. Upon addition of fresh nucleoside phosphorylase, a new equilibrium is generated since one of the products was (partially) removed from the equilibrium. Thus, the reaction system reestablishes reactant concentrations through further conversion of the nucleoside to the nucleobase which again fulfill the equilibrium constraint given by the law of mass action. The apparent extent of conversion in this new equilibrium then reflects the respective loss of a product and can be used to calculate the amount of hydrolyzed pentose-1-phosphate through equations available via implementation of the adjusted mass balances in the law of mass action. For **5b**, this approach offers a surprisingly broad working space as a range of conditions enables a significant maximum equilibrium shift that can be quantified by high-throughput spectral unmixing-based reaction monitoring. In fact, nucleosides in general lend themselves to this approach as their equilibrium constants of phosphorolysis ($K = 0.01\text{--}0.80$) allow a straightforward adjustment of the reaction conditions for an apparent equilibrium shift of up to 25 percentage points, as revealed by a theoretical examination of the working space (Figure 5, bottom). This approach was demonstrated with an examination of the hydrolysis of the relatively stable ribose-1-phosphate (**10a**) in near-boiling media at different pH values. To this end,

10a was generated *in situ* by phosphorolysis of **5b** and subjected to 98 °C for various times. A continuation of phosphorolysis in these mixtures resulted in new equilibria consistent with the fundamental predictions of the theoretical framework and yielded half-lives of 1.8–11.7 h, depending on the pH of the incubation mixture.

This approach reflects how principles of thermodynamic control can be exploited to probe the stability of reactants in a coupled reaction system and provides an inexpensive and easy-to-handle method for the analysis of pentose-1-phosphate hydrolysis. Previous methods for the quantification of pentose-1-phosphate decay have relied on thin layer chromatography¹²¹ or colorimetric phosphate detection.¹⁸⁵ In contrast, this method employing UV spectroscopy i) does not require pure pentose-1-phosphates which can be expensive and/or hard to isolate, ii) enables application of various buffer systems or cosolvents and iii) delivers robust and quantitative data in a high-throughput fashion.

Paper IV includes the necessary equations, which can, in principle, be transferred to all pentose-1-phosphates as well as other thermodynamically controlled reaction systems where similar decay effects can be encountered.

Hydrolysis of pentose-1-phosphates from a phosphorolysis equilibrium



Theoretical examination of maximum equilibrium shift and experimental example

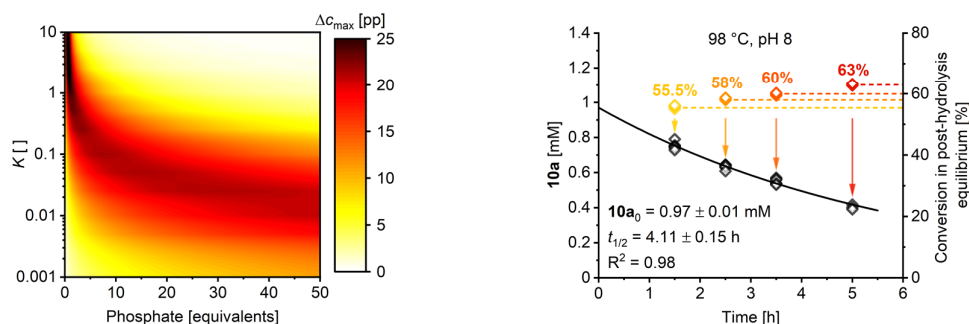


Figure 5. A flashlight approach to the quantification of pentose-1-phosphate hydrolysis via monitoring of a coupled phosphorolysis equilibrium. Adapted in part from ¹⁸⁶.

4.5 Yield Optimization of Nucleoside Transglycosylations

Having characterized the thermodynamic control of nucleoside phosphorolysis reactions, these principles were extended to transglycosylations comprising a forward and reverse phosphorolysis. Despite the fact that nucleoside transglycosylation is a well-established biocatalytic method for the synthesis of nucleosides directly from their respective nucleobases,^{41,118–130,144–149} the investigation of the thermodynamics of this coupled reaction system has been largely neglected. As such, a general characterization of nucleoside transglycosylation reactions with respect to yield optimization was missing from the literature. Thus, the interrelation between the obtained conversions and the choice of enzyme, the employed starting materials as well as the product(s) of these reactions has remained unclear and elusive. Although a recent report by Alexeev *et al.*¹¹⁷ demonstrated an approach for a system of equations for the yield prediction in nucleoside transglycosylations, the respective equations failed for higher equilibrium constants. Therefore, a general physicochemical framework for the prediction and optimization of yields in nucleoside transglycosylations was needed to enable a robust and streamlined optimization of these biocatalytic reactions. Empowered by the thermodynamic insights presented in **paper III**, this gap in the literature motivated the formulation of the fifth research hypothesis:

H5 The thermodynamic reaction control of nucleoside phosphorolysis enables a systematic prediction of transglycosylation yields.

This hypothesis was probed with a theoretical examination of nucleoside transglycosylation systems, which revealed general trends and systematic behaviors of these reactions in line with experimental observations.

Paper V presents general principles for the yield prediction and optimization of biocatalytic nucleoside transglycosylations based on thermodynamic characterizations of the individual phosphorolytic steps (Figure 6, top). As explored previously,¹⁸³ the first and second reaction steps of a nucleoside transglycosylation are both under tight thermodynamic control. Therefore, it appears logical to assume that the net reaction would follow the respective equilibrium constraints:

$$K_1 = \frac{[B1][P1P]}{[N1][P]} \quad (2)$$

$$K_2 = \frac{[B2][P1P]}{[N2][P]} \quad (3)$$

Here, K_1 and K_2 are the apparent equilibrium constants of phosphorolysis of the sugar donor and the product nucleoside, respectively, and $[B1]$, $[B2]$, $[N1]$, $[N2]$, $[P1P]$ and $[P]$ are the equilibrium concentrations of the nucleobases, nucleosides, pentose-1-phosphate and phosphate, respectively. However, these equilibrium constraints, combined with the mass balances of all reactants, yield only five non-redundant equations for a system of six variables, assuming that all reaction components are considered as species with variable concentrations. Alexeev *et al.*'s¹¹⁷ approach of a cubic expression assuming a constant phosphate concentration yielded results which were not in agreement with

experimental HPLC data for nucleosides with high equilibrium constants, such as the pharmaceutically and biologically relevant 5-ethynyluridine (**12b**, $K_2 = 0.35$). Therefore, **paper V** presents a numerical solution to this problem which was employed to access the concentrations of all reaction components directly from the equilibrium constraints (2) and (3).

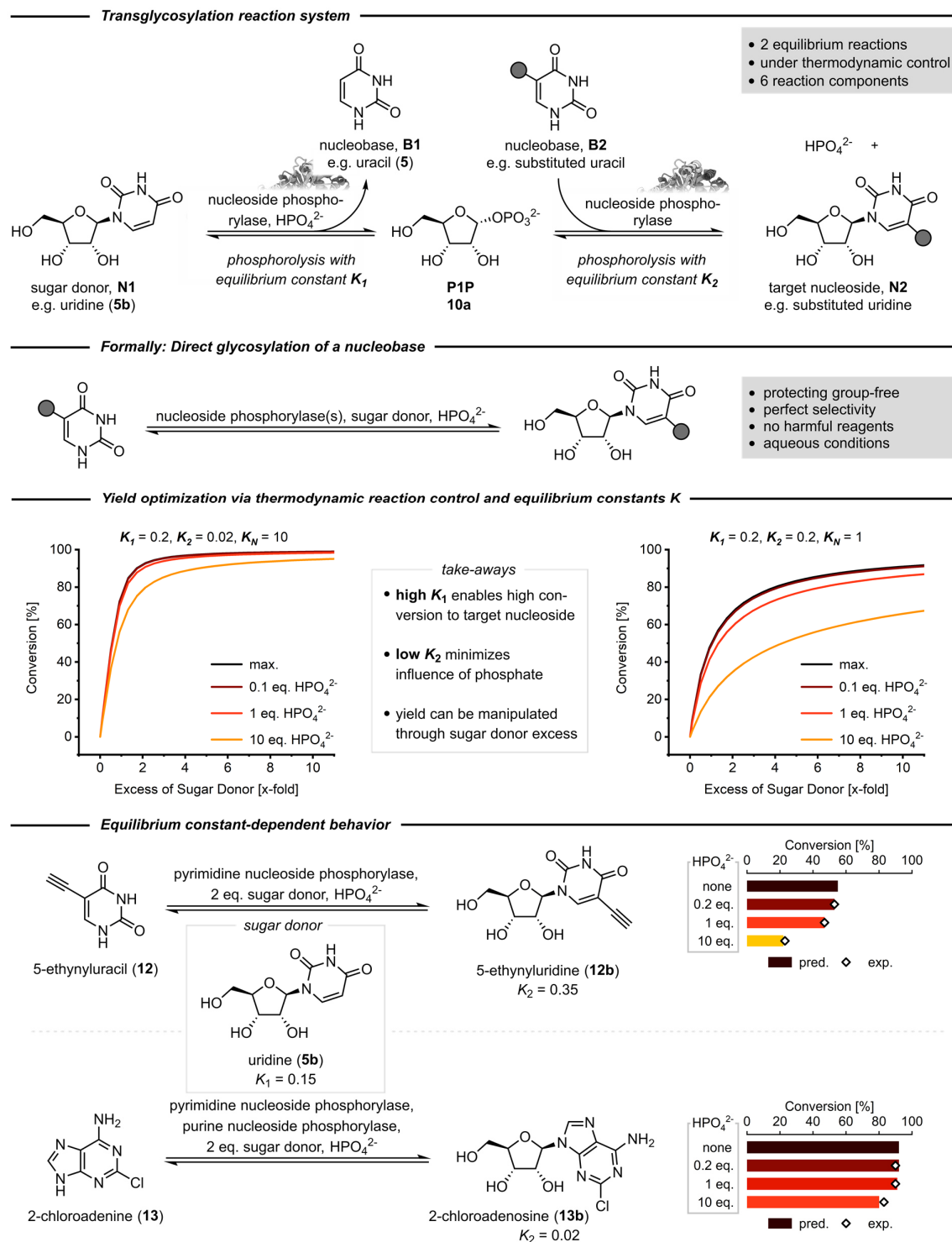


Figure 6. Thermodynamic control of nucleoside transglycosylations. Adapted in part from ¹⁸⁷.

A theoretical investigation of this reaction system with realistic equilibrium constants of phosphorolysis revealed several important characteristics which serve to guide the optimization of nucleoside transglycosylation reactions (Figure 6, center). First, high equilibrium constants of phosphorolysis of the starting nucleoside (sugar donor) are highly beneficial to conversion of the nucleobase of interest to the target nucleoside. Therefore, uridine (**5b**) and thymidine (**4a**) present very favorable thermodynamic characteristics and further recommend themselves as sugar donors by being easily commercially available and well soluble in aqueous media. Conversely, high equilibrium constants of the product nucleoside are unfavorable and limit the maximum yields that can be achieved. Although an excess of sugar donor can be employed to promote higher conversions, this comes with significantly diminished returns. Secondly, phosphate concentrations should generally be kept to a (catalytic) minimum to prevent phosphorolysis (or non-synthesis) of the product nucleoside. This is especially important for products with unfavorable equilibrium constants as these are more sensitive to higher phosphate levels. Conversely, reaction systems working towards purine nucleosides are very robust, insensitive to phosphate concentrations and high-yielding even with moderate excesses of the sugar donor, because of the low equilibrium constants of these products. Experimental data of selected examples reflecting the characteristic behavior of transglycosylation systems depending on the thermodynamic properties of the nucleosides involved supported these predictions (Figure 6, bottom). Thus, **paper V** demonstrates the value of fundamental thermodynamic insights for the prediction and optimization of synthetically useful biocatalytic equilibrium reactions.

Paper V additionally provides a simplified equation for the calculation of maximum yields in transglycosylation reactions via robust analytical solutions and highlights further examples of nucleoside transglycosylation systems with different nucleosides from a theoretical and experimental perspective. The tools available in the supplementary information enable straightforward reaction optimization based on either i) previously reported equilibrium constants¹⁸³ or ii) at least one selected preliminary experiment for the determination of the equilibrium constants of phosphorolysis of the target nucleoside. The latter approach was already applied for the optimization of the biocatalytic synthesis of dihalogenated purine nucleosides,⁴⁰ where data from one analytical-scale experiment per target compound was sufficient for yield predictions. Reactions under *in silico* optimized conditions gave the anticipated conversions, which could easily be transferred to the preparative scale, demonstrating the predictability and tunability of nucleoside transglycosylations based on principles of thermodynamic reaction control.

4.6 Synthesis of Selenium-Modified Pyrimidine Nucleosides

The principles of yield optimization in transglycosylation reactions were applied to the synthesis of selenium-containing pyrimidine nucleosides. These compounds are valuable tools for structure and function studies of nucleic acids and have been employed for the crystallographic characterization of ribozymes¹⁸⁸ and riboswitches,¹⁸⁹ among others.^{190,191} Previous syntheses of 2-Se-pyrimidine nucleosides via selenation of isocytidine^{192,193} or methylated sulfo-nucleosides^{194–197} require long routes of 7 steps or more and considerable purification effort, as discussed in chapter 4.1 (**paper I**).⁷⁰ Therefore, it was envisioned that a biocatalytic approach via glycosylation of a selenium-containing nucleobase, which can be accessed in 1 step from selenourea,¹⁹⁸ would provide a concise and straightforward route to these selenium-containing nucleosides. There was literature precedence that such a transformation would, in principle, be feasible since the substrate scope of some thermostable pyrimidine nucleoside phosphorylases enabled conversion of the respective 2-Se-nucleobases.¹⁴⁹ However, several challenges needed to be addressed to transition from the previously reported conditions to a synthetically useful procedure, including low conversions, low substrate solubility and oxidative loss of the substrate and product in aqueous solution. This prompted the sixth research hypothesis:

H6 Equilibrium thermodynamics can be employed to rationally improve the yields of hard-to-access nucleosides such as selenium-modified pyrimidines in transglycosylation reactions.

This hypothesis was examined with a series of analytical-scale experiments under conditions which improved the solubility and stability of 2-Se-pyrimidines and enabled the biocatalytic preparation of these synthetically challenging nucleosides.

Paper VI presents a biocatalytic synthesis of 2-Se-pyrimidine nucleosides via transglycosylation from natural uridine (**5b**) or thymidine (**4a**, Figure 7, top). To improve the low solubility of the starting materials, the reaction pH was adjusted to 9, which facilitated dissolution of the deprotonated 2-Se-nucleobase (Figure 7, center). The instability and oxidative deselenation of these nucleobases in aqueous solution¹⁹⁹ was addressed by the addition of dithioerythritol (DTT) and nitrogen-sparging of reaction mixtures, which promoted the stability of the starting materials for more than 24 h even at high temperatures (Figure 7, center). While DTT slightly reduced the activity of the applied pyrimidine nucleoside phosphorylase, all other modifications to the reaction conditions were tolerated without loss of enzymatic activity. With these conditions in hand, analytical-scale transglycosylation reactions were performed, which revealed remarkably high equilibrium constants of phosphorolysis of the target nucleosides ($K = 5$ to 10 , $\Delta_R G = -4$ to -5 kJ·mol⁻¹). These unfavorable thermodynamic properties indicated that high yields in transglycosylation reactions were beyond reach, since unreasonably high sugar donor excesses of 20 equiv. (or higher) would need to be applied to achieve even 60% conversion to the target nucleoside (Figure 7, bottom). Therefore, a tradeoff between yield and sugar donor excess was met by applying 10 equiv. of sugar donor. Small-scale reactions under optimized conditions yielded the anticipated conversions, which could easily be transferred to the semi-preparative scale, where identical results were achieved. However, purification of the desired products from the reaction mixtures presented a considerable bottleneck due to the presence of large quantities of unreacted sugar donor (which was required for the equilibrium shift). The 2-Se-nucleosides either i) did not retain on preparative HPLC columns or ii) the purified fractions persistently contained unreacted sugar donor,

which necessitated a rather laborious two-step purification process. Although the combination of a silica column chromatography step on normal phase followed by preparative HPLC on a reverse phase finally yielded pure products, it was not without considerable expense of solvent and loss of product. Nonetheless, the isolated yields of 6–40% achieved via this approach using only one reaction step^v compared favorably to most established routes where total yields of < 10% are typically achieved over 7 steps or more. Consequently, **paper VI** demonstrates that even synthetically challenging and sensitive nucleosides such as selenium-modified pyrimidine nucleoside can be accessed via transglycosylations catalyzed by nucleoside phosphorylases. However, it also serves as an example that the thermodynamic properties of the target nucleoside (with respect to phosphorolysis) can severely limit the possible maximum yields in these reactions. It also became evident that while high sugar donor excesses do promote higher conversions to the target nucleoside, this can complicate work-up and purification procedures immensely. Ultimately, the unfavorable thermodynamics displayed by selenium-modified nucleosides call for the development of methodologies that bypass the equilibrium constraints which limited the yields in this proof-of-concept study.

Paper VI additionally presents an in-depth discussion of the solubility and instability challenges encountered with the starting materials and provides further rationale and analytical evidence supporting the choice of reaction conditions.

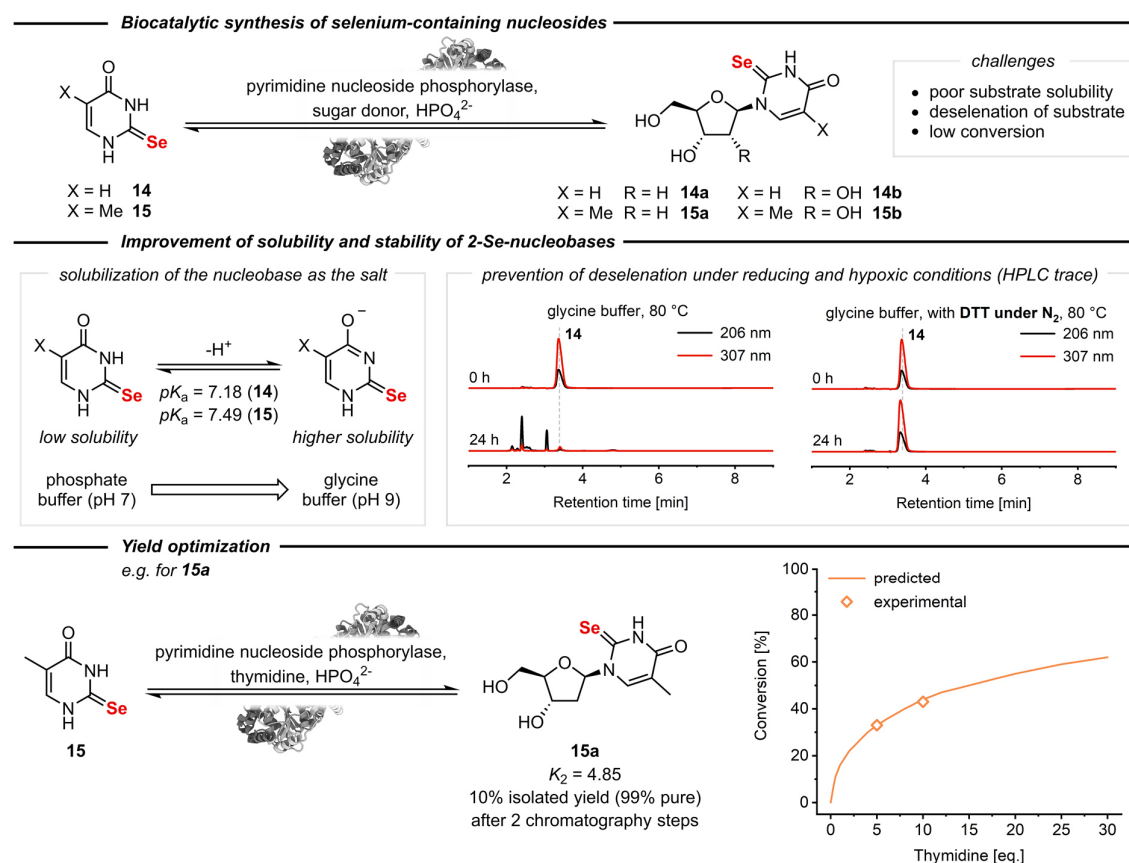


Figure 7. Optimization of the biocatalytic synthesis of 2-Se-pyrimidine nucleosides. Adapted in part from ²⁰⁰.

^v Two steps, if one counts the preparation of the selenium-containing nucleobase via condensation of selenourea and ethyl formylacetate (for **14**) or ethyl acetoacetate (for **15**).¹⁹⁸

4.7 A Hyperthermostable Enzyme for Reactions Under Harsh Conditions

Since the thermodynamic characterization of nucleoside phosphorolysis¹⁸³ and transglycosylation¹⁸⁷ reactions enabled yield robust prediction and optimization, the second bottleneck for efficient biocatalytic nucleoside synthesis was addressed next: substrate solubility.⁷⁰ Many nucleobases are poorly soluble in aqueous solution with typical substrate concentrations in transglycosylation reactions ranging from 1 to 10 mM.^{40,41,124} However, for preparative-scale and industrial applications, much higher substrate concentrations of more than 200 mM are generally sought after.^{71,153,154,201} This necessitates the application of harsh reaction conditions in the form of base, heat and cosolvent to facilitate the solubility of nucleobases. Consequently, thermostable nucleoside phosphorylases have received increased attention since these enzymes are known to be robust and retain activity even under harsh conditions.¹⁴⁴ In this context, the pyrimidine nucleoside phosphorylase from *Thermus thermophilus* (*TtPyNP*) appeared particularly attractive because it has been reported to be active at up to 100 °C and tolerate cosolvents such as DMSO and DMF.^{127,150} Therefore, it presented an ideal candidate to probe the seventh research hypothesis:

H7 Thermostable nucleoside phosphorylases enable reactions under harsh conditions facilitating increased substrate loading.

This hypothesis was interrogated through kinetic experiments with *TtPyNP* to probe the limits of its tolerance to harsh reaction conditions.

Paper VII presents investigations on the activity as well as the thermal and cosolvent stability of *TtPyNP*. In accordance with literature reports, *TtPyNP* was active at up to 100 °C with the rate constant following Eyring relationships (Figure 8).²⁰² Combined with the enzyme tolerating a remarkably broad pH range and cosolvents (DMSO or ethylene glycol) at up to 60–80% (v/v), this suggested that the performance of *TtPyNP* would primarily be limited by its stability, rather than activity under the applied conditions. Indeed, *TtPyNP* displayed a rather low half-life of only around 2 min at 100 °C but proved much more stable at slightly lower temperatures, which enabled more than 10⁶ predicted total turnovers with the model substrate **5b**. Remarkably, the enzyme was even quite stable and active at high cosolvent concentrations such as 40% DMSO or 60% ethylene glycol (v/v) at 80 °C (Figure 8, center). Together with the substrate scope of *TtPyNP* including a range of substituted uridine analogs, these results indicated that this enzyme would indeed be useful as a catalyst for transglycosylation reactions under harsh conditions, which would then enable higher substrate loadings. However, attempts to determine the Michaelis-Menten constant K_M of *TtPyNP* for a model substrate under conditions far from those reported in the literature revealed an atypical inhibition behavior. While substrate inhibition is well known in uridine phosphorylases (which belong to the purine nucleoside phosphorylases from a structural perspective),^{92,203} inhibition of pyrimidine nucleoside phosphorylases had not yet been described. Although the kinetics of *TtPyNP* at higher substrate concentrations first suggested a substrate inhibition by nucleosides, a series of follow-up experiments i) in the presence of either product and ii) running the reverse reaction revealed that this enzyme is in fact inhibited by nucleobases (Figure 8, bottom). Given that this inhibitory effect already occurs at substrate concentrations below 1 mM, it renders *TtPyNP*'s performance in preparative settings with higher substrate loadings rather subpar. While this inhibition probably holds no physiological relevance for the host organism since the intracellular concentrations of nucleosides and nucleobases are in the low

micromolar range (more than two orders of magnitude lower than the concentrations necessary to effect significant inhibition),²⁰⁴ it does discourage the use of *Tt*PyNP in preparative applications. Ultimately, these characteristics make *Tt*PyNP an oddity among pyrimidine nucleoside phosphorylases, displaying unparalleled stability and a rare case of product^{VI} inhibition.

Paper VII additionally presents kinetic and stability data exploring the cosolvent space of the enzyme and in-depth discussions of the inhibitory effects observed.

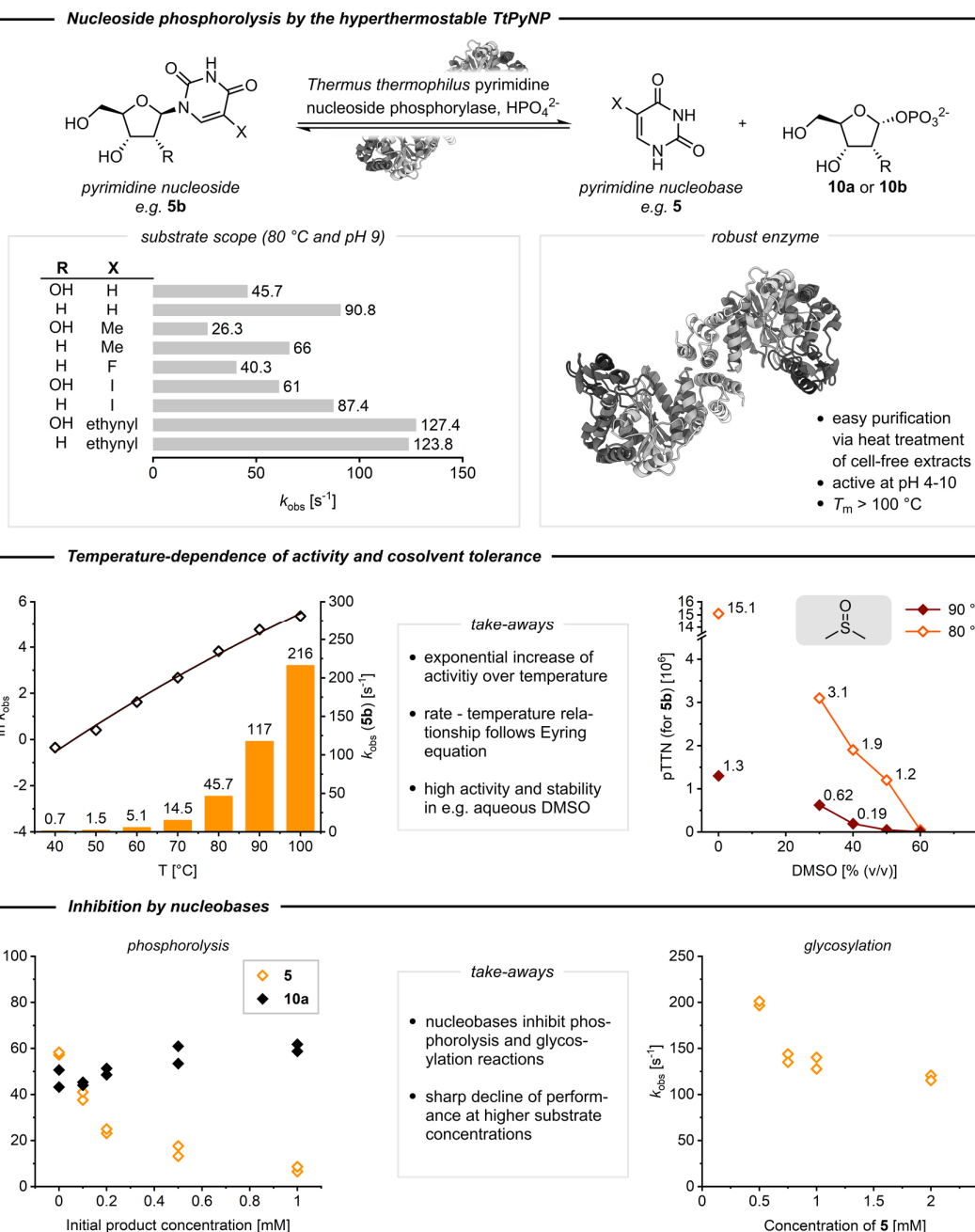


Figure 8. The peculiar case of the hyperthermostable pyrimidine nucleoside phosphorylase from *Thermus thermophilu* (PDB 2dsj). Adapted in part from ²⁰⁵.

^{VI} Or substrate inhibition, depending on the direction in which the reversible reaction is run.

5 Conclusion and Outlook

The synthesis of nucleosides directly from their corresponding nucleobases is a long-standing challenge in synthetic organic chemistry. Although a range of glycosylation methods has been developed to this end, these currently come with significant drawbacks rendering them inefficient and laborious. Biocatalytic approaches via nucleoside phosphorylases promise perfect selectivity and function under harmless aqueous conditions but have previously suffered from a limited understanding of i) the equilibrium thermodynamics in phosphorolysis and transglycosylation reactions, ii) the stability of the reactants involved and iii) thermostable enzymes enabling the application of conditions permitting higher substrate solubility.

This thesis presents analytical methods and thermodynamic frameworks for efficient nucleoside synthesis via nucleoside phosphorylases. Encouraged by a route efficiency assessment which revealed the bottlenecks plaguing traditional as well as biocatalytic nucleoside synthesis (**paper I**),⁷⁰ a systematic characterization of the equilibrium thermodynamics of nucleoside phosphorolysis reactions was pursued. Therefore, a high-throughput method for reaction monitoring via deconvolution of UV absorption spectra was developed (**paper II**)¹⁷⁷ and applied to the characterization of the phosphorolysis equilibria of a range of natural and modified nucleosides (**paper III**).¹⁸³ Building on this thermodynamic foundation, a UV-based method for the kinetic analysis of the hydrolytic decay of UV-inactive pentose-1-phosphates was realized (**paper IV**).¹⁸⁶ The transfer of these thermodynamic groundworks to nucleoside transglycosylation reactions then yielded a set of general principles for the yield prediction in these reactions as well as means for their straightforward optimization (**paper V**).¹⁸⁷ Subsequently, these insights enabled the preparation of sensitive and synthetically challenging selenium-containing pyrimidine nucleosides in a biocatalytic one-step process (**paper VI**).²⁰⁰ Lastly, a hyperthermostable pyrimidine nucleoside phosphorylase was characterized with the aim of enabling its application in preparative settings reaching beyond the low substrate loadings currently troubling nucleoside transglycosylations (**paper VII**).²⁰⁵ The thermodynamic insights and tools presented in this thesis aid the development and optimization of biocatalytic processes for nucleoside synthesis by i) streamlining the (high-throughput) characterization of biocatalysts, ii) uncovering the equilibrium thermodynamics of previously unexplored nucleosides and iii) enabling the yield prediction in transglycosylations based on minimal experimental information. As such, several projects surrounding the synthesis of nucleosides and nucleotides already profited from the work in this thesis. These have either been published recently,⁴⁰ are under review for publication or are currently in preparation for submission in due course.

Since this work describes the thermodynamics of nucleoside phosphorolysis and transglycosylations, as well as their limitations, future work should aspire to look beyond equilibrium reactions in these systems. As **paper VI** demonstrated,²⁰⁰ unfavorable equilibrium thermodynamics can severely limit the maximum yields and make biocatalytic transglycosylations a challenging endeavor. Although some approaches have been developed to render the first phosphorolysis step irreversible,^{41,82} they shared the same primary obstacles of other nucleoside transglycosylation reactions and performed equally well (or worse) regarding their efficiency as quantified by the E-factor. Therefore, future efforts in the field should be focused on i) escaping the inherent equilibrium limitations of transglycosylation

reactions, ii) improving the solubility of nucleobase substrates (or enable higher net substrate loadings otherwise) and iii) expanding the biocatalytic repertoire for modified nucleosides by engineering enzymes capable of accepting challenging substrates such as nucleosides with fluorinated or arabinosyl sugar moieties. Ultimately, biocatalytic nucleoside synthesis already holds great potential to augment existing chemical routes to a range of nucleoside targets. With future work addressing the remaining bottlenecks and challenges, enzymatic nucleoside synthesis will undoubtedly become a standard method for the concise and efficient synthesis of nucleosides directly from their nucleobases.

6 References

- (1) Brand, A.; Allen, L.; Altman, M.; Hlava, M.; Scott, J. Beyond Authorship: Attribution, Contribution, Collaboration, and Credit. *Learn. Publ.* **2015**, *28* (2), 151–155. <https://doi.org/doi:10.1087/20150211>.
- (2) Kossel, A.; Steudel, H. Weitere Untersuchungen Über Das Cytosin. *Biol. Chem.* **1903**, *38* (1–2), 49–59. <https://doi.org/10.1515/bchm2.1903.38.1-2.49>.
- (3) Kossel, A. Ueber Eine Neue Base Aus Dem Thierkörper. *Berichte der Dtsch. Chem. Gesellschaft* **1885**, *18* (1), 79–81. <https://doi.org/10.1002/cber.18850180119>.
- (4) Kossel, A.; Neumann, A. Ueber Das Thymin, Ein Spaltungsproduct Der Nucleinsäure. *Berichte der Dtsch. Chem. Gesellschaft* **1893**, *26* (3), 2753–2756. <https://doi.org/10.1002/cber.18930260379>.
- (5) Kossel, A. Zur Chemie Des Zellkern. *Zeitschrift für Physiol. Chemie* **1882**, No. 7, 7. <https://doi.org/10.1515/bchm1.1883.7.1.7>.
- (6) Behrend, R. Versuche Zur Synthese von Körpern Der Harnsäurereihe. *Justus Liebigs Ann. Chem.* **1885**, *229* (1-2), 1–44. <https://doi.org/10.1002/jlac.18852290102>.
- (7) Wöhler, F.; Liebig, J. Untersuchungen Über Die Natur Der Harnsäure. *Ann. der Pharm.* **1838**, *26* (3), 241–336. <https://doi.org/10.1002/jlac.18380260302>.
- (8) Seley-Radtke, K. L.; Yates, M. K. The Evolution of Nucleoside Analogue Antivirals: A Review for Chemists and Non-Chemists. Part 1: Early Structural Modifications to the Nucleoside Scaffold. *Antiviral Res.* **2018**, *154*, 66–86. <https://doi.org/10.1016/j.antiviral.2018.04.004>.
- (9) Jordheim, L. P.; Durantel, D.; Zoulim, F.; Dumontet, C. Advances in the Development of Nucleoside and Nucleotide Analogues for Cancer and Viral Diseases. *Nat. Rev. Drug Discov.* **2013**, *12*, 447–464. <https://doi.org/10.1038/nrd4010>.
- (10) Shelton, J.; Lu, X.; Hollenbaugh, J. A.; Cho, J. H.; Amblard, F.; Schinazi, R. F. Metabolism, Biochemical Actions, and Chemical Synthesis of Anticancer Nucleosides, Nucleotides, and Base Analogs. *Chem. Rev.* **2016**, *116* (23), 14379–14455. <https://doi.org/10.1021/acs.chemrev.6b00209>.
- (11) Clercq, E. De. The History of Antiretrovirals: Key Discoveries over the Past 25 Years. *Rev. Med. Virol.* **2009**, *19* (5), 287–299. <https://doi.org/10.1002/rmv.624>.
- (12) Damaraju, V. L.; Damaraju, S.; Young, J. D.; Baldwin, S. A.; Mackey, J.; Sawyer, M. B.; Cass, C. E. Nucleoside Anticancer Drugs: The Role of Nucleoside Transporters in Resistance to Cancer Chemotherapy. *Oncogene* **2003**, *22* (47), 7524–7536. <https://doi.org/10.1038/sj.onc.1206952>.
- (13) Ghanem, H.; Jabbour, E.; Faderl, S.; Ghandhi, V.; Plunkett, W.; Kantarjian, H. Clofarabine in Leukemia. *Expert Rev. Hematol.* **2010**, *3* (1), 15–22. <https://doi.org/10.1586/ehm.09.70>.
- (14) Genini, D.; Adachi, S.; Chao, Q.; Rose, D. W.; Carrera, C. J.; Cottam, H. B.; Carson, D. A.; Leoni, L. M. Deoxyadenosine Analogs Induce Programmed Cell Death in Chronic Lymphocytic Leukemia Cells by Damaging the DNA and by Directly Affecting the Mitochondria. *Blood* **2000**, *96* (10), 3537–3543. <https://doi.org/10.1182/blood.V96.10.3537>.
- (15) Braasch, D. A.; Corey, D. R. Locked Nucleic Acid (LNA): Fine-Tuning the Recognition of DNA and RNA. *Chem. Biol.* **2001**, *8* (1), 1–7. [https://doi.org/10.1016/S1074-5521\(00\)00058-2](https://doi.org/10.1016/S1074-5521(00)00058-2).

- (16) Thayer, M. B.; Lade, J. M.; Doherty, D.; Xie, F.; Basiri, B.; Barnaby, O. S.; Bala, N. S.; Rock, B. M. Application of Locked Nucleic Acid Oligonucleotides for siRNA Preclinical Bioanalytics. *Sci. Rep.* **2019**, *9* (1), 3566. <https://doi.org/10.1038/s41598-019-40187-4>.
- (17) Guo, F.; Li, Q.; Zhou, C. Synthesis and Biological Applications of Fluoro-Modified Nucleic Acids. *Org. Biomol. Chem.* **2017**, *15* (45), 9552–9565. <https://doi.org/10.1039/C7OB02094E>.
- (18) Xu, W.; Chan, K. M.; Kool, E. T. Fluorescent Nucleobases as Tools for Studying DNA and RNA. *Nat. Chem.* **2017**, *9* (11), 1043–1055. <https://doi.org/10.1038/nchem.2859>.
- (19) Dvořáčková, M.; Fajkus, J. Visualization of the Nucleolus Using Ethynyl Uridine. *Front. Plant Sci.* **2018**, *9*. <https://doi.org/10.3389/fpls.2018.00177>.
- (20) Jao, C. Y.; Salic, A. Exploring RNA Transcription and Turnover in Vivo by Using Click Chemistry. *Proc. Natl. Acad. Sci.* **2008**, *105* (41), 15779–15784. <https://doi.org/10.1073/pnas.0808480105>.
- (21) Vorbrüggen, H.; Ruh-Pohlenz, C. Synthesis Of Nucleosides. *Org. React.* **2004**, 1–630. <https://doi.org/10.1002/0471264180.or055.01>.
- (22) Hesse, R. H.; Barton, D. H. R.; Toh, H. T.; Pechet, M. M. Convenient Synthesis of 5-Fluorouracil. *J. Org. Chem.* **1972**, *37* (2), 329–330. <https://doi.org/10.1021/jo00967a037>.
- (23) Kagan, J.; Melnick, B. The Synthesis and Photochemistry of 4-Amino-3-Cyanopyrazole. *J. Heterocycl. Chem.* **1979**, *16* (6), 1113–1115. <https://doi.org/10.1002/jhet.5570160607>.
- (24) Andersen, K. E.; Pedersen, E. B. Synthesis of New 2-Azaadenines and 2-Azahypoxanthines from 4-Diazo-4H-Imidazoles. *Liebigs Ann. der Chemie* **1986**, *1986* (6), 1012–1020. <https://doi.org/10.1002/jlac.198619860606>.
- (25) Richter, E.; Loeffler, J. E.; Taylor, E. C. Studies in Purine Chemistry. VIII. A Convenient Synthesis of Hypoxanthines and Adenines. *J. Am. Chem. Soc.* **1960**, *82* (12), 3144–3146. <https://doi.org/10.1021/ja01497a041>.
- (26) Ferris, J. P.; Kuder, J. E.; Catalano, A. W. Photochemical Reactions and the Chemical Evolution of Purines and Nicotinamide Derivatives. *Science (80-.)*. **1969**, *166* (3906), 765–766. <https://doi.org/10.1126/science.166.3906.765>.
- (27) ORÓ, J.; KAMAT, S. S. Amino-Acid Synthesis from Hydrogen Cyanide under Possible Primitive Earth Conditions. *Nature* **1961**, *190* (4774), 442–443. <https://doi.org/10.1038/190442a0>.
- (28) Hong, C. M.; Xu, Y.; Chung, J. Y. L.; Schultz, D. M.; Weisel, M.; Varsolona, R. J.; Zhong, Y.-L.; Purohit, A. K.; He, C. Q.; Gauthier, D. R.; Humphrey, G. R.; Maloney, K. M.; Lévesque, F.; Wang, Z.; Whittaker, A. M.; Sirota, E.; McMullen, J. P. Development of a Commercial Manufacturing Route to 2-Fluoroadenine, The Key Unnatural Nucleobase of Islatravir. *Org. Process Res. Dev.* **2020**. <https://doi.org/10.1021/acs.oprd.0c00304>.
- (29) Harrison, S. A.; Lane, N. Life as a Guide to Prebiotic Nucleotide Synthesis. *Nat. Commun.* **2018**, *9* (1), 5176. <https://doi.org/10.1038/s41467-018-07220-y>.
- (30) Xu, J.; Chmela, V.; Green, N. J.; Russell, D. A.; Janicki, M. J.; Góra, R. W.; Szabla, R.; Bond, A. D.; Sutherland, J. D. Selective Prebiotic Formation of RNA Pyrimidine and DNA Purine Nucleosides. *Nature* **2020**, *582* (7810), 60–66. <https://doi.org/10.1038/s41586-020-2330-9>.
- (31) Stairs, S.; Nikmal, A.; Bučar, D.-K.; Zheng, S.-L.; Szostak, J. W.; Powner, M. W. Divergent Prebiotic Synthesis of Pyrimidine and 8-Oxo-Purine Ribonucleotides. *Nat. Commun.* **2017**, *8*

- (1), 15270. <https://doi.org/10.1038/ncomms15270>.
- (32) Oba, Y.; Takano, Y.; Naraoka, H.; Watanabe, N.; Kouchi, A. Nucleobase Synthesis in Interstellar Ices. *Nat. Commun.* **2019**, *10* (1), 4413. <https://doi.org/10.1038/s41467-019-12404-1>.
- (33) Cafferty, B. J.; Fialho, D. M.; Khanam, J.; Krishnamurthy, R.; Hud, N. V. Spontaneous Formation and Base Pairing of Plausible Prebiotic Nucleotides in Water. *Nat. Commun.* **2016**, *7* (1), 11328. <https://doi.org/10.1038/ncomms11328>.
- (34) Roberts, S. J.; Szabla, R.; Todd, Z. R.; Stairs, S.; Bučar, D.-K.; Šponer, J.; Sasselov, D. D.; Powner, M. W. Selective Prebiotic Conversion of Pyrimidine and Purine Anhydronucleosides into Watson-Crick Base-Pairing Arabino-Furanosyl Nucleosides in Water. *Nat. Commun.* **2018**, *9* (1), 4073. <https://doi.org/10.1038/s41467-018-06374-z>.
- (35) Whitaker, D.; Powner, M. W. Prebiotic Nucleic Acids Need Space to Grow. *Nat. Commun.* **2018**, *9* (1), 5172. <https://doi.org/10.1038/s41467-018-07221-x>.
- (36) Fialho, D. M.; Roche, T. P.; Hud, N. V. Prebiotic Syntheses of Noncanonical Nucleosides and Nucleotides. *Chem. Rev.* **2020**, *120* (11), 4806–4830. <https://doi.org/10.1021/acs.chemrev.0c00069>.
- (37) Zhang, Q.; Sun, J.; Zhu, Y.; Zhang, F.; Yu, B. An Efficient Approach to the Synthesis of Nucleosides: Gold(I)-Catalyzed N-Glycosylation of Pyrimidines and Purines with Glycosyl Ortho-Alkynyl Benzoates. *Angew. Chemie Int. Ed.* **2011**, *50* (21), 4933–4936. <https://doi.org/10.1002/anie.201100514>.
- (38) Li, P.; He, H.; Zhang, Y.; Yang, R.; Xu, L.; Chen, Z.; Huang, Y.; Bao, L.; Xiao, G. Glycosyl Ortho-(1-Phenylvinyl)Benzoates Versatile Glycosyl Donors for Highly Efficient Synthesis of Both O-Glycosides and Nucleosides. *Nat. Commun.* **2020**, *11* (1), 405–414. <https://doi.org/10.1038/s41467-020-14295-z>.
- (39) Hu, Z.; Tang, Y.; Yu, B. Glycosylation with 3,5-Dimethyl-4-(2'-Phenylethynylphenyl)Phenyl (EPP) Glycosides via a Dearomative Activation Mechanism. *J. Am. Chem. Soc.* **2019**, *141* (12), 4806–4810. <https://doi.org/10.1021/jacs.9b00210>.
- (40) Yehia, H.; Westarp, S.; Röhrs, V.; Kaspar, F.; Giessmann, T. R.; Klare, F. T. H.; Paulick, K.; Neubauer, P.; Kurreck, J.; Wagner, A. Efficient Biocatalytic Synthesis of Dihalogenated Purine Nucleoside Analogues Applying Thermodynamic Calculations. *Molecules* **2020**, *25* (4), 934. <https://doi.org/10.3390/molecules25040934>.
- (41) Alexeev, C. S.; Drenichev, M. S.; Dorinova, E. O.; Esipov, R. S.; Kulikova, I. V.; Mikhailov, S. N. Use of Nucleoside Phosphorylases for the Preparation of 5-Modified Pyrimidine Ribonucleosides. *Biochim. Biophys. Acta - Proteins Proteomics* **2020**, *1868* (1), 140292. <https://doi.org/10.1016/j.bbapap.2019.140292>.
- (42) Köllmann, C.; Sake, S. M.; Jones, P. G.; Pietschmann, T.; Werz, D. B. Protecting-Group-Mediated Diastereoselective Synthesis of C4'-Methylated Uridine Analogs and Their Activity against the Human Respiratory Syncytial Virus. *J. Org. Chem.* **2020**, *85* (6), 4267–4278. <https://doi.org/10.1021/acs.joc.9b03425>.
- (43) Eyer, L.; Nencka, R.; Huvarová, I.; Palus, M.; Joao Alves, M.; Gould, E. A.; De Clercq, E.; Růžek, D. Nucleoside Inhibitors of Zika Virus. *J. Infect. Dis.* **2016**, *214* (5), 707–711. <https://doi.org/10.1093/infdis/jiw226>.
- (44) Wang, G.; Dyatkina, N.; Prhavic, M.; Williams, C.; Serebryany, V.; Hu, Y.; Huang, Y.; Wan, J.;

- Wu, X.; Deval, J.; Fung, A.; Jin, Z.; Tan, H.; Shaw, K.; Kang, H.; Zhang, Q.; Tam, Y.; Stoycheva, A.; Jekle, A.; Smith, D. B.; Beigelman, L. Synthesis and Anti-HCV Activities of 4'-Fluoro-2'-Substituted Uridine Triphosphates and Nucleotide Prodrugs: Discovery of 4'-Fluoro-2'-C-Methyluridine 5'-Phosphoramidate Prodrug (AL-335) for the Treatment of Hepatitis C Infection. *J. Med. Chem.* **2019**, *62* (9), 4555–4570. <https://doi.org/10.1021/acs.jmedchem.9b00143>.
- (45) Youssefyeh, R. D.; Verheyden, J. P. H.; Moffatt, J. G. 4'-Substituted Nucleosides. 4. Synthesis of Some 4'-Hydroxymethyl Nucleosides. *J. Org. Chem.* **1979**, *44* (8), 1301–1309. <https://doi.org/10.1021/jo01322a024>.
- (46) Meanwell, M.; Silverman, S. M.; Lehmann, J.; Adluri, B.; Wang, Y.; Cohen, R.; Campeau, L.-C.; Britton, R. A Short de Novo Synthesis of Nucleoside Analogs. *Science (80-.)*. **2020**, *369* (6504), 725–730. <https://doi.org/10.1126/science.abb3231>.
- (47) Mukaiyama, T.; Shiina, I.; Kobayashi, S. A Convenient and Versatile Route for the Stereoselective Synthesis of Monosaccharides via Key Chiral Synthons Prepared from Achiral Sources. *Chem. Lett.* **1990**, *19* (12), 2201–2204. <https://doi.org/10.1246/cl.1990.2201>.
- (48) Wang, G.; Deval, J.; Hong, J.; Dyatkina, N.; Prhavc, M.; Taylor, J.; Fung, A.; Jin, Z.; Stevens, S. K.; Serebryany, V.; Liu, J.; Zhang, Q.; Tam, Y.; Chanda, S. M.; Smith, D. B.; Symons, J. A.; Blatt, L. M.; Beigelman, L. Discovery of 4'-Chloromethyl-2'-Deoxy-3',5'-Di-O-Isobutyryl-2'-Fluorocytidine (ALS-8176), A First-in-Class RSV Polymerase Inhibitor for Treatment of Human Respiratory Syncytial Virus Infection. *J. Med. Chem.* **2015**, *58* (4), 1862–1878. <https://doi.org/10.1021/jm5017279>.
- (49) Moreau, C.; Kirchberger, T.; Swarbrick, J. M.; Bartlett, S. J.; Fliegert, R.; Yorgan, T.; Bauche, A.; Harneit, A.; Guse, A. H.; Potter, B. V. L. Structure–Activity Relationship of Adenosine 5'-Diphosphoribose at the Transient Receptor Potential Melastatin 2 (TRPM2) Channel: Rational Design of Antagonists. *J. Med. Chem.* **2013**, *56* (24), 10079–10102. <https://doi.org/10.1021/jm401497a>.
- (50) Hocková, D.; Hocek, M.; Dvořáková, H.; Votruba, I. Synthesis and Cytostatic Activity of Nucleosides and Acyclic Nucleoside Analogues Derived from 6-(Trifluoromethyl)Purines. *Tetrahedron* **1999**, *55* (36), 11109–11118. [https://doi.org/10.1016/S0040-4020\(99\)00615-8](https://doi.org/10.1016/S0040-4020(99)00615-8).
- (51) Ackermann, D.; Famulok, M. Pseudo-Complementary PNA Actuators as Reversible Switches in Dynamic DNA Nanotechnology. *Nucleic Acids Res.* **2013**, *41* (8), 4729–4739. <https://doi.org/10.1093/nar/gkt121>.
- (52) Freskos, J. N. Synthesis of 2'-Deoxypyrimidine Nucleosides via Copper (I) Iodide Catalysis. *Nucleosides and Nucleotides* **1989**, *8* (4), 549–555. <https://doi.org/10.1080/07328318908054197>.
- (53) Kazimierczuk, Z.; Cottam, H. B.; Revankar, G. R.; Robins, R. K. Synthesis of 2'-Deoxytubercidin, 2'-Deoxyadenosine, and Related 2'-Deoxynucleosides via a Novel Direct Stereospecific Sodium Salt Glycosylation Procedure. *J. Am. Chem. Soc.* **1984**, *106* (21), 6379–6382. <https://doi.org/10.1021/ja00333a046>.
- (54) Fraser-Reid, B.; Ganney, P.; Ramamurty, C. V. S.; Gómez, A. M.; López, J. C. A Reverse Strategy for Synthesis of Nucleosides Based on N-Pentenyl Orthoester Donors. *Chem. Commun.* **2013**, *49* (31), 3251–3253. <https://doi.org/10.1039/C3CC41036F>.
- (55) Rao, B. V.; Manmode, S.; Hotha, S. Propargyl 1,2-Orthoesters for a Catalytic and Stereoselective Synthesis of Pyrimidine Nucleosides. *J. Org. Chem.* **2015**, *80* (3), 1499–1505.

- <https://doi.org/10.1021/jo502413z>.
- (56) Liao, J.; Sun, J.; Yu, B. Effective Synthesis of Nucleosides with Glycosyl Trifluoroacetimidates as Donors. *Tetrahedron Lett.* **2008**, *49* (34), 5036–5038. <https://doi.org/10.1016/j.tetlet.2008.06.042>.
- (57) Liao, J.; Sun, J.; Yu, B. An Improved Procedure for Nucleoside Synthesis Using Glycosyl Trifluoroacetimidates as Donors. *Carbohydr. Res.* **2009**, *344* (8), 1034–1038. <https://doi.org/10.1016/j.carres.2009.03.010>.
- (58) Liu, G.; Zhang, X.; Xing, G. A General Method for N-Glycosylation of Nucleobases Promoted by (p-Tol)2SO/Tf2O with Thioglycoside as Donor. *Chem. Commun.* **2015**, *51* (64), 12803–12806. <https://doi.org/10.1039/C5CC03617H>.
- (59) Downey, A. M.; Pohl, R.; Roithová, J.; Hocek, M. Synthesis of Nucleosides through Direct Glycosylation of Nucleobases with 5-O-Monoprotected or 5-Modified Ribose: Improved Protocol, Scope, and Mechanism. *Chem. Eur. J.* **2017**, *23* (16), 3910–3917. <https://doi.org/10.1002/chem.201604955>.
- (60) Downey, A. M.; Richter, C.; Pohl, R.; Mahrwald, R.; Hocek, M. Direct One-Pot Synthesis of Nucleosides from Unprotected or 5-O-Monoprotected d-Ribose. *Org. Lett.* **2015**, *17* (18), 4604–4607. <https://doi.org/10.1021/acs.orglett.5b02332>.
- (61) Chow, K.; Danishefsky, S. Stereospecific Vorbrueggen-like Reactions of 1,2-Anhydro Sugars. An Alternative Route to the Synthesis of Nucleosides. *J. Org. Chem.* **1990**, *55* (13), 4211–4214. <https://doi.org/10.1021/jo00300a049>.
- (62) Ramamurty, C. V. S.; Ganney, P.; Rao, C. S.; Fraser-Reid, B. Ready Preparation of Furanosyl N-Pentenyl Orthoesters from Corresponding Methyl Furanosides. *J. Org. Chem.* **2011**, *76* (7), 2245–2247. <https://doi.org/10.1021/jo1021376>.
- (63) Azuma, T.; Isono, K. Transnucleosidation : An Improved Method for Transglycosylation from Pyrimidines to Purines. *Chem. Pharm. Bull. (Tokyo)*. **1977**, *25* (12), 3347–3353. <https://doi.org/10.1248/cpb.25.3347>.
- (64) Miyaki, M.; Saito, A.; Shimizu, B. N→N Alkyl and Glycosyl Migrations of Purines and Pyrimidines. IV. Trans-Glycosylation from Pyrimidines to Purines. (A Novel Synthetic Method of Purine Nucleosides and Nucleotides). *Chem. Pharm. Bull. (Tokyo)*. **1970**, *18* (12), 2459–2468. <https://doi.org/10.1248/cpb.18.2459>.
- (65) Boryski, J. A Novel Approach to Synthesis of 2'-Deoxy-β-D-Ribonucleosides Via Transglycosylation of 6-Oxopurine Ribonucleosides. *Nucleosides and Nucleotides* **1998**, *17* (9–11), 1547–1556. <https://doi.org/10.1080/07328319808004685>.
- (66) Niedballa, U.; Vorbrüggen, H. A General Synthesis of Pyrimidine Nucleosides. *Angew. Chemie Int. Ed. English* **1970**, *9* (6), 461–462. <https://doi.org/10.1002/anie.197004612>.
- (67) Kim, H. O. Synthesis of 2-Alkyl-Substituted-N6-Methyladenine Derivatives as Potential Adenosine Receptor Ligand. *Arch. Pharm. Res.* **2001**, *24* (6), 508–513. <https://doi.org/10.1007/BF02975154>.
- (68) Parmenopoulou, V.; Chatzileontiadou, D. S. M.; Manta, S.; Bougiatioti, S.; Maragozidis, P.; Gkaragkouni, D.-N.; Kaffesaki, E.; Kantsadi, A. L.; Skamnaki, V. T.; Zographos, S. E.; Zounpoulakis, P.; Balatsos, N. A. A.; Komiotis, D.; Leonidas, D. D. Triazole Pyrimidine Nucleosides as Inhibitors of Ribonuclease A. Synthesis, Biochemical, and Structural Evaluation.

- Bioorg. Med. Chem.* **2012**, *20* (24), 7184–7193. <https://doi.org/10.1016/j.bmc.2012.09.067>.
- (69) Shirouzu, H.; Morita, H.; Tsukamoto, M. Synthesis of Modified Pyrimidine Nucleosides via Vorbrüggen-Type N-Glycosylation Catalyzed by 2-Methyl-5-Phenylbenzoxazolium Perchlorate. *Tetrahedron* **2014**, *70* (22), 3635–3639. <https://doi.org/10.1016/j.tet.2014.03.013>.
- (70) Kaspar, F.; Stone, M. R. L.; Neubauer, P.; Kurreck, A. Route Efficiency Assessment and Review of the Synthesis of β -Nucleosides via N-Glycosylation of Nucleobases. *Green Chem.* **2020**. <https://doi.org/10.1039/D0GC02665D>.
- (71) Sheldon, R. A. The E Factor 25 Years on: The Rise of Green Chemistry and Sustainability. *Green Chem.* **2017**, *19* (1), 18–43. <https://doi.org/10.1039/C6GC02157C>.
- (72) Sheldon, R. A. The E Factor: Fifteen Years On. *Green Chem.* **2007**, *9* (12), 1273–1283. <https://doi.org/10.1039/B713736M>.
- (73) Sheldon, R. A. Metrics of Green Chemistry and Sustainability: Past, Present, and Future. *ACS Sustain. Chem. Eng.* **2018**, *6* (1), 32–48. <https://doi.org/10.1021/acssuschemeng.7b03505>.
- (74) Tang, Y.; Li, J.; Zhu, Y.; Li, Y.; Yu, B. Mechanistic Insights into the Gold(I)-Catalyzed Activation of Glycosyl Ortho-Alkynylbenzoates for Glycosidation. *J. Am. Chem. Soc.* **2013**, *135* (49), 18396–18405. <https://doi.org/10.1021/ja4064316>.
- (75) Alder, C. M.; Hayler, J. D.; Henderson, R. K.; Redman, A. M.; Shukla, L.; Shuster, L. E.; Sneddon, H. F. Updating and Further Expanding GSK's Solvent Sustainability Guide. *Green Chem.* **2016**, *18* (13), 3879–3890. <https://doi.org/10.1039/C6GC00611F>.
- (76) Constable, D. J. C.; Dunn, P. J.; Hayler, J. D.; Humphrey, G. R.; Leazer Johnnie L., J.; Linderman, R. J.; Lorenz, K.; Manley, J.; Pearlman, B. A.; Wells, A.; Zaks, A.; Zhang, T. Y. Key Green Chemistry Research Areas—a Perspective from Pharmaceutical Manufacturers. *Green Chem.* **2007**, *9* (5), 411–420. <https://doi.org/10.1039/B703488C>.
- (77) Pessel, F.; Augé, J.; Billault, I.; Scherrmann, M.-C. The Weight of Flash Chromatography: A Tool to Predict Its Mass Intensity from Thin-Layer Chromatography. *Beilstein J. Org. Chem.* **2016**, *12*, 2351–2357. <https://doi.org/10.3762/bjoc.12.228>.
- (78) Bzowska, A.; Kulikowska, E.; Shugar, D. Purine Nucleoside Phosphorylases: Properties, Functions, and Clinical Aspects. *Pharmacol. Ther.* **2000**, *88* (3), 349–425. [https://doi.org/10.1016/S0163-7258\(00\)00097-8](https://doi.org/10.1016/S0163-7258(00)00097-8).
- (79) Lewkowicz, E. S.; Iribarren, A. M. Nucleoside Phosphorylases. *Curr. Org. Chem.* **2006**, *10* (11), 1197–1215. <https://doi.org/10.2174/138527206777697995>.
- (80) Tozzi, M. G.; Camici, M.; Mascia, L.; Sgarrella, F.; Ipata, P. L. Pentose Phosphates in Nucleoside Interconversion and Catabolism. *FEBS J.* **2006**, *273* (6), 1089–1101. <https://doi.org/10.1111/j.1742-4658.2006.05155.x>.
- (81) Kalckar, H. M. Enzymatic Synthesis of a Nucleoside. *J. Biol. Chem.* **1945**, *158* (3), 723–724.
- (82) Kalckar, H. M. The Enzymatic Synthesis of Purine Ribosides. *J. Biol. Chem.* **1947**, *167* (2), 477–486.
- (83) Friedkin, M.; Kalckar, H. M. Desoxyribose-1-Phosphate: I. The Phosphorolysis and Resynthesis of Purine Desoxyribose Nucleoside. *J. Biol. Chem.* **1950**, *184* (2), 437–448.
- (84) Friedkin, M.; Kalckar, H. M.; Hoff-Jorgensen, E. Enzymatic Synthesis of Desoxyribose

- Nucleoside with Desoxyribose Phosphate Ester. *J. Biol. Chem.* **1949**, *178* (1), 527.
- (85) Friedkin, M. Desoxyribose-1-Phosphate. II. The Isolation of Crystalline Desoxyribose-1-Phosphate. *J. Biol. Chem.* **1950**, *184* (2), 449–459.
- (86) Hoff-Jorgenses, E.; Friedkin, M.; Kalckar, H. M. Desoxyribose-1-Phosphate. III. Comparison of Microbiological and Spectrophotometric Estimations of Enzymatically Produced Purine Desoxyribose Nucleoside. *J. Biol. Chem.* **1950**, *184* (2), 461–464.
- (87) Heppel, L. A.; Hilme, R. J. Phosphorolysis and Hydrolysis of Purine Ribosides by Enzymes From Yeast. *J. Biol. Chem.* **1952**, *198* (2), 683–694.
- (88) Rowen, J. W.; Kornberg, A. The Phosphorolysis of Nicotinamide Riboside. *J. Biol. Chem.* **1951**, *193* (2), 497–507.
- (89) Salamone, S. J.; Jordan, F.; Jordan, R. R. ³¹P NMR Studies on Purine Nucleoside Phosphorylases: Determination of the Scissile Bond and of the Equilibrium Constant. *Arch. Biochem. Biophys.* **1982**, *217* (1), 139–143. [https://doi.org/10.1016/0003-9861\(82\)90487-8](https://doi.org/10.1016/0003-9861(82)90487-8).
- (90) Senesi, S.; Falcone, G.; Mura, U.; Sgarrella, F.; Ipata, P. L. A Specific Adenosine Phosphorylase, Distinct from Purine Nucleoside Phosphorylase. *FEBS Lett.* **1976**, *64* (2), 353–357. [https://doi.org/10.1016/0014-5793\(76\)80327-4](https://doi.org/10.1016/0014-5793(76)80327-4).
- (91) Silva, R. G.; Hirschi, J. S.; Ghanem, M.; Murkin, A. S.; Schramm, V. L. Arsenate and Phosphate as Nucleophiles at the Transition States of Human Purine Nucleoside Phosphorylase. *Biochemistry* **2011**, *50* (13), 2701–2709. <https://doi.org/10.1021/bi200279s>.
- (92) Silva, R. G.; Schramm, V. L. Uridine Phosphorylase from *Trypanosoma Cruzi*: Kinetic and Chemical Mechanisms. *Biochemistry* **2011**, *50* (42), 9158–9166. <https://doi.org/10.1021/bi2013382>.
- (93) Stoeckler, J. D.; Poirot, A. F.; Smith, R. M.; Parks Robert E.; Ealick, S. E.; Takabayashi, K.; Erion, M. D. Purine Nucleoside Phosphorylase. 3. Reversal of Purine Base Specificity by Site-Directed Mutagenesis. *Biochemistry* **1997**, *36* (39), 11749–11756. <https://doi.org/10.1021/bi961971n>.
- (94) Erion, M. D.; Stoeckler, J. D.; Guida, W. C.; Walter, R. L. Purine Nucleoside Phosphorylase. 2. Catalytic Mechanism. *Biochemistry* **1997**, *36* (39), 11735–11748. <https://doi.org/10.1021/bi961970v>.
- (95) Utagawa, T.; Morisawa, H.; Yamanaka, S.; Yamazaki, A.; Yoshinaga, F.; Hirose, Y. Properties of Nucleoside Phosphorylase from *Enterobacter Aerogenes*. *Agric. Biol. Chem.* **1985**, *49* (11), 3239–3246. <https://doi.org/10.1080/00021369.1985.10867255>.
- (96) De Verdier, C.-H.; Gould, B. J. Purine Ribonucleoside and Deoxyribonucleoside Phosphorylase in Human Erythrocytes. *Biochim. Biophys. Acta - Spec. Sect. Nucleic Acids Relat. Subj.* **1963**, *68*, 333–341. [https://doi.org/10.1016/0926-6550\(63\)90451-1](https://doi.org/10.1016/0926-6550(63)90451-1).
- (97) Vita, A.; Huang, C. Y.; Magni, G. Uridine Phosphorylase from *Escherichia Coli* B.: Kinetic Studies on the Mechanism of Catalysis. *Arch. Biochem. Biophys.* **1983**, *226* (2), 687–692. [https://doi.org/10.1016/0003-9861\(83\)90339-9](https://doi.org/10.1016/0003-9861(83)90339-9).
- (98) Porter, D. J. Purine Nucleoside Phosphorylase. Kinetic Mechanism of the Enzyme from Calf Spleen. *J. Biol. Chem.* **1992**, *267* (11), 7342–7351.
- (99) Bose, R.; Yamada, E. W. Uridine Phosphorylase, Molecular Properties, and Mechanism of Catalysis. *Biochemistry* **1974**, *13* (10), 2051–2056. <https://doi.org/10.1021/bi00707a008>.

- (100) Bzowska, A.; Kulikowska, E.; Shugar, D. Linear Free Energy Relationships for N(7)-Substituted Guanosines as Substrates of Calf Spleen Purine Nucleoside Phosphorylase. Possible Role of N(7)-Protonation as an Intermediary in Phosphorolysis. *Zeitschrift für Naturforsch. C* **1993**, *48* (9–10), 803–811. <https://doi.org/10.1515/znc-1993-9-1020>.
- (101) Jensen, K. F.; Nygaard, P. Purine Nucleoside Phosphorylase from Escherichia Coli and Salmonella Typhimurium. *Eur. J. Biochem.* **1975**, *51* (1), 253–265. <https://doi.org/10.1111/j.1432-1033.1975.tb03925.x>.
- (102) Kulikowska, E.; Bzowska, A.; Wierzchowski, J.; Shugar, D. Properties of Two Unusual, and Fluorescent, Substrates of Purine-Nucleoside Phosphorylase: 7-Methylguanosine and 7-Methylinosine. *Biochim. Biophys. Acta - Protein Struct. Mol. Enzymol.* **1986**, *874* (3), 355–363. [https://doi.org/10.1016/0167-4838\(86\)90035-X](https://doi.org/10.1016/0167-4838(86)90035-X).
- (103) Lehtikoinen, P. K.; Sinnott, M. L.; Krenitsky, T. A. Investigation of α -Deuterium Kinetic Isotope Effects on the Purine Nucleoside Phosphorylase Reaction by the Equilibrium-Perturbation Technique. *Biochem. J.* **1989**, *257* (2), 355–359. <https://doi.org/10.1042/bj2570355>.
- (104) Murakami, K.; Tsushima, K. Crystallization and Some Properties of Purine Nucleoside Phosphorylase from Chicken Liver. *Biochim. Biophys. Acta - Enzymol.* **1975**, *384* (2), 390–398. [https://doi.org/10.1016/0005-2744\(75\)90040-6](https://doi.org/10.1016/0005-2744(75)90040-6).
- (105) Bennett, E. M.; Li, C.; Allan, P. W.; Parker, W. B.; Ealick, S. E. Structural Basis for Substrate Specificity of Escherichia Coli Purine Nucleoside Phosphorylase. *J. Biol. Chem.* **2003**, *278* (47), 47110–47118. <https://doi.org/10.1074/jbc.M30462200>.
- (106) Pugmire, M. J.; Ealick, S. E. The Crystal Structure of Pyrimidine Nucleoside Phosphorylase in a Closed Conformation. *Structure* **1998**, *6* (11), 1467–1479. [https://doi.org/10.1016/S0969-2126\(98\)00145-2](https://doi.org/10.1016/S0969-2126(98)00145-2).
- (107) Grenha, R.; Levnikov, V. M.; Fogg, M. J.; Blagova, E. V.; Brannigan, J. A.; Wilkinson, A. J.; Wilson, K. S. Structure of Purine Nucleoside Phosphorylase (DeoD) from Bacillus Anthracis. *Acta Crystallogr. Sect. F* **2005**, *61* (5), 459–462. <https://doi.org/10.1107/S174430910501095X>.
- (108) Tahirov, T. H.; Inagaki, E.; Ohshima, N.; Kitao, T.; Kuroishi, C.; Ukita, Y.; Takio, K.; Kobayashi, M.; Kuramitsu, S.; Yokoyama, S.; Miyano, M. Crystal Structure of Purine Nucleoside Phosphorylase from Thermus Thermophilus. *J. Mol. Biol.* **2004**, *337* (5), 1149–1160. <https://doi.org/10.1016/j.jmb.2004.02.016>.
- (109) Mikleušević, G.; Štefanić, Z.; Narczyk, M.; Wielgus-Kutrowska, B.; Bzowska, A.; Luić, M. Validation of the Catalytic Mechanism of Escherichia Coli Purine Nucleoside Phosphorylase by Structural and Kinetic Studies. *Biochimie* **2011**, *93* (9), 1610–1622. <https://doi.org/10.1016/j.biochi.2011.05.030>.
- (110) Pugmire, M. J.; Cook, W. J.; Jasanoff, A.; Walter, M. R.; Ealick, S. E. Structural and Theoretical Studies Suggest Domain Movement Produces an Active Conformation of Thymidine Phosphorylase. Edited by I. Wilson. *J. Mol. Biol.* **1998**, *281* (2), 285–299. <https://doi.org/10.1006/jmbi.1998.1941>.
- (111) Balaev, V. V.; Lashkov, A. A.; Gabdulkhakov, A. G.; Dontsova, M. V.; Seregina, T. A.; Mironov, A. S.; Betzel, C.; Mikhailov, A. M. Structural Investigation of the Thymidine Phosphorylase from Salmonella Typhimurium in the Unliganded State and Its Complexes with Thymidine and Uridine. *Acta Crystallogr. Sect. F* **2016**, *72* (3), 224–233. <https://doi.org/10.1107/S2053230X1600162X>.

- (112) Balaev, V. V.; Prokofev, I. I.; Gabdoulkhakov, A. G.; Betzel, C.; Lashkov, A. A. Crystal Structure of Pyrimidine-Nucleoside Phosphorylase from *Bacillus Subtilis* in Complex with Imidazole and Sulfate. *Acta Crystallogr. Sect. F* **2018**, *74* (4), 193–197. <https://doi.org/10.1107/S2053230X18002935>.
- (113) Mitsiki, E.; Papageorgiou, A. C.; Iyer, S.; Thiyagarajan, N.; Prior, S. H.; Sleep, D.; Finnis, C.; Acharya, K. R. Structures of Native Human Thymidine Phosphorylase and in Complex with 5-Iodouracil. *Biochem. Biophys. Res. Commun.* **2009**, *386* (4), 666–670. <https://doi.org/10.1016/j.bbrc.2009.06.104>.
- (114) Norman, R. A.; Barry, S. T.; Bate, M.; Breed, J.; Colls, J. G.; Ernill, R. J.; Luke, R. W. A.; Minshull, C. A.; McAlister, M. S. B.; McCall, E. J.; McMiken, H. H. J.; Paterson, D. S.; Timms, D.; Tucker, J. A.; Pauptit, R. A. Crystal Structure of Human Thymidine Phosphorylase in Complex with a Small Molecule Inhibitor. *Structure* **2004**, *12* (1), 75–84. <https://doi.org/10.1016/j.str.2003.11.018>.
- (115) Caradoc-Davies, T. T.; Cutfield, S. M.; Lamont, I. L.; Cutfield, J. F. Crystal Structures of *Escherichia Coli* Uridine Phosphorylase in Two Native and Three Complexed Forms Reveal Basis of Substrate Specificity, Induced Conformational Changes and Influence of Potassium. *J. Mol. Biol.* **2004**, *337* (2), 337–354. <https://doi.org/10.1016/j.jmb.2004.01.039>.
- (116) Koellner, G.; Bzowska, A.; Wielgus-Kutrowska, B.; Luić, M.; Steiner, T.; Saenger, W.; Stępiński, J. Open and Closed Conformation of the *E. Coli* Purine Nucleoside Phosphorylase Active Center and Implications for the Catalytic Mechanism¹¹ Edited by R. Huber. *J. Mol. Biol.* **2002**, *315* (3), 351–371. <https://doi.org/10.1006/jmbi.2001.5211>.
- (117) Alexeev, C. S.; Kulikova, I. V.; Gavryushov, S.; Tararov, V. I.; Mikhailov, S. N. Quantitative Prediction of Yield in Transglycosylation Reaction Catalyzed by Nucleoside Phosphorylases. *Adv. Synth. Catal.* **2018**, *360* (16), 3090–3096. <https://doi.org/10.1002/adsc.201800411>.
- (118) Ubiali, D.; Rocchietti, S.; Scaramozzino, F.; Terreni, M.; Albertini, A. M.; Fernández-Lafuente, R.; Guisán, J. M.; Pregnolato, M. Synthesis of 2'-Deoxynucleosides by Transglycosylation with New Immobilized and Stabilized Uridine Phosphorylase and Purine Nucleoside Phosphorylase. *Adv. Synth. Catal.* **2004**, *346* (11), 1361–1366. <https://doi.org/10.1002/adsc.200404019>.
- (119) Ubiali, D.; Serra, C. D.; Serra, I.; Morelli, C. F.; Terreni, M.; Albertini, A. M.; Manitto, P.; Speranza, G. Production, Characterization and Synthetic Application of a Purine Nucleoside Phosphorylase from *Aeromonas Hydrophila*. *Adv. Synth. Catal.* **2012**, *354* (1), 96–104. <https://doi.org/10.1002/adsc.201100505>.
- (120) Calleri, E.; Cattaneo, G.; Rabuffetti, M.; Serra, I.; Bavaro, T.; Massolini, G.; Speranza, G.; Ubiali, D. Flow-Synthesis of Nucleosides Catalyzed by an Immobilized Purine Nucleoside Phosphorylase from *Aeromonas Hydrophila*: Integrated Systems of Reaction Control and Product Purification. *Adv. Synth. Catal.* **2015**, *357* (11), 2520–2528. <https://doi.org/10.1002/adsc.201500133>.
- (121) Kamel, S.; Weiß, M.; Klare, H. F. T.; Mikhailopulo, I. A.; Neubauer, P.; Wagner, A. Chemo-Enzymatic Synthesis of α -D-Pentofuranose-1-Phosphates Using Thermostable Pyrimidine Nucleoside Phosphorylases. *Mol. Catal.* **2018**, *458*, 52–59. <https://doi.org/10.1016/j.mcat.2018.07.028>.
- (122) Yehia, H.; Kamel, S.; Paulick, K.; Wagner, A.; Neubauer, P. Substrate Spectra of Nucleoside Phosphorylases and Their Potential in the Production of Pharmaceutically Active Compounds. *Curr. Pharm. Des.* **2017**, *23* (45), 6913–6935. <https://doi.org/10.2174/1381612823666171024155811>.

- (123) Kulikova, I. V.; Drenichev, M. S.; Soltyev, P. N.; Alexeev, C. S.; Mikhailov, S. N. Enzymatic Synthesis of 2-Deoxyribose 1-Phosphate and Ribose 1 Phosphate and Subsequent Preparation of Nucleosides. *European J. Org. Chem.* **2019**, 2019 (41), 6999–7004. <https://doi.org/10.1002/ejoc.201901454>.
- (124) Drenichev, M. S.; Alexeev, C. S.; Kurochkin, N. N.; Mikhailov, S. N. Use of Nucleoside Phosphorylases for the Preparation of Purine and Pyrimidine 2'-Deoxynucleosides. *Adv. Synth. Catal.* **2018**, 360 (2), 305–312. <https://doi.org/10.1002/adsc.201701005>.
- (125) Panova, N. G.; Shcheveleva, E. V.; Alexeev, C. S.; Mukhortov, V. G.; Zuev, A. N.; Mikhailov, S. N.; Esipov, R. S.; Chuvikovskiy, D. V.; Miroshnikov, A. I. Use of 4-Thiouridine and 4-Thiothymidine in Studies on Pyrimidine Nucleoside Phosphorylases. *Mol. Biol.* **2004**, 38 (5), 770–776. <https://doi.org/10.1023/B:MBIL.0000043946.44742.c8>.
- (126) Zhou, X.; Szeker, K.; Jiao, L.-Y.; Oestreich, M.; Mikhailopulo, I. A.; Neubauer, P. Synthesis of 2,6-Dihalogenated Purine Nucleosides by Thermostable Nucleoside Phosphorylases. *Adv. Synth. Catal.* **2015**, 357 (6), 1237–1244. <https://doi.org/10.1002/adsc.201400966>.
- (127) Szeker, K.; Zhou, X.; Schwab, T.; Casanueva, A.; Cowan, D.; Mikhailopulo, I. A.; Neubauer, P. Comparative Investigations on Thermostable Pyrimidine Nucleoside Phosphorylases from *Geobacillus Thermoglucosidarius* and *Thermus Thermophilus*. *J. Mol. Catal. B Enzym.* **2012**, 84, 27–34. <https://doi.org/10.1016/j.molcatb.2012.02.006>.
- (128) Zhou, X.; Szeker, K.; Janocha, B.; Böhme, T.; Albrecht, D.; Mikhailopulo, I. A.; Neubauer, P. Recombinant Purine Nucleoside Phosphorylases from Thermophiles: Preparation, Properties and Activity towards Purine and Pyrimidine Nucleosides. *FEBS J.* **2013**, 280 (6), 1475–1490. <https://doi.org/10.1111/febs.12143>.
- (129) Rabuffetti, M.; Bavaro, T.; Semproli, R.; Cattaneo, G.; Massone, M.; Morelli, F. C.; Speranza, G.; Ubiali, D. Synthesis of Ribavirin, Tecadenoson, and Cladribine by Enzymatic Transglycosylation. *Catalysts* **2019**, 9 (4), 355. <https://doi.org/10.3390/catal9040355>.
- (130) Serra, I.; Bavaro, T.; Cecchini, D. A.; Daly, S.; Albertini, A. M.; Terreni, M.; Ubiali, D. A Comparison between Immobilized Pyrimidine Nucleoside Phosphorylase from *Bacillus Subtilis* and Thymidine Phosphorylase from *Escherichia Coli* in the Synthesis of 5-Substituted Pyrimidine 2'-Deoxyribonucleosides. *J. Mol. Catal. B Enzym.* **2013**, 95, 16–22. <https://doi.org/10.1016/j.molcatb.2013.05.007>.
- (131) Kamel, S.; Yehia, H.; Neubauer, P.; Wagner, A. Enzymatic Synthesis of Nucleoside Analogues by Nucleoside Phosphorylases. In *In Enzymatic and Chemical Synthesis of Nucleic Acid Derivatives*; J., F., Ed.; 2018; pp 1–28. <https://doi.org/10.1002/9783527812103.ch1>.
- (132) Pugmire, M. J.; Ealick, S. E. Structural Analyses Reveal Two Distinct Families of Nucleoside Phosphorylases. *Biochem. J.* **2002**, 361 (Pt 1), 1–25. <https://doi.org/10.1042/0264-6021:3610001>.
- (133) Oliva, I.; Zuffi, G.; Barile, D.; Orsini, G.; Tonon, G.; Gioia, L. De; Ghisotti, D. Characterization of *Escherichia Coli* Uridine Phosphorylase by Single-Site Mutagenesis. *J. Biochem.* **2004**, 135 (4), 495–499. <https://doi.org/10.1093/jb/mvh057>.
- (134) Komissarov, A. A.; Moltchan, O. K.; Romanova, D. V.; Debabov, V. G. Enzyme-Catalyzed Uridine Phosphorolysis: SN2 Mechanism with Phosphate Activation by Desolvation. *FEBS Lett.* **1994**, 355 (2), 192–194. [https://doi.org/10.1016/0014-5793\(94\)01204-0](https://doi.org/10.1016/0014-5793(94)01204-0).
- (135) Mendieta, J.; Martín-Santamaría, S.; Priego, E.-M.; Balzarini, J.; Camarasa, M.-J.; Pérez-Pérez,

- M.-J.; Gago, F. Role of Histidine-85 in the Catalytic Mechanism of Thymidine Phosphorylase As Assessed by Targeted Molecular Dynamics Simulations and Quantum Mechanical Calculations. *Biochemistry* **2004**, *43* (2), 405–414. <https://doi.org/10.1021/bi034793o>.
- (136) Barnett, C. B.; Naidoo, K. J. PNP Diminishes Guanosine Glycosidic Bond Strength Through Restrictive Ring Pucker as a Precursor to Phosphorylation. *J. Phys. Chem. B* **2013**, *117* (20), 6019–6026. <https://doi.org/10.1021/jp3109013>.
- (137) Birck, M. R.; Schramm, V. L. Binding Causes the Remote [5'-3H]Thymidine Kinetic Isotope Effect in Human Thymidine Phosphorylase. *J. Am. Chem. Soc.* **2004**, *126* (22), 6882–6883. <https://doi.org/10.1021/ja0492642>.
- (138) Birck, M. R.; Schramm, V. L. Nucleophilic Participation in the Transition State for Human Thymidine Phosphorylase. *J. Am. Chem. Soc.* **2004**, *126* (8), 2447–2453. <https://doi.org/10.1021/ja039260h>.
- (139) Edwards, P. N. A Kinetic, Modeling and Mechanistic Re-Analysis of Thymidine Phosphorylase and Some Related Enzymes. *J. Enzyme Inhib. Med. Chem.* **2006**, *21* (5), 483–518. <https://doi.org/10.1080/14756360600721075>.
- (140) Fedorov, A.; Shi, W.; Kicska, G.; Fedorov, E.; Tyler, P. C.; Furneaux, R. H.; Hanson, J. C.; Gainsford, G. J.; Larese, J. Z.; Schramm, V. L.; Almo, S. C. Transition State Structure of Purine Nucleoside Phosphorylase and Principles of Atomic Motion in Enzymatic Catalysis. *Biochemistry* **2001**, *40* (4), 853–860. <https://doi.org/10.1021/bi002499f>.
- (141) Ghanem, M.; Li, L.; Wing, C.; Schramm, V. L. Altered Thermodynamics from Remote Mutations Altering Human toward Bovine Purine Nucleoside Phosphorylase. *Biochemistry* **2008**, *47* (8), 2559–2564. <https://doi.org/10.1021/bi702132e>.
- (142) Isaksen, G. V.; Åqvist, J.; Brandsdal, B. O. Thermodynamics of the Purine Nucleoside Phosphorylase Reaction Revealed by Computer Simulations. *Biochemistry* **2017**, *56* (1), 306–312. <https://doi.org/10.1021/acs.biochem.6b00967>.
- (143) Schwartz, P. A.; Vetticatt, M. J.; Schramm, V. L. Transition State Analysis of the Arsenolytic Depyrimidination of Thymidine by Human Thymidine Phosphorylase. *Biochemistry* **2011**, *50* (8), 1412–1420. <https://doi.org/10.1021/bi101900b>.
- (144) Kamel, S.; Thiele, I.; Neubauer, P.; Wagner, A. Thermophilic Nucleoside Phosphorylases: Their Properties, Characteristics and Applications. *Biochim. Biophys. Acta - Proteins Proteomics* **2020**, *1868* (2), 140304. <https://doi.org/10.1016/j.bbapap.2019.140304>.
- (145) Krajewska, E.; Shugar, D. Pyrimidine Ribonucleoside Phosphorylase Activity vs 5- and/or 6-Substituted Uracil and Uridine Analogues, Including Conformational Aspects. *Biochem. Pharmacol.* **1982**, *31* (6), 1097–1102. [https://doi.org/10.1016/0006-2952\(82\)90348-3](https://doi.org/10.1016/0006-2952(82)90348-3).
- (146) Fateev, I. V.; Antonov, K. V.; Konstantinova, I. D.; Muravyova, T. I.; Seela, F.; Esipov, R. S.; Miroshnikov, A. I.; Mikhailopulo, I. A. The Chemoenzymatic Synthesis of Clofarabine and Related 2'-Deoxyfluoroarabinosyl Nucleosides: The Electronic and Stereochemical Factors Determining Substrate Recognition by E. Coli Nucleoside Phosphorylases. *Beilstein J. Org. Chem.* **2014**, *10*, 1657–1669. <https://doi.org/10.3762/bjoc.10.173>.
- (147) Winkler, M.; Domarkas, J.; Schweiger, L. F.; O'Hagan, D. Fluorinase-Coupled Base Swaps: Synthesis of [18F]-5'-Deoxy-5'-Fluorouridines. *Angew. Chemie* **2008**, *120* (52), 10295–10297. <https://doi.org/10.1002/ange.200804040>.

- (148) Morisawa, H.; Utagawa, T.; Yamanaka, S.; Yamazaki, A. A New Method for the Synthesis of 2'-Amino-2'-Deoxyguanosine and -Adenosine and Their Derivatives. *Chem. Pharm. Bull. (Tokyo)*. **1981**, 29 (11), 3191–3195. <https://doi.org/10.1248/cpb.29.3191>.
- (149) Zhou, X.; Yan, W.; Zhang, C.; Yang, Z.; Neubauer, P.; Mikhailopulo, I. A.; Huang, Z. Biocatalytic Synthesis of Seleno-, Thio- and Chloro-Nucleobase Modified Nucleosides by Thermostable Nucleoside Phosphorylases. *Catal. Commun.* **2019**, 121, 32–37. <https://doi.org/10.1016/j.catcom.2018.12.004>.
- (150) Almendros, M.; Berenguer, J.; Sinisterra, J.-V. Thermus Thermophilus Nucleoside Phosphorylases Active in the Synthesis of Nucleoside Analogues. *Appl. Environ. Microbiol.* **2012**, 78 (9), 3128–3135. <https://doi.org/10.1128/AEM.07605-11>.
- (151) Huffman, M. A.; Fryszkowska, A.; Alvizo, O.; Borra-Garske, M.; Campos, K. R.; Canada, K. A.; Devine, P. N.; Duan, D.; Forstater, J. H.; Grosser, S. T.; Halsey, H. M.; Hughes, G. J.; Jo, J.; Joyce, L. A.; Kolev, J. N.; Liang, J.; Maloney, K. M.; Mann, B. F.; Marshall, N. M.; McLaughlin, M.; Moore, J. C.; Murphy, G. S.; Nawrat, C. C.; Nazor, J.; Novick, S.; Patel, N. R.; Rodriguez-Granillo, A.; Robaire, S. A.; Sherer, E. C.; Truppo, M. D.; Whittaker, A. M.; Verma, D.; Xiao, L.; Xu, Y.; Yang, H. Design of an in Vitro Biocatalytic Cascade for the Manufacture of Islatravir. *Science (80-.)*. **2019**, 366 (6470), 1255–1259. <https://doi.org/10.1126/science.aay8484>.
- (152) Nawrat, C. C.; Whittaker, A. M.; Huffman, M. A.; McLaughlin, M.; Cohen, R. D.; Andreani, T.; Ding, B.; Li, H.; Weisel, M.; Tschäen, D. M. Nine-Step Stereoselective Synthesis of Islatravir from Deoxyribose. *Org. Lett.* **2020**, 22 (6), 2167–2172. <https://doi.org/10.1021/acs.orglett.0c00239>.
- (153) Ni, Y.; Holtmann, D.; Hollmann, F. How Green Is Biocatalysis? To Calculate Is To Know. *ChemCatChem* **2014**, 6 (4), 930–943. <https://doi.org/10.1002/cctc.201300976>.
- (154) Tieves, F.; Tonin, F.; Fernández-Fueyo, E.; Robbins, J. M.; Bommarius, B.; Bommarius, A. S.; Alcalde, M.; Hollmann, F. Energising the E-Factor: The E⁺-Factor. *Tetrahedron* **2019**, 75 (10), 1311–1314. <https://doi.org/10.1016/j.tet.2019.01.065>.
- (155) Tewari, Y. B.; Steckler, D. K.; Goldberg, R. N.; Gitomer, W. L. Thermodynamics of Hydrolysis of Sugar Phosphates. *J. Biol. Chem.* **1988**, 263 (8), 3670–3675.
- (156) Alberty, R. A. Use of Standard Gibbs Free Energies and Standard Enthalpies of Adenosine(Aq) and Adenine(Aq) in the Thermodynamics of Enzyme-Catalyzed Reactions. *J. Chem. Thermodyn.* **2004**, 36 (7), 593–601. <https://doi.org/10.1016/j.jct.2004.03.010>.
- (157) Camici, M.; Sgarrella, F.; Ipata, P. L.; Mura, U. The Standard Gibbs Free Energy Change of Hydrolysis of α -D-Ribose 1-Phosphate. *Arch. Biochem. Biophys.* **1980**, 205 (1), 191–197. [https://doi.org/10.1016/0003-9861\(80\)90098-3](https://doi.org/10.1016/0003-9861(80)90098-3).
- (158) Krenitsky, T. A.; Koszalka, G. W.; Tuttle, J. V. Purine Nucleoside Synthesis: An Efficient Method Employing Nucleoside Phosphorylases. *Biochemistry* **1981**, 20 (12), 3615–3621. <https://doi.org/10.1021/bi00515a048>.
- (159) Schrittwieser, J. H.; Coccia, F.; Kara, S.; Grischek, B.; Kroutil, W.; d'Alessandro, N.; Hollmann, F. One-Pot Combination of Enzyme and Pd Nanoparticle Catalysis for the Synthesis of Enantiomerically Pure 1,2-Amino Alcohols. *Green Chem.* **2013**, 15 (12), 3318–3331. <https://doi.org/10.1039/C3GC41666F>.
- (160) Li, J.; Albrecht, J.; Borovika, A.; Eastgate, M. D. Evolving Green Chemistry Metrics into Predictive Tools for Decision Making and Benchmarking Analytics. *ACS Sustain. Chem. Eng.*

- 2018**, 6 (1), 1121–1132. <https://doi.org/10.1021/acssuschemeng.7b03407>.
- (161) Li, J.; Simmons, E. M.; Eastgate, M. D. A Data-Driven Strategy for Predicting Greenness Scores, Rationally Comparing Synthetic Routes and Benchmarking PMI Outcomes for the Synthesis of Molecules in the Pharmaceutical Industry. *Green Chem.* **2017**, 19 (1), 127–139. <https://doi.org/10.1039/C6GC02359B>.
- (162) Kaspar, F. A Chemical Definition of Efficiency. *ChemRxiv* **2020**. <https://doi.org/10.26434/chemrxiv.13251344.v1>.
- (163) Wierzchowski, J.; Stachelska-Wierzchowska, A.; Wielgus-Kutrowska, B.; Bzowska, A. 1,N6-Ethenoadenine and Other Fluorescent Nucleobase Analogs as Substrates for Purine-Nucleoside Phosphorylases: Spectroscopic and Kinetic Studies. *Curr. Pharm. Des.* **2017**, 23 (45), 6948–6966. <https://doi.org/10.2174/1381612823666171011103551>.
- (164) Wierzchowski, J.; Ogiela, M.; Iwańska, B.; Shugar, D. Selective Fluorescent and Fluorogenic Substrates for Purine-Nucleoside Phosphorylases from Various Sources, and Direct Fluorimetric Determination of Enzyme Levels in Human and Animal Blood. *Anal. Chim. Acta* **2002**, 472 (1), 63–74. [https://doi.org/10.1016/S0003-2670\(02\)00938-8](https://doi.org/10.1016/S0003-2670(02)00938-8).
- (165) Wierzchowski, J.; Stachelska-Wierzchowska, A.; Wielgus-Kutrowska, B.; Mikleušević, G. Two Fluorogenic Substrates for Purine Nucleoside Phosphorylase, Selective for Mammalian and Bacterial Forms of the Enzyme. *Anal. Biochem.* **2014**, 446, 25–27. <https://doi.org/10.1016/j.ab.2013.10.017>.
- (166) Stachelska-Wierzchowska, A.; Wierzchowski, J.; Bzowska, A.; Wielgus-Kutrowska, B. Tricyclic Nitrogen Base 1,N6-Ethenoadenine and Its Ribosides as Substrates for Purine-Nucleoside Phosphorylases: Spectroscopic and Kinetic Studies. *Nucleosides, Nucleotides and Nucleic Acids* **2018**, 37 (2), 89–101. <https://doi.org/10.1080/15257770.2017.1419255>.
- (167) Stachelska-Wierzchowska, A.; Wierzchowski, J.; Górka, M.; Bzowska, A.; Wielgus-Kutrowska, B. Tri-Cyclic Nucleobase Analogs and Their Ribosides as Substrates of Purine-Nucleoside Phosphorylases. II Guanine and Isoguanine Derivatives. *Molecules* **2019**, 24 (8), 1493. <https://doi.org/10.3390/molecules24081493>.
- (168) Singh, D.; Schaaper, R. M.; Hochkoeppler, A. A Continuous Spectrophotometric Enzyme-Coupled Assay for Deoxynucleoside Triphosphate Triphosphohydrolases. *Anal. Biochem.* **2016**, 496, 43–49. <https://doi.org/10.1016/j.ab.2015.11.027>.
- (169) Seamon, K. J.; Stivers, J. T. A High-Throughput Enzyme-Coupled Assay for SAMHD1 DNTase. *J. Biomol. Screen.* **2015**, 20 (6), 801–809. <https://doi.org/10.1177/1087057115575150>.
- (170) Yamada, E. W. Uridine Phosphorylase from Rat Liver. *Methods Enzymol.* **1978**, 51, 423–431. [https://doi.org/10.1016/S0076-6879\(78\)51058-6](https://doi.org/10.1016/S0076-6879(78)51058-6).
- (171) Surette, M.; Gill, T.; MacLean, S. Purification and Characterization of Purine Nucleoside Phosphorylase from *Proteus Vulgaris*. *Appl. Environ. Microbiol.* **1990**, 56 (5), 1435–1439.
- (172) Wittenburg, E. Untersuchung Der Tautomeren Struktur von Thymin Und Seinen Alkylderivaten Mit Hilfe von UV-Spektren. *Chem. Ber.* **1966**, 99 (7), 2391–2398. <https://doi.org/10.1002/cber.19660990737>.
- (173) Fox, J. J.; Yung, N.; Wempfen, I. Spectrophotometric Studies of Nucleic Acid Derivatives and Related Compounds as a Function of PH: IV. On the Structure of Orotidine. A Study of N-Methylated Orotic Acids. *Biochim. Biophys. Acta* **1957**, 23, 295–305.

[https://doi.org/10.1016/0006-3002\(57\)90331-1](https://doi.org/10.1016/0006-3002(57)90331-1).

- (174) Fox, J. J.; Shugar, D. Spectrophotometric Studies on Nucleic Acid Derivatives and Related Compounds as a Function of PH: II. Natural and Synthetic Pyrimidine Nucleosides. *Biochim. Biophys. Acta* **1952**, *9*, 369–384. [https://doi.org/10.1016/0006-3002\(52\)90181-9](https://doi.org/10.1016/0006-3002(52)90181-9).
- (175) Giessmann, R. T.; Krausch, N.; Kaspar, F.; Cruz Bournazou, N. M.; Wagner, A.; Neubauer, P.; Gimpel, M. Dynamic Modelling of Phosphorolytic Cleavage Catalyzed by Pyrimidine-Nucleoside Phosphorylase. *Processes* **2019**, *7* (6), 380. <https://doi.org/10.3390/pr7060380>.
- (176) Kaspar, F.; Giessmann, R. T.; Krausch, N.; Neubauer, P.; Wagner, A.; Gimpel, M. A UV/Vis Spectroscopy-Based Assay for Monitoring of Transformations Between Nucleosides and Nucleobases. *Methods Protoc.* **2019**, *2* (3), 60. <https://doi.org/10.3390/mps2030060>.
- (177) Kaspar, F.; Giessmann, R. T.; Westarp, S.; Hellendahl, K. F.; Krausch, N.; Thiele, I.; Walczak, M. C.; Neubauer, P.; Wagner, A. Spectral Unmixing-Based Reaction Monitoring of Transformations between Nucleosides and Nucleobases. *ChemBioChem* **2020**, *21* (18), 2604. <https://doi.org/10.1002/cbic.202000204>.
- (178) Alberty, R. A. Thermodynamic Properties of Enzyme-Catalyzed Reactions Involving Cytosine, Uracil, Thymine, and Their Nucleosides and Nucleotides. *Biophys. Chem.* **2007**, *127* (1–2), 91–96. <https://doi.org/10.1016/j.bpc.2006.12.010>.
- (179) Goldberg, R. N.; Tewari, Y. B.; Bhat, T. N. Thermodynamics of Enzyme-Catalyzed Reactions: Part 7—2007 Update. *J. Phys. Chem. Ref. Data* **2007**, *36* (4), 1347–1397. <https://doi.org/10.1063/1.2789450>.
- (180) Visser, D. F.; Hennessy, F.; Rashamuse, J.; Pletschke, B.; Brady, D. Stabilization of Escherichia Coli Uridine Phosphorylase by Evolution and Immobilization. *J. Mol. Catal. B Enzym.* **2011**, *68* (3), 279–285. <https://doi.org/10.1016/j.molcatb.2010.11.018>.
- (181) Nannemann, D. P.; Kaufmann, K. W.; Meiler, J.; Bachmann, B. O. Design and Directed Evolution of a Dideoxy Purine Nucleoside Phosphorylase. *Protein Eng. Des. Sel.* **2010**, *23* (8), 607–616. <https://doi.org/10.1093/protein/gzq033>.
- (182) Xie, X.; Huo, W.; Xia, J.; Xu, Q.; Chen, N. Structure-Activity Relationship of a Cold-Adapted Purine Nucleoside Phosphorylase by Site-Directed Mutagenesis. *Enzyme Microb. Technol.* **2012**, *51* (1), 59–65. <https://doi.org/10.1016/j.enzmictec.2012.04.002>.
- (183) Kaspar, F.; Giessmann, R. T.; Neubauer, P.; Wagner, A.; Gimpel, M. Thermodynamic Reaction Control of Nucleoside Phosphorolysis. *Adv. Synth. Catal.* **2020**, *362* (4), 867–876. <https://doi.org/10.1002/adsc.201901230>.
- (184) Giessmann, R. T.; Kaspar, F.; Neubauer, P. in preparation, preliminary dataset available at <https://doi.org/10.5281/zenodo.3572070>.
- (185) Bunton, C. A.; Humeres, E. The Hydrolyses of Alpha-D-Ribose and -Glucose 1-Phosphates. *J. Org. Chem.* **1969**, *34* (3), 572–576. <https://doi.org/10.1021/jo01255a019>.
- (186) Kaspar, F.; Neubauer, P.; Kurreck, A. Kinetic Analysis of the Hydrolysis of Pentose-1-Phosphates Through Apparent Nucleoside Phosphorolysis Equilibrium Shifts. *ChemPhysChem* **2020**, accepted article. <https://doi.org/10.1002/cphc.202000901>.
- (187) Kaspar, F.; Giessmann, R. T.; Hellendahl, K. F.; Neubauer, P.; Wagner, A.; Gimpel, M. General Principles for Yield Optimization of Nucleoside Phosphorylase-Catalyzed Transglycosylations. *ChemBioChem* **2020**, *21*, 1428–1432. <https://doi.org/10.1002/cbic.201900740>.

- (188) Serganov, A.; Keiper, S.; Malinina, L.; Tereshko, V.; Skripkin, E.; Höbartner, C.; Polonskaia, A.; Phan, A. T.; Wombacher, R.; Micura, R.; Dauter, Z.; Jäschke, A.; Patel, D. J. Structural Basis for Diels-Alder Ribozyme-Catalyzed Carbon-Carbon Bond Formation. *Nat. Struct. Mol. Biol.* **2005**, *12* (3), 218–224. <https://doi.org/10.1038/nsmb906>.
- (189) Serganov, A.; Yuan, Y.-R.; Pikovskaya, O.; Polonskaia, A.; Malinina, L.; Phan, A. T.; Hobartner, C.; Micura, R.; Breaker, R. R.; Patel, D. J. Structural Basis for Discriminative Regulation of Gene Expression by Adenine- and Guanine-Sensing MRNAs. *Chem. Biol.* **2004**, *11* (12), 1729–1741. <https://doi.org/10.1016/j.chembiol.2004.11.018>.
- (190) Egli, M.; Pallan, P. S.; Pattanayek, R.; Wilds, C. J.; Lubini, P.; Minasov, G.; Dobler, M.; Leumann, C. J.; Eschenmoser, A. Crystal Structure of Homo-DNA and Nature's Choice of Pentose over Hexose in the Genetic System. *J. Am. Chem. Soc.* **2006**, *128* (33), 10847–10856. <https://doi.org/10.1021/ja062548x>.
- (191) Freisz, S.; Lang, K.; Micura, R.; Dumas, P.; Ennifar, E. Binding of Aminoglycoside Antibiotics to the Duplex Form of the HIV-1 Genomic RNA Dimerization Initiation Site. *Angew. Chemie Int. Ed.* **2008**, *47* (22), 4110–4113. <https://doi.org/10.1002/anie.200800726>.
- (192) Wise, D. S.; Townsend, L. B. Synthesis of the Selenopyrimidine Nucleosides 2-Seleno- and 4-Selenouridine. *J. Heterocycl. Chem.* **1972**, *9* (6), 1461–1462. <https://doi.org/10.1002/jhet.5570090655>.
- (193) Shiue, C.-Y.; Chu, S.-H. Facile Synthesis of 1-β-D-Arabinofuranosyl-2-Seleno- and-4-Selenouracil and Related Compounds. *J. Org. Chem.* **1975**, *40* (20), 2971–2974. <https://doi.org/10.1021/jo00908a032>.
- (194) Sun, H.; Sheng, J.; Hassan, A. E. A.; Jiang, S.; Gan, J.; Huang, Z. Novel RNA Base Pair with Higher Specificity Using Single Selenium Atom. *Nucleic Acids Res.* **2012**, *40* (11), 5171–5179. <https://doi.org/10.1093/nar/gks010>.
- (195) Bartos, P.; Maciaszek, A.; Rosinska, A.; Sochacka, E.; Nawrot, B. Transformation of a Wobble 2-Thiouridine to 2-Selenouridine via S-Geranyl-2-Thiouridine as a Possible Cellular Pathway. *Bioorg. Chem.* **2014**, *56*, 49–53. <https://doi.org/10.1016/j.bioorg.2014.05.012>.
- (196) Kogami, M.; Davis, D.; Koketsu, M. An Efficient Synthesis of 2-Selenouridine and Its Phosphoramidite Precursor. *Heterocycles* **2016**, *92*, 64. <https://doi.org/10.3987/COM-15-13349>.
- (197) Hassan, A. E. A.; Sheng, J.; Zhang, W.; Huang, Z. High Fidelity of Base Pairing by 2-Selenothymidine in DNA. *J. Am. Chem. Soc.* **2010**, *132* (7), 2120–2121. <https://doi.org/10.1021/ja909330m>.
- (198) Mautner, H. G. The Synthesis and Properties of Some Selenopurines and Selenopyrimidines. *J. Am. Chem. Soc.* **1956**, *78* (20), 5292–5294. <https://doi.org/10.1021/ja01601a037>.
- (199) Payne, N. C.; Geissler, A.; Button, A.; Sasuclark, A. R.; Schroll, A. L.; Ruggles, E. L.; Gladyshev, V. N.; Hondal, R. J. Comparison of the Redox Chemistry of Sulfur- and Selenium-Containing Analogs of Uracil. *Free Radic. Biol. Med.* **2017**, *104*, 249–261. <https://doi.org/10.1016/j.freeradbiomed.2017.01.028>.
- (200) Hellendahl, K. F.; Kaspar, F.; Zhou, X.; Yang, Z.; Huang, Z.; Neubauer, P.; Kurreck, A. Biocatalytic Synthesis of 2-Seleno Pyrimidine Nucleosides via Transglycosylation. *ChemRxiv* **2020**. <https://doi.org/10.26434/chemrxiv.13318202.v1>.

- (201) Sheldon, R. A.; Brady, D. Broadening the Scope of Biocatalysis in Sustainable Organic Synthesis. *ChemSusChem* **2019**, *12* (13), 2859–2881. <https://doi.org/10.1002/cssc.201900351>.
- (202) Eyring, H. The Activated Complex in Chemical Reactions. *J. Chem. Phys.* **1935**, *3* (2), 107–115. <https://doi.org/10.1063/1.1749604>.
- (203) Krenitsky, T. A. Uridine Phosphorylase from Escherichia Coli: Kinetic Properties and Mechanism. *Biochim. Biophys. Acta - Enzymol.* **1976**, *429* (2), 352–358. [https://doi.org/10.1016/0005-2744\(76\)90283-7](https://doi.org/10.1016/0005-2744(76)90283-7).
- (204) Traut, T. W. Physiological Concentrations of Purines and Pyrimidines. *Mol. Cell. Biochem.* **1994**, *140* (1), 1–22. <https://doi.org/10.1007/BF00928361>.
- (205) Kaspar, F.; Neubauer, P.; Kurreck, A. The Peculiar Case of the Hyperthermostable Pyrimidine Nucleoside Phosphorylase from Thermus Thermophilus. *ChemBioChem* **2020**. <https://doi.org/10.1002/cbic.202000679>.
- (206) Kalckar, H. M.; Macnutt, W. S.; Hoff-Jørgensen, E. Trans-N-Glycosidase Studied with Radioactive Adenine. *Biochem. J.* **1952**, *50* (3), 397–400. <https://doi.org/10.1042/bj0500397>.
- (207) Macnutt, W. S. The Enzymically Catalysed Transfer of the Deoxyribosyl Group from One Purine or Pyrimidine to Another. *Biochem. J.* **1952**, *50* (3), 384–397. <https://doi.org/10.1042/bj0500384>.

7 Ten Theses

The following ten theses are a condensate of the cumulative scientific insights presented in this work. Naturally, they are not comprehensive and, certainly, more than ten fundamental statements could be drawn from the work in this thesis. As such, this selection of ten theses also reflects the priorities of the author.

- 1 The efficiency of a synthetic route (in the sense of resource efficiency) is primarily a function of route length and solvent use throughout that route.
- 2 Contaminated water is the main source of waste in nucleoside phosphorylase-catalyzed nucleoside syntheses due to the low water-solubility of many nucleosides and nucleobases.
- 3 Spectral deconvolution is a powerful analytical tool for the monitoring of nucleoside phosphorylase-catalyzed reactions and other transformations in which the substrate and product have different but highly overlapping UV absorption spectra.
- 4 Nucleoside phosphorolysis is a thermodynamically controlled reversible endothermic reaction with Gibbs free energies of -5 to 15 kJ mol⁻¹.
- 5 The equilibrium constant of nucleoside phosphorolysis is a function of temperature.
- 6 The hydrolysis of pentose-1-phosphates can be monitored quantitatively via equilibrium shifts of a nucleoside phosphorolysis reaction.
- 7 In a predictable manner, the maximum conversions in nucleoside transglycosylation reactions depend on the thermodynamic properties of the target nucleoside and the starting nucleoside serving as the sugar donor as well as the concentrations of this sugar donor and inorganic phosphate.
- 8 Yields and conversions in nucleoside transglycosylation reactions cannot be quantitative due to the system's nature as a reversible equilibrium reaction. Maximum yields are therefore always the result of a tradeoff between i) the addition of sugar donor pushing the equilibrium to higher conversions and ii) wasting this sugar donor due to diminished returns effects.
- 9 Selenium-containing pyrimidine nucleosides can be accessed directly from their corresponding nucleobases via nucleoside transglycosylation, despite the unfavorable equilibrium constants of phosphorolysis of these compounds in the range of 5–10 and the sensitivity of the nucleobases to oxidation in aqueous solution.
- 10 The pyrimidine nucleoside phosphorylase from *Thermus thermophilus* resists high concentrations of the organic cosolvents DMSO and ethylene glycol at temperatures of up to 90 °C, facilitating the solubilization of poorly water-soluble nucleobases.

8 Publications

Paper I

Kaspar, F.; Stone, M.R.L.; Neubauer, P.; Wagner, A. Route efficiency assessment and review of the synthesis of β -nucleosides via *N*-glycosylation of nucleobases. *Green Chem.* **2020**, accepted article, <https://doi.org/10.1039/D0GC02665D>.

This article was published under an RSC Green license which permits the author reproduction of the unaltered material in a thesis such as this one, given that proper acknowledgement of the source is provided.

Author contributions (with definitions by Brand *et al.*¹)

Conceptualization, F.K.; Data curation, F.K.; Formal analysis, F.K. and M.R.L.S.; Funding acquisition, P.N. and A.W.; Investigation, F.K. and M.R.L.S.; Methodology, F.K.; Project administration, F.K. and A.W.; Resources, A.W. and P.N.; Software, - ; Supervision, F.K.; Validation, - ; Visualization, F.K.; Writing—original draft, F.K.; Writing—review & editing, F.K., M.R.L.S., P.N. and A.W.

Specifically, my contribution included formulation of the research idea, literature search, data acquisition, data extraction from the original literature, data curation, calculation of the E-factors, interpretation of the results as well as illustration and lead writing of the publication.

Preamble

Although biocatalysis is often hailed as the “greener” or “sustainable” alternative to traditional chemical synthesis routes, there has been a growing recognition that this might not always be the case. In fact, the “greenness” of a biocatalytic synthesis can vary drastically, just like that of its chemical counterparts, as work from Hollmann and colleagues continues to demonstrate quite nicely. Given that typical nucleoside transglycosylation reactions from our laboratory and those of others are performed on a 1–5 mM scale with incomplete conversion of the starting material and non-negligible loss of product during purification, I had some reservations about our routes being much greener than their chemical competitors. However, proof of any kind was missing. Since the Covid-19 pandemic effectively halted all practical work in our laboratory for a few months, I suddenly found the time to investigate the fundamental question “*Is biocatalytic nucleoside synthesis greener than chemical nucleoside synthesis?*” from my desk at home. To answer this question, I took stock of the entire literature on nucleoside synthesis via *N*-glycosylation and extracted experimental details and procedures to calculate environmental factors (E-factors), as a representative metric for efficiency and, in extension, greenness. Not only did this literature search reveal that not one efficiency analysis had been published for synthetic routes with glycosylation-type chemistry, but also that nucleoside synthesis, biocatalytic or otherwise, was generally far from efficient. Although we were pleased to see that this data highlighted that biocatalytic nucleoside synthesis has tremendous potential by providing a concise single-step route, it became clear that issues arising from poor substrate solubility and unfavorable reaction equilibria urgently needed to be addressed.

CRITICAL REVIEW

[View Article Online](#)
[View Journal](#)


Cite this: DOI: 10.1039/d0gc02665d

Route efficiency assessment and review of the synthesis of β -nucleosides via *N*-glycosylation of nucleobases†

Felix Kaspar, ^{a,b} M. Rhia L. Stone, ^c Peter Neubauer ^a and Anke Kurreck ^{a,b}

Nucleosides and their analogs are biomolecules central to nearly all areas of life science. Consequently, a variety of approaches have been developed to prepare these compounds. These methods typically employ *N*-glycosylation as a key step which installs a sugar moiety on a heterocyclic nucleobase. However, these methods vary drastically regarding their synthetic strategy, number of steps, yield, reagents, and conditions employed, making it difficult to compare and evaluate different approaches. Herein, we review the state of art for the synthesis of β -nucleosides by *N*-glycosylation and present a comprehensive sustainability assessment of these routes via an E-factor analysis. Our data reveal that the current methods and protocols are, in general, laborious and inefficient. Although impressive yields have been achieved in many cases, these typically came at the cost of long routes, leading to high overall E-factors (primarily composed of solvent contributions). Shorter routes using fewer protecting groups tended to perform equally well or better regarding their route E-factors, despite lower yields in many cases. Nearly all available approaches are currently hampered by a heavy reliance on chromatography, multiple protecting groups and bulky leaving groups. Biocatalytic methods bypass these limitations but suffer from poor substrate solubility and unfavorable reaction equilibria. To enable more efficient and sustainable nucleoside synthesis via *N*-glycosylation, future efforts should focus on using non-chromatographic purification steps, running shorter routes and higher substrate loading to minimize (solvent) waste accumulation.

Received 3rd August 2020,
Accepted 16th November 2020

DOI: 10.1039/d0gc02665d

rsc.li/greenchem

Introduction

Nucleosides are highly functionalized biomolecules essential to life on earth and were among the first organic molecules on our planet.¹ Now β -nucleosides serve as the building blocks of DNA and RNA, part of cellular energy transfer systems, and as enzymatic cofactors in all known organisms on earth. In recent years, nucleoside analogs have become indispensable as pharmaceutical agents against various cancers as well as viral infections and as molecular biology tools.^{2–4} For example, fluorinated nucleoside analogs such as floxuridine and islatravir are used for the treatment of colorectal cancer and HIV infections, respectively.^{5,6} Alkyne-containing nucleosides such as 5-ethynyluridine have been broadly applied for the labelling of nucleic acids, including the analysis of RNA synthesis and visualization of cellular localization.⁴ Consequently, the

demand for these molecules in nearly all areas of life science has necessitated the development of chemical methods for their synthesis. More than six decades of research in the field have yielded a variety of robust methods to access these compounds.

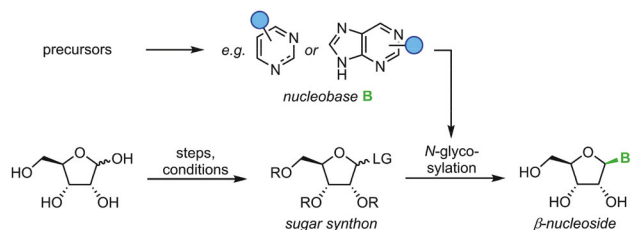
Nucleoside synthesis is generally performed in a convergent manner via *N*-glycosylation of a nucleobase, which installs a ribosyl moiety on a heterocyclic base (Scheme 1). Although the glycosylation of a nucleobase as a key step may appear rather simple at first glance, it is complicated by challenges in regio- and diastereoselectivity.⁷ These issues typically arise from the low nucleophilicity of nucleobases as well as the density of functional groups decorating the ribosyl moiety. Thus, the desired linkage of a nucleobase to the anomeric center of a ribosyl moiety to yield a β -nucleoside often competes with several side reactions, including unselective nucleophilic attack (forming the α -nucleoside) and attack of other nucleophilic functional groups, affording complex mixtures of products. To address these obstacles, a variety of creative approaches have been developed to prepare β -nucleosides in high yield and selectivity. However, these methods vary drastically regarding their strategy, number of steps, yield, reagents, and conditions employed, making it difficult to compare and evaluate different approaches.

^aInstitute of Biotechnology, Chair of Bioprocess Engineering, Technische Universität Berlin, ACK24, Ackerstraße 76, 13355 Berlin, Germany. E-mail: felix.kaspar@web.de

^bBioNukleo GmbH, Ackerstraße 76, 13355 Berlin, Germany

^cCentre for Superbug Solutions, Institute for Molecular Biosciences, University of Queensland, 306 Carmody Road, St. Lucia, 4072 Queensland, Australia

†Electronic supplementary information (ESI) available. See DOI: 10.1039/d0gc02665d



Scheme 1 Convergent synthesis of nucleosides with *N*-glycosylation as the key step. *N*-Heterocyclic nucleobases such as pyrimidines and purines with variable substitution patterns (blue circles) can be accessed directly from cheap precursors via condensation reactions while sugar synthons need to be prepared by multistep routes from unprotected sugars.

Driven by the increasing global effort to establish a sustainable economy, most branches of chemistry have questioned their practices and aimed to design “greener” processes and reagents.^{8,9} Among others, these efforts include the use of sustainably sourced solvents (and recycling thereof), the development of more concise and high-yielding routes to pharmaceuticals and the establishment of waste-minimizing cascade syntheses, to name just a few. The pharmaceutical industry (and related fields) has been quick to adopt green chemistry principles and environmental concerns are increasingly recognized in this area.¹⁰ Subsequent research has made a wealth of information publicly available to benchmark and predict various metrics of sustainability and efficiency of chemical syntheses.^{11–19} Several comprehensive assessments of different routes for the preparation of pharmaceutically relevant target molecules have been published, which have provided further insights into the pitfalls of some synthetic approaches and highlighted successful strategies from a sustainability perspective.^{20–25} Beyond that, assessments of individual newly

published reactions or approaches *versus* established methods have become a common sight in the literature and continue to provide a valuable and critical evaluation of the state of the art.^{26–45} However, most of the above approaches focus either on (i) drug-like molecules and, consequently, the heterocycle chemistry commonly involved or (ii) single transformations. To the best of our knowledge, a comprehensive assessment of sustainability or efficiency for glycosylation-type chemistry is missing from the literature. Spurred by this lack of information, we were curious which of the available methods for nucleoside synthesis would be most compatible with a low-waste economy and be efficient in a sense of resource usage.

Since nucleosides will undoubtedly continue to be central to all areas of life science, we aimed to provide a transparent evaluation and specifically investigated which routes to nucleosides would yield the most efficient and sustainable synthesis. Rather than starting an assessment at a randomly chosen synthon, we opted to consider the entire route necessary for a given strategy. Since preparation of the sugar synthon is generally the most time- and material-intensive part of these routes,⁷ we assumed that all routes had to start from unprotected readily available materials. To this end, we surveyed the literature for glycosylation methods for the synthesis of β-nucleosides and extracted experimental data and protocols for several nucleoside examples to calculate representative environmental factors (E-factors, EF)^{9,46–50} for the entire synthetic routes. The E-factor is a mass-based metric to assess the amount of waste produced during a synthetic process or route, where

$$EF = \frac{m_{\text{waste}}}{m_{\text{product}}}$$

with m_{product} being the weight of the pure product and m_{waste} being the mass of all materials involved in a synthesis that are not the product. In our analysis, we both considered the simple



Felix Kaspar

Felix Kaspar is a Ph.D. candidate at the Institute for Biotechnology at the Technische Universität Berlin, Germany. He obtained a Bachelor's (Biotechnology, 2016) and Master's degree (Biochemistry, 2019) from the Technische Universität Braunschweig, Germany, and completed several research internships during his studies, leading him to Australia (Charles Sturt University, 2015; University of Queensland,

2017–2018) and the USA (University of Alabama, 2016). His research interests include all things biocatalysis, particularly biocatalytic nucleoside synthesis, as well as equilibrium thermodynamics, method development and environmentally acceptable chemistry.



M. Rhia L. Stone

Dr M. Rhia L. Stone completed her BSc and MSc (I) in Chemistry from Victoria University of Wellington in New Zealand, before moving to the University of Queensland, Australia for her PhD. Rhia completed her doctorate in July 2020, working on tagged antibiotics for the examination of bacterial resistance and infection. Rhia is currently a Postdoctoral Researcher at Rutgers University, the State University of New Jersey, where she is studying the Chemical Biology of nucleic acids.

E-factor (sEF) which, as pioneered by Sheldon,⁹ only considers the reagents used as

$$\text{sEF} = \frac{\sum m_{\text{reagents}} - m_{\text{product}}}{m_{\text{product}}}$$

as well as the complete E-factor (cEF)⁹ which considers all materials used as

$$\text{cEF} = \frac{\sum m_{\text{reagents}} + \sum m_{\text{auxiliaries}} + \sum m_{\text{solvents}} - m_{\text{product}}}{m_{\text{product}}}$$

where $\sum m_{\text{reagents}}$ is the sum of the masses of all reagents (including starting materials), $\sum m_{\text{auxiliaries}}$ is the sum of the masses of all auxiliary materials (such as inorganic salts and silica gel, for example) and $\sum m_{\text{solvents}}$ is the sum of the masses of all solvents, including organic solvents and water. Considering the number of reactions and routes we aimed to assess, as well as their heterogeneity, we herein opted for the use of the E-factor as a simple and accessible metric. A full life cycle assessment^{51–53} would have far surpassed the scope of this work and, given the (sometimes) incomplete literature data, also proven unrealistic. Likewise, we did not consider energy consumption (e.g. for inclusion in an E⁺-factor)⁵⁴ as this data was not available from the literature. It should therefore also be recognized that our data only describe the amount and not the sort of waste generated, how harmful this waste is to the environment or how costly its treatment is (i.e. a kilogram of NaCl or water had the same E-factor as a kilogram of fluorinated Lewis acids or methylation reagents).

This article reviews the state of the art for β -nucleoside synthesis *via* N-glycosylation and provides an assessment of the performance and efficiency of all available methods and their routes. Since the last comprehensive review of nucleoside synthesis by Vorbrüggen,⁷ there have been some notable additions to the toolbox, which we briefly introduce along with

some general considerations. We further present a collection of 80 route E-factors (covering up to 11 total steps) which were extracted from over 30 papers using 12 different N-glycosylation methods. Our data highlight prominent sources of waste, reveal the inefficiency of some strategies and underscore that route and reaction design tremendously impact the overall E-factor of the synthesis. Based on these findings, we outline current obstacles and bottlenecks which future synthetic efforts should seek to address. Lastly, our freely available data allow straightforward benchmarking of future syntheses to evaluate their efficiency.

Nucleoside synthesis *via* N-glycosylation

All methods for N-glycosylation of nucleobases are united in employing a reactive (activated) glycosyl intermediate that is subjected to nucleophilic attack by a nucleobase (Scheme 2, top). All approaches published to date proceed *via* one of three key intermediates for attack by the nucleobase (Scheme 2, middle). Selective attack at the anomeric center is encouraged either by (i) generation of a 1,3-dioxolane cation through recruitment of the neighboring protecting group, (ii) formation of a reactive glycosyl cation with charge delocalization across the ring oxygen or (iii) employment of a good leaving group that sets the right configuration upon S_N2-type substitution at the anomeric position. These intermediates can be accessed from various synthons, all of which typically bear one or more protecting groups and need to be prepared from (deoxy)ribose in 1–7 steps (Scheme 2, bottom). Despite these shared basic strategies, conditions and methodologies employed by the available methods differ significantly and are generally guided by the sugar synthon employed for N-glycosylation. It should



Peter Neubauer

Peter Neubauer is Professor of Bioprocess Engineering at the Department of Biotechnology at the Technische Universität Berlin, Germany, since 2008. He holds a doctoral degree in Microbiology from Universität Greifswald, Germany, and completed postdocs at the Royal Institute of Technology (KTH), Sweden, and Martin-Luther-Universität of Halle, Germany, before he received a professorship in bioprocess engineering

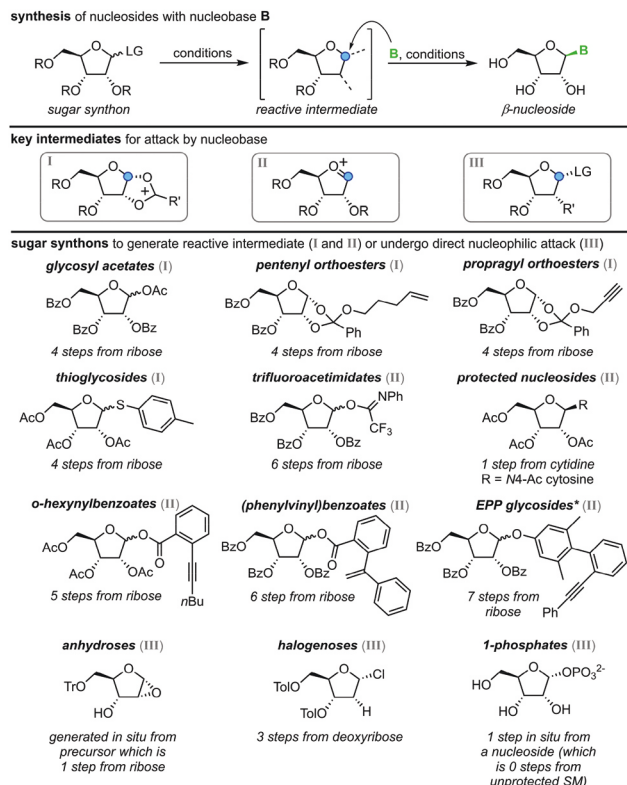
from the University of Oulu, Finland (2000–2008). His research is concerned with bioprocess scale up/scale down and microbial physiology in industrial scale bioprocesses, as well as the development of strategies for the production of difficult-to-express proteins and the mathematical modelling of bioprocesses.



Anke Kurreck

Anke Kurreck is a Postdoctoral Researcher in the Bioprocess Engineering group at the Technische Universität Berlin, Germany, and CEO of the Biotech company BioNukleo GmbH since 2014. She holds a doctoral degree in Microbiology from Martin-Luther-Universität of Halle (Germany) and completed a research internship at Wageningen University during her PhD. Subsequently she worked as a Postdoctoral

Researcher in the Applied Biochemistry Group at the Technische Universität Berlin. Her research focusses on applied sciences with the aim to reduce the environmental burden and to bring (chemo) enzymatic synthesis routes increasingly into pharmaceutical application.

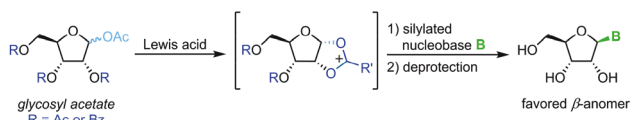


Scheme 2 Synthesis of nucleosides via *N*-glycosylation, including key intermediates and sugar synthons. Under varying conditions, a sugar synthon is transformed to a reactive intermediate primed for nucleophilic attack by an (activated) nucleobase, which furnishes a β -nucleoside. LG = leaving group, R = protecting group, B = nucleobase, SM = starting material, *EPP = (phenylethynylphenyl)phenyl.

be noted that the following overview only includes methods which predominantly yield the β -nucleoside in reasonable yield and selectivity. Therefore, nucleoside syntheses which favor α -nucleosides, afford minimal yields and/or poor selectivity, or do not employ an *N*-glycosylation step were not included. Furthermore, methods whose reports did not include sufficient detail to reconstruct the experimental procedures are also not included below or in our E-factor assessment.

Glycosyl acetates

Vorbrüggen's classic synthesis of nucleosides built on silyl Hilbert-Johnson conditions and was originally only described for pyrimidine nucleosides.⁵⁵ A fully protected glycosyl acetate is subjected to Lewis acid catalysis, yielding a glycosyl cation intermediate upon displacement of the anomeric acetate (Scheme 3). This labile species is then reacted with a silylated



Scheme 3 Nucleobase glycosylation with glycosyl acetates.

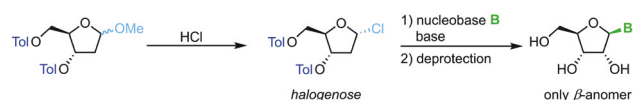
nucleobase to afford a nucleoside after global deprotection. Its exceptional substrate scope, easy adaptability and reliability have made it the most popular method for nucleoside synthesis in academia and industry. Nonetheless, downsides of this method include the need for silylated nucleobases, harsh reaction conditions and the stoichiometric amounts of Lewis acid generally used.^{56–59}

Halogenoses

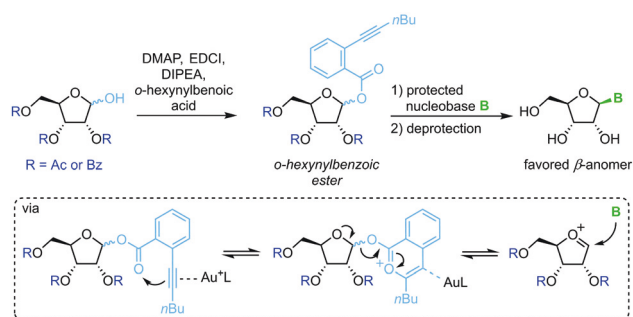
Direct glycosylation of nucleobases with halogenoses can be achieved through nucleophilic substitution at the anomeric center. This method is particularly popular for the synthesis of 2'-deoxy nucleosides that are otherwise difficult to access due to the lack of anchimeric assistance. Halogenoses can be accessed from the respective methoxyriboside and are subject to direct nucleophilic attack by the nucleobase (Scheme 4). To this end, different methods for nucleobase activation, including silylation and deprotonation by strong bases, have been employed.^{60–63} However, the functional group tolerance of this approach is hampered by the harsh conditions needed for this transformation. Further, the regioselectivity for purine nucleoside synthesis, as well as glycosylation yield, are generally limited. Despite its shortcomings, glycosylation with halogenoses offers a favorable atom economy compared to other methods.

o-Hexynylbenzoates

Spurred on by the difficulty to glycosylate purine bases *via* Vorbrüggen-type conditions, Yu and colleagues developed a glycosylation method based on *ortho*-hexynylbenzoic esters.⁶⁴ Under gold catalysis, the benzoic ester at the anomeric position reversibly rearranges to an isocoumarin scaffold and yields a glycosyl cation (Scheme 5). This effectively minimizes competition of the leaving group with the nucleobase for attack at the anomeric center, enabling productive attack by



Scheme 4 Nucleobase glycosylation with halogenoses.



Scheme 5 Nucleobase glycosylation with *o*-hexynylbenzoates.

weak nucleophiles such as purine nucleobases. Although this method allows glycosylation under mild conditions without the use of stoichiometric activating reagents, it demands a long reaction sequence and extensive use of protecting groups on both the sugar and the nucleobase.

o-(1-Phenylvinyl)benzoates

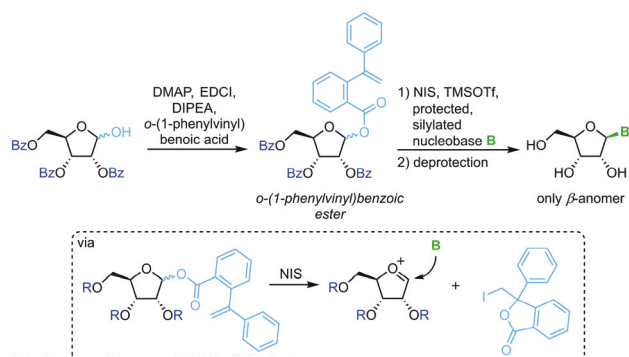
A similar strategy that eliminates competition of the leaving group with the nucleobase relies on irreversible sequestration of a vinylbenzoic ester (Scheme 6).⁶⁵ Esterification of tribenzoylated ribose with *o*-(1-phenylvinyl)benzoic acid accesses a stable sugar synthon. When subjected to an iodine source this synthon affords a glycosyl cation which can be intercepted by a silylated nucleobase. This method provides excellent glycosylation yields and regioselectivity under mild conditions. However, the need for a long reaction sequence with multiple protecting group manipulations make this approach rather laborious.

3,5-Dimethyl-4-(2'-phenylethynylphenyl)phenyl (EPP) glycosides

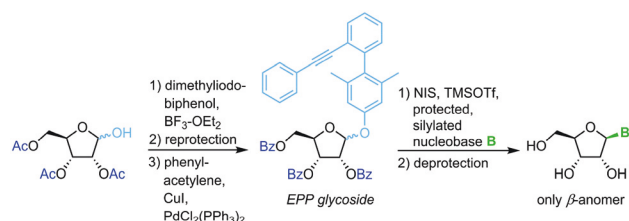
The same strategy and conditions can also be employed with (phenylethynylphenyl)phenyl glycosides as alternative leaving groups (Scheme 7).⁶⁶

Pentenyl glycosides

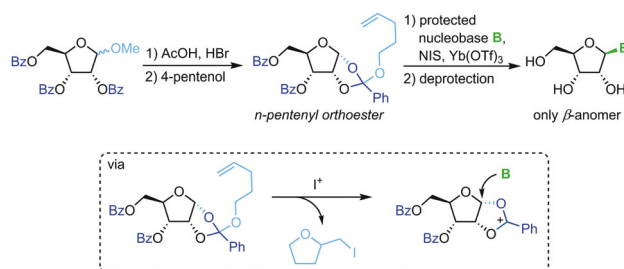
Sequestration of a *n*-pentenyloxy group as an iodomethyl tetrahydrofuran to avoid competition of the leaving group with weakly nucleophilic nucleobases is a strategy developed recently by Fraser-Reid and colleagues.⁶⁷ Starting from a per-



Scheme 6 Nucleobase glycosylation with *o*-(1-phenylvinyl)benzoates.



Scheme 7 Nucleobase glycosylation with EPP glycosides.



Scheme 8 Nucleobase glycosylation with pentenyl glycosides.

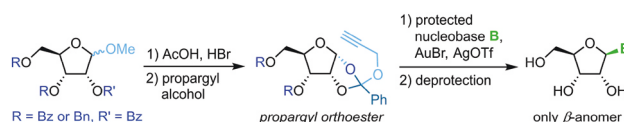
benzoylated methyl riboside, a *n*-pentenyl orthoester is prepared through recruitment of the 2-benzoyl group. Similar to the above approaches, treatment of this ester with an iodonium source and a silylated nucleobase affords the corresponding β -nucleoside after global deprotection (Scheme 8). While this approach also suffers from a rather long reaction sequence (7 steps from unprotected starting materials) and a strict limitation to 2'-hydroxy nucleosides, it does provide excellent stereoselectivity and little problems with regioselectivity. Nonetheless, the substrate scope is limited and the need for the extensive use of protecting groups raises concerns from an efficiency perspective.

Propargyl-1,2-orthoesters

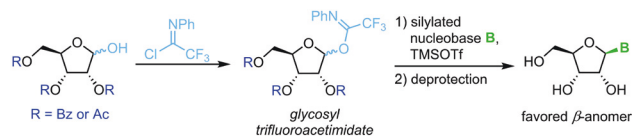
A similar methodology to Fraser-Reid *et al.* was developed by Rao and coworkers⁶⁸ to facilitate high yields in the *N*-glycosylation of nucleobases. A propargyl-1,2-orthoester can be obtained from the respective perbenzoylated riboside through base-promoted attack of the alcohol to enable subsequent glycosylation under mild conditions. Addition of a silylated pyrimidine nucleobase under Lewis acid catalysis affords exclusively the β -anomer of the nucleoside (Scheme 9). Despite the method's promise of excellent stereo- and regioselectivity, it has only been applied to two nucleobases to date, presumably since the preparation of the sugar synthon is rather lengthy and labor-intensive.

Trifluoroacetimidate glycosides

N-Glycosylation under mild conditions can also be achieved through activation of glycosyl donors as trifluoroacetimidates, which are excellent leaving groups.^{69,70} Nucleophilic attack of a silylated nucleobase provides near-quantitative yields of the thermodynamically favored β -nucleoside under Lewis acid catalysis (Scheme 10). However, this method has only been demonstrated for a small selection of pyrimidine nucleosides thus far. The extensive use of protecting groups, stoichiometric



Scheme 9 Nucleobase glycosylation with propargyl-1,2-orthoesters.



Scheme 10 Nucleobase glycosylation with trifluoroacetimidates.

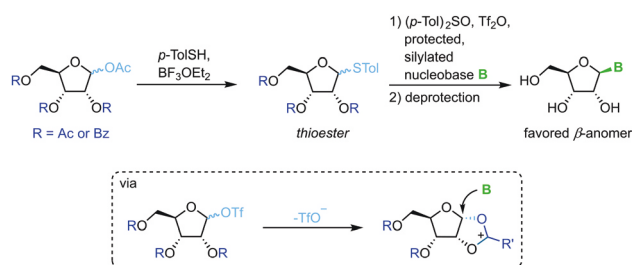
application of activating agents and unfavorable atom economy make the viability of this approach rather questionable, despite its impressive yields.

Thioglycosides

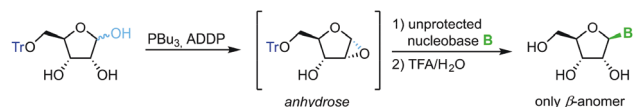
Thioglycosides have been employed in carbohydrate synthesis for various glycosylations and are notable for their versatility. Their use in nucleoside synthesis is rather rare, yet there are examples in the literature.⁷¹ Similar to other approaches, this method relies on *in situ* formation of a charged five-membered ring through recruitment of the protecting group at the 2-position after treatment of the thioglycoside with a triflate source (Scheme 11). This reactive intermediate is then intercepted by an activated nucleobase to generate the favored β -anomer. While yields of the glycosylation step are good to excellent, this approach requires a rather lengthy synthesis of the sugar synthons (4–5 steps) and suffers from similar drawbacks concerning protecting groups and silylating agents to analogous methods. It is noteworthy that even 2'-deoxynucleosides can be accessed with this approach, although not in high yield or anomeric selectivity.

Anhydroses

Building on Mitsunobu glycosylation conditions and pioneering work by Chow and Danishefsky,⁷² Hock and colleagues developed⁷³ and optimized⁷⁴ a glycosylation strategy that relies on *in situ* tributylphosphine-mediated formation of a mono-protected anhydroses. Subsequent nucleophilic attack of a deprotonated nucleobase at the electronically favored 1-position exclusively provides the β -anomer of the nucleoside (Scheme 12). This concise route profits from employing only one protecting group (which can be installed in one high-yielding step from D-ribose), a respectable substrate scope and moderate to good yields of only the desired anomer, which significantly simplifies purification. Drawbacks of this method are



Scheme 11 Nucleobase glycosylation with thioglycosides.



Scheme 12 Nucleobase glycosylation with anhydroses.

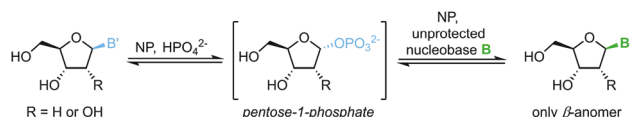
few and mainly comprise the strict limitation to 2-hydroxy sugars.

1-Phosphates

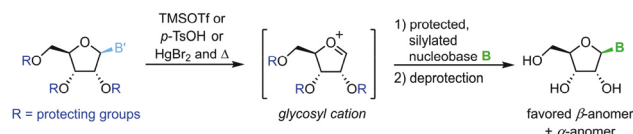
The biocatalytic synthesis of nucleosides *via* nucleoside phosphorylases (NPs) is well established and has recently attracted renewed interest.⁷⁵ NP-catalyzed nucleoside transglycosylations employ an easily accessible nucleoside, such as natural uridine or thymidine, as the synthetic starting point.⁷⁶ A pentose-1-phosphate is generated by phosphorolytic cleavage of the starting nucleoside and then serves as the glycosyl donor to a second nucleobase, which furnishes the nucleoside of interest (Scheme 13).^{77–83} These reactions capitalize on their promise of mild reaction conditions, perfect regio- and stereoselectivity of NPs, and overall excellent functional group tolerance. Both ribosyl and 2'-deoxyribosyl nucleosides with various nucleobases can be accessed easily with this methodology. While the substrate scope is somewhat limited by the capabilities of the available enzymes, further expansion of the substrate scope by enzyme engineering can be expected.⁸⁴ Recent progress in the thermodynamic characterization of these reactions has further enabled robust optimization of reaction conditions by leveraging principles of thermodynamic reaction control.^{80,85} Thus, considerable progress in this field may be anticipated.

Protected nucleosides

Transglycosylation can also be achieved through heat- and Lewis acid-mediated dissociation of the nucleobase from a donor nucleoside (Scheme 14).^{86–88} This yields an unstable glycosyl cation which can be intercepted by a silylated nucleobase, affording the nucleoside of interest after global deprotection. Owing to several drawbacks of this approach, literature examples are rare and date back to the late 20th century.



Scheme 13 Nucleobase glycosylation with 1-phosphates.



Scheme 14 Nucleobase glycosylation with protected nucleosides.

These include, among others, the need to protect every functional group, the limitation to purine nucleosides, poor control of the configuration at the anomeric center, as well as exceptionally harsh and hazardous reaction conditions.

E-factor assessment of glycosylation methods for nucleobases

Considering the route length, methodology and yield of the individual steps of the available approaches, it is to be expected that these routes for nucleobase glycosylation would differ significantly regarding their efficiency and waste production.

Data collection

We sought to provide a fully transparent assessment of the efficiency and sustainability of the available methods for nucleobase glycosylation. Therefore, we surveyed the literature for examples of applications for these approaches and calculated the E-factor for the entire routes. In all cases, performing these calculations for every example in the literature (or even every example in a given publication) would have far surpassed the scope of this work. Thus, we selected representative examples that cover multiple pyrimidine and purine nucleosides each with various functional groups, as far as available from the literature (please see Chart S1† for an overview of all nucleosides considered herein).

To generate a level playing field for all methods, we opted to have all routes start from readily available unprotected starting materials. Consequently, we assumed that all routes started either from (deoxy)ribose or a natural nucleoside. Whenever possible and provided in the literature, we considered the E-factor for the synthesis of the sugar donor employed for glycosylation based on the route and procedures reported by the authors of that paper. However, this information was not available in most cases (*i.e.* the explicit methodology for synthon preparation was not always reported). Therefore, we assumed that whatever synthon these authors used for their synthesis was prepared according to classic literature procedures.^{89–102} Similarly, many nucleoside syntheses ended with the protected nucleoside and in those cases, we assumed that a suitable classic deprotection protocol from the literature was used.⁹⁴ To avoid favoring one method over another, we applied these same assumptions equally across the board to all methods that built on a given synthon or required a given deprotection.

Calculations

To calculate the sEF and cEF of each route over all steps, we extracted experimental details and procedures from the reports of these methods. However, many reports across different journals did not provide a sufficient description of the experimental procedures to allow a precise reconstruction of the protocol. To still permit a calculation of cEF (which includes, for example, reaction solvents and solutions for quenching and

extractions), several quantities had to be estimated. We based these estimates on previous reports of this kind,⁴⁵ original papers on the matter^{44,103} as well as our own experience with typical laboratory procedures. A complete and transparent description of all calculations and estimates is given in the ESI.†

Route cEF and sEF

As expected, the sEF and cEF of the available routes differed significantly, both within and between methods. The sEFs in our dataset of 80 route E-factors (please see the ESI† for details) were as low as 1.8 and as high as 73.3, with most methods scoring between 10 and 30 (all kg_{waste} per kg_{product} which is omitted from hereon for clarity). In contrast, the cEFs covered more than 2 orders of magnitude, with values from 165 to 42 499 (Fig. 1). Interestingly, some methods had E-factors in a rather narrow range, whereas others displayed significant variation between substrates/routes. Downey *et al.*'s anhydrose-based method is good example of the latter. While their originally reported procedure⁷³ had quite unfavorable E-factors in a broad range (sEF = 11–53.8, cEF = 20 195–42 499, routes N1–N7 in the ESI†), the subsequently published improved protocol⁷⁴ fared much better, but still displayed considerable variability (sEF = 1.8–9.6, cEF = 1760–6017, routes N8–N13). On the other hand, alternative methods such as Fraser-Reid and colleagues' *n*-pentenyl orthoester-based procedure⁶⁷ showed little E-factor variation (sEF = 22.2–29.7, cEF = 10 590–14 495), except for substrates where glycosylation yield suffered tremendously (N32–N37).

In general, we were surprised to find how high most of these E-factors were. Both well-established and newly developed methods, and even biocatalytic approaches, typically had cEFs in the range of 5000–10 000. This significantly surpasses many other types of transformations employed in industrial settings that typically have cEFs of less than 100 per step.^{15,16}

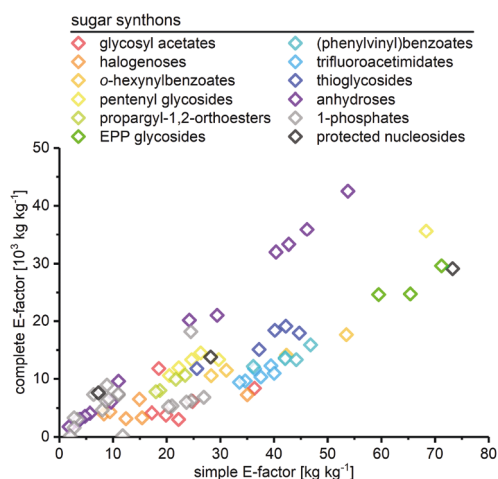


Fig. 1 Complete and simple E-factors of *N*-glycosylation methods for nucleobases cover an extensive range with great variability within and between methods. All E-factors represent route E-factors over all steps. Please see the ESI† for all details of the calculations.

While some of this may be ascribed to the fact that nucleosides are complex molecules with a high density of sensitive functional groups, these E-factors are still comparably high, considering the high demand and broad applicability of these compounds. Notably, none of the available methods performed well for all nucleobase substrates and/or delivered significantly lower E-factors than all other methods. Motivated by this lack of true efficiency¹⁰⁴ in the sense of resource usage (and consequently high waste production), we were curious to find the sources of these high E-factors and identify areas where improvement is needed. At the same time, we sought to identify strategies that worked particularly well and may be employed by future “greener” nucleoside syntheses.

Yield

Most methods in the literature for nucleoside synthesis focused on optimization of glycosylation yield as the key metric. To this end, several strategies have been developed that employ highly reactive sugar synthons or disable competition of the leaving group with the nucleobase for (re)attack at the anomeric position. In many cases, these strategies succeeded in achieving glycosylation yields upwards of 90%. However, while the yield of an individual step is certainly a critical variable, it should always be viewed in light of the entire synthesis. Indeed, we found no correlation between glycosylation yield and sEF or cEF (Fig. 2A). Many of the strategies that sought to optimize glycosylation yield also performed quite lengthy routes and employed large leaving groups. Consequently, both the total yield and the atom economy of these routes suffered immensely, which is reflected by these E-factors.

In contrast to glycosylation yield, we found that total yield (over the entire route) correlated negatively with route sEF and cEF, albeit only moderately (Fig. 2B). This comes as no surprise, as one would generally expect a higher efficiency for high-yielding routes *versus* those that barely generated any product. Nonetheless, there were some interesting outliers in the literature. The glycosylation and total yields of Downey's improved anhydrose-based approach were modest by most standards (in the range of 30% and 20%, respectively), yet this method displayed some of the lowest sEFs in our entire dataset (sEF = 1.8–9.6, see the grey diamonds in Fig. 2B).⁷⁴ By employing a concise route (2 steps) and managing the atom economy by using only one protecting group that could be cleaved *in situ*, they were able to outweigh the rather moderate yields. Obviously, these sEFs could have been even lower with higher yields under the same conditions. However, these yields were still sufficient to achieve what could be considered an efficient (lower waste) synthesis. Other methods that had higher glycosylation and total yields, for example those employing trifluoroacetimidates (>88% glycosylation yield, **N38–N43**, please see the ESI† for details) or propargyl-orthoesters⁶⁸ (>85% glycosylation yield, **N44–N47**), also necessitated longer routes and had more unfavorable atom economies, leading to much higher sEFs of 18–40. Clearly, yield is an important variable, but only to a certain extent. Even excellent yields are generally offset by cumulative reagent usage across a

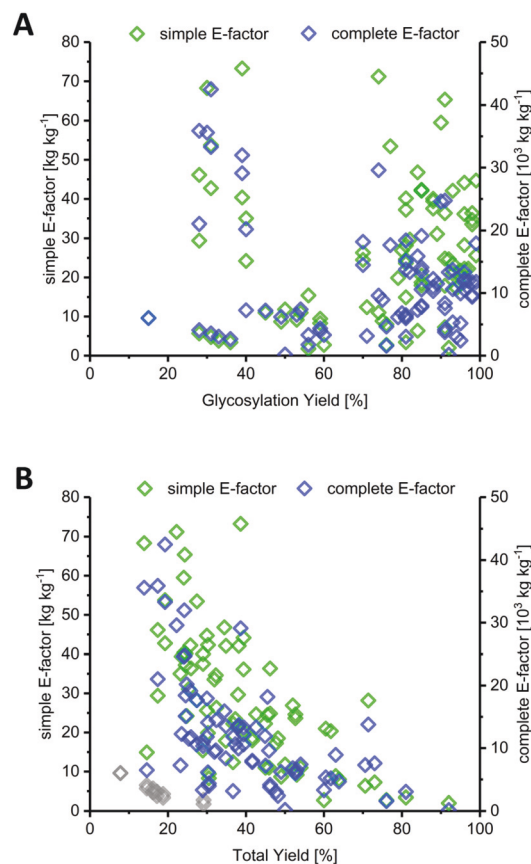


Fig. 2 Yield of the glycosylation step is a misleading predictor of method efficiency compared to total yield across the route. (A) Glycosylation yield shows no correlation with route sEF or cEF. (B) Total yield over the entire route correlates negatively with route sEF and cEF. Downey *et al.*'s improved anhydrose-based method (**N8–N13**) is shown as grey diamonds (sEF and cEF).

long route. Although yield of the key glycosylation step constitutes a bottleneck for some nucleobases, it appears that, from an efficiency standpoint, chasing maximum yields is not a fruitful strategy if it entails following longer routes.

Route length

The length of a route, as given by the number of total steps,¹⁰⁵ varied drastically among different glycosylation methods and appeared to dictate the lower bounds for possible route E-factors. The shortest available routes relied on nucleoside phosphorylases for biocatalytic glycosylation and had only one step, whereas the longest routes had around 9 to 11 steps, with several protecting group transformations. The cumulative sEFs and cEFs of all methods covered a broad range over all route lengths, and trended upwards with increasing route length (Fig. 3). This data highlights two important points for consideration. Routes employing only one step tended to perform rather favorably (sEF < 11), probably because the potential for waste accumulation in a one-step route is quite limited. On the other end of the spectrum, long routes with 9–11 steps all had sEFs higher than 40 and cEFs well above

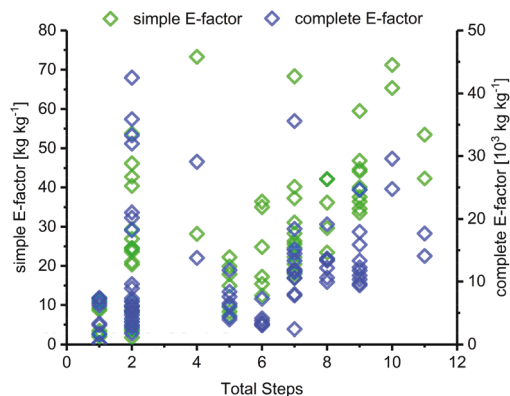


Fig. 3 sEF and cEF generally increase with route length. The total number of steps denotes the number of steps from an unprotected sugar starting material to an unprotected nucleoside. A step is considered as every transformation that was followed by a workup and/or purification of some sort.

10 000. While these routes still displayed great heterogeneity, it appears that waste accumulation to a certain extent was a natural consequence of the number of transformations. It should be noted, however, that short routes don't guarantee lower E-factors, as our dataset featured 22 routes with 2 steps (all from Downey *et al.*'s method or biocatalytic) which mostly performed favorably regarding their E-factor, but also included a few outliers with cEFs above 15 000 (Fig. 3). These data demonstrate that shorter routes do not necessarily translate to lower E-factors, but clearly have the potential to perform more efficiently than longer alternatives, especially if several protecting group transformations are involved.

E-factor contributions

Irrespective of yield and route length, the cEFs of all routes were mainly composed of solvent contributions (Fig. 4). The reagents used throughout a synthesis, as well as inorganics only added minorly to the route cEFs, as contributions from organic solvents and (for biocatalytic routes) water typically made up more than 95% of the cEF. This observation is somewhat intuitive as nucleobases and many nucleosides are generally poorly soluble in all solvents and solvents are known to be the main determiner for E-factors, if they are included in the calculation.^{11,36,44,45} Nonetheless, we were surprised to find that even routes which employed heterogenous steps were characterized by overshadowing solvent contributions. Biocatalytic routes were particularly plagued by the low water solubility of many nucleobases, which has so far largely restricted these syntheses to working concentrations in the low millimolar range. However, some routes which sought to prepare especially insoluble guanosine derivatives used this to their advantage to realize the lowest cEFs in our dataset. Zuffi *et al.*'s⁸² (cEF = 200, route N29) and Ubiali *et al.*'s⁸³ (cEF = 165, route N31) one-step syntheses of 2'-deoxyguanosine from thymidine *via* transglycosylation employed a substrate loading which was an order of magnitude higher than other biocatalytic

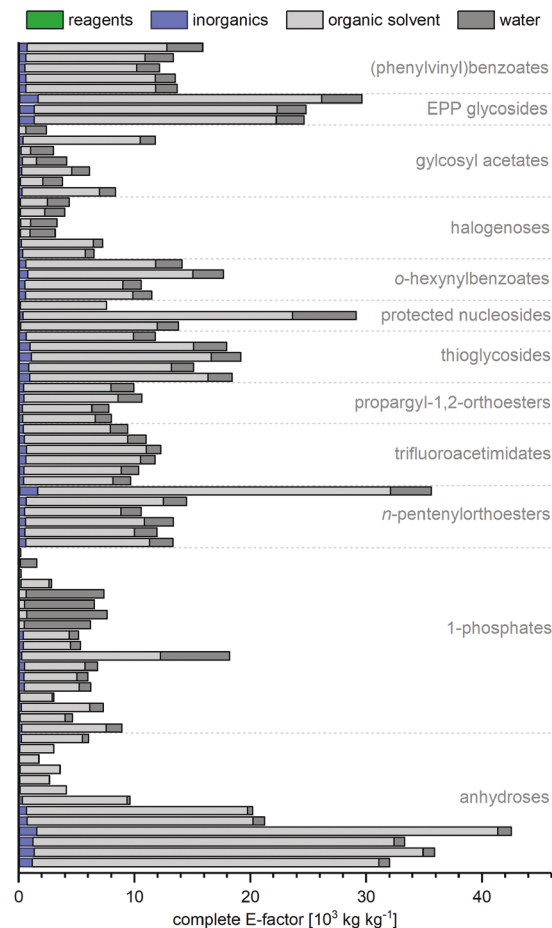


Fig. 4 Complete E-factors of nearly all routes are mainly composed of solvent contributions. All contributions are also given in the ESI† with reference to the procedure and details for calculation.

routes and profited from the target compound readily precipitating from the reaction mixture. Thus, the higher substrate loading in heterogenous reaction steps appears particularly attractive for sugar or nucleobase transformations. Based on our data it could be reasoned that (beyond heterogenous reactions) any strategy that allows higher substrate/reagent loading will result in lower E-factors. Yet even if one or multiple steps of a route can be realized heterogeneously, or with otherwise high substrate loading, solvent contributions from other steps may still be the main contributors to the cEF of that route. Again, this underscores that the demands and opportunities of a single step need to be considered as part of the entire route, and that shorter routes offer more potential for minimizing E-factors. It should also be noted that we did not consider recycling of any solvents in this analysis. Clearly, some solvents can be and are recycled in industrial settings to reduce the net waste arising from a reaction, especially in the case of low-boiling solvents such as dichloromethane or hexane. However, other solvents like pyridine, water or acetonitrile may be harder and much more energy-intensive to recover, purify and reuse. Thus, given the heterogeneity of sol-

vents employed and their role in the respective syntheses, we opted to consider all solvents as waste without any recycling.

Chromatography

Solvent contributions for many steps originated to a large extent from chromatographic purification steps. In fact, the number of chromatography steps was equally good at setting the lower bounds for cEF as the total number of steps in a route – irrespective of the transformations, yields and types of workup performed (Fig. 5). It should be noted that very few syntheses in our dataset included quantities for their chromatography solvents, which required us to estimate these for most of the routes discussed herein. Like Hollmann and colleagues,⁴⁵ we estimated 500 mL of solvent per gram of crude product and calculated the E-factor contributions *via* the density of the chromatography solvents employed (which are generally reported). Depending on the solvent used and the crude product, this equaled a cEF contribution of around 500–1500 per chromatography step in most cases. Considering published experimental data on this issue,^{44,103} and the fact that most chromatography steps in our dataset were done to isolate material from complex mixtures, this is a very conservative estimate for most syntheses analyzed here. Still, chromatography solvents dominated the cEFs of all routes that employed chromatographic purifications. Naturally, longer routes featured more chromatography steps, which is reflected in their cEFs (see *e.g.* N50–N52 or N56–N59). Conversely, the two routes that did not employ any chromatography steps (N29 and N31, see above) had the by far lowest cEFs. Admittedly, chromatography probably cannot be avoided altogether given the nature of the transformations required for nucleoside synthesis but limiting chromatography steps should be a primary goal to achieve more efficient and “greener” nucleoside synthesis.

Protecting groups

All non-biocatalytic syntheses considered herein employed protected sugar synthons, whose synthesis constitutes the most

labor- and resource-intensive part of the route. Most sugar synthons need to be accessed in 3–7 steps from (deoxy)ribose through selective protection and introduction of the anomeric leaving group. Thus, the synthesis of these synthons accumulates a considerable E-factor even before the key glycosylation step. Even though yields for the required transformations are generally high to excellent, reagent usage and purification throughout these routes is reflected in the high sEFs and cEFs (Chart 1). Please note that these E-factors are somewhat skewed by the high molecular weights of the protected synthons and may not directly translate to full route E-factors since the E-factor is a mass-based metric, and the nucleoside products are generally a lot lighter than these synthons. Exceptions to these observations are presented by biocatalytic routes^{77–83} requiring no protecting groups (which considerably shortens these syntheses by all protecting and deprotecting steps) and Downey's method^{73,74} which only employs one (albeit large) protecting group, that can be installed in one step and cleaved *in situ* after the reaction. The only other method that consistently delivered E-factors close to these two approaches is halogenose-based glycosylation, which uses an easy to prepare synthon with a small leaving group. Clearly, the non-biocatalytic synthesis of nucleosides requires at least some protecting groups due to the complex arrangement of reactive functional groups in the target compounds. However, the choice of protecting groups and synthon for glycosylation should be made based on the most concise and efficient route to that synthon. Every protecting and deprotecting step that can be avoided in a synthesis typically results in lower waste production through a better atom economy and less purification effort.

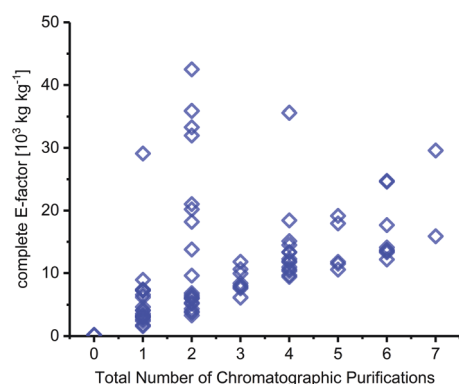


Fig. 5 The number of chromatography steps sets the lower bounds for route cEF. For all details regarding calculation of chromatography contributions to cEF, please see the ESI†

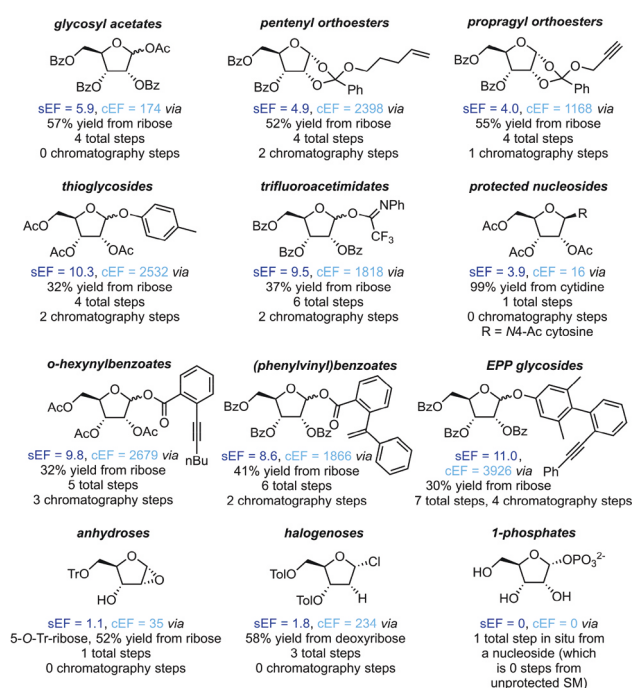


Chart 1 Please see the ESI† for procedures and references.

Transitioning to more efficient nucleoside synthesis

Benchmarks

Based on these observations, we propose some benchmarks for nucleoside synthesis to be termed “efficient”. Future synthetic efforts should seek to achieve sEFs below 10 and cEFs below 2000 in a route that takes 4 steps or less. We explicitly opt against inclusion of any recommendations regarding glycosylation or total yield, protecting groups, solvent usage or chromatographic purifications. However, a balance and improvement of all these metrics will be reflected in the E-factor. We chose to include route length as a relevant parameter, since the average step for nucleoside synthesis took roughly one day (Fig. S1†) and time investment in a synthesis is certainly a relevant factor. Selected routes in our dataset already meet these benchmarks (N11 and N29–N31), although only for some purines. We believe that there is potential for nucleoside synthesis to become more efficient in general by striving to meet these proposed benchmarks. To this end, there are some areas which require and deserve attention by researchers to effect immediate improvement.

Areas for improvement

The above data illustrate that nucleoside synthesis is currently hampered by several bottlenecks that manifest themselves in inefficient routes with high E-factors. Most notably, chromatographic purification steps present a significant source of waste in the form of solvent. Although some of this solvent may be recycled to reduce the net waste from these steps, they remain notoriously inefficient separation processes from a sustainability perspective. However, at least one chromatography step will probably be required for most target nucleosides to achieve sufficient purity, since *N*-glycosylation is a non-trivial transformation that (beyond the desired nucleoside) often yields several hard-to-separate byproducts. Thus, reduction of additional chromatography steps should be a central aim for all synthetic routes to the relevant sugar synthons. Whenever possible, precipitation or recrystallization steps allow tremendously lower resource investment and, therefore, lower E-factors. For some of the routes outlined above, it would also be worth considering if some of the steps required for either sugar donor synthesis or post-glycosylation deprotection could be performed in a one-pot manner to avoid intermediary purifications. This may also help to cut down the use of solvents like dichloromethane or hexane which serve as popular extraction and purification solvents but are recognized as environmentally concerning.¹⁰⁶ To facilitate these aims, applied routes should be as short as possible, since additional steps such as protecting group manipulations on the sugar moiety have the potential to render the entire route inefficient – irrespective of metrics such as glycosylation or total yield. Therefore, glycosylation approaches which employ few protecting groups and do not rely on large leaving groups (which themselves necessitate prior installment) appear to have the

most potential going forward. Future efforts to optimize existing methods or devise new methods may therefore focus on avoiding chromatography, shortening routes and/or doing multiple transformations in one pot. Furthermore, heterogeneous reactions present an attractive strategy to cut down non-chromatography solvent waste, particularly since nucleosides are generally poorly soluble. This holds especially true for biocatalytic approaches which are currently severely hampered by the low water solubility of both the starting materials and products, as well as unfavorable reaction equilibria for some nucleosides. To overcome these obstacles, strategies to enable increased substrate loading and equilibrium shifts in favor of the target nucleosides should be key research goals.

Conclusions

Nucleosides and their analogs are indispensable biomolecules in nearly all areas of life science. However, the available methods to prepare these compounds *via N*-glycosylation of nucleobases suffer from severe drawbacks, which render these routes laborious and inefficient. Our comprehensive literature survey and E-factor analysis revealed that glycosylation methods for nucleoside synthesis cover an extended range of route E-factors and that glycosylation yield is an overrated metric of efficiency. Solvents, predominantly from chromatographic purification steps, are the main contributors to cEF and a heavy reliance on protecting groups tremendously increased both the sEF and cEF of most routes. Future syntheses should seek to address these bottlenecks to enable more efficient and sustainable nucleoside syntheses.

Conflicts of interest

A. K. is CEO of the biotech company BioNukleo GmbH. F. K. is a scientist at BioNukleo GmbH and P. N. is a member of the advisory board. These affiliations constitute no conflict of interest with the results presented and discussed in this report.

Acknowledgements

The authors thank Kerstin Heinecke (TU Berlin) for fruitful discussions.

Notes and references

- 1 K. Ruiz-Mirazo, C. Briones and A. de la Escosura, *Chem. Rev.*, 2014, **114**, 285–366.
- 2 L. P. Jordheim, D. Durantel, F. Zoulim and C. Dumontet, *Nat. Rev. Drug Discovery*, 2013, **12**, 447–464.
- 3 W. Xu, K. M. Chan and E. T. Kool, *Nat. Chem.*, 2017, **9**, 1043–1055.

- 4 C. Y. Jao and A. Salic, *Proc. Natl. Acad. Sci. U. S. A.*, 2008, **105**, 15779–15784.
- 5 T. G. Allen-Merish, S. Earlam, C. Fordy, K. Abrams and J. Houghton, *Lancet*, 1994, **344**, 1255–1260.
- 6 D. Schürmann, D. J. Rudd, S. Zhang, I. De Lepeleire, M. Robberechts, E. Friedman, C. Keicher, A. Hüser, J. Hofmann, J. A. Grobler, *et al.*, *Lancet HIV*, 2020, **7**, 164–172.
- 7 H. Vorbrüggen and C. Ruh-Pohlenz, *Org. React.*, 2004, **1**, 630.
- 8 P. Anastas and N. Eghbali, *Chem. Soc. Rev.*, 2010, **39**, 301–312.
- 9 R. A. Sheldon, *Green Chem.*, 2017, **19**, 18–43.
- 10 D. J. C. Constable, P. J. Dunn, J. D. Hayler, G. R. Humphrey, J. Leazer, L. Johnnie, R. J. Linderman, K. Lorenz, J. Manley, B. A. Pearlman, A. Wells, *et al.*, *Green Chem.*, 2007, **9**, 411–420.
- 11 C. Jimenez-Gonzalez, C. S. Ponder, Q. B. Broxterman and J. B. Manley, *Org. Process Res. Dev.*, 2011, **15**, 912–917.
- 12 H. Loureiro, M. Prem and G. Wuitschik, *Chim. Int. J. Chem.*, 2019, **73**, 724–729.
- 13 D. Kaiser, J. Yang and G. Wuitschik, *Org. Process Res. Dev.*, 2018, **22**, 1222–1235.
- 14 T. Li and X. Li, *Green Chem.*, 2014, **16**, 4241–4256.
- 15 J. Li, J. Albrecht, A. Borovika and M. D. Eastgate, *ACS Sustainable Chem. Eng.*, 2018, **6**, 1121–1132.
- 16 J. Li, E. M. Simmons and M. D. Eastgate, *Green Chem.*, 2017, **19**, 127–139.
- 17 J. Li and M. D. Eastgate, *React. Chem. Eng.*, 2019, **4**, 1595–1607.
- 18 E. R. Monteith, P. Mampuy, L. Summerton, J. H. Clark, B. U. W. Maes and C. R. McElroy, *Green Chem.*, 2020, **22**, 123–135.
- 19 A. G. Parvatker, H. Tunceroglu, J. D. Sherman, P. Coish, P. Anastas, J. B. Zimmerman and M. J. Eckelman, *ACS Sustainable Chem. Eng.*, 2019, **7**, 6580–6591.
- 20 J. Tian, H. Shi, X. Li, Y. Yin and L. Chen, *Green Chem.*, 2012, **14**, 1990–2000.
- 21 G. Rosini, V. Borzatta, C. Paolucci and P. Righi, *Green Chem.*, 2008, **10**, 1146–1151.
- 22 Z. Amara, J. F. B. Bellamy, R. Horvath, S. J. Miller, A. Beeby, A. Burgard, K. Rossen, M. Poliakov and M. W. George, *Nat. Chem.*, 2015, **7**, 489–495.
- 23 J. Andraos, *Org. Process Res. Dev.*, 2009, **13**, 161–185.
- 24 J. Andraos, E. Ballerini and L. Vaccaro, *Green Chem.*, 2015, **17**, 913–925.
- 25 S. K. Ma, J. Gruber, C. Davis, L. Newman, D. Gray, A. Wang, J. Grate, G. W. Huisman and R. A. Sheldon, *Green Chem.*, 2010, **12**, 81–86.
- 26 K. C. Badgular and B. M. Bhanage, *Biomass Bioenergy*, 2016, **84**, 12–21.
- 27 E. Busto, R. C. Simon, B. Grischek, V. Gotor-Fernández and W. Kroutil, *Adv. Synth. Catal.*, 2014, **356**, 1937–1942.
- 28 A. Cavezza, C. Boule, A. Guéguiniat, P. Pichaud, S. Trouille, L. Ricard and M. Dalko-Csiba, *Bioorg. Med. Chem. Lett.*, 2009, **19**, 845–849.
- 29 F. Fringuelli, D. Lanari, F. Pizzo and L. Vaccaro, *Green Chem.*, 2010, **12**, 1301–1305.
- 30 Y. Gaber, U. Törnqvall, C. Orellana-Coca, M. Ali Amin and R. Hatti-Kaul, *Green Chem.*, 2010, **12**, 1817–1825.
- 31 S. M. Kelly and B. H. Lipshutz, *Org. Lett.*, 2014, **16**, 98–101.
- 32 D. Kuhn, M. K. Julsing, E. Heinzle and B. Bühler, *Green Chem.*, 2012, **14**, 645–653.
- 33 D. Kuhn, M. A. Kholiq, E. Heinzle, B. Bühler and A. Schmid, *Green Chem.*, 2010, **12**, 815–827.
- 34 A. Ledoux, L. Sandjong Kuigwa, E. Framery and B. Andrioletti, *Green Chem.*, 2015, **17**, 3251–3254.
- 35 J. Liang, J. Lalonde, B. Borup, V. Mitchell, E. Mundorff, N. Trinh, D. A. Kochrekar, R. Nair Cherat and G. G. Pai, *Org. Process Res. Dev.*, 2010, **14**, 193–198.
- 36 B. H. Lipshutz, N. A. Isley, J. C. Fennewald and E. D. Slack, *Angew. Chem., Int. Ed.*, 2013, **52**, 10952–10958.
- 37 S. Handa, J. C. Fennewald and B. H. Lipshutz, *Angew. Chem., Int. Ed.*, 2014, **53**, 3432–3435.
- 38 B. H. Lipshutz and S. Ghorai, *Green Chem.*, 2014, **16**, 3660–3679.
- 39 L. Martínez-Montero, V. Gotor, V. Gotor-Fernández and I. Lavandera, *Green Chem.*, 2017, **19**, 474–480.
- 40 O. Maurin, P. Verdié, G. Subra, F. Lamaty, J. Martinez and T.-X. Métro, *Beilstein J. Org. Chem.*, 2017, **13**, 2087–2093.
- 41 T.-X. Métro, J. Bonnamour, T. Reidon, A. Duprez, J. Sarpoulet, J. Martinez and F. Lamaty, *Chem. – Eur. J.*, 2015, **21**, 12787–12796.
- 42 A. R. C. Morais, S. Dworakowska, A. Reis, L. Gouveia, C. T. Matos, D. Bogdał and R. Bogel-Lukasik, *Catal. Today*, 2015, **239**, 38–43.
- 43 A. Palmieri, S. Gabrielli and R. Ballini, *Green Chem.*, 2013, **15**, 2344–2348.
- 44 M. L. Parisi, A. Dessi, L. Zani, S. Maranghi, S. Mohammadpourasl, M. Calamante, A. Mordini, R. Basosi, G. Reginato and A. Sinicropi, *Front. Chem.*, 2020, **8**, 214.
- 45 J. H. Schrittwieser, F. Coccia, S. Kara, B. Grischek, W. Kroutil, N. d'Alessandro and F. Hollmann, *Green Chem.*, 2013, **15**, 3318–3331.
- 46 R. A. Sheldon, *Green Chem.*, 2007, **9**, 1273–1283.
- 47 R. A. Sheldon, *J. R. Soc., Interface*, 2016, **13**, 20160087.
- 48 F. Roschangar, J. Colberg, P. J. Dunn, F. Gallou, J. D. Hayler, S. G. Koenig, M. E. Kopach, D. K. Leahy, I. Mergelsberg, J. L. Tucker, *et al.*, *Green Chem.*, 2017, **19**, 281–285.
- 49 R. A. Sheldon, *ACS Sustainable Chem. Eng.*, 2018, **6**, 32–48.
- 50 R. A. Sheldon, *Green Chem.*, 2016, **18**, 3180–3183.
- 51 M. A. F. Delgove, A.-B. Laurent, J. M. Woodley, S. M. A. De Wildeman, K. V. Bernaerts and Y. van der Meer, *ChemSusChem*, 2019, **12**, 1349–1360.
- 52 M. C. McManus and C. M. Taylor, *Biomass Bioenergy*, 2015, **82**, 13–26.
- 53 A. A. Burgess and D. J. Brennan, *Chem. Eng. Sci.*, 2001, **56**, 2589–2604.
- 54 F. Tieves, F. Tonin, E. Fernández-Fueyo, J. M. Robbins, B. Bommarius, A. S. Bommarius, M. Alcalde and F. Hollmann, *Tetrahedron*, 2019, **75**, 1311–1314.

- 55 U. Niedballa and H. Vorbrüggen, *Angew. Chem., Int. Ed. Engl.*, 1970, **9**, 461–462.
- 56 H. O. Kim, *Arch. Pharmacol. Res.*, 2001, **24**, 508–513.
- 57 V. Parmenopoulou, D. S. M. Chatzileontiadou, S. Manta, S. Bougiatioti, P. Maragozidis, D.-N. Gkaragkouni, E. Kaffesaki, A. L. Kantsadi, V. T. Skamnaki, S. E. Zographos, *et al.*, *Bioorg. Med. Chem.*, 2012, **20**, 7184–7193.
- 58 H. Shirouzu, H. Morita and M. Tsukamoto, *Tetrahedron*, 2014, **70**, 3635–3639.
- 59 C. Moreau, T. Kirchberger, J. M. Swarbrick, S. J. Bartlett, R. Fliegert, T. Yorgan, A. Bauche, A. Harneit, A. H. Guse and B. V. L. Potter, *J. Med. Chem.*, 2013, **56**, 10079–10102.
- 60 D. Hocková, M. Hocek, H. Dvořáková and I. Votruba, *Tetrahedron*, 1999, **55**, 11109–11118.
- 61 D. Ackermann and M. Famulok, *Nucleic Acids Res.*, 2013, **41**, 4729–4739.
- 62 J. N. Freskos, *Nucleosides Nucleotides*, 1989, **8**, 549–555.
- 63 Z. Kazimierzczuk, H. B. Cottam, G. R. Revankar and R. K. Robins, *J. Am. Chem. Soc.*, 1984, **106**, 6379–6382.
- 64 Q. Zhang, J. Sun, Y. Zhu, F. Zhang and B. Yu, *Angew. Chem., Int. Ed.*, 2011, **50**, 4933–4936.
- 65 P. Li, H. He, Y. Zhang, R. Yang, L. Xu, Z. Chen, Y. Huang, L. Bao and G. Xiao, *Nat. Commun.*, 2020, **11**, 405–414.
- 66 Z. Hu, Y. Tang and B. Yu, *J. Am. Chem. Soc.*, 2019, **141**, 4806–4810.
- 67 B. Fraser-Reid, P. Ganney, C. V. S. Ramamurty, A. M. Gómez and J. C. López, *Chem. Commun.*, 2013, **49**, 3251–3253.
- 68 B. V. Rao, S. Manmode and S. Hotha, *J. Org. Chem.*, 2015, **80**, 1499–1505.
- 69 J. Liao, J. Sun and B. Yu, *Tetrahedron Lett.*, 2008, **49**, 5036–5038.
- 70 J. Liao, J. Sun and B. Yu, *Carbohydr. Res.*, 2009, **344**, 1034–1038.
- 71 G. Liu, X. Zhang and G. Xing, *Chem. Commun.*, 2015, **51**, 12803–12806.
- 72 K. Chow and S. Danishefsky, *J. Org. Chem.*, 1990, **55**, 4211–4214.
- 73 A. M. Downey, C. Richter, R. Pohl, R. Mahrwald and M. Hocek, *Org. Lett.*, 2015, **17**, 4604–4607.
- 74 A. M. Downey, R. Pohl, J. Roithová and M. Hocek, *Chem. – Eur. J.*, 2017, **23**, 3910–3917.
- 75 S. Kamel, H. Yehia, P. Neubauer and A. Wagner, in *Enzym. Chem. Synth. Nucleic Acid Deriv.*, 2019, pp. 1–28.
- 76 F. Kaspar, R. T. Giessmann, K. F. Hellendahl, P. Neubauer, A. Wagner and M. Gimpel, *ChemBioChem*, 2020, **21**, 1428–1432.
- 77 M. S. Drenichev, C. S. Alexeev, N. N. Kurochkin and S. N. Mikhailov, *Adv. Synth. Catal.*, 2018, **360**, 305–312.
- 78 C. S. Alexeev, M. S. Drenichev, E. O. Dorinova, R. S. Esipov, I. V. Kulikova and S. N. Mikhailov, *Biochim. Biophys. Acta, Proteins Proteomics*, 2020, **1868**, 140292.
- 79 V. N. Barai, A. I. Zinchenko, L. A. Eroshevskaya, E. N. Kalinichenko, T. I. Kulak and I. A. Mikhailopulo, *Helv. Chim. Acta*, 2002, **85**, 1901–1908.
- 80 H. Yehia, S. Westarp, V. Röhrs, F. Kaspar, T. R. Giessmann, F. T. H. Klare, K. Paulick, P. Neubauer, J. Kurreck and A. Wagner, *Molecules*, 2020, **25**, 934.
- 81 X. Zhou, K. Szeker, L.-Y. Jiao, M. Oestreich, I. A. Mikhailopulo and P. Neubauer, *Adv. Synth. Catal.*, 2015, **357**, 1237–1244.
- 82 G. Zuffi, D. Ghisotti, I. Oliva, E. Capra, G. Frascotti, G. Tonon and G. Orsini, *Biocatal. Biotransform.*, 2004, **22**, 25–33.
- 83 D. Ubiali, S. Rocchietti, F. Scaramozzino, M. Terreni, A. M. Albertini, R. Fernández-Lafuente, J. M. Guisán and M. Pregnotato, *Adv. Synth. Catal.*, 2004, **346**, 1361–1366.
- 84 M. A. Huffman, A. Fryszkowska, O. Alvizo, M. Borra-Garske, K. R. Campos, K. A. Canada, P. N. Devine, D. Duan, J. H. Forstater, S. T. Grosser, *et al.*, *Science*, 2019, **366**, 1255–1259.
- 85 F. Kaspar, R. T. Giessmann, P. Neubauer, A. Wagner and M. Gimpel, *Adv. Synth. Catal.*, 2020, **362**, 867–876.
- 86 T. Azuma and K. Isono, *Chem. Pharm. Bull.*, 1977, **25**, 3347–3353.
- 87 M. Miyaki, A. Saito and B. Shimizu, *Chem. Pharm. Bull.*, 1970, **18**, 2459–2468.
- 88 J. Boryski, *Nucleosides Nucleotides*, 1998, **17**, 1547–1556.
- 89 O. V. Andreeva, M. G. Belenok, L. F. Saifina, M. M. Shulaeva, A. B. Dobrynin, R. R. Sharipova, A. D. Voloshina, A. F. Saifina, A. T. Gubaidullin, B. I. Khairutdinov, *et al.*, *Tetrahedron Lett.*, 2019, **60**, 151276.
- 90 Y. Kawase, M. Koizumi, S. Iwai and E. Ohtsuka, *Chem. Pharm. Bull.*, 1989, **37**, 2313–2317.
- 91 H. M. Kissman, C. Pidacks and B. R. Baker, *J. Am. Chem. Soc.*, 1955, **77**, 18–24.
- 92 N.-S. Li and J. A. Piccirilli, *Synthesis*, 2005, **2005**, 2865–2870.
- 93 Q. Liu, X. Cai, D. Yang, Y. Chen, Y. Wang, L. Shao and M.-W. Wang, *Bioorg. Med. Chem.*, 2017, **25**, 4579–4594.
- 94 P. Nauš, O. Caletková, P. Konečný, P. Džubák, K. Bogdanová, M. Kolář, J. Vrbková, L. Slavětinská, E. Tloušťová, P. Perlíková, *et al.*, *J. Med. Chem.*, 2014, **57**, 1097–1110.
- 95 R. K. Ness and H. G. Fletcher, *J. Am. Chem. Soc.*, 1953, **75**, 3289–3290.
- 96 I. Nowak, M. Conda-Sheridan and M. J. Robins, *J. Org. Chem.*, 2005, **70**, 7455–7458.
- 97 A. Nudelman, J. Herzig, H. E. Gottlieb, E. Keinan and J. Sterling, *Carbohydr. Res.*, 1987, **162**, 145–152.
- 98 V. Rolland, M. Kotera and J. Lhomme, *Synth. Commun.*, 1997, **27**, 3505–3511.
- 99 C. V. S. Ramamurty, P. Ganney, C. S. Rao and B. Fraser-Reid, *J. Org. Chem.*, 2011, **76**, 2245–2247.

- 100 M. Thomas, J.-P. Gesson and S. Papot, *J. Org. Chem.*, 2007, **72**, 4262–4264.
- 101 S. A. Thadke, B. Mishra and S. Hotha, *J. Org. Chem.*, 2014, **79**, 7358–7371.
- 102 M. Kurosu and K. Li, *J. Org. Chem.*, 2008, **73**, 9767–9770.
- 103 F. Pessel, J. Augé, I. Billault and M.-C. Scherrmann, *Beilstein J. Org. Chem.*, 2016, **12**, 2351–2357.
- 104 'Efficiency' is typically defined as the ability to obtain a result or desired product in a way that does not waste resources in the form of materials, money or time. Herein, we focus on the aspect of resource efficiency as quantified by the E-factor.
- 105 We herein considered a step as any kind or number of transformations which was followed by a workup and/or purification of some sort.
- 106 C. M. Alder, J. D. Hayler, R. K. Henderson, A. M. Redman, L. Shukla, L. E. Shuster and H. F. Sneddon, *Green Chem.*, 2016, **18**, 3879–3890.

Paper II

Kaspar, F.; Giessmann, R.T.; Westarp, S.; Hellendahl, K.F.; Krausch, N.; Thiele, I.; Walczak, M.C.; Neubauer, P.; Wagner, A. Spectral Unmixing-Based Reaction Monitoring of Transformations Between Nucleosides and Nucleobases. *ChemBioChem* **2020**, *21*, 2604, <https://doi.org/10.1002/cbic.202000204>.

This article was published as open access under a CC BY license which permits reproduction of the material with proper attribution, such as in this thesis.

Author contributions (with definitions by Brand *et al.* ¹)

Conceptualization, F.K.; Data curation, F.K. and R.T.G.; Formal analysis, F.K., R.T.G. and N.K.; Funding acquisition, R.T.G., P.N. and A.W.; Investigation, F.K., S.W., K.F.H., I.T. and C.W.; Methodology, F.K., R.T.G. and N.K.; Project administration, F.K.; Resources, R.T.G., A.W. and P.N.; Software, R.T.G. and N.K.; Supervision, F.K.; Validation, - ; Visualization, F.K.; Writing—original draft, F.K.; Writing—review & editing, F.K., R.T.G., S.W., K.F.H., N.K., I.T., C.W., P.N. and A.W.

Specifically, my contribution included development of robust and transferable conditions as well as the development of alternative quenching and sample treatment protocols enabling analysis of nucleosides with sensitive UV absorption spectra. Further, I developed and evaluated principles for background management and designed and performed the experiments in the publication. I curated the data, illustrated the publication and lead the writing. As this work was featured on the cover of *ChemBioChem* (<https://doi.org/10.1002/cbic.202000569>), I co-designed the artwork with Annie Voigt.

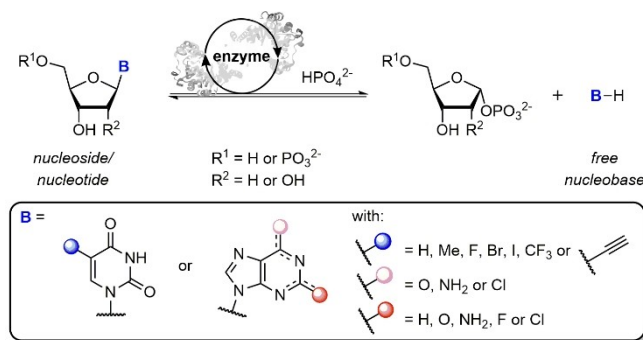
Preamble

Much of the work presented in this thesis heavily relied on high throughput experimentation enabled by an efficient analytical tool. Like many others, our group had historically relied on HPLC analysis of enzymatic reaction mixtures for kinetic experiments, screenings and general reaction monitoring. Although some non-HPLC methods for the monitoring of nucleoside phosphorolysis reactions were known from the literature, none of these satisfied the needs of our reactions featuring unconventional substrates and high temperatures. Sparked by the observation that nucleosides and their nucleobases have different UV absorption spectra at pH 12+ as reported by Fox, Sugar and Wittenburg in the 1950s and 60s, Robert Giessmann and Niels Krausch had developed an assay for thymidine phosphorolysis which employed base-induced spectral shifts around the time I joined the institute. In collaboration with Robert, I extended this method to a spectrum of other nucleosides, exploiting a deprotonation-driven aromatization and spectral shift of free nucleobases which allowed their discrimination from the corresponding nucleosides. Although the respective spectra still overlapped significantly and background absorption continues to be the prime challenge, I developed analysis conditions and sample treatment protocols which enabled spectral deconvolution of pyrimidines and purines alike. As of this thesis, this versatile method has put through north of 18,000 datapoints and has risen to become the to-go method for reaction monitoring in our group.

Spectral Unmixing-Based Reaction Monitoring of Transformations between Nucleosides and Nucleobases**

Felix Kaspar,^{*,[a, b]} Robert T. Giessmann,^[a] Sarah Westarp,^[a, b] Katja F. Hellendahl,^[a] Niels Krausch,^[a] Isabel Thiele,^[a] Miriam C. Walczak,^[a, b] Peter Neubauer,^[a] and Anke Wagner^{*,[a, b]}

The increased interest in (enzymatic) transformations between nucleosides and nucleobases has demanded the development of efficient analytical tools. In this report, we present an update and extension of our recently described method for monitoring these reactions by spectral unmixing. The presented method uses differences in the UV absorption spectra of nucleosides and nucleobases after alkaline quenching to derive their ratio based on spectral shape by fitting normalized reference spectra. It is applicable to a broad compound spectrum comprising more than 35 examples, offers HPLC-like accuracy, ease of handling and significant reductions in both cost and data acquisition time compared to other methods. This contribution details the principle of monitoring reactions by spectral unmixing, gives recommendations regarding solutions to common problems and applications that necessitate special sample treatment. We provide software, workflows and reference spectra that facilitate the straightforward and versatile application of the method.



Scheme 1. Nucleoside/nucleotide phosphorolysis of pyrimidine or purine species. With the exceptions of cytosine and 1,2,4-triazole-3-carboxamide, all nucleobases featured in this report are described.

Nucleoside-altering enzymes harbor significant potential for the synthesis of nucleoside analogues. Nucleoside phosphorylases (NPs), for instance, catalyze the reversible phosphorolytic cleavage of nucleosides into the corresponding free nucleobase and pentose-1-phosphate (Scheme 1) and are widely applied for the preparation of modified nucleosides.^[1–11] Consequently, their kinetic and thermodynamic characterization has attracted increased interest and demanded the development of efficient analytical tools.^[12,13]

Recently, we reported a UV/Vis spectroscopy-based method for the monitoring of these reactions that largely eliminated the need for HPLC.^[14] For this method, we employed spectral unmixing to derive nucleoside/nucleobase ratios from experimental UV absorption spectra based on suitable reference spectra. Implemented into the workflow of a high-throughput assay, this methodology facilitated a >20-fold reduction of data acquisition time and a roughly fivefold decrease in cost compared to conventional HPLC, while maintaining very comparable accuracy and excellent reproducibility. Unlike other non-HPLC-based methods,^[15–27] our approach offers a uniquely broad substrate spectrum, including all natural and several examples of modified nucleosides, as well as high adaptability and the straightforward application to any substrate without the need for laborious method development.

Following the initial report of our method, it has found wide-spread use in our laboratory and was successfully applied to several projects. Most notably, previous spectral characterization of a range of nucleoside substrates and their corresponding nucleobases enabled the investigation of the thermodynamic reaction control of nucleoside phosphorolysis.^[12] Here we were able to measure slight temperature-induced changes of reaction equilibria of the phosphorolysis of 24 nucleosides that allowed convenient experimental access to thermodynamic properties of those reactions. Knowledge of the UV absorption spectra of nucleosides and nucleobases also enabled qualitative reaction monitoring of nucleoside transglycosylations to determine the time to equilibrium and reduce sampling effort.^[11] Further work to employ our method for the kinetic character-

[a] F. Kaspar, R. T. Giessmann, S. Westarp, K. F. Hellendahl, N. Krausch, I. Thiele, M. C. Walczak, Prof. Dr. P. Neubauer, Dr. A. Wagner
Institute of Biotechnology, Chair of Bioprocess Engineering
Technische Universität Berlin
ACK 24, Ackerstraße 76, 13355 Berlin (Germany)
E-mail: anke.wagner@tu-berlin.de

[b] F. Kaspar, S. Westarp, M. C. Walczak, Dr. A. Wagner
BioNukleo GmbH
Ackerstraße 76, 13355 Berlin (Germany)
E-mail: felix.kaspar@web.de

[**] A previous version of this manuscript has been deposited on a preprint server (<https://doi.org/10.26434/chemrxiv.12044424.v1>)

Supporting information for this article is available on the WWW under <https://doi.org/10.1002/cbic.202000204>

© 2020 The Authors. Published by Wiley-VCH Verlag GmbH & Co. KGaA. This is an open access article under the terms of the Creative Commons Attribution License, which permits use, distribution and reproduction in any medium, provided the original work is properly cited.

ization of several NPs across their broad working space to probe the limits of their tolerance to harsh reaction conditions is currently underway.^[28] In addition, this method has greatly aided our efforts to explore the substrate spectra of other nucleobase-cleaving enzymes,^[29] empowered screening projects^[30] and overall alleviated our dependence on HPLC.^[31] Ultimately, these examples showcase the remarkable potential of our spectral unmixing-based method for high sample throughput and efficient monitoring of nucleobase cleavage reactions.

In this update we expand the scope of established substrates, share our experience and recommendations regarding solutions to common problems and describe some examples of alternative uses of the original method that necessitate deviation from the previously reported protocol. This contribution highlights the utility of spectral unmixing for the monitoring and analysis of (enzymatic) nucleobase cleavage reactions and will prove helpful to all current and future users of our previously published method.^[14]

The principle of reaction monitoring by spectral unmixing

Spectral unmixing in this case describes the concept of linear combination of absorption spectra that can be traced back to its individual components. In this sense, any mixture of two (or more) compounds with known absorption spectra can be deconvoluted into its constituents if appropriate reference spectra are available.^[32]

Our method for monitoring of nucleobase cleavage reactions employs this concept by deriving nucleoside/nucleobase ratios from experimental spectra recorded after alkaline dilution of samples from a reaction mixture.^[14] Under alkaline conditions the UV absorption spectra of nucleosides and nucleobases (Figure 1A) differ sufficiently to allow discrimination (Figure 1B).^[33–35] Therefore, previously recorded reference spectra can be fitted to a background-corrected experimental spectrum (Figure 1C) to determine the contribution and ratio of its individual constituents (namely substrate and product of the reaction). This approach allows for efficient reaction monitoring when multiple UV absorption spectra from a given reaction are available and can be deconvoluted into their individual components to derive the respective degree of conversion (Figure 1D). Conveniently, nearly all nucleoside-nucleobase pairs display an isosbestic point of base cleavage that allows for normalization to correct for differences in signal intensity which in turn eliminates potential errors from pipetting inaccuracy. At the isosbestic point, the nucleoside and nucleobase in question possess the same extinction coefficient which manifests itself as a constant signal intensity at this wavelength throughout a reaction (see Figure 1D for the pair of 1 and 3).

In this workflow, alkaline dilution of the sample serves a threefold purpose. This step simultaneously terminates the reaction by denaturing the enzyme, adjusts the concentration of the analytes and regulates the pH value of the sample to achieve deprotonation and spectral shifting of the UV absorption spectra. The suitable degree of alkaline dilution as well as

the concentration of the base used for dilution (in our case aqueous NaOH) varies between different nucleoside-nucleobase pairs, since the extinction coefficients and the pH range for stable and reproducible spectra needed for analysis differ. For example, purine nucleosides generally display a stronger UV absorption than pyrimidine nucleosides, which requires smaller sampling volumes to achieve the same peak signal intensity for these substrates.

Although we mainly discuss nucleobase cleavage (e.g., by nucleoside phosphorolysis) in this report, spectral unmixing-based reaction monitoring can also be applied to observe the reverse reaction. The same principles, strategies and challenges considered below for phosphorolysis reactions also pertain to the corresponding transformations in the glycosylation direction.

Updated list of established substrates

Extending our previously reported list of 20 nucleosides,^[14] we herein present the spectral characteristics of 38 substrates (Table 1). Reference spectra for all compounds and their bases listed in Table 1 are freely available from the externally hosted supplementary material.^[36] The updated list of established substrates now includes several modified purine nucleosides (22–27 and 33–36) and highly modified pyrimidines such as 5-trifluoromethyluridine (15). Notably, we also characterized some 5'-phosphorylated nucleotides and found their spectral properties to be essentially identical to their respective non-phosphorylated counterparts, conveniently allowing the reaction monitoring for these substrates without the need for additional reference spectra or method development.

Dealing with background

The most common obstacle with the presented method is background absorption. Different types of background absorption are typically observed and need to be addressed individually (Figure 2). Please note that while we use the phosphorolysis of thymidine (1, Figure 2A) as an example reaction in this manuscript, the same principles translate to all nucleosides and nucleotides and can be applied in the same manner.

An occasional and unavoidable type of background signal is atypical UV absorption of the multiwell plate or of particles. A typical background signal is in the range of 0.03 absorption units (AU) at 300 nm and curves up towards slightly higher intensities at 250 nm (Figure 2B). This background is very well reproducible and easily adjusted for, as described in our original method. However, on average in approximately 1–2% of all measurements, we observed increased absorption across the entire spectrum apparent as a distinct baseline shift (Figure 2C). This results in an inability to obtain accurate fits without manual spectral processing (which we choose to explicitly abstain from), as in these cases the baseline can be shifted >0.10 AU. The straightforward solution in this case is remeasurement of

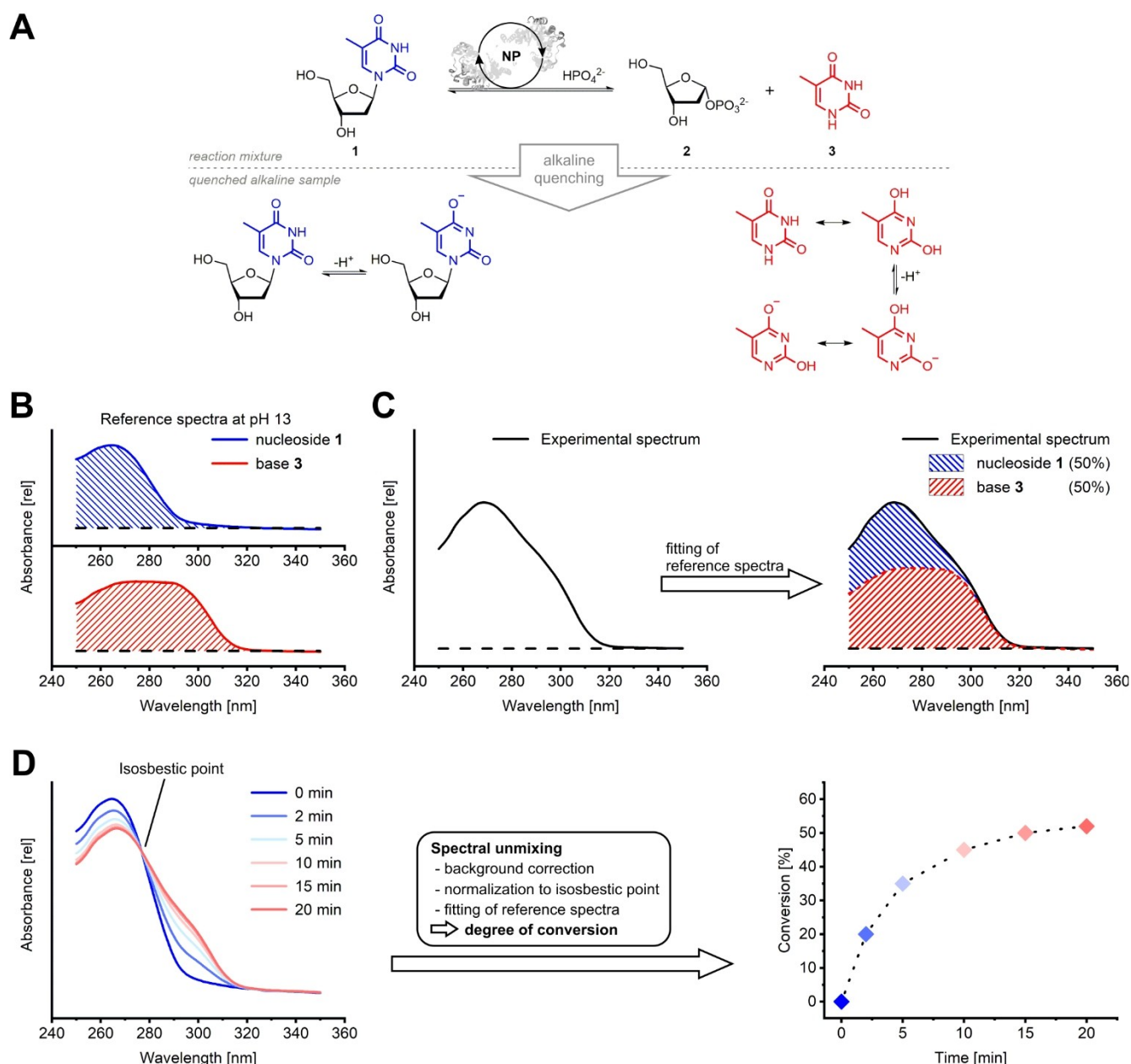


Figure 1. The principle of spectral unmixing-based reaction monitoring. A) Enzymatic phosphorolysis of thymidine (1) into 2-deoxyribose-1-phosphate (2) and the free nucleobase 3 as well as deprotonation after alkaline quenching. Representative resonance structures are shown. B) The substrate 1 and product 3 of the reaction have markedly different UV absorption spectra under alkaline conditions. C) The spectra of 1 (blue) and 3 (red) can be fitted to an experimental spectrum (black line) obtained during a reaction to derive the individual contributions of both species to the observed spectrum (hashed areas). D) Unmixing of multiple experimental spectra obtained during a reaction (left) enables reaction monitoring by deriving the degree of conversion at every sampled timepoint (right). Spectral unmixing of nucleoside transformations generally includes background correction, normalization to the isosbestic point of base cleavage, and fitting of the respective reference spectra. The spectra and conversions presented in this figure serve an illustrative purpose and were generated from the reference spectra of 1 and 3, as described in the externally hosted Supporting Information.^[36] Typical reaction conditions include a nucleoside concentration of 2 mM, 10 mM phosphate, 50 mM buffer of choice and $10\ \mu\text{g}\cdot\text{mL}^{-1}$ NP in a total volume of 500 μL .^[12]

the sample in a different well, which generally resolves the problem.

We did not mention correction for protein background in our initial report. That is because in most cases enzyme background absorption in the considered range of 250–350 nm is quasi undetectable when using protein concentrations of 50 $\mu\text{g}/\text{mL}$ or less in the reaction mixture that is sampled. In

selected instances where either higher concentrations and/or especially UV-active enzymes are used, appropriate background correction of the experimental sample may be necessary (Figure 2D). This can easily be carried out with a spectrum of a suitably diluted sample of the enzyme. Note that one may keep using the previously obtained reference spectra for the

Table 1. Spectral properties of nucleosides, nucleotides, and their bases under alkaline conditions.

Compound ^[a]		pH ^[b]	λ_{max} nucleoside/nucleotide [nm]	λ_{max} nucleobase [nm]	Isosbestic point of base cleavage [nm]	Spectral extension [nm]
Pyrimidines	uridine (4) ^[c]	13	262	281	271	310
	2'-deoxyuridine (5) ^[c]	13	262	281	272	310
	5-methyluridine (6) ^[c]	13	267	290	277	320
	thymidine (1) ^[c]	13	266	290	278	320
	5-fluorouridine (7) ^[c]	13.3	269	281	282	325
	2'-deoxy-5-fluorouridine (8) ^[c]	13.3	268	281	280	325
	5-bromouridine (9) ^[c]	13	276	290	283	330
	5-bromo-2'-deoxyuridine (10) ^[c]	13	275	290	282	330
	5-iodouridine (11) ^[c]	13.3	281	291	283	340
	2'-deoxy-5-iodouridine (12) ^[c]	13.3	279	291	282	340
	5-ethynyluridine (13) ^[c]	13.3	285	298	262, 288	340
	2'-deoxy-5-ethynyluridine (14) ^[c]	13.3	284	298	262, 288	340
	5-trifluoromethyluridine (15)	10	259	279	267	310
	cytidine (16) ^[c]	13.7	271	281	271	310
	2'-deoxycytidine (17) ^[c]	13.7	271	281	271	310
	uridine-5'-monophosphate (18)	13	262	281	271	310
	cytidine-5'-monophosphate (19)	13.7	271	281	271	310
Purines	adenosine (20) ^[c]	13	259	268	267	310
	2'-deoxyadenosine (21) ^[c]	13	259	268	267	310
	2-fluoroadenosine (22)	13	260	268	271	310
	2'-deoxy-2-fluoroadenosine (23)	13	260	268	271	310
	2-chloroadenosine (24)	13	264	271	271	310
	2-chloro-2'-deoxyadenosine (25)	13	264	271	271	310
	2-aminoadenosine (26)	13	279	284	285	320
	2-amino-2'-deoxyadenosine (27)	13	279	284	285	320
	guanosine (28) ^[c]	13	264	273	279	310
	2'-deoxyguanosine (29) ^[c]	13	264	273	279	310
	inosine (30) ^[c]	13	252	262	263	320
	2'-deoxyinosine (31) ^[c]	13	252	262	263	320
	xanthosine (32)	13.3	276	282	276	320
	2,6-dichloropurine riboside (33)	9	274	279	278	310
	2,6-dichloro 2'-deoxyriboside (34)	9	274	279	278	310
	6-chloro-2-fluoropurine riboside (35)	9	269	273	271	310
	6-chloro-2-fluoropurine 2'-deoxyriboside (36)	9	269	273	271	310
	adenosine-5'-monophosphate (37)	13	259	268	267	310
	guanosine-5'-monophosphate (38)	13	264	273	279	310
	inosine-5'-monophosphate (39)	13	252	262	263	320
	1,2,4-triazole-3-carboxamide riboside (40) ^[d]	13	— ^[e]	— ^[e]	— ^[e]	— ^[e]

[a] See Figure S1 for the structures of all compounds. [b] pH 9 was generally achieved in 50 mM Tris/NaOH buffer, pH 10 in 100 mM glycine/NaOH buffer, pH 13 in 100 mM NaOH, pH 13.3 in 200 mM NaOH and pH 13.7 in 500 mM NaOH. [c] From the original report.^[14] [d] Ribavirin. [e] Both λ_{max} values are at < 250 nm, and there is no isosbestic point of base cleavage. Note that reaction monitoring can still be performed by single- or multi-wavelength detection, but normalization to the isosbestic point of base cleavage is not possible for this substrate.

substrate and product without any further alterations as those are already corrected for their respective background.

Background absorption by UV-active components in the reaction mixture needs to be addressed on a case-to-case basis. Generally, all common buffers, protein stabilizing agents or even artifacts from protein purification such as imidazole do not represent any challenge to the method and allow straightforward use of the standard procedure without any additional background correction. When using some organic cosolvents, however, we noticed significant background absorption in the lower wavelength region. Whereas alcohols including methanol, ethanol, isopropanol, ethylene glycol and glycerol may be used without alterations to the method (see Supporting Information for details), solvents like dimethyl sulfoxide (DMSO) and dimethyl formamide (DMF) create background signals that need to be accounted for (Figure 2E). In

these cases we found success employing background spectra that reflect the specific content of UV-active solvent in the sample and, if appropriate, limiting the wavelength range for fitting of pyrimidine UV absorption spectra to the information-rich tail region (i.e., 265–295 nm for uridine, 4). We even found success when using especially UV-active reaction components, such as dithiothreitol (DTT), that proved problematic in some instances, by selecting appropriate substrates and selectively limiting the fitting range (see the Supporting Information for details and Figure S3 for an example).

In rare cases, we observed elevated baselines when using very concentrated buffers for dilution and spectral measurement. Again, appropriate background spectra to correct for this shift succeeded in resolving this issue.

Nonetheless, it should be stressed that background correction does not always lead to accurate and reliable data. We

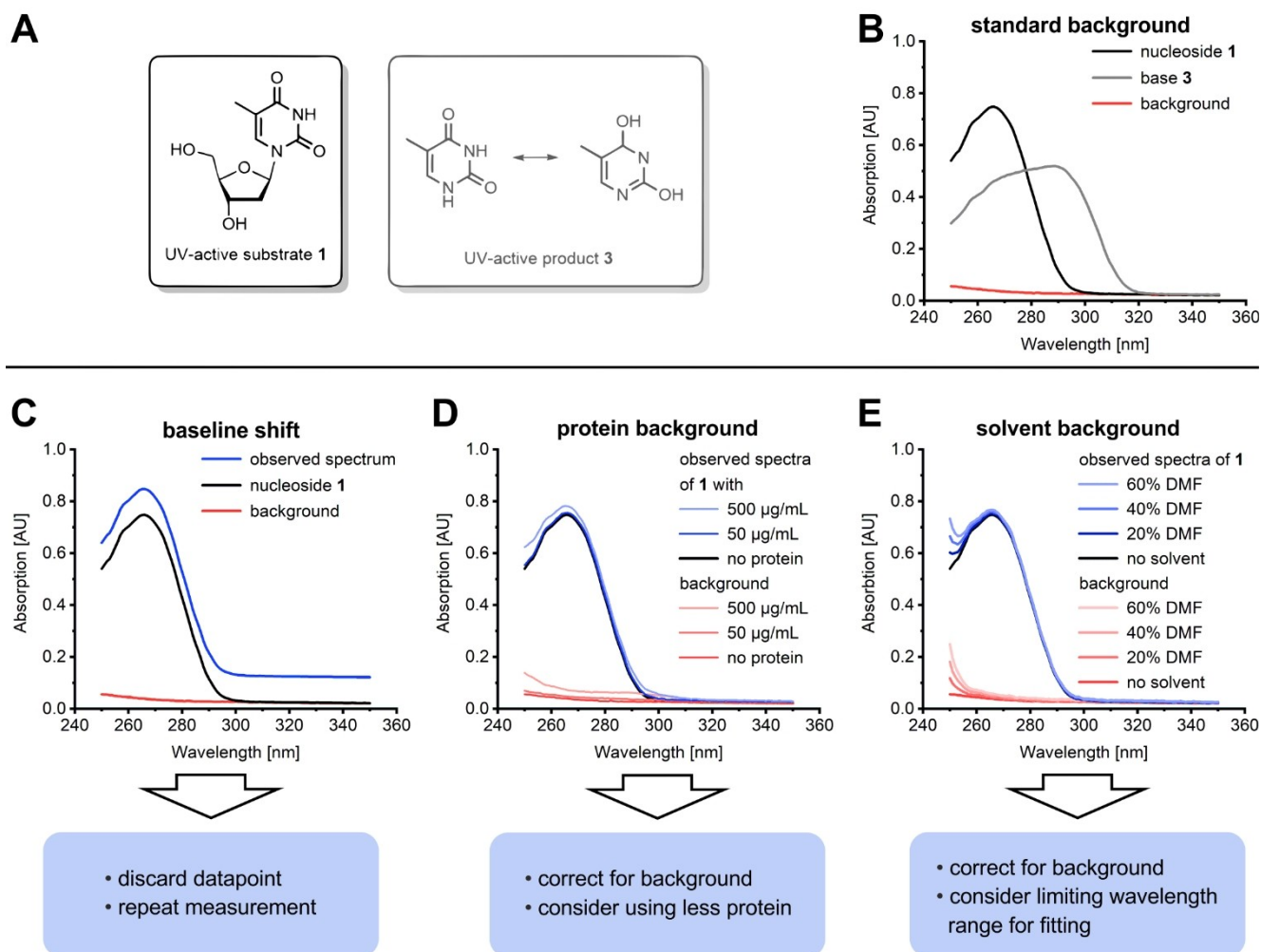


Figure 2. Common background signals. A) Exemplary UV-active reactants 1 and 3. B) Standard background observed from the absorption of the 96-well plate filled with water or aqueous NaOH. Signals for 1 and 3 represent typical signal intensities observed for reactions with 2 mM nucleoside substrate and a dilution factor of 15 during sampling. C) Baseline shift observed in approximately 1–2% of measurements. D) Background observed in reactions with significant protein content. Purified *Escherichia coli* thymidine phosphorylase was used to recreate typical protein backgrounds by 15-fold dilution in 100 mM NaOH. Note that some proteins can cause significantly more or less background. E) Representative background observed with some organic solvents. DMF was diluted tenfold in 100 mM NaOH to record the background signals.

experienced serious difficulties to correct for noise in instances where the background signal intensity is comparable to the signal intensity of the nucleoside-nucleobase pair under investigation and directly and/or completely overlaps with this signal (i.e., when examining the effect of enzyme inhibitors in stoichiometric quantities). In principle, background subtraction from the experimental spectrum is still possible and yields a processed spectrum that can be fitted, but fit quality and, consequently, accuracy of this approach suffered tremendously. We ascribed this to the fact that the signal intensity of the dynamic analytes (substrate and product) is largely irrelevant as those values are normalized to the isosbestic point and considered only in relation to one another, but background signals from most sources are absolute quantities and thus vary with and are very sensitive to pipetting accuracy. As a rule of thumb, we recommend our method for cases where back-

ground absorption does not exceed 20% of the relevant signals (i.e., signal-to-noise ratio should remain > 5).

Reactant Instability

A critical factor for any method is stability and detectability of the analytes. While all nucleosides and nucleobases in our original report displayed excellent stability towards the quenching and analysis conditions, we noted some issues within the extended substrate range. Fluorinated purine nucleosides 22 and 23 were found to be quite sensitive to alkaline conditions as these nucleosides underwent a temperature- and base-promoted side reaction (Figure S2), presumably by 5'-OH attack at the purine ring. We were able to bypass this issue by quick sample processing avoiding any unnecessary storage. At room

temperature and pH 13, compounds **22** and **23** remained stable enough for analysis for at least 10 min.

Further applications of the method

While the original protocol has proven to be a robust and versatile method, we have used spectral unmixing-based reaction monitoring in instances that deviated from the original conditions. Some applications that necessitated adjusted sample treatment are worth mentioning.

In our earlier report we have used purified protein in all reactions.^[14] The subsequently published applications also featured pure protein in all instances.^[12] However, the use of unpurified protein, for example, in the form of crude cell lysate, is highly desirable for screening of mutants or whole-cell reactions. We were pleased to find that even crude protein preparations (as lysed cells or cell-free extract) permitted the use of spectral unmixing-based reaction monitoring, if appropriate background correction is considered and the background signal remains within a manageable range (see above and the Supporting Information). In cases where heterogeneous reactions were applied, centrifugation of the quenched alkaline samples prior to analysis was necessary and successfully reduced background noise and baseline shifts caused by particles.

Conveniently, spectral shifting of the UV absorption spectra of the free nucleobases doesn't always require application of a strong base. Selected nucleoside-nucleobase pairs feature a marked spectral shift and stable spectra in a pH region easily accessible by established buffer systems (e.g., **33–36**, Table 1). This also presents an opportunity to monitor live reactions, either by applying a continuous assay or discontinuously monitoring very slow reactions by diluting samples of the reaction mixture in appropriate buffer (see the Supporting Information for details).

Some nucleosides precluded application of the original protocol that involves quenching of reaction samples in aqueous NaOH. Chlorinated scaffolds **33–36** display remarkably dynamic UV absorption spectra at pH values above 11 (Figure S4) and we were unable to obtain reproducible spectral fits using alkaline quenching. Fortunately, this issue could be resolved by employing organic solvents like methanol as an alternative quenching medium and subsequently adjusting the pH value to 9 for analysis (see the Supporting Information for details). A similar methodology featuring a different buffer system succeeded for the trifluorinated pyrimidine **15** (Table 1, Figure S6).

These examples only present a snapshot of the diverse applications of spectral unmixing-based reaction monitoring of transformations between nucleosides and nucleobases that one may envision. Nonetheless, we are confident that the lessons learned thus far will translate well to other scenarios, reaction systems, enzymes and applications where similar issues might be encountered.

Conclusion

Spectral unmixing presents a powerful tool for the efficient reaction monitoring of nucleobase cleavage reactions, with nucleoside phosphorolysis representing a highly relevant example. Spectral unmixing of UV absorption spectra conveniently allows for increased sample throughput compared to other methods and doesn't require expensive equipment or reagents. We have employed this method extensively and demonstrated its precision, versatility, robustness and ease of handling. This report extends the range of established substrates and discusses common problems and notable modifications to the original protocol. Reference spectra for all substrates and nucleobases listed in this article^[36] as well as our Python code used for spectral unmixing^[37,38] can be obtained from an external online repository and we are happy to assist with their use. While specific scenarios may require evaluation and troubleshooting on a case-to-case basis, the strategies discussed herein will facilitate the straightforward and versatile application of this method.

Experimental Section

All chemicals were purchased from Sigma Aldrich, TCI, Carl Roth, Carbosynth or BioNukleo GmbH at the highest available quality and used without prior purification. Solutions of all compounds were prepared in water deionized to 18.2 MW-cm with a Werner water purification system. NaOH solutions were prepared with deionized water. Enzymatic reactions were typically prepared from stock solutions of substrates and buffer and started via the addition of enzyme. Various NPs were used, including among others Y01, Y02, N01 and N02 from BioNukleo GmbH, *E. coli* uridine and thymidine phosphorylase and purine NP and *Bacillus subtilis* pyrimidine NP, as described previously.^[12] UV absorption spectra were recorded on a BioTek PowerWave HT plate reader, using UV/Vis-transparent 96-well plates (UV-STAR F-Bottom #655801, Greiner Bio-One). Spectral processing, unmixing and data generation were performed as described previously^[14] with software freely available online.^[37,38] All data presented in this report and the Supporting Information are freely available from an external online repository.^[36]

Reference spectra for pure compounds were prepared from 2 mM solutions by 10- to 20-fold dilution in aqueous NaOH. Reactions with purine or pyrimidine nucleosides were typically performed with either 1 or 2 mM of UV-active compounds. From the 2 mM reactions, 20 μ L (purines) or 30 μ L (pyrimidines) were withdrawn and quenched in NaOH to give a final volume of 500 μ L. From the 1 mM reactions, twice as much sample volume was withdrawn and treated analogously. Note that exact adherence to these volumes is not necessary, as normalization to the isosbestic point accounts for differences in signal intensity. For halogenated nucleosides **33–36**, typically, samples of 20 μ L were withdrawn and either diluted in 50 mM Tris/NaOH buffer (pH 9) to a volume of 500 μ L or quenched in an equal volume of MeOH or *i*PrOH before dilution in 50 mM Tris/NaOH buffer to give a final volume of 500 μ L. Similarly, the fluorinated pyrimidine **15** was sampled by quenching in *i*PrOH or MeOH followed by dilution with 100 mM glycine/NaOH buffer (pH 10) to a final volume of 500 μ L. Subsequently, 200 μ L of the diluted alkaline samples were transferred to wells of a UV/Vis-transparent 96-well plate to record the UV absorption spectra. All spectra were recorded from 250–350 nm in steps of 1 nm. For exact

sampling procedures and example reactions, please see our earlier reports^[12,14] and the Supporting Information.

Acknowledgements

This work was funded by the Deutsche Forschungsgemeinschaft (DFG, German Research Foundation) under Germany's Excellence Strategy–EXC 2008/1–390540038. We are grateful for the support of R.T.G. by the Einstein Foundation Berlin (ESB)–Einstein Center of Catalysis (EC²). K.F.H. is funded by DFG grant no. 392246628. We thank the Open Access Publishing funds of the TU Berlin for the support of this publication. Open access funding enabled and organized by Projekt DEAL.

Keywords: nucleobases · nucleoside phosphorylase · nucleosides · spectral unmixing · UV/Vis spectroscopy

- [1] S. Kamel, H. Yehia, P. Neubauer, A. Wagner, in *Enzym. Chem. Synth. Nucleic Acid Deriv.* (Ed.: J. Fernández-Lucas), **2018**, 1–28.
- [2] S. Kamel, M. Weiß, H. F. T. Klare, I. A. Mikhailopulo, P. Neubauer, A. Wagner, *Mol. Catal.* **2018**, 458, 52–59.
- [3] I. V. Fateev, K. V. Antonov, I. D. Konstantinova, T. I. Muravyova, F. Seela, R. S. Esipov, A. I. Miroshnikov, I. A. Mikhailopulo, *Beilstein J. Org. Chem.* **2014**, 10, 1657–1669.
- [4] H. Komatsu, T. Araki, *Nucleosides Nucleotides Nucleic Acids* **2005**, 24, 1127–1130.
- [5] I. D. Konstantinova, K. V. Antonov, I. V. Fateev, A. I. Miroshnikov, V. A. Stepchenko, A. V. Baranovsky, I. A. Mikhailopulo, *Synthesis*. **2011**, 1555–1560.
- [6] M. Rabuffetti, T. Bavaro, R. Semproli, G. Cattaneo, M. Massone, F. C. Morelli, G. Speranza, D. Ubiali, *Catalysts* **2019**, 9, 355.
- [7] H. Yehia, S. Westarp, V. Röhrs, F. Kaspar, T. R. Giessmann, F. T. H. Klare, K. Paulick, P. Neubauer, J. Kurreck, A. Wagner, *Molecules* **2020**, 25, 934.
- [8] B. Z. Eletskaia, D. A. Gruzdev, V. P. Krasnov, G. L. Levit, M. A. Kostromina, A. S. Paramonov, A. L. Kayushin, I. S. Muzyka, T. I. Muravyova, R. S. Esipov, et al., *Chem. Biol. Drug Des.* **2019**, 93, 605–616.
- [9] X. Zhou, K. Szeker, B. Janocha, T. Böhme, D. Albrecht, I. A. Mikhailopulo, P. Neubauer, *FEBS J.* **2013**, 280, 1475–1490.
- [10] K. Szeker, X. Zhou, T. Schwab, A. Casanueva, D. Cowan, I. A. Mikhailopulo, P. Neubauer, *J. Mol. Catal. B* **2012**, 84, 27–34.
- [11] F. Kaspar, R. T. Giessmann, K. Hellendahl, P. Neubauer, A. Wagner, M. Gimpel, *ChemBioChem* **2020**.
- [12] F. Kaspar, R. T. Giessmann, P. Neubauer, A. Wagner, M. Gimpel, *Adv. Synth. Catal.* **2020**, 362, 867–876.
- [13] R. T. Giessmann, N. Krausch, F. Kaspar, N. M. Cruz Bournazou, A. Wagner, P. Neubauer, M. Gimpel, *Processes* **2019**, 7, 380.
- [14] F. Kaspar, R. T. Giessmann, N. Krausch, P. Neubauer, A. Wagner, M. Gimpel, *Methods Protoc.* **2019**, 2, 60.
- [15] E. W. Yamada, *Methods Enzymol.* **1978**, 51, 423–431.
- [16] D. Ubiali, S. Rocchietti, F. Scaramozzino, M. Terreni, A. M. Albertini, R. Fernández-Lafuente, J. M. Guisán, M. Pregnotato, *Adv. Synth. Catal.* **2004**, 346, 1361–1366.
- [17] D. Singh, R. M. Schaaper, A. Hochkoeppler, *Anal. Biochem.* **2016**, 496, 43–49.
- [18] K. J. Seamon, J. T. Stivers, *J. Biomol. Screening* **2015**, 20, 801–809.
- [19] M. Surette, T. Gill, S. MacLean, *Appl. Environ. Microbiol.* **1990**, 56, 1435–1439.
- [20] A. Stachelska-Wierzchowska, J. Wierzchowski, M. Górka, A. Bzowska, B. Wielgus-Kutrowska, *Molecules* **2019**, 24, 1493.
- [21] A. Bzowska, E. Kulikowska, D. Shugar, *Pharmacol. Ther.* **2000**, 88, 349–425.
- [22] N. G. Panova, E. V. Shcheveleva, C. S. Alexeev, V. G. Mukhortov, A. N. Zuev, S. N. Mikhailov, R. S. Esipov, D. V. Chuvikovsky, A. I. Miroshnikov, *Mol. Biol.* **2004**, 38, 770–776.
- [23] J. Wierzchowski, A. Stachelska-Wierzchowska, B. Wielgus-Kutrowska, A. Bzowska, *Curr. Pharm. Des.* **2017**, 23, 6948–6966.
- [24] J. Wierzchowski, M. Ogiela, B. Iwańska, D. Shugar, *Anal. Chim. Acta* **2002**, 472, 63–74.
- [25] J. Wierzchowski, A. Stachelska-Wierzchowska, B. Wielgus-Kutrowska, G. Mikleušević, *Anal. Biochem.* **2014**, 446, 25–27.
- [26] A. Stachelska-Wierzchowska, J. Wierzchowski, A. Bzowska, B. Wielgus-Kutrowska, *Nucleosides Nucleotides Nucleic Acids* **2018**, 37, 89–101.
- [27] D. J. Porter, *J. Biol. Chem.* **1992**, 267, 7342–7351.
- [28] F. Kaspar, P. Neubauer, A. Wagner, **2020**, unpublished results.
- [29] S. Kamel, C. Walczak, P. Neubauer, A. Wagner, **2020**, unpublished results.
- [30] S. Westarp, J. Schollmeyer, P. Neubauer, A. Wagner, **2020**, unpublished results.
- [31] K. F. Hellendahl, F. Kaspar, P. Neubauer, A. Wagner, **2020**, unpublished results.
- [32] C. Quintano, A. Fernández-Manso, Y. E. Shimabukuro, G. Pereira, *Int. J. Remote Sens.* **2012**, 33, 5307–5340.
- [33] E. Wittenburg, *Chem. Ber.* **1966**, 99, 2391–2398.
- [34] J. J. Fox, D. Sugar, *Biochim. Biophys. Acta* **1952**, 9, 199–218.
- [35] J. J. Fox, D. Sugar, *Biochim. Biophys. Acta* **1952**, 9, 369–384.
- [36] F. Kaspar, **2020**, DOI: 10.5281/zenodo.3716126.
- [37] R. T. Giessmann, N. Krausch, **2019**, DOI: 10.5281/zenodo.3243376.
- [38] R. T. Giessmann, https://gitlab.com/rgiessmann/data_toolbox.

Manuscript received: April 1, 2020
Revised manuscript received: April 21, 2020
Accepted manuscript online: April 23, 2020
Version of record online: June 18, 2020

Paper III

Kaspar, F.;[#] Giessmann, R.T.;[#] Neubauer, P.; Wagner, A.; Gimpel, M. Thermodynamic Reaction Control of Nucleoside Phosphorolysis. *Adv. Synth. Catal.* **2020**, 362, 867–876, <https://doi.org/10.1002/adsc.201901230>. [#]equal contribution

This article was published as open access under a CC BY license which permits reproduction of the material with proper attribution, such as in this thesis.

Author contributions (with definitions by Brand *et al.* ¹)

Conceptualization, F.K., R.T.G., P.N., A.W. and M.G.; Data curation, F.K. and R.T.G.; Formal analysis, F.K. and R.T.G.; Funding acquisition, R.T.G., P.N. and A.W.; Investigation, F.K.; Methodology, F.K. and R.T.G.; Project administration, F.K., R.T.G. and A.W.; Resources, R.T.G., A.W., P.N., S.W. and N.K.; Software, - ; Supervision, R.T.G., P.N., A.W. and M.G.; Validation, - ; Visualization, F.K.; Writing—original draft, F.K.; Writing—review & editing, F.K., R.T.G., P.N., A.W. and M.G.

Specifically, my contribution included formulation of the research idea regarding the temperature-sensitivity of the equilibrium constant of phosphorolysis, design of experiments, execution of experiments, data curation, calculations, formulation and verification of the derived equations as well as illustration and lead writing of the publication.

Preamble

Although reports of the thermodynamic reaction control of some nucleoside phosphorolysis reactions dated back to the 1950s and 70s, this knowledge was largely forgotten as nucleoside phosphorylases regained attention as biocatalysts for the synthesis of pharmaceutically interesting nucleosides in the 2010s. As work of Robert Giessmann and Niels Krausch had shown that the phosphorolysis of thymidine behaved quite nicely according an equilibrium constant of 0.1, it was a small jump to show that the phosphorolysis of *all* nucleosides is under tight thermodynamic control. This held true irrespective of the enzyme or conditions used, which was not really met with acceptance by the community at the time. Nonetheless, my experiments further revealed that purines and pyrimidines had significantly different Gibbs free energies of phosphorolysis, explaining why purines were so easy to synthesize via transglycosylation (more on that in paper V). Since fundamental thermodynamics dictate that equilibrium constants are a function of temperature, I then set out to answer the basic question of “*Can we measure that?*”. Fortunately for me, i) we had a good grip on the UV-based assay by then ii) I had access to robust and thermostable enzymes enabling me to cover a 40 °C temperature range and iii) our favorite substrate at the time (thymidine) had a significant entropic contribution to phosphorolysis, answering that question with a resounding “yes!”. Although the temperature-dependence of the equilibrium constants of phosphorolysis remains to have practical significance beyond a curiosity perspective, the spectrum of equilibrium constants reported in this paper proved a highly valuable resource for following projects and guided us in much of our reaction engineering of nucleoside transglycosylations (papers V and VI).

Thermodynamic Reaction Control of Nucleoside Phosphorolysis

Felix Kaspar,^{+a, b} Robert T. Giessmann,^{+a} Peter Neubauer,^a Anke Wagner,^{a, b,*} and Matthias Gimpel^a

^a Bioprocess Engineering, Department of Biotechnology, Technische Universität Berlin, Ackerstraße 76, ACK24, D-13355 Berlin, Germany

Tel.: +49 30 314 72183

E-mail: anke.wagner@tu-berlin.de

^b BioNukleo GmbH, Ackerstraße 76, D-13355 Berlin, Germany

⁺ The authors contributed equally

Manuscript received: September 24, 2019; Revised manuscript received: November 15, 2019;

Version of record online: January 7, 2020



Supporting information for this article is available on the WWW under <https://doi.org/10.1002/adsc.201901230>



© 2019 The Authors. Published by Wiley-VCH Verlag GmbH & Co. KGaA.

This is an open access article under the terms of the Creative Commons Attribution License, which permits use, distribution and reproduction in any medium, provided the original work is properly cited.

Abstract: Nucleoside analogs represent a class of important drugs for cancer and antiviral treatments. Nucleoside phosphorylases (NPases) catalyze the phosphorolysis of nucleosides and are widely employed for the synthesis of pentose-1-phosphates and nucleoside analogs, which are difficult to access via conventional synthetic methods. However, for the vast majority of nucleosides, it has been observed that either no or incomplete conversion of the starting materials is achieved in NPase-catalyzed reactions. For some substrates, it has been shown that these reactions are reversible equilibrium reactions that adhere to the law of mass action. In this contribution, we broadly demonstrate that nucleoside phosphorolysis is a thermodynamically controlled endothermic reaction that proceeds to a reaction equilibrium dictated by the substrate-specific equilibrium constant of phosphorolysis, irrespective of the type or amount of NPase used, as shown by several examples. Furthermore, we explored the temperature-dependency of nucleoside phosphorolysis equilibrium states and provide the apparent transformed reaction enthalpy and apparent transformed reaction entropy for 24 nucleosides, confirming that these conversions are thermodynamically controlled endothermic reactions. This data allows calculation of the Gibbs free energy and, consequently, the equilibrium constant of phosphorolysis at any given reaction temperature. Overall, our investigations revealed that pyrimidine nucleosides are generally more susceptible to phosphorolysis than purine nucleosides. The data disclosed in this work allow the accurate prediction of phosphorolysis or transglycosylation yields for a range of pyrimidine and purine nucleosides and thus serve to empower further research in the field of nucleoside biocatalysis.

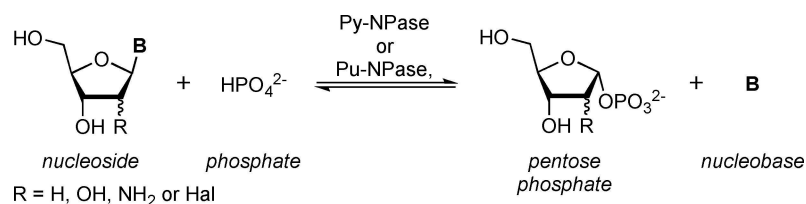
Keywords: nucleosides; nucleoside phosphorylase; nucleoside phosphorolysis; equilibrium constant; temperature

Introduction

Nucleosides serve as drugs against a variety of cancers and viral infections.^[1] Thus, their cost- and time-efficient preparation is of high interest. However, the synthesis of nucleosides and nucleoside analogs via conventional synthetic methods comes with several challenges posed by regio- and stereochemical complexity, functional group sensitivity and, consequently, heavy reliance on protecting groups.^[2] Biocatalytic methods are a valuable alternative as pyrimidine and

purine nucleosides can be synthesized with high selectivity in sustainable enzyme-catalyzed processes.^[3] Here, the use of nucleoside phosphorylases (NPases) has been firmly established and these enzymes are widely applied for the synthesis of nucleosides and their analogues.^[3]

NPases catalyze the phosphorolysis of nucleosides to pentose-1-phosphates, as well as the corresponding reverse reaction (Scheme 1). They are generally classified as either pyrimidine nucleoside phosphorylases



Scheme 1. Generalized biocatalytic nucleoside phosphorolysis reaction. A nucleoside is subjected to phosphorolytic cleavage of the nucleobase, yielding a pentose-1-phosphate and a free nucleobase.

(Py-NPases) or purine nucleoside phosphorylases (Pu-NPases), depending on their substrate spectra.^[4]

The use of NPases as biocatalysts in organic chemistry offers the advantage of using mild aqueous reaction conditions, a broad substrate spectrum regarding sugar and base moieties, as well as perfect regio- and stereoselectivity at the C1' position. Employing these enzymes, pentose-1-phosphates can be obtained as important synthetic intermediates from the accessible pool of nucleosides^[5,6] which have been shown to be highly valuable precursors for the synthesis of base- and sugar-modified nucleosides.^[7–9] Furthermore, NPases are widely used for the synthesis of nucleoside analogues in transglycosylation reactions.^[10–12]

Current research activities mainly focus on kinetic aspects of individual NPase-catalyzed reactions. Hence, kinetic data for a variety of NPases are available. To increase the final yield of phosphorolysis, mainly the choice of enzyme,^[13,14] enzyme immobilization^[15] or enzyme engineering^[16,17] have been investigated. Nonetheless, NPases generally fail to facilitate full conversion.^[18] A recent report by Alexeev and coworkers has shed more light on the cause of this phenomenon and showed that the thermodynamic properties of the nucleosides involved in the reaction influence the yields of NPase-catalyzed reactions.^[19]

Since nucleoside phosphorolysis is a reversible reaction (Scheme 1), there is a point, where the rates of the forward and the backward reactions are equal and no apparent change in concentrations is observed. In this equilibrium state, the reaction quotient defined as the quotient of the concentrations of the products and the substrates can be derived from the law of mass action and is generally referred to as the apparent equilibrium constant K' .^[20] The following expression results for nucleoside phosphorolysis reactions:

$$K' = \frac{[B][P1P]}{[N][P]} \quad (1)$$

where K' is the apparent equilibrium constant of phosphorolysis, $[B]$ is the equilibrium concentration of the free nucleobase [mM], $[P1P]$ is the equilibrium concentration of the pentose-1-phosphate [mM], $[N]$ is the equilibrium concentration of the nucleoside [mM]

and $[P]$ is the equilibrium concentration of inorganic phosphate [mM].

This equilibrium constant exists irrespective of the (bio)catalyst used and K' values for some substrates in NPase-catalyzed reactions have been reported.^[19,21–26] Thus, according to the law of mass action, only the reaction conditions influence the final equilibrium concentrations and not the enzyme used for catalysis. Alexeev and colleagues^[19] recently employed this dependency in their method for accurate yield prediction of nucleoside transglycosylation reactions based on the equilibrium constants of the individual reactions. Ultimately, this allows for thermodynamic reaction control by adjusting the concentrations of the starting materials to facilitate an optimal yield.

In this work we provide extensive evidence for the universal interpretation of nucleoside phosphorolysis reactions as thermodynamically controlled endothermic equilibrium reactions that adhere to the law of mass action. To this end, we performed and monitored several biocatalytic nucleoside phosphorolysis reactions. We demonstrate that nucleoside phosphorolysis proceeds to a reaction equilibrium dictated by the substrate-specific equilibrium constant of phosphorolysis, irrespective of the type or amount of NPase used. Furthermore, we show that the equilibrium constant is temperature dependent. Therefore, we determined the equilibrium constants of phosphorolysis of 24 nucleosides at different temperatures and derived the apparent transformed enthalpies and entropies. The resulting data show that pyrimidine nucleosides are generally more susceptible to phosphorolysis than purine nucleosides. Additionally, our enthalpy and entropy data allow calculation of equilibrium constants at different temperatures as well as prediction of phosphorolysis yields, as demonstrated herein.

Results and Discussion

Maximum Conversions of Nucleosides in Phosphorolysis Reactions are Independent of the Applied Biocatalyst

Previous research activities have focused on the discovery of new enzymes^[13,14] or enzyme immobilization strategies^[15] to increase the obtained yield for

nucleoside phosphorolysis and transglycosylation reactions. Based on the thermodynamic characteristics of these reactions, however, we anticipated that the maximum conversion in phosphorolysis reactions would behave independently of the enzyme used.

To investigate the impact of different NPases on the equilibrium states of nucleoside phosphorolysis reactions, we initially performed the phosphorolysis of uridine (**1**) with *Escherichia coli* uridine phosphorylase (*E. coli* UP), *E. coli* thymidine phosphorylase (*E. coli* TP), *Bacillus subtilis* Py-NPase (*B. subtilis* Py-NPase) and two commercially available thermostable Py-NPases (Py-NPase Y01 and Py-NPase Y02). All enzymes readily accepted this substrate and reaction completion could be observed after 5 to 80 min using $10\text{ }\mu\text{g}\cdot\text{mL}^{-1}$ of the respective enzymes (Figure 1A). Using 5 equivalents (eq.) of phosphate with respect to the nucleoside substrate, a maximum conversion of 55% was achieved regardless of the enzyme used.

To exclude any concentration effects of the enzyme preparations, we additionally conducted the phosphorolysis of **1** with different concentrations of Py-NPase Y02 (Figure 1B). Higher enzyme concentrations led to faster reaction completion. However, irrespective of the amount of the enzyme used, the same equilibrium as previously observed was reached.

To eliminate the possibility of enzyme inactivation preventing the completion of the reaction, we performed the phosphorolysis of **1** with Py-NPase Y02 and added additional enzyme after apparent reaction completion (Figure 1C).

This experiment resulted in no change of reactant concentrations after addition of more enzyme, confirm-

ing that this reaction was not terminated by means of inhibition and/or enzyme inactivation.

This evidence confirms that the phosphorolysis of uridine (**1**) is a thermodynamically controlled equilibrium reaction which is consistent with previous reports.^[19,21–24,27] From the data collected, the apparent equilibrium constant of phosphorolysis K' under these conditions was 0.15, as calculated from equation (1).

To broadly confirm the thermodynamic reaction control of nucleoside phosphorolysis, we investigated the conversion of other nucleosides by NPases. We observed a similar behavior for the phosphorolysis of the pyrimidine nucleosides 2'-deoxyuridine (**2**), 5-fluorouridine (**3**) and 2'-deoxy-5-fluorouridine (**4**), employing the same Py-NPases (Figure 2A–2C). As observed for uridine (**1**), the choice of enzyme had no effect on the equilibrium conversions. Pyrimidines **2–4** displayed very similar apparent equilibrium constants to **1** (0.20 for **2**, 0.14 for **3** and **4**).

To extend this investigation to purine nucleosides, we performed the phosphorolysis of two natural (adenosine, **5**, and 2'-deoxyadenosine, **6**) and two modified purine nucleosides (2-chloroadenosine, **7**, and 2-chloro-2'-deoxyadenosine, **8**) with three different NPases (thermostable Pu-NPases N01 and N02 and *E. coli* Pu-NPase). Similar to the pyrimidine nucleosides mentioned above, the choice of the enzyme had no effect on the equilibrium concentrations of these reactions (Figure 2D–2G). Here, the equilibrium conversions with 5 eq. of phosphate were significantly lower, in the range of 20%. Calculation of the apparent equilibrium constants of phosphorolysis yielded values

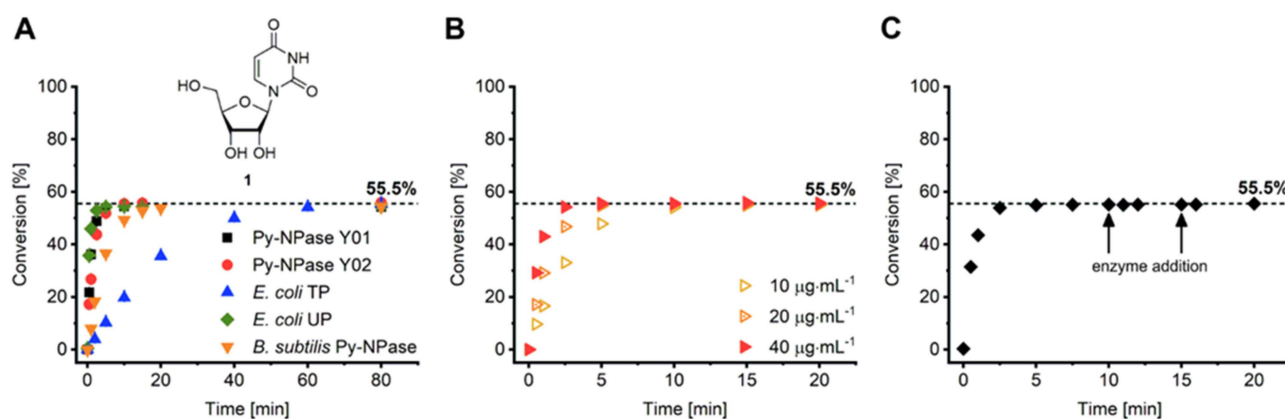


Figure 1. Enzymatic phosphorolysis of uridine (**1**). **A** Phosphorolysis of **1** with five different Py-NPases. **B** Phosphorolysis of **1** with Py-NPase Y02 using different enzyme concentrations. **C** Phosphorolysis of **1** with Py-NPase Y02 employing spiking of enzyme upon apparent reaction completion. All reactions reach the same equilibrium, regardless of the enzyme or its amount used for catalysis. Reactions were performed with 2 mM nucleoside substrate and 10 mM K_2HPO_4 in 50 mM MOPS buffer at pH 7.5 and 37°C in a total volume of 500 μL . $10\text{ }\mu\text{g}\cdot\text{mL}^{-1}$ of the respective enzyme were used in A and $10\text{--}40\text{ }\mu\text{g}\cdot\text{mL}^{-1}$ Py-NPase Y02 were used in B. The reaction in C was started with $40\text{ }\mu\text{g}\cdot\text{mL}^{-1}$ (20 μg total enzyme) Py-NPase Y02 and $10\text{ }\mu\text{g}$ of the enzyme were added at 10 min and 15 min each, indicated by the arrows. Reactions in A were performed in duplicate and the standard deviation (SD) is shown as error bars.

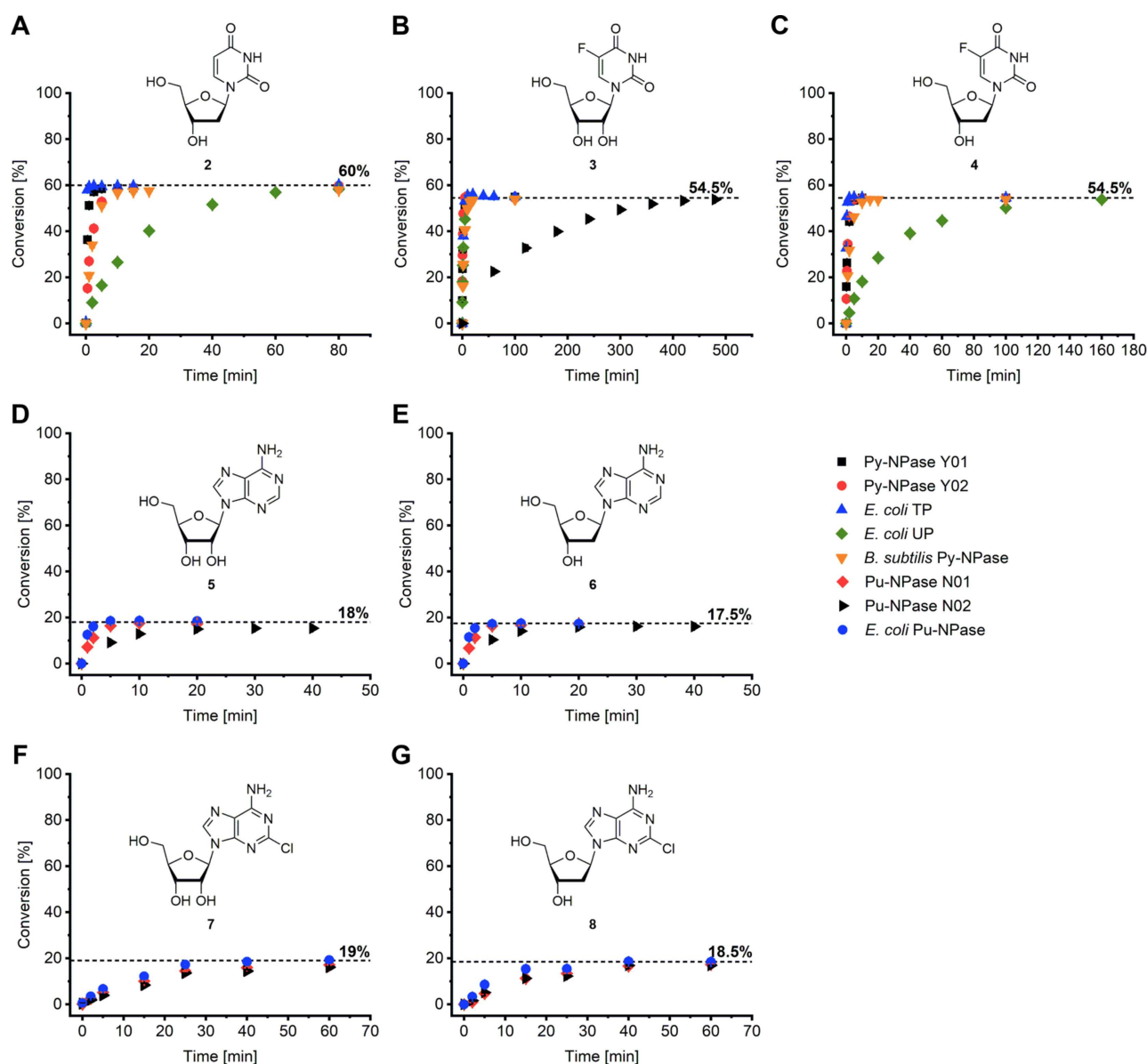


Figure 2. Enzymatic phosphorolysis of pyrimidine and purine nucleosides. The phosphorolysis of **A** 2'-deoxyuridine (**2**), **B** 5-fluorouridine (**3**), **C** 2'-deoxy-5-fluorouridine (**4**), **D** adenosine (**5**), **E** 2'-deoxyadenosine (**6**), **F** 2-chloroadenosine (**7**) and **G** 2-chloro-2'-deoxyadenosine (**8**) was performed in duplicate with 2 mM nucleoside substrate, 10 mM K_2HPO_4 and $10 \mu\text{g}\cdot\text{mL}^{-1}$ of the respective enzyme (except for the phosphorolysis of **3** with Pu-NPase N02, where $600 \mu\text{g}\cdot\text{mL}^{-1}$ were used) in 50 mM MOPS buffer at pH 7.5 and 37°C in a total volume of 500 μL . Note the different time scales. Error bars show the SD.

around 0.01, which is consistent with previous reports for **5**.^[19,28]

Interestingly, Py-NPases Y01, Y02 and *B. subtilis* Py-NPase performed roughly equally well with uridine (**1**) compared to 2'-deoxyuridine (**2**), whereas our data nicely reflect the inverse substrate specificity of *E. coli* UP and TP, as reported previously.^[29,30] *E. coli* UP showed excellent activity with uridine (**1**) but significantly diminished activity with the 2'-deoxy analogue **2**. *E. coli* TP, on the other hand, displayed only low

activity with **1** but facilitated remarkably quick reaction completion with **2** (Figure 1A and 2A).

Notably, although it is commonly believed that Pu-NPases should be specific to purine nucleosides, they generally also catalyze the phosphorolysis of pyrimidine nucleosides. Compared to corresponding Py-NPases they usually exhibit $>2,000$ -fold lower turnover rates. Nonetheless, given the thermodynamic reaction control of nucleoside phosphorolysis, Pu-NPases should still be expected to complete the phosphorolysis of their unfavored substrates, despite

their kinetic handicap. Consequently, for the phosphorolysis of the pyrimidine 5-fluorouridine (**3**), even the use of the thermostable Pu-NPase N02 proved successful in reaching the thermodynamic equilibrium (Figure 2B). In this case, a 60-fold higher amount of enzyme had to be employed and the reaction took considerably longer than with any of the Py-NPases under the same reaction conditions. Thus far, to the best of our knowledge, only the phylogenetically peculiar *Plasmodium falciparum* Pu-NPase has been reported to perform the phosphorolysis of a pyrimidine nucleoside.^[31] Here, we not only show for the first time that the thermostable Pu-NPase N02 accepts pyrimidine substrates such as **3**, but also achieves reaction completion given sufficient time. This strikingly emphasizes the non-significance of the enzyme kinetics for the ultimate reaction outcome, as it is possible to drive these phosphorolysis reactions into their chemical equilibrium even with an extremely small enzyme activity, in a range commonly considered negligible.

Thus, all nucleoside phosphorolysis reactions we investigated behaved according to the law of mass action and reached maximum product concentrations after a variable run time. Despite differences in reaction speed, the maximum conversion yields in the equilibrium are dictated by a characteristic and substrate-specific equilibrium constant which was shown to be independent of the type and amount of enzyme used. It may be reasonable to assume that this holds true for all nucleosides that are subjected to phosphorolysis. Important exceptions from this are nucleosides that are not converted by NPases because of issues such as excessive steric demands or severely unfavored transition states which prevent transformation.

Higher Reaction Temperature yields Higher Conversion of Nucleosides by NPases

The absolute values of the equilibrium constants of phosphorolysis of the nucleosides discussed above were all found to be well below 1. This means that they describe endothermic reactions, which are not favored under standard conditions. Consequently, we anticipated a temperature-dependence of K' and set out to investigate the effect of higher reaction temperatures on the equilibrium states of nucleoside phosphorolysis. Profiting from the use of the thermostable NPases Y02 and N02, we were able to perform the phosphorolysis of 24 nucleosides, including 12 pyrimidine and 12 purine nucleosides, at temperatures of 40 to 70 °C. To prevent decomposition of the produced pentose-1-phosphates, which is known to happen rapidly at high temperatures and neutral pH values,^[5] we increased the reaction pH to 9. Under these conditions, both enzymes displayed excellent activity with all substrates **1–24**

and allowed efficient reaction completion and monitoring. Consistent with our initial assumptions, we observed a trend towards higher conversions at higher temperatures. For example, under these conditions the phosphorolysis of 2'-deoxy-5-fluorouridine (**4**; Figure 3A) showed equilibrium conversions in the range of 51% at 40 °C and values around 55% at 70 °C. A similar behavior could be observed for all nucleosides investigated which confirms that the phosphorolysis of **1–24** are thermodynamically controlled endothermic reactions (Table S1).

The difference between the equilibrium conversions determined at pH 9 (this section) and the ones determined at pH 7.5 (see above) were insignificant (compare Figure 1 and Figure 2 with Table S1). Although a difference between them might be expected from the definition of the biochemical equilibrium, it seems that pH only minorly influences the equilibrium constant by changing the contribution of charged species.

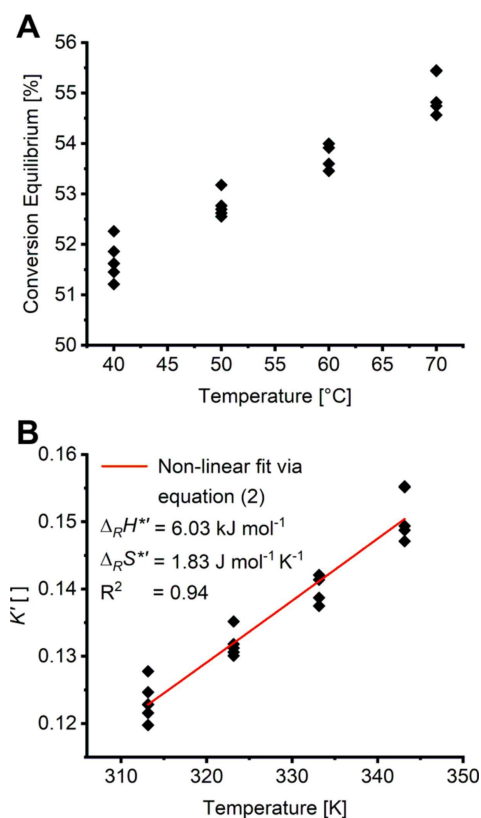


Figure 3. Examples of nucleoside phosphorolysis thermodynamic data processing. **A** Raw data of the phosphorolysis of **4** at different temperatures. The reactions were performed with 2 mM nucleoside substrate, 10 mM K_2HPO_4 and $16 \mu\text{g} \cdot \text{mL}^{-1}$ Py-NPase Y02 in 50 mM glycine buffer at pH 9 and 40–70 °C in a total volume of 500 μL . **B** Transformed and fitted data for the derivation of $\Delta_R H''$ and $\Delta_R S''$. Raw data were processed via equation (1) and then fitted with equation (2).

Pyrimidine Nucleosides are Generally more Susceptible to Phosphorolysis than Purine Nucleosides

From the described data, we derived K' at various temperatures and determined the transformed apparent reaction enthalpy $\Delta_R H'^*$ and transformed apparent reaction entropy $\Delta_R S'^*$ via fitting of the data to:

$$K' = e^{-\frac{\Delta_R G'}{RT}} = e^{-\frac{\Delta_R H'^* - T\Delta_R S'^*}{RT}} \quad (2)$$

where $\Delta_R G'$ is the transformed apparent Gibbs free energy of phosphorolysis [$\text{J} \cdot \text{mol}^{-1}$], T is the temperature [K], R is the universal gas constant ($8.314 \text{ J} \cdot \text{mol}^{-1} \cdot \text{K}^{-1}$), $\Delta_R H'^*$ is the transformed apparent enthalpy of phosphorolysis [$\text{J} \cdot \text{mol}^{-1}$], $\Delta_R S'^*$ is the transformed apparent entropy of phosphorolysis [$\text{J} \cdot \text{mol}^{-1} \cdot \text{K}^{-1}$], and the definitions from above.

Here, we carried out direct determinations through a non-linear fit to prevent error propagation by linearization (Figure 3A and 3B; see Table S1 for all derived values for $\Delta_R H'^*$ and $\Delta_R S'^*$; note that we communicate transformed thermodynamic values, as they were measured at constant pH and do not consider charged species, and explicitly abstain from referring to our results as “standard” values, but apparent ones, as they were not measured under standard biochemical conditions).

The knowledge of $\Delta_R H'^*$ and $\Delta_R S'^*$ then allowed access to the transformed apparent Gibbs free energy $\Delta_R G'$ of these phosphorolysis reactions at different temperatures. The Gibbs free energy of phosphorolysis $\Delta_R G'$ at 40°C of pyrimidine nucleosides was found to be in the range of $1.2\text{--}5.5 \text{ kJ} \cdot \text{mol}^{-1}$, which is notably lower than for the investigated purine nucleosides that display values of $5.7\text{--}12.6 \text{ kJ} \cdot \text{mol}^{-1}$ (Figure 4A). These values correspond to apparent equilibrium constants K' in the range of $0.12\text{--}0.62$ for pyrimidine nucleosides and $0.01\text{--}0.11$ for purine nucleosides. Accordingly, noticeably different equilibrium conversions can be observed across these nucleosides, with pyrimidines generally featuring higher equilibrium conversions than purines, as dictated by their respective equilibrium constants (Figure 4B).

The practical value of our collection of $\Delta_R H'^*$ and $\Delta_R S'^*$ data lies within their use for the prediction of the equilibrium phosphorolysis conversion of the nucleosides investigated here. Using equation (2), the equilibrium constants of phosphorolysis of any of the nucleosides investigated here can easily be obtained for any given temperature. Employing then:

$$[B] = [P1P] = \frac{K'([N]_0 + [P]_0) - \sqrt{(K'[N]_0 + K'[P]_0)^2 - 4(K' - 1)K'[N]_0[P]_0}}{2(K' - 1)} \quad (3)$$

where $[N]_0$ is the initial concentration of the nucleoside [mM], $[P]_0$ is the initial concentration of phosphate [mM] and definitions from above yields the concentrations of the free nucleobase and pentose-1-phosphate with variable initial concentrations of nucleoside and phosphate. Thus, conversions of these nucleosides can be predicted. To ease these calculations, we provided an Excel spreadsheet that is freely available from the externally hosted online supplementary material.^[32]

To verify the predictions available through equation (3), we performed the NPase-catalyzed phosphorolysis of uridine (**1**) and adenosine (**5**) at pH 9 and 40°C with different concentrations of phosphate (Figure 5). For example, pyrimidine **1** reached a conversion of 80% with 20 eq. of phosphate whereas for purine **5** we only observed a conversion of 37% under the same conditions, which is consistent with the predictions obtained via our collection of $\Delta_R H'^*$ and $\Delta_R S'^*$ data (Table S1). This emphasizes the practical value of the knowledge of the equilibrium constants of phosphorolysis of these nucleosides, as they allow for accurate prediction of phosphorolysis yields to optimize the reaction conditions.

Conclusion

In the present work, we broadly demonstrated that nucleoside phosphorolysis catalyzed by NPases is a thermodynamically controlled endothermic reversible equilibrium reaction. Therefore, maximum yields for each substrate are independent of the NPase used, as demonstrated by several examples, and can be predicted via the substrate-specific apparent equilibrium constant K' . We anticipate that this holds true for all nucleosides that can be subjected to phosphorolysis. Furthermore, we presented data on the temperature-dependency of the equilibrium constants of phosphorolysis of 24 nucleosides that display characteristic behavior. The available data allow for the calculation of K' at any given temperature and enable accurate prediction of phosphorolysis or transglycosylation yields for a range of pyrimidine and purine nucleosides.^[33] Subsequently, the equations described by Alexeev *et al.*,^[19] the thermodynamic data reported in this study, as well as the tools provided herein (see external supplementary material)^[32] serve to facilitate streamlined reaction engineering of NPase-catalyzed reactions by *in silico* yield prediction and thermodynamic reaction control.^[33]

Since our findings show that maximum yields in NPase-catalyzed reactions can be achieved independently of the enzyme applied, we believe that efforts to influence the yield of these reactions by varying the enzyme are unlikely to bear fruit. Instead, extending the toolbox of available NPases to improve kinetic parameters to reach reaction equilibrium faster or to

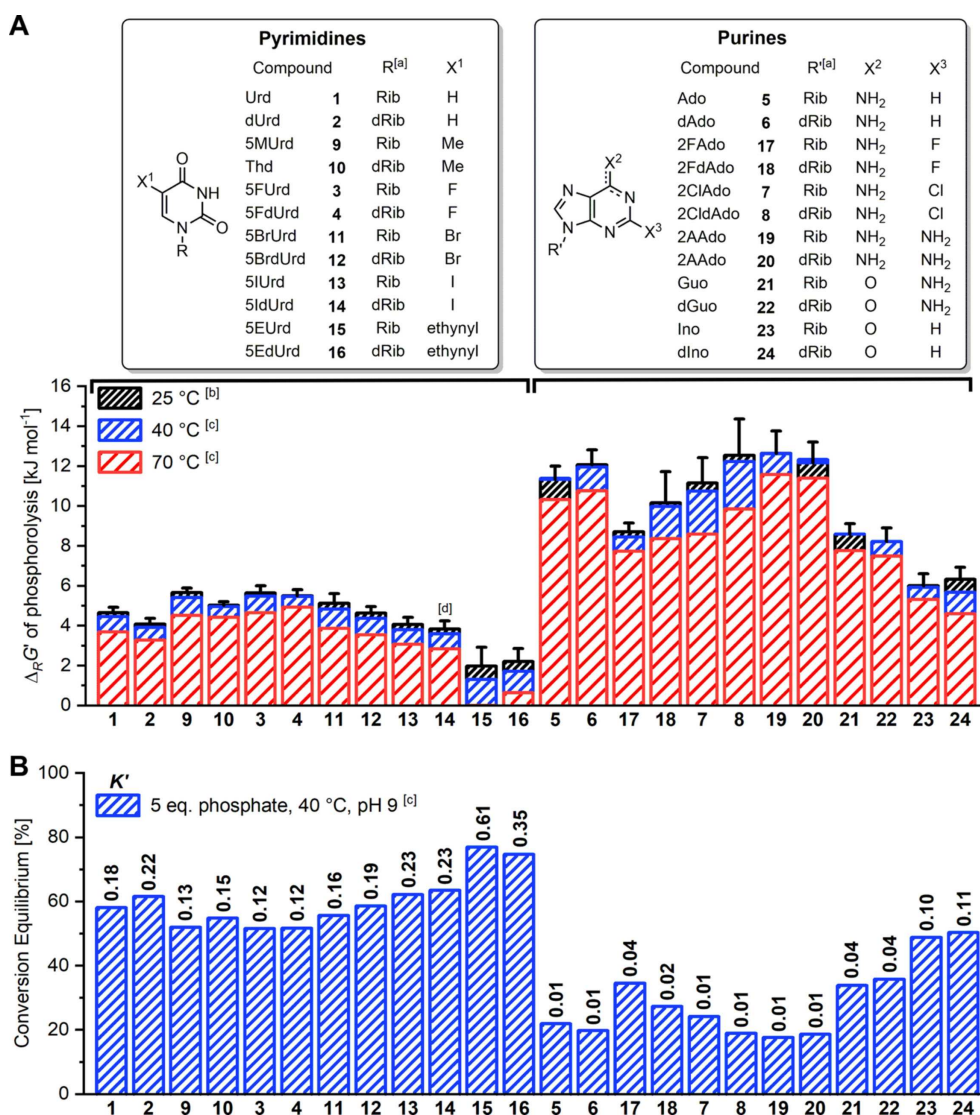


Figure 4. Gibb's free energy of phosphorolysis and conversion of nucleosides. **A** Gibb's free energy of phosphorolysis determined via equations (1) and (2) from the equilibrium concentrations of nucleoside phosphorolysis reactions with 2 mM nucleoside substrate, 10 mM K₂HPO₄ and 16 μg·ml⁻¹ Py-NPase Y02 or 66 μg·ml⁻¹ Pu-NPase N02 in 50 mM glycine buffer at pH 9 in a total volume of 500 μL performed at 40–70 °C. Error bars quantify the uncertainty of the prediction at 25 °C calculated via equation (4). **B** Equilibrium conversion of nucleosides in a phosphorolysis reaction at 40 °C and pH 9 employing 5 eq. of phosphate and equilibrium constant *K'* (also see Table S1). [a] Rib = ribosyl, dRib = 2'-deoxyribosyl, [b] extrapolated from experimental data for Δ_R*H*[°] and Δ_R*S*[°], [c] experimental data (conditions as above), [d] calculated from data for 50–70 °C since data for 40 °C were excluded from analysis (see Supplementary Material for full dataset).

convert challenging substrates such as arabinosyl nucleosides, fluorinated glycosides or bulky nucleobases will certainly prove beneficial.

Lastly, the quantification of effects of reaction conditions such as ionic strength, different salts, pH and chelating agents on the equilibrium states of nucleoside phosphorolysis may be explored experimentally by future studies.

Experimental Section

General Remarks

All chemicals were of analytical grade or higher and purchased, if not stated otherwise, from Sigma Aldrich (Steinheim, Germany), Carbosynth (Berkshire, UK), Carl Roth (Karlsruhe, Germany), TCI Deutschland (Eschborn, Germany) or VWR (Darmstadt, Germany). All nucleosides (Figure S1) and nucleobases were used without prior purification. Water deionized to 18.2 MΩ·cm with a Werner water purification system was used. For the preparation of NaOH solutions deionized water was used.

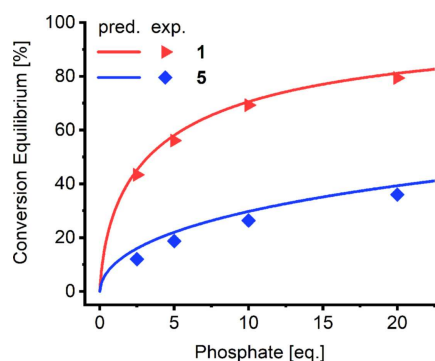


Figure 5. Predicted (pred.) and experimental (exp.) phosphorolytic conversion of uridine (**1**) and adenosine (**5**). Reactions were performed with 2 mM substrate and 5, 10, 20 or 40 mM (2.5, 5, 10 or 20 eq.) K_2HPO_4 and $40 \mu\text{g}\cdot\text{mL}^{-1}$ Py-NPase Y02 or $40 \mu\text{g}\cdot\text{mL}^{-1}$ Pu-NPase N02 in 50 mM glycine buffer at pH 9 and 40°C in a total volume of 500 μL . Samples were taken after 10, 15 and 20 min to confirm equilibrium. The datapoints show the average of the three equilibrium data points. The predictions were calculated with equation (3) using K' (T) obtained through the $\Delta_r H^*$ and $\Delta_r S^*$ data for these substrates.

Enzymes

Enzymes were either purchased from BioNukleo GmbH (Berlin, Germany) or Sigma Aldrich (see Table S2). Enzymes provided by BioNukleo were E-PyNP-0001 (Py-NPase Y01; EC 2.4.2.2), E-PyNP-0002 (Py-NPase Y02; EC 2.4.2.2), E-PNP-0001 (Pu-NPase N01; EC 2.4.2.1), E-PNP-0002 (Pu-NPase N02; EC 2.4.2.1), E-UP-0001 (*Escherichia coli* uridine phosphorylase; *E. coli* UP; EC 2.4.2.3), E-TP-0001 (*E. coli* thymidine phosphorylase; *E. coli* TP; EC 2.4.2.4) and E-PNP-04 (*E. coli* purine nucleoside phosphorylase; *E. coli* Pu-NPase; EC 2.4.2.1). Enzymes were desalted against 2 mM KH_2PO_4 (pH 7.0, measured at 25°C) buffer and stored at 4°C at concentrations listed in Table S2. *Bacillus subtilis* pyrimidine phosphorylase (*B. subtilis* Py-NPase; EC 2.4.2.2) was obtained from Sigma Aldrich and prepared as a $1 \text{ mg}\cdot\text{mL}^{-1}$ solution in 2 mM KH_2PO_4 buffer (pH 7.5, measured at 25°C) prior to use.

The activity of the stock solutions of Py-NPase Y02 and Pu-NPase N02 was assessed by the UV/Vis spectroscopy-based method described recently (also see below).^[34] Reactions were performed with 1 mM of nucleoside substrate in 50 mM glycine buffer and 50 mM K_2HPO_4 at pH 9 and 40°C . One unit (U) is defined as the conversion of 1 μmol of substrate per minute. For Py-NPase Y02 and Pu-NPase N02 an activity of $40 \text{ U}\cdot\text{mg}^{-1}$ ($65 \text{ U}\cdot\text{mL}^{-1}$) and $57 \text{ U}\cdot\text{mg}^{-1}$ ($379 \text{ U}\cdot\text{mL}^{-1}$) for their natural substrates uridine (**1**) and adenosine (**5**), respectively, was determined.

Phosphorolysis of Pyrimidine and Purine Nucleosides

Enzymatic nucleoside phosphorolysis reactions were prepared from stock solutions of nucleoside, phosphate, buffer and water in 1.5 mL reaction tubes (Sarstedt, Nümbrecht, Germany) and started by the addition of the enzyme. Reactions were

performed in duplicate with 2 mM nucleoside and 10 mM K_2HPO_4 in 50 mM MOPS buffer (pH 7.5, measured at 30°C) in a total volume of 500 μL . Prior to the addition of enzyme solution, reactions were preheated to 37°C . Unless stated otherwise, final enzyme concentrations of $10 \mu\text{g}\cdot\text{mL}^{-1}$ were used for all enzymes and substrates. For the phosphorolysis of 5-fluorouridine (**3**) with Pu-NPase N02, $600 \mu\text{g}\cdot\text{mL}^{-1}$ of enzyme were employed.

To investigate possible effects of the enzyme concentration, uridine (**1**) was subjected to phosphorolysis using 10–40 $\mu\text{g}\cdot\text{mL}^{-1}$ of Py-NPase Y02. To exclude possible enzyme inactivation effects, **1** was also subjected to phosphorolysis with 40 $\mu\text{g}\cdot\text{mL}^{-1}$ of Py-NPase Y02 (20 μg total enzyme) and 10 μg of the enzyme were added after apparent reaction completion at 10 min and 15 min each. To validate the predictions of phosphorolysis conversion with different phosphate concentrations, 2 mM of **1** and **5**, respectively, were converted with 40 $\mu\text{g}\cdot\text{mL}^{-1}$ Py-NPase Y02 or 40 $\mu\text{g}\cdot\text{mL}^{-1}$ Pu-NPase N02 in 50 mM glycine buffer at pH 9 and 40°C with 5, 10, 20 or 40 mM (2.5, 5, 10 or 20 eq.) K_2HPO_4 . The reactions were monitored, and equilibrium samples were taken after 10, 15 and 20 min.

Monitoring of Enzyme Reactions

Sampling, data collection and analysis were carried out as described previously.^[34] Briefly, samples of 30 μL (for pyrimidine nucleosides) or 20 μL (for purine nucleosides) were withdrawn from the reaction mixture and pipetted into 100 mM NaOH solution (200 mM NaOH solution for **3**, **4** and **13–16**) to give a final volume of 500 μL of diluted alkaline sample. From this mixture, 200 μL were pipetted into wells of a UV/Vis-transparent 96-well plate (UV-STAR F-Bottom #655801, Greiner Bio-One). The UV/Vis absorption spectra of these alkaline samples were recorded from 250 to 350 nm to determine the nucleoside/nucleobase ratio via spectra unmixing. All data presented in this study can be obtained from an external online repository^[32] along with the software for spectral unmixing and metadata treatment detailed in our previous work.^[34,35]

Temperature Dependence of the Equilibrium Constant

Equilibrium constants for the phosphorolysis of 24 nucleosides (**1–24**) were determined at pH 9 and at 40, 50, 60 and 70°C . All reactions were performed with 2 mM nucleoside substrate and 10 mM K_2HPO_4 in 50 mM glycine buffer at pH 9. Unless stated otherwise, $16 \mu\text{g}\cdot\text{mL}^{-1}$ ($0.6 \text{ U}\cdot\text{mL}^{-1}$) Py-NPase Y02 (for pyrimidine nucleosides) or $66 \mu\text{g}\cdot\text{mL}^{-1}$ ($3.7 \text{ U}\cdot\text{mL}^{-1}$) Pu-NPase N02 (for purine nucleosides) were applied. For inosine (**23**) and 2'-deoxyinosine (**24**) $330 \mu\text{g}\cdot\text{mL}^{-1}$ of Pu-NPase N02 were used and for 5-iodouridine (**13**) and 2'-deoxy-5-iodouridine (**14**) $32 \mu\text{g}\cdot\text{mL}^{-1}$ of Py-NPase Y02. All reactions were performed in duplicate at temperatures from 40 – 70°C in steps of 10°C . Three samples were taken from each reaction once equilibrium was reached to confirm reaction completion. The time points used for sampling are given in Table S3. In total, 576 data points were recorded. Outliers that either displayed an elevated baseline due to UV absorption of the 96-well plate or differed

more than 1.5 percentage points from the other two data points within a sample set of a given temperature and reaction mixture were excluded from data interpretation. Consequently, 519 data points were considered for further evaluation. Data treatment and fitting was carried out with Origin ProLab 9. All data, as well as all subsequent calculations can be inspected as freely available data from an external online repository.^[32] For each data point, K' was calculated via equation (1) and transformed apparent reaction enthalpy $\Delta_R H'^*$ [J·mol⁻¹] and transformed apparent reaction entropy $\Delta_R S'^*$ [J·mol⁻¹·K⁻¹] were fitted directly to all available datapoints for a substrate with equation (2). Similarly, $\Delta_R G'$ was calculated with equation (2) assuming that the apparent values $\Delta_R H'^*$ and $\Delta_R S'^*$ are independent of the reaction temperature in the considered range. The errors $\Delta\Delta_R H'^*$ [J·mol⁻¹], and $\Delta\Delta_R S'^*$ [J·mol⁻¹·K⁻¹] were derived from the fit and $\Delta\Delta_R G'$ was calculated via Gaussian error propagation:

$$\Delta\Delta_R G' = \sqrt{\Delta\Delta_R H'^{*2} + T^2 \Delta\Delta_R S'^{*2}} \quad (4)$$

with definitions from above.

Conflict of Interest

A.W. is CEO of the biotech company BioNukleo GmbH. F.K. is a researcher at BioNukleo GmbH and P. N. is a member of the advisory board.

Acknowledgements

We would like to thank Sarah von Westarp for her support with enzyme preparation, Niels Krausch for initial support with software development, and Dr. Erik Wade for revision of the manuscript. We are grateful for the support of R.T.G. by the German Research Foundation (DFG) under Germany's Excellence Strategy – EXC 2008/1 – 390540038 (UniSysCat), and by the Einstein Foundation Berlin (ESB) – Einstein Center of Catalysis (EC²).

References

- [1] L. P. Jordheim, D. Durantel, F. Zoulim, C. Dumontet, *Nat. Rev. Drug Discovery* **2013**, *12*, 447–464.
- [2] J. Shelton, X. Lu, J. A. Hollenbaugh, J. H. Cho, F. Amblard, R. F. Schinazi, *Chem. Rev.* **2016**, *116*, 14379–14455.
- [3] S. Kamel, H. Yehia, P. Neubauer, A. Wagner, in *Enzym. Chem. Synth. Nucleic Acid Deriv.*, **2019**, pp. 1–28.
- [4] H. Yehia, S. Kamel, K. Paulick, A. Wagner, P. Neubauer, *Curr. Pharm. Des.* **2017**, *23*, 6913–6935.
- [5] S. Kamel, M. Weiß, H. F. T. Klare, I. A. Mikhailopulo, P. Neubauer, A. Wagner, *Mol. Cancer* **2018**, *458*, 52–59.
- [6] I. V. Kulikova, M. S. Drenichev, P. N. Solyev, C. S. Alexeev, S. N. Mikhailov, *Eur. J. Org. Chem.* **2019**, 6999–7004.
- [7] I. V. Fateev, K. V. Antonov, I. D. Konstantinova, T. I. Muravyova, F. Seela, R. S. Esipov, A. I. Miroshnikov, I. A. Mikhailopulo, *Beilstein J. Org. Chem.* **2014**, *10*, 1657–1669.
- [8] H. Komatsu, T. Araki, *Nucleosides Nucleotides Nucleic Acids* **2005**, *24*, 1127–1130.
- [9] I. D. Konstantinova, K. V. Antonov, I. V. Fateev, A. I. Miroshnikov, V. A. Stepchenko, A. V. Baranovsky, I. A. Mikhailopulo, *Synthesis* **2011**, 1555–1560.
- [10] M. Rabuffetti, T. Bavaro, R. Sempoli, G. Cattaneo, M. Massone, F. C. Morelli, G. Speranza, D. Ubiali, *Catalysts* **2019**, *9*, 355.
- [11] B. Z. Eletskaya, D. A. Gruzdev, V. P. Krasnov, G. L. Levit, M. A. Kostromina, A. S. Paramonov, A. L. Kayushin, I. S. Muzyka, T. I. Muravyova, R. S. Esipov, *Chem. Biol. Drug Des.* **2019**, *93*, 605–616.
- [12] X. Zhou, K. Szeker, B. Janocha, T. Böhme, D. Albrecht, I. A. Mikhailopulo, P. Neubauer, *FEBS J.* **2013**, *280*, 1475–1490.
- [13] K. Szeker, X. Zhou, T. Schwab, A. Casanueva, D. Cowan, I. A. Mikhailopulo, P. Neubauer, *J. Mol. Catal. B* **2012**, *84*, 27–34.
- [14] I. Serra, T. Bavaro, D. A. Cecchini, S. Daly, A. M. Albertini, M. Terreni, D. Ubiali, *J. Mol. Catal. B* **2013**, *95*, 16–22.
- [15] D. F. Visser, F. Hennessy, J. Rashamuse, B. Pletschke, D. Brady, *J. Mol. Catal. B* **2011**, *68*, 279–285.
- [16] D. P. Nannemann, K. W. Kaufmann, J. Meiler, B. O. Bachmann, *Protein Eng. Des. Sel.* **2010**, *23*, 607–616.
- [17] X. Xie, W. Huo, J. Xia, Q. Xu, N. Chen, *Enzyme Microb. Technol.* **2012**, *51*, 59–65.
- [18] R. T. Giessmann, N. Krausch, F. Kaspar, N. M. Cruz Bournazou, A. Wagner, P. Neubauer, M. Gimpel, *Process* **2019**, *7*, 380.
- [19] C. S. Alexeev, I. V. Kulikova, S. Gavryushov, V. I. Tararov, S. N. Mikhailov, *Adv. Synth. Catal.* **2018**, *360*, 3090–3096.
- [20] IUPAC, *Compendium of Chemical Terminology*, Blackwell Scientific Publications, Oxford, **1997**.
- [21] N. G. Panova, E. V. Shcheveleva, C. S. Alexeev, V. G. Mukhortov, A. N. Zuev, S. N. Mikhailov, R. S. Esipov, D. V. Chuvikovsky, A. I. Miroshnikov, *Mol. Biol.* **2004**, *38*, 770–776.
- [22] R. A. Alberty, *Biophys. Chem.* **2007**, *127*, 91–96.
- [23] A. Vita, C. Y. Huang, G. Magni, *Arch. Biochem. Biophys.* **1983**, *226*, 687–692.
- [24] R. Bose, E. W. Yamada, *Biochemistry* **1974**, *13*, 2051–2056.
- [25] R. A. Alberty, *J. Chem. Thermodyn.* **2004**, *36*, 593–601.
- [26] R. N. Goldberg, Y. B. Tewari, T. N. Bhat, *J. Phys. Chem. Ref. Data* **2007**, *4*, 1347–1397.
- [27] T. A. Krenitsky, G. W. Koszalka, J. V. Tuttle, *Biochemistry* **1981**, *20*, 3615–3621.
- [28] M. Camici, F. Sgarrella, P. L. Ipata, U. Mura, *Arch. Biochem. Biophys.* **1980**, *205*, 191–197.
- [29] A. Hatano, A. Harano, Y. Takigawa, Y. Naramoto, K. Toda, Y. Nakagomi, H. Yamada, *Bioorg. Med. Chem.* **2008**, *16*, 3866–3870.
- [30] J. C. Leer, K. Hammer-Jespersen, M. Schwartz, *Eur. J. Biochem.* **1977**, *75*, 217–224.

- [31] G. A. Kicska, P. C. Tyler, G. B. Evans, R. H. Furneaux, K. Kim, V. L. Schramm, *J. Biol. Chem.* **2002**, 277, 3219–3225.
- [32] F. Kaspar, R. T. Giessmann, **2019**, 10.5281/zenodo.3530526
- [33] F. Kaspar, R. T. Giessmann, K. Hellendahl, P. Neubauer, A. Wagner, M. Gimpel, ChemBioChem, in press.
- [34] F. Kaspar, R. T. Giessmann, N. Krausch, P. Neubauer, A. Wagner, M. Gimpel, *Methods Protoc.* **2019**, 2, 60.
- [35] R. T. Giessmann, N. Krausch, **2019**, 10.5281/zenodo.3243376.
-

Paper IV

Kaspar, F.; Neubauer, P.; Kurreck, A. Kinetic Analysis of the Hydrolysis of Pentose-1-Phosphates through Apparent Nucleoside Phosphorolysis Equilibrium Shifts. *ChemPhysChem* **2020**, accepted article, <https://doi.org/10.1002/cphc.202000901>.

This article was published as open access under a CC BY license which permits reproduction of the material with proper attribution, such as in this thesis.

Author contributions (with definitions by Brand *et al.* ¹)

Conceptualization, F.K.; Data curation, F.K.; Formal analysis, F.K.; Funding acquisition, P.N. and A.K.; Investigation, F.K.; Methodology, F.K.; Project administration, F.K. and A.K.; Resources, P.N. and A.K.; Software, - ; Supervision, P.N. and A.K.; Validation, - ; Visualization, F.K.; Writing—original draft, F.K.; Writing—review & editing, F.K., P.N. and A.K.

Specifically, my contribution included development of the specific research idea, design of experiments and development of the mathematical methodology for equilibrium shifts after hydrolysis of one product feeding back one substrate. I executed the experiments, curated the data and performed the calculations. Further, I illustrated the publication and lead the writing.

Preamble

One of the greatest challenges for nucleoside (trans)glycosylations at high temperatures is the instability of sugar phosphates, which has been plaguing projects in our group for years. Since these molecules are typically quite elusive to most analytical methods, their stability has remained virtually unexplored. Preliminary work from our laboratory and early hydrolysis experiments by Bunton and Humeres in the 1960s had shown that high temperatures and low pH promote hydrolysis of pentose-1-phosphates, but much of the temperature and pH space accessible in water has remained untouched. To tackle this analytical challenge, I developed a method which built upon the UV-based assay in paper II and the thermodynamic insights in paper III. The underlying idea was simple: A reaction in equilibrium will remain in equilibrium until one reactant is removed or added. Thus, *if a certain percentage of pentose-1-phosphate in a nucleoside phosphorolysis reaction mixture in equilibrium hydrolyses, this should cause an equilibrium shift reflecting that degree of hydrolysis*. Indeed, my equations supported the idea in theory. Proof-of-concept experiments then confirmed the feasibility and yielded data via simple analytical solutions of the problem – a method was born. As it turned out, the thermodynamics of nucleoside phosphorolysis even worked in our favor by allowing a significant equilibrium shift under very accessible reaction conditions. As an added bonus, this approach allows one to analyze valuable sugar phosphates in minute quantities directly from a nucleoside phosphorolysis reaction mixture without the need for any (typically low-yielding) purification. Despite the early disagreements of some publishers on the subfield this work belongs to, I am confident it will prove a useful method, especially for nucleosides with modified sugar moieties which have not been characterized yet.

Kinetic Analysis of the Hydrolysis of Pentose-1-phosphates through Apparent Nucleoside Phosphorolysis Equilibrium Shifts**

Felix Kaspar,^{*,[a], [b]} Peter Neubauer,^[a] and Anke Kurreck^{*,[a], [b]}

Herein, we report an addition to the toolbox for the monitoring and quantification of the hydrolytic decay of pentose-1-phosphates, which are known to be elusive and difficult to quantify. This communication describes how apparent equilibrium shifts of a nucleoside phosphorolysis reaction can be employed to calculate hydrolytic loss of pentose-1-phosphates based on the measurement of post-hydrolysis equilibrium concentrations of a nucleoside and a nucleobase. To demonstrate this approach, we assessed the stability of the relatively stable ribose-1-phosphate at 98 °C and found half-lives of 1.8–11.7 h depending on the medium pH. This approach can be extended to other sugar phosphates and related reaction systems to quantify the stability of UV-inactive and hard-to-detect reaction products and intermediates.

Many biomolecules of the central metabolism are rather elusive, owed to their nature as highly polar UV-inactive small molecules.^[1–3] Prominent examples include non-aromatic amino acids (building blocks of proteins), sugar phosphates (intermediates of glycolysis and nucleoside catabolism) and small carboxylic acids (intermediates of amino acid metabolism and Krebs cycle). Nonetheless, research of cellular processes as well as enzymatic reactions, both *in vivo* and *in vitro*, requires a fundamental quantitative understanding of the turnover and the stability of these molecules. Where common high-throughput HPLC-based detection of analytes fails, sensitive GC-based methods, mass spectrometry, derivatization of target molecules (or a combination of the above) or detection via coupled fluoro- or chromogenic reactions can serve as alternatives. Detection and quantification via NMR, TLC, polarimetry, refractometry or

specific enzymatic assays might also be employed, depending on the target analyte. However, many of these methods typically suffer from limited throughput and, often, a narrow working space. Furthermore, detection from complex mixtures, such as enzymatic reactions or buffered aqueous solutions, can prove difficult or impossible with some of the above methods.


Herein, we report an addition to the toolbox for the monitoring and quantification of the hydrolytic decay of pentose-1-phosphates. These compounds are central to nucleoside catabolism, nucleoside/nucleotide salvage pathways as well as the pentose phosphate pathway.^[4] Further, they serve as synthetic intermediates and sugar donors in nucleoside phosphorylase-catalyzed transglycosylations.^[5–7] Their synthesis typically occurs via phosphorolytic cleavage of a nucleoside, liberating the corresponding nucleobase and pentose-1-phosphate (Figure 1A). Once generated, pentose-1-phosphates are valuable intermediates as they allow direct glycosylation of (nearly) any other nucleobase. Thus, irreversible hydrolysis of these sugar synthons represents a costly loss – both *in vivo* and *in synthesis*.^[8–11] Previous work from Bunton and Hummeres^[12] had employed a colorimetric phosphate assay and work from our lab^[13] had used TLC for a preliminary screening of pentose-1-phosphate stability. Both studies revealed that acidic conditions as well as high temperatures promote hydrolysis. However, painting of a clearer picture requires more sensitivity and throughput than TLC or colorimetric phosphate detection from diluted mixtures offer. Furthermore, direct analysis of pure pentose-1-phosphates is discouraged by their limited commercial availability and deterring price point (ca. 50 € mg^{−1} for ribose- and 2-deoxyribose-1-phosphate as of September 2020).


This report details how apparent equilibrium shifts of nucleoside phosphorolysis can be used to assess the hydrolysis of *in situ* generated pentose-1-phosphates. For this approach we relied on nucleoside phosphorolysis as a tightly thermodynamically controlled reaction with equilibrium constants in the range of 0.01–0.8,^[14] which allows one to calculate all reagent concentrations of an enzymatic reaction in equilibrium solely by measuring two UV-active components (Figure 1A). We anticipated that knowledge of the equilibrium constant of a given transformation would enable us to quantify loss of one reagent (pentose-1-phosphate) via the mass balances off all reagents and a shifted apparent equilibrium position caused by the reaction system compensating the loss of a product via additional substrate consumption following Le Chatelier's principle. Having previously employed spectral unmixing-based reaction monitoring to detect slight temperature-dependent changes in the chemical equilibrium of many nucleoside

[a] F. Kaspar, Prof. Dr. P. Neubauer, Dr. A. Kurreck
Chair of Bioprocess Engineering
Technische Universität Berlin
Straße des 17. Juni 135, 10632 Berlin, Germany
E-mail: anke.wagner@tu-berlin.de

[b] F. Kaspar, Dr. A. Kurreck
BioNukleo GmbH
Ackerstraße 76, 13355 Berlin, Germany
E-mail: felix.kaspar@web.de

[**] A previous version of this manuscript has been deposited on a preprint server (<https://doi.org/10.26434/chemrxiv.13090244.v1>)

 Supporting information for this article is available on the WWW under <https://doi.org/10.1002/cphc.202000901>

 © 2020 The Authors. ChemPhysChem published by Wiley-VCH GmbH. This is an open access article under the terms of the Creative Commons Attribution License, which permits use, distribution and reproduction in any medium, provided the original work is properly cited.

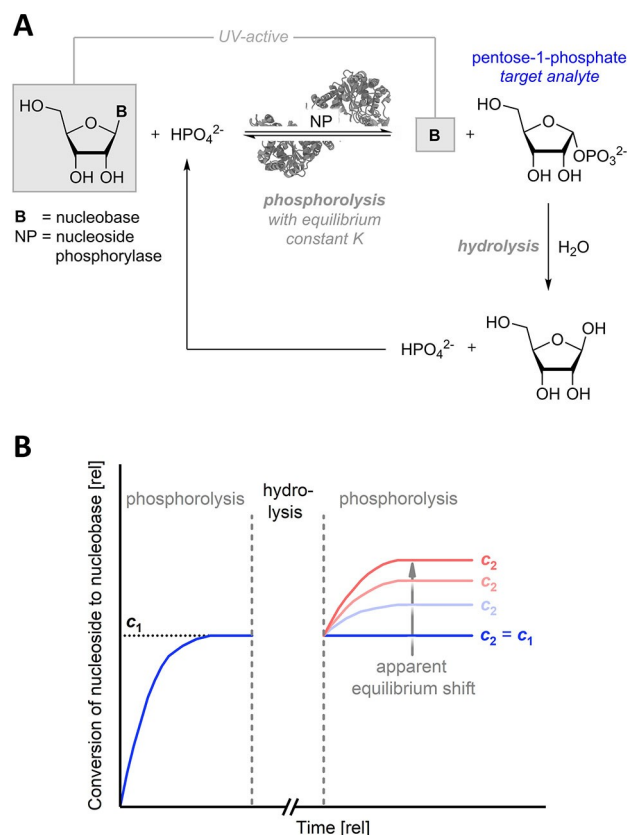


Figure 1. Enzymatic reversible phosphorolysis of a nucleoside with subsequent irreversible hydrolysis of the product pentose-1-phosphate (A) and illustrative reaction time course of a discontinuous performance of phosphorolysis and hydrolysis (B). c_1 and c_2 are the degrees of conversion from the nucleoside to the nucleobase in the pre- and post-hydrolysis equilibria as defined below. Phosphate liberated by hydrolysis of the target analyte feeds back into the substrate reservoir *in situ*. Monitoring of the phosphorolysis reaction can be achieved via the two UV-active components (nucleoside and nucleobase).^[15,16] The graphs shown in B only serve an illustrative purpose and do not represent real data.

phosphorolysis reactions,^[14–16] we again turned to this method to record small spectral differences to quantify minor equilibrium shifts. To effect these equilibrium shifts, we let nucleoside phosphorolysis reactions reach a stable equilibrium, then subjected these mixtures to hydrolyzing conditions and, upon addition of fresh enzyme and continuation of phosphorolysis, allowed the reaction to establish a new equilibrium (Figure 1B). This incubation time-dependent deviation of the new equilibrium from the old equilibrium could then be used to calculate the amount of lost pentose-1-phosphate.

The mathematical basis for this approach is given by the law of mass action,^[17] which describes the concentrations of all reaction components in a chemical equilibrium. In the case of nucleoside phosphorolysis, the concentrations of the nucleoside and nucleobase are easily accessible and the unknown concentrations of UV-inactive components (phosphate and the sugar phosphate) are generally available through the assumption of stoichiometry and the derived mass balances.^[14] The equilibrium constant K of nucleoside phosphorolysis is defined as

$$K = \frac{[P1P][B]}{[N][P]} \quad (1)$$

where $[P1P]$, $[B]$, $[N]$ and $[P]$ are the equilibrium concentrations of the pentose-1-phosphate, nucleobase, nucleoside and phosphate, respectively. Before hydrolysis to any significant degree has taken place, the following mass balances hold true for this reaction:

$$[P1P] = [B] = [P1P]_1 = [B]_1 \quad (2)$$

$$[N] = [N]_0 - [B]_1 \quad (3)$$

$$[P] = [P]_0 - [B]_1 \quad (4)$$

where $[N]_0$ and $[P]_0$ are the starting (initial) concentrations of the nucleoside and phosphate and $[P1P]_1$ and $[B]_1$ are the concentrations of the pentose-1-phosphate and the nucleobase and the first (pre-hydrolysis) equilibrium, respectively (assuming that the initial concentrations of both products, $[P1P]_0$ and $[B]_0$, are equal to zero). The degree of conversion of the nucleoside to the nucleobase in this first equilibrium c_1 is given as

$$c_1 = \frac{[B]_1}{[N]_0} \quad (5)$$

After the establishment of an initial equilibrium, termination of the enzymatic reaction and subsequent hydrolysis of the pentose-1-phosphate the mass balances of the nucleoside and the nucleobase remain identical. However, the hydrolysis of some fraction of the sugar phosphate results in adjusted mass balances for this reagent and its hydrolysis product phosphate (and ribose, which is not part of this equilibrium and will therefore not be considered herein). At this point, addition of fresh nucleoside phosphorylase leads to further conversion of the nucleoside to equalize the loss of pentose-1-phosphate and reestablish reagent concentrations which fulfill the equilibrium constraint (1). The degree of conversion in this new equilibrium then reflects the amount of hydrolyzed pentose-1-phosphate (see the Supporting Information for more details and derivations). This results in the adjusted mass balances:

$$[P1P] = c_2[N]_0 - [P1P]_h \quad (6)$$

$$[B] = c_2[N]_0 \quad (7)$$

$$[N] = [N]_0 - c_2[N]_0 \quad (8)$$

$$[P] = [P]_0 - c_2[N]_0 + [P1P]_h \quad (9)$$

where $[P1P]_h$ is the amount of hydrolyzed pentose-1-phosphate and c_2 is the degree of conversion of the nucleoside to the nucleobase in the post-hydrolysis equilibrium defined as

$$c_2 = \frac{[B]_2}{[N]_0} \quad (10)$$

where $[B]_2$ is the nucleobase concentration in the second (post-hydrolysis) equilibrium. These mass balances then allow the calculation of the concentration of hydrolyzed sugar phosphate upon insertion into the law of mass action (1). Solving of the resulting expression for $[P1P]_h$ yields an equation which returns analytical solutions for known values of c_2 , $[N]_0$, $[P]_0$ and K .

$$[P1P]_h = \frac{K([P]_0 - c_2[N]_0 - c_2[P]_0 + c_2^2[N]_0) - c_2^2[N]_0}{Kc_2 - c_2 - K} \quad (11)$$

The expected maximum degree of conversion in the second equilibrium $c_{2,max}$ can be obtained through the assumption of full hydrolysis of the initially generated sugar phosphate ($[P1P]_h = c_1[N]_0$) and is given by the expression:

$$c_{2,max} = \frac{-X}{2[N]_0(1-K)} + \frac{\sqrt{X^2 + 4([N]_0 - K[N]_0)(c_1[N]_0K + K[P]_0)}}{2[N]_0(1-K)} \quad (12)$$

where

$$X = c_1[N]_0K - c_1[N]_0 + [N]_0K + K[P]_0 \quad (13)$$

The incubation time-dependent conversion c_2 is available directly through monitoring of the reaction at its second equilibrium, K can either be determined experimentally or obtained from the respective literature^[14] and the initial concentrations $[N]_0$ and $[P]_0$ are known from the experimental setup. Thus, equation (11) allows direct quantification of hydro-

lyzed pentose-1-phosphate solely by measuring post-hydrolysis equilibrium positions of a nucleoside phosphorolysis reaction. Please note, however, that these equations assume that the equilibrium constant K can be determined with sufficient accuracy. Alternatively, replacement of K in (11) with the terms in equations (1) and (2) allows simultaneous determination of K and $[P1P]_h$ but demands monitoring of the first equilibrium via observation of the equilibrium conversion c_1 (also see the equations in^[14]). Calculation of

$$\Delta c_{max} = c_{2,max} - c_1 \quad (14)$$

then provides insight into the maximum apparent equilibrium shift Δc_{max} as a function of $[N]_0$, $[P]_0$ and K .

A theoretical examination of the solutions of this derived set of equations reveals a relatively broad operational window for equilibrium constants between 1 and 0.01 (Figure 2A). For the cheaply available sugar donor uridine ($K=0.15$ at 37 °C and pH 7.5),^[14] any phosphate to nucleoside ratio of 2.5–10 yields a potential equilibrium shift Δc_{max} of > 20 percentage points (pp; from the equilibrium position of no hydrolysis to the new equilibrium corresponding to full hydrolysis of the generated pentose-1-phosphate; Figure 2B), with the extreme ends of nucleoside conversion either generating almost no sugar phosphate ($c_1 < 10\%$) or offering little space for equilibrium adjustment ($c_1 > 80\%$).

To demonstrate this method with a practical example, we assessed the hydrolysis kinetics of the relatively stable ribose-1-phosphate (Rib1P). While pentose-1-phosphates lacking the 2-hydroxy group are prone to hydrolysis,^[13] ribosyl scaffolds offer much more stability.^[12,13] In fact, even high temperatures are known to effect only minimal decay of these molecules and previous work had largely limited their working space to acidic conditions – presumably to permit operation within a reason-

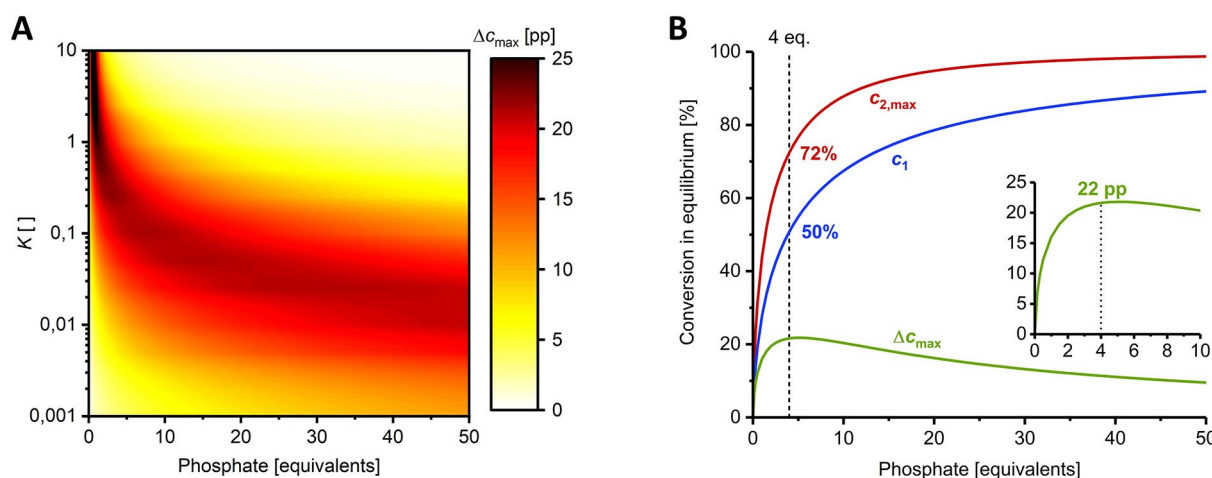


Figure 2. Working window for hydrolysis-induced equilibrium shifts of nucleoside phosphorolysis. The working window should enable a maximum equilibrium shift Δc_{max} as large as possible to permit accurate measurements of the effect. Suitable reaction conditions regarding phosphate excess depend on the equilibrium constant of the system (A). For uridine ($K=0.15$) the system is quite robust and offers a $\Delta c_{max} > 20$ pp over a broad phosphate excess range with an optimal zone of 4–6 equivalents (B). c_1 was calculated by solving equation (1) for the mass balances (2)–(4), as described previously,^[14] and $c_{2,max}$ and Δc_{max} were calculated via equations (12) and (14) for different equilibrium constants. Please see the externally hosted Supplementary Information for the calculations.^[18]

able timeframe. To benchmark the stability of **Rib1P** at higher pH values, we generated this compound *in situ* and subjected it to pH values from 7–9 at a temperature of 98 °C. The application of 4 equivalents of phosphate (2 mM uridine, 8 mM phosphate), yielded a stable equilibrium of 50% conversion to the corresponding nucleobase uracil and **Rib1P** (1 mM each at c_1 which agrees with previous reports).^[14] Rebuffering and incubation of this mixture at 98 °C for 1.5–5 h effected hydrolysis of **Rib1P** and gave new equilibrium positions of 54–69% after additional pH adjustment and addition of fresh nucleoside phosphorylase (see Figure 3 for exemplary data for pH 8). Consistent with the fundamental assumptions and the predictions of equation (12), the new equilibrium position approached but did not surpass 72% conversion, which would correspond to full hydrolysis of the initially generated **Rib1P**. Calculation of the amount of hydrolyzed **Rib1P** via equation (11) and fitting of the time-dependent decrease of remaining **Rib1P** as a first order exponential decay yielded half-lives of 1.8–11.7 h under these conditions (Figures 3, S1 and S2). These results strongly support the observation that **Rib1P** is quite tolerant to high temperatures, with alkaline pH values promoting additional stability.^[12] Considering the significant differences in experimental conditions, our derived first-order rate constants of hydrolysis are comparable to those reported by Bunton and Humeres^[12] more than 50 years ago (Figure S3) and reveal that the exponential decrease of the rate constant over pH extends well into the alkaline region, up to at least pH 9. One may expect that the half-life of **Rib1P** under moderate conditions far exceeds the values we obtained at 98 °C (presumably following Eyring relationships), suggesting that hydrolysis of this compound is a negligible factor in most scenarios employing

neutral or alkaline pH values and moderate temperatures. However, in applications where harsher conditions or acidic media are applied, hydrolysis of **Rib1P** should certainly be taken into consideration.

In conclusion, we outlined and demonstrated a tool for the assessment of the stability of pentose-1-phosphates based on apparent equilibrium shifts of a nucleoside phosphorolysis reaction. Our results reveal that spectral unmixing-based reaction monitoring can be used in conjunction with equilibrium thermodynamics to uncover the hydrolysis kinetics of relatively stable sugar phosphates such as ribose-1-phosphate. We anticipate that this approach can be extended to other sugar phosphates and related reaction systems where similar effects can be observed.

Experimental Section

Rib1P was generated *in situ* via phosphorolysis of 2 mM uridine with 8 mM potassium phosphate catalyzed by *Geobacillus thermoglucosidasius* pyrimidine nucleoside phosphorylase. Reaction mixtures in equilibrium were aliquoted into PCR tubes and diluted with a buffer mix for pH adjustment. These mixtures were incubated at 98 °C for various times and stored at 4 °C until analysis. To determine the amount of hydrolyzed **Rib1P**, further phosphorolysis of this mixture was initiated by the addition of fresh nucleoside phosphorylase and buffer. This second phosphorolysis reaction was run into its equilibrium and samples were withdrawn and quenched in 100 mM aqueous NaOH. Aliquots of these alkaline samples were transferred to an UV/Vis-transparent 96-well plate and UV absorption spectra were recorded from 250 to 350 nm. The respective degree of conversion of the nucleoside to the nucleobase was then obtained via deconvolution of the experimental UV absorption spectra using suitable reference spectra.^[15,16] Please see the Supporting Information for all experimental details. All raw data presented in this report, along with metadata and calculations are freely available from an external online repository.^[18] Likewise, reference spectra and software for spectral unmixing are available from the same repository^[19,20] and detailed in previous works.^[15,16]

Acknowledgements

The authors are grateful to Robert Giessmann (orcid.org/0000-0002-0254-1500) for inspiration and initial conceptualization and thank Kerstin Heinecke (Technische Universität Berlin) for proof-reading and critical comments. The authors thank the Open Access Publishing funds of the TU Berlin for the support of this publication. Open access funding enabled and organized by Projekt DEAL. Open access funding enabled and organized by Projekt DEAL.

Keywords: decay · phosphate · ribose · sugar phosphate · UV spectroscopy

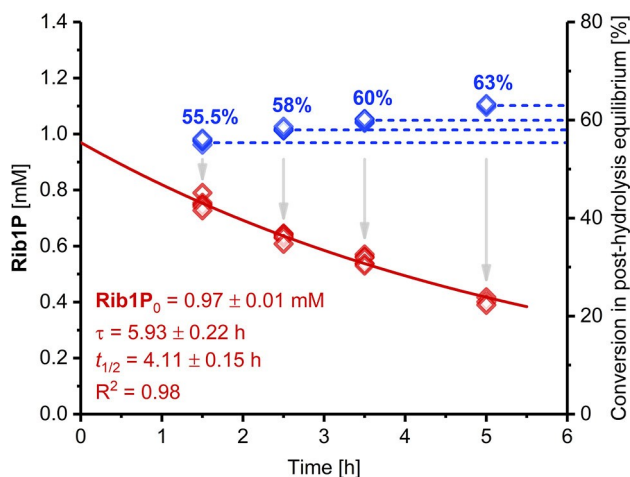


Figure 3. Hydrolysis of **Rib1P** at pH 8 and 98 °C as quantified by phosphorolysis equilibrium shifts. **Rib1P** was generated enzymatically *in situ* through phosphorolysis of uridine catalyzed by *Geobacillus thermoglucosidasius* pyrimidine nucleoside phosphorylase and then subjected to hydrolyzing conditions. Hydrolyzed **Rib1P** after various incubation times was calculated via equations (11) and (S23) from post-hydrolysis equilibrium positions (blue) and residual **Rib1P** (red) was fitted with a first-order exponential decay (equation (S23) in the Supplementary Information). Please see the Supporting Information for more experimental details and the externally hosted Supplementary Information for all raw and calculated data.^[18]

[1] S. Mikkelsen, D. Eduardo, *Bioanalytical Chemistry*, John Wiley & Sons, 2004.

[2] H. Scherz, G. Bonn, *Analytical Chemistry of Carbohydrates*, Wiley-VCH, 2002.

- [3] M. Alterman, P. Hunziker, *Amino Acid Analysis*, Springer, **2012**.
- [4] M. G. Tozzi, M. Camici, L. Mascia, F. Sgarrella, P. L. Ipata, *FEBS J.* **2006**, *273*, 1089–1101.
- [5] S. Kamel, H. Yehia, P. Neubauer, A. Wagner, *Enzym. Chem. Synth. Nucleic Acid Deriv.* (Ed.: F. J.), **2018**, 1–28.
- [6] F. Kaspar, R. T. Giessmann, K. F. Hellendahl, P. Neubauer, A. Wagner, M. Gimpel, *ChemBioChem* **2020**, *21*, 1428–1432.
- [7] F. Kaspar, M. R. L. Stone, P. Neubauer, A. Kurreck, *Green Chem.* **2017**, *19*, 18–43.
- [8] P. G. Loncke, P. J. Berti, *J. Am. Chem. Soc.* **2006**, *128*, 6132–6140.
- [9] C. A. Bunton, *Acc. Chem. Res.* **1970**, *3*, 257–265.
- [10] M. Camici, F. Sgarrella, P. L. Ipata, U. Mura, *Arch. Biochem. Biophys.* **1980**, *205*, 191–197.
- [11] Y. B. Tewari, D. K. Steckler, R. N. Goldberg, W. L. Gitomer, *J. Biol. Chem.* **1988**, *263*, 3670–3675.
- [12] C. A. Bunton, E. Humeres, *J. Org. Chem.* **1969**, *34*, 572–576.
- [13] S. Kamel, M. Weiß, H. F. T. Klare, I. A. Mikhailopulo, P. Neubauer, A. Wagner, *J. Mol. Catal.* **2018**, *458*, 52–59.
- [14] F. Kaspar, R. T. Giessmann, P. Neubauer, A. Wagner, M. Gimpel, *Adv. Synth. Catal.* **2020**, *362*, 867–876.
- [15] F. Kaspar, R. T. Giessmann, N. Krausch, P. Neubauer, A. Wagner, M. Gimpel, *Methods Protoc.* **2019**, *2*, 60.
- [16] F. Kaspar, R. T. Giessmann, S. Westarp, K. F. Hellendahl, N. Krausch, I. Thiele, M. C. Walczak, P. Neubauer, A. Wagner, *ChemBioChem* **2020**, *21*, 2604.
- [17] IUPAC, *Compendium of Chemical Terminology*, Blackwell Scientific Publications, Oxford, **1997**.
- [18] F. Kaspar, **2020**, DOI 10.5281/zenodo.4274088.
- [19] R. T. Giessmann, N. Krausch, **2019**, DOI 10.5281/zenodo.3243376.
- [20] R. T. Giessmann, F. Kaspar, **2019**, DOI 10.5281/zenodo.3333469.

Manuscript received: October 30, 2020

Revised manuscript received: November 17, 2020

Accepted manuscript online: November 20, 2020

Version of record online: ■■■, ■■■■

Paper V

Kaspar, F.;[#] Giessmann, R.T.;[#] Hellendahl, K.F.; Neubauer, P.; Wagner, A.; Gimpel, M. General Principles of Yield Optimization of Nucleoside Phosphorylase-Catalyzed Transglycosylations. *ChemBioChem* **2020**, *21*, 1428–1432, <https://doi.org/10.1002/cbic.201900740>. [#]equal contribution

This article was published as open access under a CC BY license which permits reproduction of the material with proper attribution, such as in this thesis.

Author contributions (with definitions by Brand *et al.* ¹)

Conceptualization, F.K., R.T.G., P.N., A.W. and M.G.; Data curation, F.K. and R.T.G.; Formal analysis, F.K. and R.T.G.; Funding acquisition, R.T.G., P.N. and A.W.; Investigation, F.K. and K.H.; Methodology, F.K. and R.T.G.; Project administration, F.K., R.T.G. and A.W.; Resources, R.T.G., K.H., A.W. and P.N.; Software, R.T.G.; Supervision, R.T.G., P.N. A.W. and M.G.; Validation, -; Visualization, F.K.; Writing—original draft, F.K. and R.T.G.; Writing—review & editing, F.K., R.T.G., K.H., P.N., A.W. and M.G.

Specifically, my contribution included co-development of the specific research idea, formulation of the simplified equations, design of experiments, execution of experiments, data curation, calculations, as well as illustration and lead writing of the publication.

Preamble

Following the thermodynamic characterization of nucleoside phosphorolysis, transfer of this knowledge to nucleoside transglycosylations was the logical next step. At the time, the literature already offered a wealth of examples for nucleoside transglycosylations and quite a few examples of reaction optimizations which had revealed that lower phosphate and higher sugar donor concentrations are beneficial to conversion of the starting nucleobase to a nucleoside of interest. This felt intuitive to me, given that a nucleoside transglycosylation is just two coupled phosphorolysis reactions – each of which behaves according to its respective equilibrium constant of phosphorolysis. On that basis, Robert Giessmann and I realized that we should be able to predict the equilibrium conversion of a transglycosylation as a function of the initial conditions. Although a simplifying assumption (“*there is no phosphate*”) allowed quite straightforward calculation of the transglycosylation conversion yielding very practicable and robust solutions for a range of purine nucleosides, this approach did not satisfy our needs for pyrimidines as those systems tend to be more sensitive due to their lower net Gibbs energies of phosphorolysis. Although a framework for more precise solutions had been reported in 2018 by Alexeev *et al.*, their mathematical basis contained a fundamental misassumption causing their equations to fail when equilibrium constants became too high. We overcame this hurdle by obtaining numerical solutions for the full set of equilibrium constraints, revealing a characteristic behavior of the reaction system depending on the starting nucleoside and desired product. Simply put, purines are really easy to make. Pyrimidine products on the other hand can be tricky and low-yielding. In principle, yields can be improved by simply adding more sugar donor, but this can create quite a few problems with downstream processing, as evident in paper VI.

General Principles for Yield Optimization of Nucleoside Phosphorylase-Catalyzed Transglycosylations**

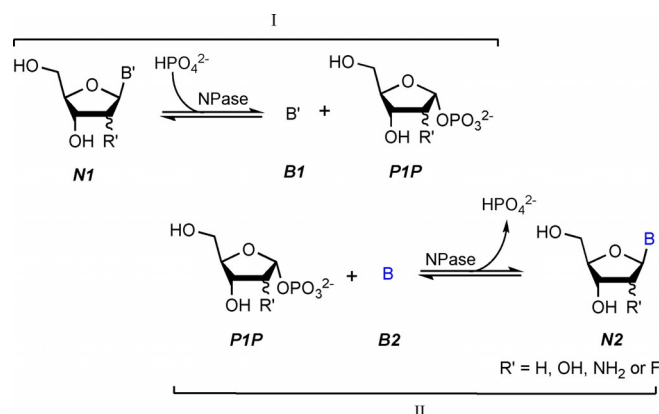
Felix Kaspar⁺,^{*,[a]} Robert T. Giessmann⁺,^[b] Katja F. Hellendahl,^[b] Peter Neubauer,^[b] Anke Wagner,^{*,[a, b]} and Matthias Gimpel^[b]

The biocatalytic synthesis of natural and modified nucleosides with nucleoside phosphorylases offers the protecting-group-free direct glycosylation of free nucleobases in transglycosylation reactions. This contribution presents guiding principles for nucleoside phosphorylase-mediated transglycosylations alongside mathematical tools for straightforward yield optimization. We illustrate how product yields in these reactions can easily be estimated and optimized using the equilibrium constants of phosphorolysis of the nucleosides involved. Furthermore, the varying negative effects of phosphate on transglycosylation yields are demonstrated theoretically and experimentally with several examples. Practical considerations for these reactions from a synthetic perspective are presented, as well as freely available tools that serve to facilitate a reliable choice of reaction conditions to achieve maximum product yields in nucleoside transglycosylation reactions.

Nucleosides are highly functionalized biomolecules essential for the storage of information as DNA and RNA, cellular energy transfer and as enzyme cofactors. Modified nucleosides are widely employed as pharmaceuticals for the treatment of cancers and viral infections.^[1] Consequently, their synthetic accessibility is crucial. However, the preparation of nucleosides and nucleoside analogues by conventional synthetic methods heavily relies on protecting groups and, thus, suffers from poor atomic efficiency and low yields.^[2–5]

Biocatalytic methods offer the efficient and protecting group-free synthesis of pyrimidine and purine nucleosides. The use of nucleoside phosphorylases (NPases) for the preparation of nucleosides and their analogues in transglycosylation reac-

tions is firmly established^[6] and numerous examples of enzymatic or chemoenzymatic syntheses can be found in the literature.^[7–14] NPases catalyze the reversible phosphorolysis of nucleosides to pentose-1-phosphates (Scheme 1, I). In transglycosylation reactions, a forward and a reverse nucleoside phosphorolysis are coupled in situ to glycosylate a free nucleobase with the pentose-1-phosphate generated by the first reaction (Scheme 1, I and II). Formally, this equals a direct glycosylation of the nucleobase to yield a nucleoside of interest. Conveniently, nature has provided an arsenal of robust biocatalysts that offer a broad substrate spectrum, excellent tolerance to harsh reaction conditions as well as perfect regio- and diastereoselectivity at the C1' position.^[11,12]



Scheme 1. Reaction sequence of a nucleoside transglycosylation.

Despite their great versatility, enzymatically catalyzed nucleoside transglycosylation reactions have previously suffered from an unclear interrelation between yields and the employed enzymes and starting materials. Particularly, the impact of different sugar donors and/or nucleobases as well as varying phosphate concentrations on the product yield had remained unclear until recently. The pioneering work of Alexeev et al.^[15] demonstrated that yields of nucleoside transglycosylation reactions involving uridine and adenosine can be accurately predicted based on the equilibrium constants of phosphorolysis of the sugar donor and the product nucleoside. They concluded that the ratio of the equilibrium constants of the sugar donor and the product nucleoside (K_1/K_2) determines maximum product yields and that an excess of sugar donor is further beneficial. On the other hand, increasing phosphate concentrations were shown to have a negative impact on product

[a] F. Kaspar,⁺ Dr. A. Wagner
BioNukleo GmbH
Ackerstrasse 76, 13355 Berlin (Germany)
E-mail: felix.kaspar@web.de

[b] R. T. Giessmann,⁺ K. F. Hellendahl, Dr. P. Neubauer, Dr. A. Wagner,
Dr. M. Gimpel
Department of Biotechnology, Technical University of Berlin
ACK24, Ackerstrasse 76, 13355 Berlin (Germany)
E-mail: anke.wagner@tu-berlin.de

[⁺] These authors contributed equally to this work.

[**] A previous version of this manuscript has been deposited on a preprint server (<https://doi.org/10.26434/chemrxiv.11283296.v1>).

Supporting information and the ORCID identification numbers for the authors of this article can be found under <https://doi.org/10.1002/cbic.201900740>.

© 2019 The Authors. Published by Wiley-VCH Verlag GmbH & Co. KGaA. This is an open access article under the terms of the Creative Commons Attribution License, which permits use, distribution and reproduction in any medium, provided the original work is properly cited.

yields. However, Alexeev and colleagues^[15] based their calculations on the assumption that the concentration of phosphate is constant and furthermore only investigated one example of a high-yielding NPase-catalyzed transglycosylation. As a continuation of the considerations of Alexeev et al.^[15] we explored this reaction system from a practical synthetic perspective and developed a universally applicable equation for yield prediction. We show that the yield-diminishing effect of phosphate strongly depends on the equilibrium constant of phosphorolysis of the nucleoside of interest (K_2). This important feature, which proved critical in the biocatalytic preparation of pharmaceutically relevant pyrimidine nucleosides has thus far not been described theoretically or experimentally. Alongside our freely available Python code for precise yield predictions (see below) we also provide a simplified equation for the estimation of product yield that allows for straightforward analytical solutions instead of the numerical solutions previously required.

Nucleoside transglycosylation reactions are generally considered as formal glycosylations of a nucleobase **B2**, which yields the corresponding nucleoside of interest, **N2**. Here, a starting nucleoside, **N1**, is used as a glycosylation agent with the purpose of donating the sugar moiety. In an enzyme cascade, the sugar donor **N1** is subjected to phosphorolysis yielding a pentose-1-phosphate (**P1P**), which is consumed in the sequential reaction with nucleobase **B2** to produce **N2** (Scheme 1). The yield of this reaction is generally defined as the formation of **N2** in respect to **B2**, neglecting the other reagents **P1P**, **B1**, **N1** and phosphate. Indeed, inorganic phosphate only plays a catalytic role as it is used in the first step but liberated again in the following reaction.

Generally, yields in NPase-catalyzed transglycosylations are dictated by the equilibrium constraints of the two half reactions I and II [Eqs. (1), (2)]:

$$K_1 = \frac{[\text{B1}][\text{P1P}]}{[\text{N1}][\text{P}]} \quad (1)$$

$$K_2 = \frac{[\text{B2}][\text{P1P}]}{[\text{N2}][\text{P}]} \quad (2)$$

where K_1 and K_2 are the apparent equilibrium constants of phosphorolysis of the sugar donor and product nucleoside, respectively, $[\text{P}]$ is the equilibrium concentration of phosphate, $[\text{P1P}]$ is the equilibrium concentration of the pentose-1-phosphate and $[\text{N1}]$, $[\text{N2}]$, $[\text{B1}]$, and $[\text{B2}]$ are the equilibrium concentrations of the nucleosides and bases. Alexeev et al.^[15] previously solved this system of equations by assuming a constant concentration of phosphate and numerically solving the resulting cubic equation.

When we attempted to apply their equations to the synthesis of the pharmaceutically relevant nucleoside 5-ethynyluridine we were unable to obtain results that were in agreement with experimental HPLC data, as their formula yielded negative values for this case (Table S1 in the Supporting Information). Therefore, we sought to establish a mathematical tool that allows general applicability and reaction optimization of all nu-

cleoside transglycosylations. Bypassing the simplification made by Alexeev and co-workers, we implemented the system of equilibrium constraints (1) and (2) including all reagents as variables in a Python code to obtain more precise predictions (see externally hosted Python code).^[16]

Numerical solutions of this system allowed theoretical examination of the effect of phosphate and sugar donor excess on the product yield, considering a reasonable range of equilibrium constants.^[17] Approaching zero phosphate concentration, the maximum (ideal) product yield can be obtained, but at higher phosphate concentrations an apparent loss of yield can be observed due to phosphorolysis (or non-synthesis) of the product nucleoside (Figure 1). Whereas the K_1/K_2 ratio (equal to K_N) dictates the maximum yield with minimal phosphate, K_2 determines the extent of yield loss in the presence of phosphate. A high K_N in the order of 5–15 promises good to excellent yields (i.e., >90%) with only moderate excesses (i.e., twofold) of the sugar donor. On the other hand, reactions with a low K_N require a great excess of sugar donor to facilitate yields upward of 50%. Interestingly, the effect of phosphate varies between systems with the same K_N , which results from the fact that high K_2 values dictate a greater degree of phosphorolysis of **N2** at non-negligible phosphate concentrations—even at great excess of the sugar donor **N1** (Figure 1). Notably, whereas potential formation of intermediate pentose-1-phosphate needs to be considered for a realistic assessment and prediction of synthetic yield, we only observed less than four percentage points of deviation from the ideal yield for any nucleoside transglycosylation with <0.3 equiv of phosphate in the reaction conditions we covered with our considerations.^[16]

To validate these predictions experimentally and demonstrate the varying impact of phosphate on the product yield, we prepared a series of natural and base-modified ribosyl nucleosides from their respective nucleobases, using uridine as a sugar donor. Fitting of the experimental data to the equilibrium constraints^[15,16] yielded equilibrium constants K_1 and K_2 very similar to those reported previously^[17] and revealed a great range of apparent equilibrium constants K_2 (0.01 to 0.35 at 60 °C, pH 9) and K_N (0.4 to 16.0). In all cases, the experimental yields determined by HPLC agreed well with the predictions obtained for different phosphate concentrations (Figure 2). Our data emphasize that, as illustrated in Figure 1, particularly the yields of transglycosylation reactions with high K_2 values suffer enormously from phosphate concentrations higher than strictly necessary. For instance, adenosine formation ($K_2=0.01$) was impacted only minorly by the addition of 10 equiv of phosphate (92% ideal yield vs. 88% experimental yield with 10 equiv of phosphate), but 5-ethynyluridine yield ($K_2=0.35$) dropped by more than 30 percentage points under the same conditions (53% ideal yield vs. 22% experimental yield with 10 equiv of phosphate; Figure 2). Thus, steep losses in yield should be expected for products with a high K value (K_2), whereas the synthesis of nucleosides with low K values tolerates significant amounts of phosphate (Figure 2). Consistent with our predictions, we only observed small deviations from the maximum yield in the experiments with 0.2 equivalents of phosphate. Thus, the concentration of phosphate should be

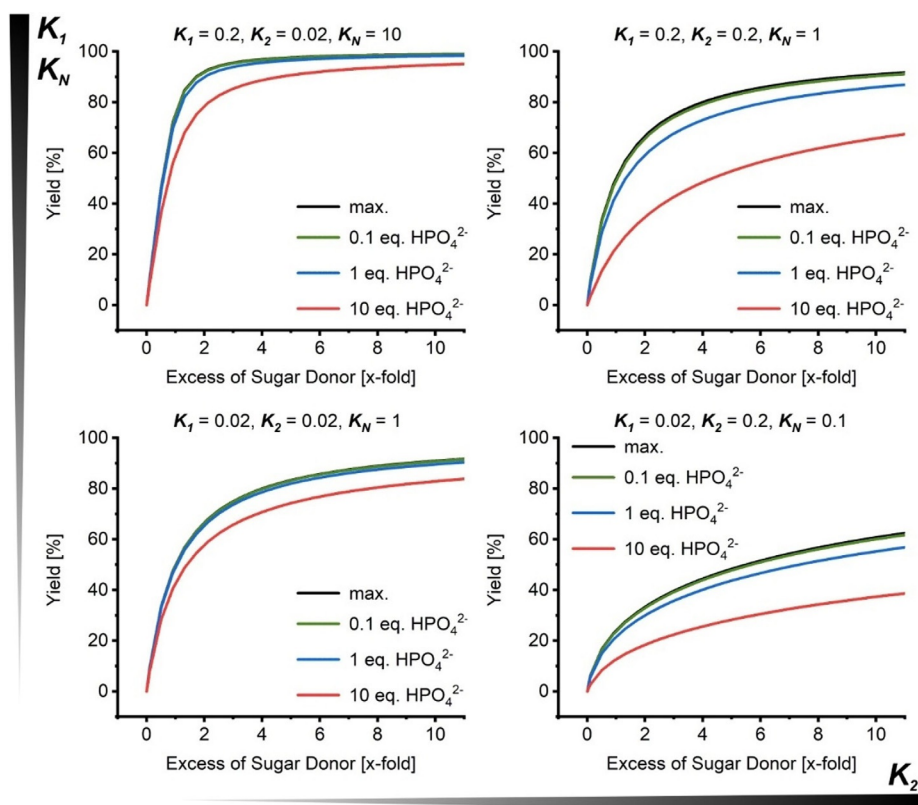


Figure 1. Impact of different K_1 and K_2 values on transglycosylation yield and phosphate gap. Realistic K_1 and K_2 values were assumed based on recently reported equilibrium constants.^[17] The graphs for maximum yield (max.; black), 0.1 equiv (green), 1 equiv (blue) and 10 equiv (red) of phosphate were plotted using numerical solutions of the system of equilibrium constraints (1) and (2) calculated with the Python code described in the external Supporting Information.^[16]

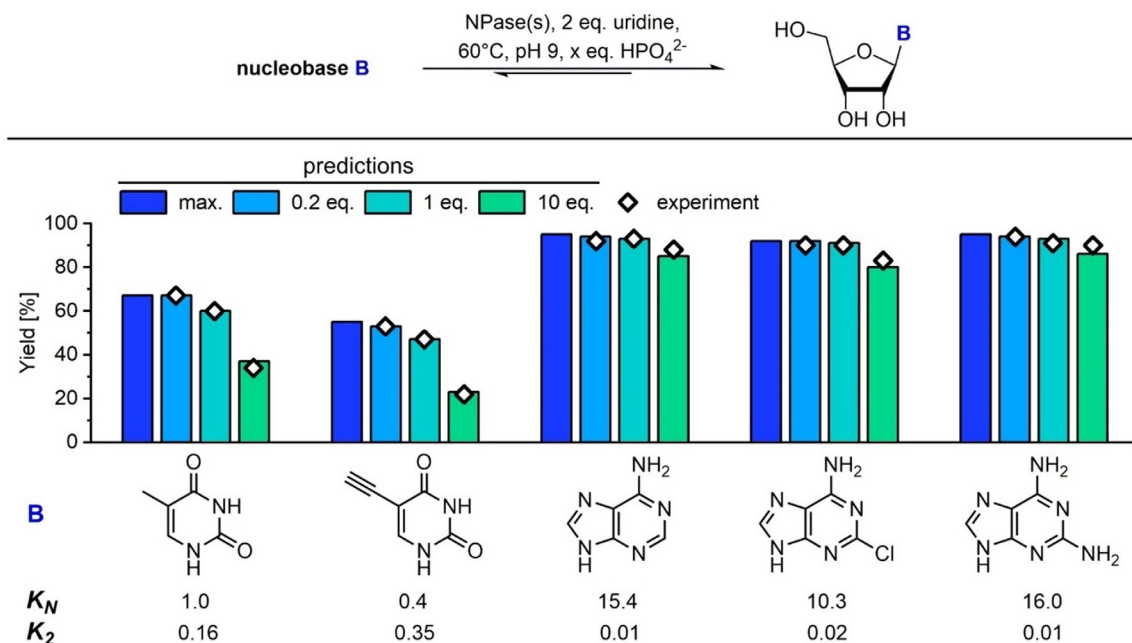


Figure 2. Biocatalytic synthesis of nucleosides by transglycosylation. Reactions were performed with 1 mM uridine as sugar donor ($K_1=0.16$), 0.5 mM nucleobase, $32 \mu\text{g mL}^{-1}$ pyrimidine NPase (2.5 U mL^{-1}) and $66 \mu\text{g mL}^{-1}$ purine NPase (5.0 U mL^{-1}) in 50 mM glycine buffer at pH 9 and 60°C with either 0.1 mM (0.2 equiv in respect to the starting base), 0.5 mM (1 equiv) or 5 mM (10 equiv) K_2HPO_4 in a total volume of 1 mL. Experimental yield (\diamond) was determined by HPLC considering conversion of the free nucleobase to its corresponding ribosyl nucleoside. Predictions (blue, light blue, turquoise and green columns) were carried out with the Python code described in the external Supporting Information.^[16] The values for the maximum yield (max.; blue) can also be obtained from Equation (4).

kept low in synthetic nucleoside transglycosylations to obtain maximum yield. For these cases, calculation of maximum (ideal) conversion provides a close approximation of the yield and allows for the use of a simplified formula.

Considering ideal (intermediate-free) coupling of the two half reactions, I and II, the terms for phosphate and **P1P** would cancel in the mathematical consideration of this system, as the production of these in one half reaction is compensated by the consumption in the other. Considering the net reaction, one may therefore define [Eq. (3)]:

$$K_N = \frac{K_1}{K_2} = \frac{[N2][B1]}{[N1][B2]} \quad (3)$$

with definitions from above. Solving this equation for the concentration of the product nucleoside, **N2**, yields only one physically possible solution that can be used to calculate ideal (phosphate- and **P1P**-free) yields of nucleoside transglycosylations with variable initial concentrations of the sugar donor **N1** and the nucleobase **B2**, $[N1]_0$ and $[B2]_0$, respectively [Eq. (4)]:

$$[N2] = \frac{K_N([N1]_0 + [B2]_0)}{2(K_N - 1)} - \frac{\sqrt{K_N(K_N[N1]_0^2 - 2K_N[N1]_0[B2]_0 + K_N[B2]_0^2 + 4[N1]_0[B2]_0)}}{2(K_N - 1)} \quad (4)$$

Thus, the maximum yield (at zero phosphate) can be calculated easily from Equation (4) to reflect a realistic estimate of the experimental yield if <0.3 equiv of phosphate are used. Ideal yields for conversions employing a range of pyrimidine and purine ribosyl and 2'-deoxyribosyl nucleosides^[17] with different reaction conditions including sugar donor excess and temperature, can be calculated with an Excel sheet freely available from the externally hosted Supporting Information.^[18]

These considerations and previous findings^[15,16] bear several practical implications for NPase-catalyzed nucleoside transglycosylations. First, a high K_1/K_2 ratio (high K_N) leads to excellent yields which can be achieved with moderate excess of the sugar donor, as mentioned by Alexeev and colleagues,^[15] and estimated easily with Equation (4). Second, pyrimidine nucleosides serve better as sugar donors than purine nucleosides.^[17] From a practical point of view, uridine and thymidine recommend themselves as ribosyl and 2'-deoxyribosyl donor, respectively, due to their simple commercial availability and high K value. Third, phosphate concentration in the transglycosylation reaction should generally be kept as low as possible to prevent loss of product yield. This becomes especially important in the synthesis of nucleosides with high K values, such as pyrimidine nucleosides like 5-ethynyluridine. Thus, 0.1–0.3 equivalents of phosphate in respect to the starting base may present an appropriate trade-off between reaction speed and maximum yield. A potential workflow for the fruitful application of the methodology presented in this work is suggested in the Supporting Information.

Given the easy accessibility of apparent equilibrium constants of phosphorolysis of any nucleoside of interest, the tools for yield prediction presented in this work aid the

straightforward design and optimization of nucleoside transglycosylations to facilitate high yields in NPase-catalyzed reactions. Exact yield prediction of transglycosylations may be performed with our Python code considering phosphate^[16] and practical estimations for ideal yield can easily be obtained from Equation (4).^[18]

Experimental Section

Enzymatic nucleoside transglycosylations were performed with 0.5 mM nucleobase, 1 mM uridine as sugar donor, 32 $\mu\text{g mL}^{-1}$ pyrimidine NPase (2.5 U mL^{-1} ; E-PyNP-0002, BioNukleo GmbH, Berlin, Germany) and 66 $\mu\text{g mL}^{-1}$ purine NPase (5.0 U mL^{-1} ; E-PNP-0002, BioNukleo GmbH) in 50 mM glycine buffer at pH 9 and 60 °C with either 0.1 mM (0.2 equivalents in respect to the starting base), 0.5 mM (1 equiv) or 5 mM (10 equiv) K_2HPO_4 in a total volume of 1 mL. Reaction mixtures were prepared from stock solutions and started by the addition of the enzyme(s). Time to equilibrium was approximated via UV/Vis spectroscopy.^[19] Allowing for additional time after apparent reaction completion, the reactions were stopped after 1 h by quenching samples of 100 μL in an equal volume of MeOH and analyzed by HPLC. All experimental and calculated data are available online.^[16,18]

Acknowledgements

We thank Sarah von Westarp for initial support. This work was funded by the Deutsche Forschungsgemeinschaft (DFG, German Research Foundation) under Germany's Excellence Strategy—EXC 2008/1-390540038. We are grateful for the support of R.T.G. by the Einstein Foundation Berlin (ESB)—Einstein Center of Catalysis (EC²). K.F.H. is funded by DFG grant no. 392246628.

Conflict of Interest

The authors declare no conflict of interest.

Keywords: equilibrium constant • nucleosides • nucleoside phosphorylases • pentose-1-phosphate • phosphates

- [1] L. P. Jordheim, D. Durantel, F. Zoulim, C. Dumontet, *Nat. Rev. Drug Discovery* **2013**, 12, 447–464.
- [2] A. M. Downey, C. Richter, R. Pohl, R. Mahrwald, M. Hocek, *Org. Lett.* **2015**, 17, 4604–4607.
- [3] A. M. Downey, R. Pohl, J. Roithová, M. Hocek, *Chem. Eur. J.* **2017**, 23, 3910–3917.
- [4] G. Framski, Z. Gdaniec, M. Gdaniec, J. Boryski, *Tetrahedron* **2006**, 62, 10123–10129.
- [5] Z. Kazimierczuk, H. B. Cottam, G. R. Revankar, R. K. Robins, *J. Am. Chem. Soc.* **1984**, 106, 6379–6382.
- [6] S. Kamel, H. Yehia, P. Neubauer, A. Wagner in *Enzymatic and Chemical Synthesis of Nucleic Acid Derivatives* (Ed.: J. Fernández-Lucas), Wiley-VCH, Weinheim, **2019**, pp. 1–28.
- [7] D. Ubiali, S. Rocchietti, F. Scaramozzino, M. Terreni, A. M. Albertini, R. Fernández-Lafuente, J. M. Guisán, M. Pregnotato, *Adv. Synth. Catal.* **2004**, 346, 1361–1366.
- [8] M. Rabuffetti, T. Bavaro, R. Semproli, G. Cattaneo, M. Massone, F. C. Morrelli, G. Speranza, D. Ubiali, *Catalysts* **2019**, 9, 355.
- [9] M. Winkler, J. Domarkas, L. F. Schweiger, D. O'Hagan, *Angew. Chem.* **2008**, 120, 10295–10297; *Angew. Chem. Int. Ed.* **2008**, 47, 10141–10143.

- [10] E. Calleri, G. Cattaneo, M. Rabuffetti, I. Serra, T. Bavaro, G. Massolini, G. Speranza, D. Ubiali, *Adv. Synth. Catal.* **2015**, *357*, 2520–2528.
- [11] K. Szeker, X. Zhou, T. Schwab, A. Casanueva, D. Cowan, I. A. Mikhailopulo, P. Neubauer, *J. Mol. Catal. B* **2012**, *84*, 27–34.
- [12] X. Zhou, K. Szeker, L.-Y. Jiao, M. Oestreich, I. A. Mikhailopulo, P. Neubauer, *Adv. Synth. Catal.* **2015**, *357*, 1237–1244.
- [13] J. Wierzchowski, A. Stachelska-Wierzchowska, B. Wielgus-Kutrowska, A. Bzowska, *Curr. Pharm. Des.* **2017**, *23*, 6948–6966.
- [14] A. Stachelska-Wierzchowska, J. Wierzchowski, A. Bzowska, B. Wielgus-Kutrowska, *Nucleosides, Nucleosides Nucleotides Nucleic Acids* **2018**, *37*, 89–101.
- [15] C. S. Alexeev, I. V. Kulikova, S. Gavryushov, V. I. Tararov, S. N. Mikhailov, *Adv. Synth. Catal.* **2018**, *360*, 3090–3096.
- [16] R. T. Giessmann, **2019**, DOI: <https://dx.doi.org/10.5281/zenodo.3522588>.
- [17] F. Kaspar, R. T. Giessmann, P. Neubauer, A. Wagner, M. Gimpel, *Adv. Synth. Catal.* **2019**, DOI: <https://doi.org/10.1002/adsc.201901230>.
- [18] F. Kaspar, R. T. Giessmann, **2019**, DOI: <https://dx.doi.org/10.5281/zenodo.3565561>.
- [19] F. Kaspar, R. T. Giessmann, N. Krausch, P. Neubauer, A. Wagner, M. Gimpel, *Methods Protoc.* **2019**, *2*, 60.

Manuscript received: December 6, 2019

Accepted manuscript online: December 10, 2019

Version of record online: January 28, 2020

Paper VI (preprint)

Hellendahl K.F.,[#] Kaspar, F.,[#] Zhou, X.; Yang, Z.; Huang, Z.; Neubauer, P.; Kurreck, A. Biocatalytic Synthesis of 2-Seleno Pyrimidine Nucleosides via Transglycosylation. *ChemRxiv* **2020**, preprint at <https://doi.org/10.26434/chemrxiv.13318202.v1>. [#]equal contribution

This preprint was published as open access under a CC BY license which permits reproduction of the material with proper attribution, such as in this thesis.

Author contributions (with definitions by Brand *et al.* ¹)

Conceptualization, K.F.H., F.K., P.N. and A.K.; Methodology, K.F.H., F.K. and A.K.; Software, F.K.; Validation, K.F.H.; Formal analysis, K.F.H and F.K.; Investigation, K.F.H and F.K.; Resources, X.Z., Z.Y., Z.H., A.K and P.N.; Writing – original draft, K.F.H and F.K.; Writing – review and editing, K.F.H., F.K., X.Z., Z.Y., Z.H., A.K. and P.N.; Visualization, K.F.H, F.K. and A.K., Supervision, A.K. and P.N.; Project administration K.F.H, F.K., A.K. and P.N.; Funding acquisition, A.K. and P.N.

Specifically, my contribution included design of experiments, execution of some kinetic experiments, calculations, as well as co-illustration and lead writing of the publication.

Preamble

With solid analytical tools in hand and a good grip on the thermodynamics of nucleoside phosphorolysis and transglycosylation reactions, we anticipated that we would have an easy time optimizing the previously low yields of selenium-containing pyrimidine nucleosides in transglycosylation reactions. As paper VI reveals, we were wrong. Not only were the starting nucleosides notoriously insoluble in water and proved sensitive to oxidation in solution, but their equilibrium constants of phosphorolysis were more than an order of magnitude higher than those of all other pyrimidine nucleosides, making their synthesis extremely unfavorable from a thermodynamic standpoint. Once we had addressed these issues through a pH shift (solubilizing the salt), working in nitrogen-sparged solutions and finding a suitable tradeoff for the amount of sugar donor to add, we discovered that the target compounds were also quite challenging to purify and our products persistently contained unreacted sugar donor. Although a two-step chromatography purification finally yielded pure product, the overall efficiency of the process was modest at best. Ultimately, this story proves a good example for the value of the fundamental work presented in papers II–V as it was quickly evident that we were fighting an uphill battle. We therefore had to find and settle for the best solution available, which was a meagre 40% isolated yield under optimized conditions. Clearly, some nucleosides require different strategies.

Biocatalytic synthesis of 2-Seleno pyrimidine nucleosides via transglycosylation

Katja F. Hellendahl,^{1,#} Felix Kaspar,^{1,2,#} Xinrui Zhou,³ Zhaoyi Yang,³ Zhen Huang,³ Peter Neubauer,¹ Anke Kurreck^{1,2*}

¹ Technische Universität Berlin, Chair of Bioprocess Engineering, Straße des 17. Juni 135, D-10623 Berlin, Germany.

² BioNukleo GmbH, Ackerstraße 76, D-13355 Berlin, Germany.

³ Sichuan University, College of Life Sciences, Key Laboratory of Bio-Resource and Eco-Environment of Ministry of Education, No. 17 People's South Road Section 3, 610041, Chengdu, China.

These authors contributed equally.

Selenium-modified nucleosides are powerful tools to study the structure and function of nucleic acids and their protein interactions. The wide-spread application of 2-seleno pyrimidine nucleosides is currently limited by low yields in established synthetic routes. Here, we describe the optimization of the synthesis of 2-Se-uridine and 2-Se-thymidine derivatives by thermostable nucleoside phosphorylases in transglycosylation reactions using natural uridine or thymidine as sugar donors. Reactions were performed at 60 or 80 °C and at pH 9 under hypoxic conditions to improve the solubility and stability of the 2-Se-nucleobases in aqueous media. To optimize the conversion, the reaction equilibria in analytical transglycosylation reactions were studied. The equilibrium constants of phosphorolysis of the 2-Se-pyrimidines were between 5 and 10 and thus belong to the highest described so far. Thus, a ten-fold excess of sugar donor was needed to achieve 40–48% conversion to the target nucleoside. Scale-up of the optimized conditions provided four Se-containing nucleosides in 6–40% isolated yield which compares favorably to established chemical routes.

Selenium derivatization is a powerful tool for structure and function studies of nucleic acids. The distinct steric and electronic properties of selenium have facilitated the X-ray structural analysis of DNA and RNA as well as their interactions with proteins.^[1–3] Notably, this technique has been applied for the investigation of ribozymes,^[4] riboswitches,^[5] homo-DNA,^[6] and for HIV-1 drug discovery.^[7] Besides their application in X-ray crystallography, selenium-modified nucleic acids are potential therapeutics for the treatment of cancer,^[8,9] as well as viral^[10–12] or bacterial infections.^[13] In addition, they have attracted interest as diagnostic agents.^[14] Several types of selenium derivatization of nucleic acids have been described which include replacement of an oxygen atom by selenium either in the nucleobase, the sugar moiety or in the phosphate groups of a nucleoside or nucleotide (please see ^[1–3] for reviews).

Despite their demand in chemical biology, a high-yielding and sustainable synthesis of Se-containing nucleosides has not yet been described. Previous work has established that 2-Se pyrimidine nucleosides can be accessed either from methylated sulfo-nucleosides or via selenation of isocytidine (Scheme 1).^[15–21] However, these chemical syntheses have several drawbacks, including the need for multi-step routes starting from a natural nucleoside, as well as an unfavorable atom economy and the extensive use of organic solvents.

In a proof-of-concept study, we recently described a protecting group-free biocatalytic route for the synthesis of Se-containing pyrimidine nucleosides (Scheme 1).^[22] We demonstrated on an analytical scale that 2- and 4-Se-substituted pyrimidine nucleosides can be prepared via transglycosylation reactions catalyzed by thermostable nucleoside phosphorylases (NPs).

NPs perform the reversible phosphorolysis of nucleosides to pentose-1-phosphates and nucleobases. By coupling the enzymatic phosphorolysis of a sugar donor with the glycosylation of a free nucleobase *in situ*, nucleosides can formally be synthesized directly from their corresponding nucleobases. The application of these enzymes resolves the need for protecting groups, laborious preparation as well as

isolation of sugar synthons,^[23] and furthermore greatly reduces the use of toxic organic solvents by employing aqueous systems^[24,25] (for reviews, see ^[26,27]).

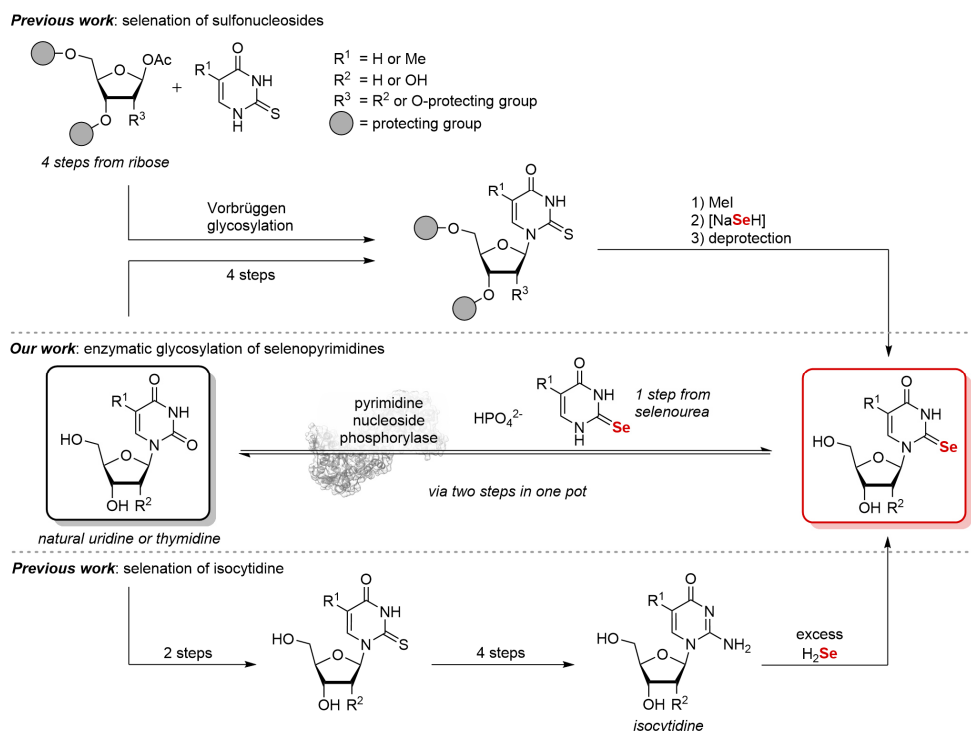
Nevertheless, several challenges remained to be addressed for the biocatalytic synthesis of Se-containing nucleosides using NPs. These include the poor solubility of the free Se-nucleobases in water, which has so far restricted substrate loading to approximately 1 mM. Furthermore, low substrate conversion was observed,^[22] indicating that the reaction equilibria of these reactions might be unfavorable. Additionally, prolonged reaction times have been shown to cause unwanted side reactions such as oxidation and deselenation of the starting material,^[22,28–30] resulting in heavy losses of the targeted product.

In this work, we addressed these obstacles by adjusting the reaction conditions to accommodate for the solubility and stability of Se-nucleobases in the biocatalytic synthesis of 2-Se-pyrimidine nucleosides. Working under hypoxic conditions prevented deselenation and oxidative loss of yield while an increased reaction pH allowed for higher substrate loading enabled by deprotonation of the Se-nucleobases. A thermodynamic characterization of the reaction equilibria via analytical transglycosylations revealed equilibrium constants well outside the known range of similar nucleosides and guided our choice of suitable reaction conditions to maximize the product yields. This report presents improved yields compared to established procedures and describes the first biocatalytic synthesis of 2-Se-pyrimidine nucleosides.

Results and Discussion

Optimization of the reaction conditions to improve substrate loading of the 2-Se-bases

We aimed to access the selenium-modified nucleosides **1a–2b** in a biocatalytic one-pot approach using thermostable NPs (Scheme 2). For this study we selected the commercially available pyrimidine nucleoside phosphorylase PyNP-04^[31] due to its thermostability and broad substrate spectrum. Analytical-scale experiments in our previous report^[22] indicated that these compounds can, in principle, be synthesized via transglycosylation starting



Scheme 1. Approaches to the synthesis of 2-Se pyrimidine nucleosides. Previous work has established introduction of selenium via a methylated sulfo-nucleoside or selenation of isocytidine. Our work aims for biocatalytic direct glycosylation of a selenium-containing nucleobase.

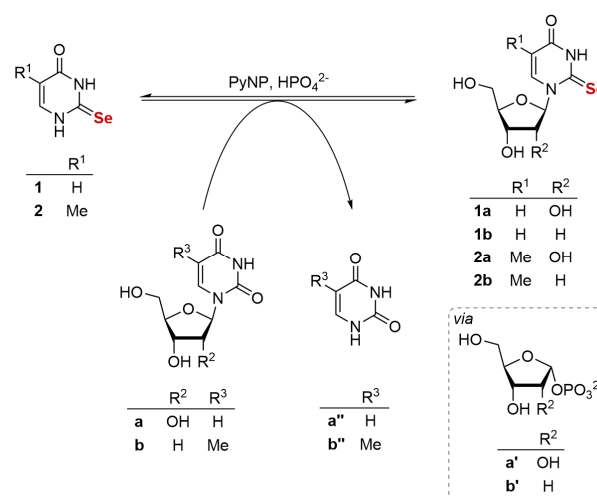
from the natural nucleosides uridine or thymidine and a selenium-containing nucleobase.

For synthetic applications, a higher substrate loading than previously employed (1 mM at pH 7) would be highly desirable to reduce solvent use and facilitate purification. Based on the pK_a of 2-Se-uracil (**1**) (7.18 at RT)^[32] we hypothesized that a slightly higher reaction pH would facilitate dissolution of **1** and 2-Se-thymine (**2**) as their corresponding anions. Since it was not available from the literature, we determined the pK_a of **2** through analysis of its UV absorption spectra at different pH values and found a similar value (7.49 ± 0.01 , Figure S1) to that of **1**. Hence, compared to the natural nucleobases, the Se-containing analogues were more acidic.^[16,32] Next, we investigated the solubility of **1** and **2** at pH values below and above their pK_a to see if a pH shift would allow higher substrate loading. At pH 7, **1** was not soluble at 10 mM, as indicated by the presence of precipitate (Figure S2). In contrast, full dissolution was observed at pH 9, confirming that a higher reaction pH can increase the solubility of the free nucleobase through deprotonation and solvation of the corresponding salt. Nonetheless, this effect was modest, as only **2** was fully soluble at 20 mM at pH 9 and RT.

A reaction temperature of 80 °C was initially chosen for the synthesis of Se-modified nucleosides as higher reaction rates are observed with the enzyme and it can be assumed that a high reaction temperature would further improve the solubility of **1** and **2**. Initial studies, however, revealed product losses during the synthesis of 2'-deoxyribo-nucleosides (data not shown) which can be correlated to the hydrolysis of the transglycosylation intermediate **b'** at higher temperatures.^[24,33] Hence, reaction temperatures of 80 °C were applied for the synthesis of ribonucleosides,

while 60 °C was chosen for reactions involving 2'-deoxynucleosides.

As the pH and temperature might influence the activity of PyNP-04, we determined specific activities of the enzyme at pH 7 or 9. To this end, we performed phosphorolysis reactions (Figure S3A) with the sugar donors uridine (**a**) and thymidine (**b**) in a MOPS (pH 7) or glycine buffer (pH 9). PyNP-04 was active under all conditions and, for instance, catalyzed the phosphorolysis of **a** at 80 °C with activities of approximately 80 U mg⁻¹ (Figure S3B). We additionally



Scheme 2. Biocatalytic synthesis of 2-Seleno pyrimidine nucleosides via transglycosylation reactions using a thermostable pyrimidine nucleoside phosphorylase (PyNP) as biocatalyst.

performed the glycosylation of **2** with the sugar phosphate **a'** to confirm that the higher reaction pH did not inhibit the second reaction step (reverse phosphorolysis). We observed no significant difference in glycosylation activity at pH 7 or 9, indicating that the deprotonated Se-base is well-accepted by the enzyme (Figure S4). Taken together, these data show that a reaction pH of 9 improves the solubility of **1** and **2** and thus permits higher substrate loadings, while still allowing excellent enzymatic activity, with reaction temperatures of 60 °C or 80 °C presumably facilitating additional solubility.

Hypoxic conditions for the stability of the 2-Se-bases

The application of an alkaline reaction environment and high temperatures guided us to explore the stability of the 2-Se-bases under these rather harsh conditions. In early experiments we noticed significant oxidation of the starting materials **1** and **2** which manifested itself as a loss of substrate and product, as observed by HPLC, as well as discoloration of the reaction mixtures from colorless to red and black (data not shown). To prevent oxidation and deselenation, reducing agents,^[28–30] such as dithiothreitol (DTT) and ascorbic acid, and inert gases^[17] like argon and nitrogen have previously been applied in chemical syntheses and redox studies. This led us to examine whether and for how long the stability of the 2-Se-bases can be increased by the application of DTT and/or a nitrogen atmosphere, which appeared compatible with our reaction system. To this end, we incubated **1** and **2** in different buffer systems (glycine/NaOH pH 9, with or without DTT and with or without a nitrogen atmosphere) at 80 °C and analyzed samples at different time points to check for the integrity of the starting material. Without any additives, oxidation products were already detected after 2 h, with most of the Se-base being degraded after 24 h (Figure 1A and S4). The addition of DTT had a slightly conserving effect, since no oxidation was apparent after 2 h, but significant deselenation was apparent after 4 and 24 h (Figure 1B and S5). In contrast, saturation of the solution with nitrogen almost completely prevented oxidation of **1** and **2**, with only minimal oxidation product being detectable after 24 h (Figure 1C and S5). As expected, combining DTT and nitrogen prevented oxidation completely and conserved the starting material for 24 h (Figure 1D and S5).

Having established that DTT and nitrogen aid in stabilization of **1** and **2**, we questioned if these conditions would affect the activity of PyNP-04. Therefore, we performed phosphorolysis experiments at 80 °C with either **a** in nitrogen-saturated buffer or the model substrate 5-iodouridine (**c**) in buffer with 5 mM DTT, as the latter nucleoside allowed us to obtain UV spectra that could be deconvoluted despite the heavy background absorption of DTT at lower wavelengths (see Figure S3 of ref. ^[34]). In contrast to the comparable activity observed in nitrogen-saturated buffer, the application of DTT caused a $\approx 40\%$ drop in enzymatic activity with our model substrate **c** (160 U mg⁻¹ to 95 U mg⁻¹; Figure S3B). However, due to the prevention of oxidation by DTT, we considered this decrease in enzymatic activity tolerable and proceeded with these conditions. In summary, the application of hypoxic conditions combined with the reducing agent DTT improved the stability of **1** and **2** in aqueous solution with

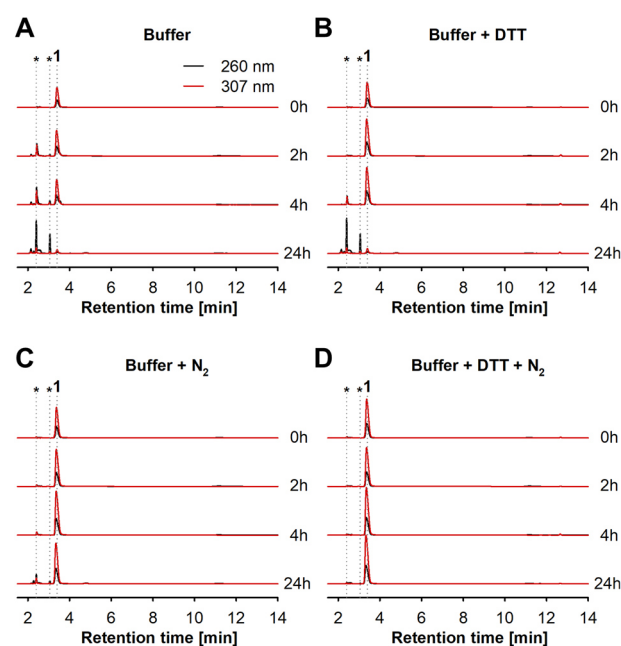


Figure 1. Stability of 5 mM **1** at 80 °C in 50 mM glycine/NaOH buffer pH 9 without additives (A), with 5 mM DTT (B), saturated with nitrogen (C) and the combination of 5 mM DTT and nitrogen (D). Samples were analyzed at 260 nm (black) and 307 nm (red). The typical retention time of **1** is 3.4 min and the degradation products appear at 2.4 min and 3 min. Similar results were obtained for **2** (Figure S5). Please see the externally hosted Supporting Information for raw data.^[34]

no detectable degradation after 24 h at 80 °C, while only slightly affecting the enzymatic activity.

Optimization of the enzymatic synthesis of 2-Se-pyrimidine nucleosides based on thermodynamic calculations

With hypoxic and alkaline reaction conditions in hand which served well to ensure solubility and stability of the nucleobases **1** and **2**, we turned our attention to the improvement of the previously observed low conversions.^[22] Recent work from our group had demonstrated the application of analytical-scale experiments and thermodynamic calculations for the yield optimization in NP-catalyzed transglycosylations.^[36] Therefore, we sought to transfer the same principles which had succeed for the synthesis of dihalogenated nucleosides^[36,37] to the preparation of Se-pyrimidines to obtain improved yields. Since nucleoside phosphorolysis (and consequently also the reverse reaction, glycosylation) is a thermodynamically controlled reaction, one may calculate the equilibrium state of transglycosylations via the corresponding equilibrium constants. Thus, when both equilibrium constants in the system are known, conversions can be optimized *in silico* to suggest conditions that enable the desired extent of product formation (for further details, please see ^[37]).

Equilibrium constants for the phosphorolysis of the sugar donors have been described recently for a broad temperature range,^[38] but the corresponding values for 2-Se-nucleosides have not been reported yet. Since these constants are

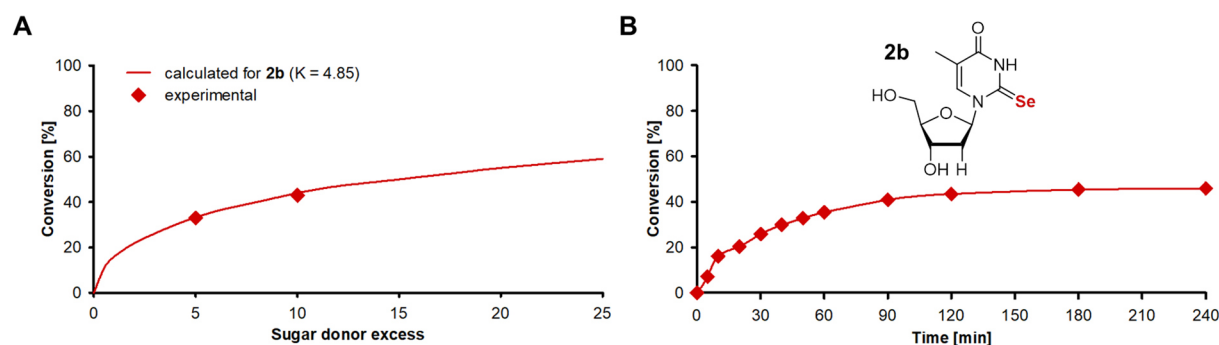


Figure 2. Optimization of the enzymatic synthesis of **2b**. Transglycosylation reactions were performed in a total volume of 1 mL using 1 mM (A) or 5 mM (B) **2** and 5 mM DTT in 50 mM glycine/NaOH buffer pH 9 at 60 °C with either 5-fold (A) or 10-fold (A, B) excess of **b** compared to the nucleobase **2**. Final concentrations of PyNP-04 of 50.4 $\mu\text{g mL}^{-1}$ (around 4 U, A) and 24.6 $\mu\text{g mL}^{-1}$ (around 2 U, B) were applied. Experimental conversion was determined by HPLC as the conversion of **2** to **2b**. The equilibrium constant of phosphorolysis was calculated based on the experimental data of the 5-fold sugar donor excess (A). Predictions of the conversion using different sugar donor to nucleobase ratios were carried out as described previously.^[37] Similar results were obtained for the other products (Table 1). Please see the externally hosted Supporting Information for raw data and calculations.^[34]

Table 1. Equilibrium state thermodynamic calculations were used to determine appropriate reaction conditions for the synthesis of **1a–2b**

Product	Product formation [%] at equilibrium for 5-fold sugar donor excess ^[a]	Equilibrium constant of phosphorolysis	Product formation [%] at equilibrium for 10-fold sugar donor excess		
			calculated ^[a]	experimental (1 mM nucleobase) ^[b]	experimental (5 mM nucleobase) ^[c]
1a	30.5	9.37	39	40	46 (4 h)
1b	30	6.07	40	40	39 (3 h)
2a	35	6.75	44	47	48 (4 h)
2b	33	4.85	44	43	45 (3 h)

Transglycosylation reactions were performed in a total volume of 1 mL in 50 mM glycine/NaOH buffer pH 9 and 5 mM DTT at 60 °C (**b**) or 80 °C (**a**). [a] 1 mM 2-Se-nucleobase (**1** or **2**), 50.4 $\mu\text{g mL}^{-1}$ (around 4 U) PyNP-04, 5 mM sugar donor (**a** or **b**). [b] 1 mM 2-Se-nucleobase (**1** or **2**), 50.4 $\mu\text{g mL}^{-1}$ (around 4 U) PyNP-04, 10 mM sugar donor (**a** or **b**). [c] 5 mM 2-Se-nucleobase (**1** or **2**), 24.6 $\mu\text{g mL}^{-1}$ (around 2 U) PyNP-04, 50 mM sugar donor (**a** or **b**).

Experimental conversion was determined by HPLC. Equilibrium constants were calculated with the experimental data of the 5-fold sugar donor excess. Predictions of the conversion using 10-fold sugar donor excess were carried out as described previously.^[37] Please see the externally hosted Supporting Information for raw data and calculations.^[34]

required for yield optimization via equilibrium thermodynamics, we performed small-scale transglycosylation reactions to determine these indirectly. Using a five-fold excess of the sugar donor over the Se-nucleobase and 0.09 equivalents of phosphate, equilibrium conversions between 30 and 35% were observed (Table 1, Figure 2A for **2b** as a visual example). This yielded equilibrium constants of the phosphorolysis of the Se-nucleosides **1a–2b** in the range of 5 to 10 (Table 1). Interestingly, these equilibrium constants surpass those of other natural and modified pyrimidine nucleosides (0.1–0.8)^[37–39] by around an order of magnitude. While the reason for these high equilibrium constants is unclear to date, we hypothesize that the increased electron density near the glycosylation site may contribute to a weaker C1'–N1 bond.

Next, we used thermodynamic calculations to predict the maximum conversions in transglycosylation reactions employing different sugar donor excesses (Figure 2A, Table 1). These predictions revealed that the high equilibrium constants of phosphorolysis of the target nucleosides limited the maximum conversion severely. For

example, to obtain 50% conversion to the Se-nucleoside **1a**, an approximately 20-fold excess of the sugar donor **a** would be necessary. However, such a high sugar donor excess is not suitable for preparative experiments due to high substrate costs and waste. In addition, we expected that this would also prevent an efficient workup and purification. Thus, we applied a sugar donor excess of 10 as a compromise to the aforementioned issues and maximum conversion. Although other sugar donors such as 5-ethynyluridine or 7-methylguanosine or direct glycosylation approaches with the sugar phosphates **a'** or **b'** might provide higher conversions than the application of natural uridine (**a**) and thymidine (**b**), these starting materials are considerably more expensive and would render this synthetic approach unfeasible (Table S1). Therefore, we decided to employ cheaply available **a** and **b** as sugar donors, which conveniently also offer some of the more favorable equilibrium constants of phosphorolysis among the natural nucleosides.^[38]

Finally, we confirmed our predictions for 10 equivalents of **a** or **b** and evaluated the reaction times until equilibrium in analytical-scale experiments under optimized conditions.

The predicted extent of product formation was observed for all four 2-Se-nucleosides (Figure 2B, Table 1) with reaction completion occurring within 3 to 4 h. Taken together, our thermodynamic characterization of the reaction system revealed unfavorable equilibrium constants of phosphorolysis of all Se-containing target nucleosides, severely limiting the maximum conversion achievable in transglycosylation reactions. However, a 10-fold excess of the sugar donors allowed for 40–48% conversion for all Se-nucleosides.

Enzymatic synthesis and purification in semi-preparative scale

After optimizing the synthesis under hypoxic and alkaline reaction conditions in small-scale experiments, we aimed to synthesize and purify the four 2-Seleno pyrimidines in semi-preparative scale. Therefore, the optimized reaction conditions were up-scaled to a volume of 50 mL with 5 mM 2-Se-nucleobase. The observed product formations in the larger scale of 41–47% after 3 (**2b**), 4 (**1b**) or 5 h (**1a**, **2a**) (Table 2) were in good accordance with the small-scale experiments. Purification of the target compounds from these reaction mixtures, however, proved rather challenging due to the presence of large quantities of unreacted sugar donor. In fact, our attempts to purify any of the products by preparative HPLC were unsuccessful as the obtained material persistently contained sugar donor starting material. Therefore, we applied an initial silica chromatography step on normal phase to remove most of the sugar donor, followed by a second purification step via preparative HPLC. Using this two-step process, we obtained 4.9–29.5 mg of the target nucleosides, corresponding to isolated yields of 6–40% (Table 2, Figure S6–S9). Despite the incomplete conversions and product losses during purification, our biocatalytic route compares favorably to its chemical counterparts where yields of less than 10% are typically achieved.^[22]

Table 2. Yields and purity of 2-Se-pyrimidine nucleosides

Product	Conversion [%] (Time [h])	Isolated yield [mg] ([%])	Purity [%] ^[a]
1a	44 (5)	4.9 (6.3)	98
1b	41 (4)	29.5 (40.5)	94
2a	47 (5)	20.8 (25.9)	99
2b	45 (3)	9.6 (12.5)	99

The 50 mL reaction mixture consisted of 5 mM 2-Se-base (**1** or **2**), 50 mM sugar donor (**a** or **b**), 5 mM DTT and 24.6 $\mu\text{g mL}^{-1}$ (around 98 U) PyNP-04 in 50 mM glycine/NaOH buffer pH 9 saturated with nitrogen. The reaction temperature was 60 °C (**1b**, **2b**) or 80 °C (**1a**, **2a**). [a] Purity was determined via analytical HPLC. Please see the externally hosted Supporting Information for raw data.

Conclusion

This work presents a biocatalytic synthesis of 2-Se-pyrimidine nucleosides via transglycosylation from uridine or thymidine. Following a thermodynamic characterization of the phosphorolysis of the target nucleosides on a small scale, four selenium-containing pyrimidine nucleosides were obtained in scale-up experiments where alkaline and hypoxic conditions, as well as high temperatures, enabled sufficient solubility and stability of the starting materials. Although the present route delivers improved yields compared to previous efforts, product purification currently represents a major bottleneck and needs to be addressed in future studies.

Experimental Section

General Information

All chemicals and solvents were of analytical grade or higher and purchased, if not stated otherwise, from Sigma-Aldrich (Steinheim, Germany), Carl Roth (Karlsruhe, Germany), TCI Deutschland (Eschborn, Germany), Carbosynth (Berkshire, UK) or VWR (Darmstadt, Germany). 2-Se-uracil (**1**) and 2-Se-thymine (**2**) were prepared according to literature procedures.^[32]

The thermostable nucleoside phosphorylase PyNP-04 (E-PyNP-0004)^[31] was obtained from BioNukleo GmbH (Berlin, Germany) and used as recommended by the manufacturer. PyNP-04 was heterologously expressed in *Escherichia coli* and purified by affinity chromatography. The provided stock solution (1.12 mg mL⁻¹) was stored at 4 °C. The enzyme originates from a thermophilic bacterium with an optimum growth temperature of 80 °C.

All UV/Vis absorption spectra were recorded with a BioTek PowerWave HT plate reader using UV/VIS-transparent 96-well plates (UV-STAR F-Bottom #655801, Greiner Bio-One). All raw and calculated data described in this article are freely available from an external online repository.^[34]

Determination of the dissociation constant (pK_a) of 2-Se-modified nucleobases

The pK_a of **1** and **2** was determined by analysis of their UV/Vis absorption spectra between pH 4 and pH 10 at RT. In a total volume of 10 mL, the nucleobases were dissolved to a concentration of 100 μM in 50 mM MOPS buffer (initially pH 9). Desired pH values were adjusted with HCl and NaOH and samples of 200 μL were transferred to a UV/Vis-transparent 96-well plate to record the UV absorption spectra in the range of 250 to 350 nm in steps of 1 nm. The spectra were analyzed via spectral unmixing as previously described^[35,40] using a fully protonated (pH 4) and a fully deprotonated (pH 10) spectrum as substrate and product reference for the deprotonation reaction, as spectra obtained near these pH values displayed identical shape (indicating no further reaction). For the determination of the pK_a, the experimental data were fitted to equation (1), whereby the pH was set as the input variable, α as the dependent variable and pK_a as the parameter to fit.^[41]

$$\alpha = \frac{x_{\text{deprot}}}{x_{\text{deprot}} + x_{\text{prot}}} = \frac{10^{\text{pH}-\text{pK}_a}}{1 + 10^{\text{pH}-\text{pK}_a}} \quad (1)$$

Solubility of the 2-Se-modified nucleobases

The solubility of **1** and **2** was tested in 50 mM MOPS/NaOH buffer pH 7 and 50 mM glycine/NaOH buffer pH 9 at RT. In a total volume of 0.3 to 10 mL, the nucleobases were dissolved to concentrations of 1 mM, 5 mM, 10 mM and 20 mM. The solutions were observed for the occurrence of precipitate.

Stability of the 2-Se-modified nucleobases

The stability of **1** and **2** was analyzed at 80 °C in Pyrex® glass tubes with screw caps. Therefore, the nucleobases were dissolved to a concentration of 5 mM in the following four buffers: (a) 50 mM glycine/NaOH buffer pH 9, (b) 50 mM glycine/NaOH buffer pH 9 with 5 mM 1,4-dithioreitol (DTT), (c) 50 mM glycine/NaOH buffer pH 9, saturated with nitrogen and (d) 50 mM glycine/NaOH buffer pH 9 with 5 mM DTT, saturated with nitrogen. Samples were taken after 0 h, 2 h, 4 h and 24 h, and diluted to a final concentration of 1 mM nucleobase with MeOH. After centrifugation (4 °C and 21,500 g for 20 min), samples were analyzed by analytical HPLC as described below.

Enzyme activity assays

The activity of PyNP-04 was determined by performing phosphorolysis reactions with the substrates uridine (**a**), thymidine (**b**) and the model substrate 5-iodouridine (**c**). Samples were analyzed by the UV/Vis spectroscopy-based assay described recently.^[35,40] Briefly, a 500 µL reaction mixture consisting of 1 mM nucleoside and 50 mM K₂HPO₄ in 50 mM buffer (glycine/NaOH pH 9 or MOPS/NaOH pH 7) was preheated to the desired temperature (60 °C or 80 °C). The reaction was started by the addition of the enzyme (typically 10 µL of enzyme stock solution prediluted in 2 mM potassium phosphate buffer pH 7). Final concentrations of PyNP-04 from 150 to 750 ng mL⁻¹ were applied. At timely intervals, samples of 60 µL were taken and quenched in 450 µL 100 mM NaOH and 200 µL of the diluted sample was transferred to a UV/Vis-transparent 96-well plate to record the UV absorption spectra from 250 to 350 nm in steps of 1 nm. Spectral analysis was carried out as described previously^[35,40] with software^[42] and reference spectra^[43] freely available online.

To assay PyNP-04 for the glycosylation of the Se-nucleobase **2**, reactions consisting of 1 mM **2**, 10 mM **b'** and 70 µg mL⁻¹ enzyme in 50 mM glycine/NaOH buffer pH 9 were monitored. For analysis, samples of 60 µL were withdrawn, quenched in an equal volume of MeOH and diluted with 400 µL 100 mM glycine/NaOH buffer pH 10. The experimental spectra were fitted with corresponding reference spectra of **2** and **2b** obtained under the same conditions.

One unit (U) of enzyme activity was defined as the amount of the enzyme catalyzing the conversion of 1 µmol of substrate per minute under the described assay conditions.

Optimization of the enzymatic synthesis of 2-Se-modified nucleosides

The 2-Se-modified nucleosides **1a–2b** were accessed in a one-pot transglycosylation reaction using the pyrimidine nucleoside phosphorylase PyNP-04 as biocatalyst. The thermodynamic characterization was performed as

described previously.^[36,37] Reaction equilibria were determined from reactions with 1 mM 2-Se-nucleobase (**1** or **2**), 5 mM sugar donor (**a** or **b**), 5 mM DTT, 50 mM glycine/NaOH buffer pH 9 and 50.4 µg mL⁻¹ (around 4 U) PyNP-04 in a total volume of 1 mL. The nitrogen-saturated reaction mixtures were incubated at 60 °C for the deoxyribosides **1b** and **2b** and 80 °C for the ribosides **1a** and **2a** until reaction completion (indicated by no further product formation; within 30 min under these conditions). Samples were diluted to 1 mM sugar donor concentration in MeOH, centrifuged (4 °C, 21,500 g, 20 min) and analyzed by HPLC.

The equilibrium constants of phosphorolysis of the 2-Se-pyrimidine nucleosides were calculated via equilibrium state thermodynamics and numerical solutions. Nucleoside phosphorolysis is a tightly thermodynamically controlled reaction and transglycosylations behave as coupled equilibrium reactions as they comprise a forward and a reverse phosphorolysis. Thus, knowledge of the equilibrium constant of the sugar donor, the concentrations of the starting materials as well as the degree of conversion to the product nucleoside allows calculation of the equilibrium constants of phosphorolysis of the product nucleoside via numerical solutions of the system of coupled equilibrium constraints (see ^[36,37]). These numerical solutions can either be obtained via the Python code described in our previous work^[44] or, more conveniently, the Excel sheet presented in the externally hosted Supplementary Information of this publication. Herein, we used the previously published equilibrium constants of phosphorolysis of the sugar donors **a** and **b** for calculation.^[38,45] Based on the obtained equilibrium constants, expected conversions for the 2-Se-nucleosides using a 10-fold sugar donor excess were calculated (please see the externally hosted Supplementary Information for details).^[34,44] To verify the theoretical calculations and to monitor the reaction progression, reactions with 5 mM 2-Se-base, 50 mM sugar donor, 5 mM DTT in 50 mM glycine/NaOH buffer pH 9 saturated with nitrogen and 24.64 µg mL⁻¹ (around 2 U) PyNP-04 in a total volume of 1 mL were performed at 60 °C for the deoxyribosides and 80 °C for the ribosides. Samples were diluted 50-fold in MeOH, centrifuged (4 °C, 21,500 g, 20 min) and analyzed by HPLC.

Analytical High-performance liquid chromatography (HPLC)

Analytical HPLC analyses were carried out with an Agilent 1200 series system equipped with an Agilent DAD detector using a Phenomenex (Aschaffenburg, Germany) reversed phase Kinetex EVO C18 column (250 × 4.6 mm). Samples were analyzed at two wavelengths (λ = 260 nm, 307 nm) at 25 °C and a flow rate of 1 mL min⁻¹. Isocratic elution was performed using 97% 20 mM ammonium acetate buffer and 3% acetonitrile for 7 min followed by a linear gradient to 60% 20 mM ammonium acetate buffer and 40% acetonitrile over 8 min. Afterwards, the initial conditions were restored and maintained for 4 min.

Conversions were determined by quantifying the 2-Se-nucleosides **1a–2b** and 2-Se-nucleobases **1** and **2** at 307 nm using equation (2), whereby P_X is the peak area of compound X and P_{total} is the sum of all peak areas at 307 nm. Substrates and products were identified based on their retention time and UV absorption spectra by

comparison to authentic standards. Typical retention times under these conditions were as follows: **1**: 3.4 min, **2**: 6 min, **a**: 3.6 min, **b**: 8.6 min, **a''**: 3 min, **b''**: 4.5 min, **1a**: 7 min, **1b**: 12 min, **2a**: 12 min and **2b**: 13 min. **a'** and **b'** are not UV-active and cannot be detected with a DAD system.

$$\text{Conversion (X) [\%]} = 100 \times \frac{P_x}{P_{\text{total}}} \quad (2)$$

Synthesis of 2-Se pyrimidine nucleosides in semi-preparative scale

2-Se nucleosides were synthesized in a reaction volume of 50 mL consisting of 5 mM 2-Se base (**1** or **2**), 50 mM sugar donor (**a** or **b**), 5 mM DTT, 50 mM glycine/NaOH buffer pH 9 and 24.6 $\mu\text{g mL}^{-1}$ (**a**: 98.5 U, **b**: 97.4 U) PyNP-04. The reaction mixture was saturated with nitrogen. Deoxyribosyl derivatives were prepared at 60 °C and ribosyl derivatives at 80 °C. The reactions were stopped after 3 to 5 h by a pH shift to 13 through addition of 10 M NaOH (monitored with a pH-electrode). The pH was shifted back to 9 using 25% HCl and proteins were removed by filtration at room temperature using a vacuum pump and 0.45 μm cellulose nitrate filters (Sartorius, Goettingen, Germany). The filtrate was saturated with nitrogen and stored at 4 °C until purification.

Purification of 2-Se pyrimidine nucleosides by Silica column chromatography

The first purification step was performed at room temperature via column chromatography (10% MeOH in DCM) using a Sigma-Aldrich silica gel (pore size 60; mesh particle size 220-440; particle size 35-75 μm). The reaction mixture was adsorbed onto silica gel by addition of 1.8 g of silica to the aqueous reaction mixture and evaporation of the solution *in vacuo*. The resulting powder was stored at -20 °C until loading on a silica column for purification. Collected fractions were analyzed by TLC (10% MeOH in DCM) using UV detection. Fractions containing the 2-Se-nucleoside were combined and dried under reduced pressure and stored at -20 °C until further purification by semi-preparative HPLC.

Purification of 2-Se pyrimidine nucleosides by semi-preparative HPLC

2-Se-nucleosides were further purified at room temperature using a Knauer HPLC system equipped with a Smartline Detector 2600 and an Azura P2.1 L pump. A reversed phase Kinetex® 5 μm Evo C18 column (250 x 21.2 mm) and a flow rate of 21.24 mL min⁻¹ were used. Samples were analyzed at 210 nm. Deionized water and acetonitrile were applied as eluents, while the gradient was modified from the analytical method as summarized in Table S2. The product purified by silica chromatography was dissolved in deionized water (Table S2) and filtered either with a 0.45 μm PES syringe filter or with a 0.45 μm cellulose nitrate filter using a vacuum pump. The collected product fractions were kept on ice to prevent product degradation during the purification process. Collected 2-Se-nucleoside fractions were dried using a Christ Gamma 1-20 freeze-dryer (Osterode am Harz, Germany).

LC-MS analysis

For LC-MS analysis, 0.1 mg sample was dissolved in 1 mL water in a HPLC vial. Samples were analyzed using a HPLC Agilent 1200 series system coupled to an ESI-Orbitrap-MS (ThermoFisher LTQ Orbitrap XL). The LC analyses were carried out using a Grace reversed phase GROM-Sil-ODS-4-HE column (50 x 2 mm, 3 μm). Samples were analyzed at 20 °C and at three wavelengths (λ = 215 nm, 280 nm, 350 nm). A flow rate of 0.3 mL min⁻¹ was applied. The gradient was linearly increased from 80% 0.1% HCOOH in water and 20% 0.1% HCOOH in ACN to 100% 0.1% HCOOH in ACN in 10 min. The mobile phase composition was held for 3 min at 100% 0.1% HCOOH in ACN. Finally, the initial conditions were restored and maintained for 5 min. The raw data was analyzed using FreeStyle (Thermo Scientific).

Compound characterization (also see Figures S6-S9)

2-Selenouridine (1a): off-white powder, R_f = 0.29 (DCM/MeOH 9:1); UV/Vis (4.5% ACN in 20 mM NH₄Ac pH 6.8): λ_{max} = 307 nm; HRMS (ESI): m/z calcd for C₉H₁₂N₂O₅Se+H⁺: 308.9984 [M+H]⁺; found: 308.9986

2'-Deoxy-2-Selenouridine (1b): yellow powder, R_f = 0.39 (DCM/MeOH 9:1); UV/Vis (26% ACN in 20 mM NH₄Ac pH 6.8): λ_{max} = 307 nm; HRMS (ESI): m/z calcd for C₉H₁₂N₂O₄Se+H⁺: 293.0035 [M+H]⁺; found: 293.0036

5-Methyl-2-selenouridine (2a): slightly cream-colored powder, R_f = 0.38 (DCM/MeOH 9:1); UV/Vis (26% ACN in 20 mM NH₄Ac pH 6.8): λ_{max} = 307 nm; HRMS (ESI): m/z calcd for C₁₀H₁₄N₂O₅Se+H⁺: 323.0141 [M+H]⁺; found: 323.0144

2-Selenothymidine (2b): off-white powder, R_f = 0.43 (DCM/MeOH 9:1); UV/Vis (30% ACN in 20 mM NH₄Ac pH 6.8): λ_{max} = 307 nm; HRMS (ESI): m/z calcd for C₁₀H₁₄N₂O₄Se+H⁺: 307.0192 [M+H]⁺; found: 307.0194

Acknowledgements

We thank the Mass Spectrometry Analytical Center of the Institute of Chemistry of Technische Universität Berlin for analysis of our samples. K.F.H. was funded by the Deutsche Forschungsgemeinschaft (DFG, German Research Foundation) - grant number 392246628.

Conflict of Interest

A. K. is CEO of the biotech company BioNukleo GmbH. F. K. is a scientist at BioNukleo GmbH and P. N. is a member of the advisory board. These affiliations constitute no conflict of interest with the results presented and discussed in this report.

Author Information

Corresponding Author

Dr. Anke Kurreck, anke.wagner@tu-berlin.de, orcid.org/0000-0001-6919-725X

Other Authors

Katja F. Hellendahl, orcid.org/0000-0002-5408-3679

Felix Kaspar, orcid.org/0000-0001-6391-043X

Dr. Xinrui Zhou, orcid.org/0000-0002-7104-6749

Zhaoyi Yang, orcid.org/0000-0003-3880-1199

Dr. Zhen Huang, orcid.org/0000-0002-8640-3227

Dr. Peter Neubauer, orcid.org/0000-0002-1214-9713

References

- [1] J. Sheng, Z. Huang, *Chem. Biodivers.* **2010**, *7*, 753–785.
- [2] L. Lin, J. Sheng, Z. Huang, *Chem. Soc. Rev.* **2011**, *40*, 4591–4602.
- [3] W. Zhang, J. W. Szostak, Z. Huang, *Front. Chem. Sci. Eng.* **2016**, *10*, 196–202.
- [4] A. Serganov, S. Keiper, L. Malinina, V. Tereshko, E. Skripkin, C. Hobartner, A. Polonskaia, A. T. Phan, R. Wombacher, R. Micura, et al., *Nat. Struct. Mol. Biol.* **2005**, *12*, 218–224.
- [5] A. Serganov, Y.-R. Yuan, O. Pikovskaya, A. Polonskaia, L. Malinina, A. T. Phan, C. Hobartner, R. Micura, R. R. Breaker, D. J. Patel, *Chem. Biol.* **2004**, *11*, 1729–1741.
- [6] M. Egli, P. S. Pallan, R. Pattanayek, C. J. Wilds, P. Lubini, G. Minasov, M. Dobler, C. J. Leumann, A. Eschenmoser, *J. Am. Chem. Soc.* **2006**, *128*, 10847–10856.
- [7] S. Freisz, K. Lang, R. Micura, P. Dumas, E. Ennifar, *Angew. Chemie Int. Ed.* **2008**, *47*, 4110–4113.
- [8] L. Lin, J. Sheng, R. K. Momin, Q. Du, Z. Huang, *Nucleosides. Nucleotides Nucleic Acids* **2009**, *28*, 56–66.
- [9] A. F. Ross, K. C. Agarwal, S. H. Chu, R. E. J. Parks, *Biochem. Pharmacol.* **1973**, *22*, 141–154.
- [10] P. K. Sahu, T. Umme, J. Yu, G. Kim, S. Qu, S. D. Naik, L. S. Jeong, *Molecules* **2017**, *22*, DOI 10.3390/molecules22071167.
- [11] P. K. Sahu, G. Kim, A. Nayak, J. Y. Ahn, M. W. Ha, C. Park, J. Yu, H. Park, L. S. Jeong, *Asian J. Org. Chem.* **2016**, *5*, 183–186.
- [12] P. K. Sahu, T. Umme, J. Yu, A. Nayak, G. Kim, M. Noh, J.-Y. Lee, D.-D. Kim, L. S. Jeong, *J. Med. Chem.* **2015**, *58*, 8734–8738.
- [13] I. Di Leo, F. Messina, V. Nascimento, F. G. Nacca, D. Pietrella, E. J. Lenardão, G. P. and L. Sancineto*, *Mini. Rev. Org. Chem.* **2019**, *16*, 589–601.
- [14] J. Caton-Williams, Z. Huang, *Angew. Chem. Int. Ed. Engl.* **2008**, *47*, 1723–1725.
- [15] D. S. Wise, L. B. Townsend, *J. Heterocycl. Chem.* **1972**, *9*, 1461–1462.
- [16] C. Y. Shiue, S. H. Chu, *J. Org. Chem.* **1975**, *40*, 2971–2974.
- [17] H. Sun, J. Sheng, A. E. A. Hassan, S. Jiang, J. Gan, Z. Huang, *Nucleic Acids Res.* **2012**, *40*, 5171–5179.
- [18] P. Bartos, A. Maciaszek, A. Rosinska, E. Sochacka, B. Nawrot, *Bioorg. Chem.* **2014**, *56*, 49–53.
- [19] M. Kogami, D. R. Davis, M. Koketsu, *Heterocycles* **2016**, *92*, 64–74.
- [20] A. E. A. Hassan, J. Sheng, W. Zhang, Z. Huang, *J. Am. Chem. Soc.* **2010**, *132*, 2120–2121.
- [21] A. Roy, C. Conlee, A. Fougerolles, *Modified Nucleic Acid Molecules and Uses Thereof*, **2014**, WO 2014/093924 A1.
- [22] X. Zhou, W. Yan, C. Zhang, Z. Yang, P. Neubauer, I. A. Mikhailopulo, Z. Huang, *Catal. Commun.* **2019**, *121*, 32–37.
- [23] F. Kaspar, M. R. L. Stone, P. Neubauer, A. Kurreck, *ChemRxiv* **2020**, DOI 10.26434/chemrxiv.12753413.v1.
- [24] S. Kamel, M. Weiß, H. F. T. Klare, I. A. Mikhailopulo, P. Neubauer, A. Wagner, *Mol. Catal.* **2018**, *458*, 52–59.
- [25] C. M. Alder, J. D. Hayler, R. K. Henderson, A. M. Redman, L. Shukla, L. E. Shuster, H. F. Sneddon, *Green Chem.* **2016**, *18*, 3879–3890.
- [26] I. A. Mikhailopulo, A. I. Miroshnikov, *Acta Naturae* **2010**, *2*, 36–59.
- [27] I. Mikhailopulo, *Curr. Org. Chem.* **2007**, *11*, 317–335.
- [28] N. C. Payne, A. Geissler, A. Button, A. R. Sasuclark, A. L. Schroll, E. L. Ruggles, V. N. Gladyshev, R. J. Hondal, *Free Radic. Biol. Med.* **2017**, *104*, 249–261.
- [29] B. Hu, Y. Wang, S. Sun, W. Yan, C. Zhang, D. Luo, H. Deng, L. R. Hu, Z. Huang, *Angew. Chemie Int. Ed.* **2019**, *58*, 7835–7839.
- [30] H. Moroder, C. Kreutz, K. Lang, A. Serganov, R. Micura, *J. Am. Chem. Soc.* **2006**, *128*, 9909–9918.
- [31] BioNukleo, “Prokaryotic pyrimidine nucleoside phosphorylase 4,” can be found under <https://www.bionukleo.com/shop/np/y04/>, **2020**.
- [32] H. G. Mautner, *J. Am. Chem. Soc.* **1956**, *78*, 5292–5294.
- [33] R. T. Giessmann, F. Kaspar, in preparation.
- [34] F. Kaspar, K. F. Hellendahl, *Zenodo* **2020**, DOI 10.5281/zenodo.4302012.
- [35] F. Kaspar, R. T. Giessmann, S. Westarp, K. F. Hellendahl, N. Krausch, I. Thiele, M. C. Walczak, P. Neubauer, A. Wagner, *Chembiochem* **2020**, DOI 10.1002/cbic.202000204.
- [36] H. Yehia, S. Westarp, V. Rohrs, F. Kaspar, R. T. Giessmann, H. F. T. Klare, K. Paulick, P. Neubauer, J. Kurreck, A. Wagner, *Molecules* **2020**, *25*, DOI 10.3390/molecules25040934.
- [37] F. Kaspar, R. T. Giessmann, K. F. Hellendahl, P. Neubauer, A. Wagner, M. Gimpel, *Chembiochem* **2019**, DOI 10.1002/cbic.201900740.
- [38] F. Kaspar, R. T. Giessmann, P. Neubauer, A. Wagner, M. Gimpel, *Adv. Synth. Catal.* **2020**, *362*, 867–876.
- [39] C. S. Alexeev, M. S. Drenichev, E. O. Dorinova, R. S. Esipov, I. V. Kulikova, S. N. Mikhailov, *Biochim. Biophys. acta. Proteins proteomics* **2020**, *1868*, 140292.
- [40] F. Kaspar, R. T. Giessmann, N. Krausch, P. Neubauer, A. Wagner, M. Gimpel, *Methods Protoc.* **2019**, *2*, 60.
- [41] J. Reijenga, A. van Hoof, A. van Loon, B. Teunissen, *Anal. Chem. Insights* **2013**, *8*, 53–71.
- [42] R. T. Giessmann, N. Krausch, *Zenodo* **2019**, DOI 10.5281/ZENODO.3243376.
- [43] F. Kaspar, *Zenodo* **2020**, DOI 10.5281/ZENODO.3723806.

- [44] F. Kaspar, R. T. Giessman, *Zenodo* **2019**, DOI 10.5281/ZENODO.3565561.
- [45] F. Kaspar, R. T. Giessman, P. Neubauer, A. Wagner, M. Gimpel, *Zenodo* **2019**, DOI 10.5281/ZENODO.3568858.

Paper VII

Kaspar, F.; Neubauer, P.; Wagner, A. The Peculiar Case of the Hyperthermostable Pyrimidine Nucleoside Phosphorylase from *Thermus thermophilus*. *ChemBioChem* **2020**, accepted article, <https://doi.org/10.1002/cbic.202000679>.

This article was published as open access under a CC BY license which permits reproduction of the material with proper attribution, such as in this thesis.

Author contributions (with definitions by Brand *et al.* ¹)

Conceptualization, F.K., P.N. and A.K.; Data curation, F.K.; Formal analysis, F.K.; Funding acquisition, P.N. and A.K.; Investigation, F.K.; Methodology, F.K.; Project administration, F.K. and A.K.; Resources, P.N. and A.K.; Software, - ; Supervision, P.N. and A.K.; Validation, - ; Visualization, F.K.; Writing—original draft, F.K.; Writing—review & editing, F.K., P.N. and A.K.

Specifically, my contribution included co-development of the specific research idea, design of experiments, development of methodology for total turnover determination of the enzyme, execution of experiments, data curation, calculations, as well as illustration and lead writing of the publication.

Preamble

Since my E-factor analysis had revealed that substrate solubility was a major bottleneck for the efficiency of biocatalytic nucleoside transglycosylation and our group has a history of working with thermostable nucleoside phosphorylases, it was only natural to search for a nucleoside phosphorylase which would withstand extremely harsh conditions enabling increased substrate solubility. Previous literature reports as well as some of my own experiments indicated that the *Thermus thermophilus* pyrimidine nucleoside phosphorylase might just be what we were looking for. Consequently, I put our high-throughput UV-based assay to good use and probed the limits of the enzyme's cosolvent and temperature tolerance with a spectrum of kinetic experiments. Quickly, it became clear that it took real effort to break this enzyme, which had little trouble withstanding harsh conditions such as 50% (v/v) DMSO at 80 °C. However, our enthusiasm was short-lived as I discovered that something unusual was happening at higher substrate concentrations. Despite the literature reporting Michaelis-Menten behavior of the enzyme (as it is typical for pyrimidine nucleoside phosphorylases), our data first suggested substrate inhibition which then turned out to be product inhibition by nucleobases (at quasi any concentration). Unfortunately, that disqualified this enzyme for applications with the desired higher substrate loadings of >200 mM (in either direction of the reaction). It nonetheless remains an interesting example of extreme thermostability and an unexpected case of inhibition. Despite its inhibitory behavior, the enzyme is still frequently in use in our laboratory and our current and future work profits from a solid understanding of its working space and stability.

The Peculiar Case of the Hyperthermostable Pyrimidine Nucleoside Phosphorylase from *Thermus thermophilus*

F. Kaspar^{[a],[b],*}, P. Neubauer^[a] and A. Kurreck^{[a],[b],*}

[a] F. Kaspar, Dr. P. Neubauer and Dr. A. Kurreck
Department of Biotechnology, Chair of Bioprocess Engineering
Technical University of Berlin
Ackerstraße 76, ACK24, D-13355, Germany
E-mail: anke.wagner@tu-berlin.de

[b] F. Kaspar and Dr. A. Kurreck
BioNukleo GmbH
Ackerstraße 76, D-13355, Berlin, Germany
E-mail: felix.kaspar@web.de

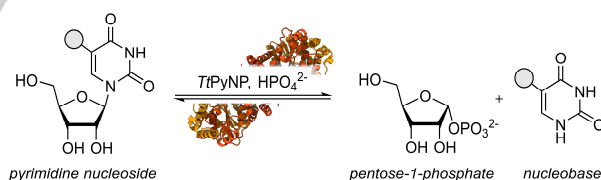
Supporting information for this article is given via a link at the end of the document.

Abstract: The poor solubility of many nucleosides and nucleobases in aqueous solution demands harsh reaction conditions (base, heat, cosolvent) in nucleoside phosphorylase-catalyzed processes to facilitate substrate loading beyond the low millimolar range. This, in turn, requires enzymes which withstand these conditions. Herein we report that the pyrimidine nucleoside phosphorylase from *Thermus thermophilus* is active over an exceptionally broad pH (4–10), temperature (up to 100 °C) and cosolvent space (up to 80% (v/v) non-aqueous medium) and displays tremendous stability under harsh reaction conditions with predicted total turnover numbers of more than 10⁶ for various pyrimidine nucleosides. However, its use as a biocatalyst for preparative applications is critically limited due to its inhibition by nucleobases at low concentrations, which is unprecedented among non-specific pyrimidine nucleoside phosphorylases.

Nucleoside phosphorylases are useful biocatalysts for the synthesis of pentose-1-phosphates and nucleoside analogs.^[1–11] These enzymes catalyze the reversible phosphorolysis of nucleosides to the corresponding pentose-1-phosphates and nucleobases (Scheme 1) and can be employed in the reverse reaction for glycosylation and transglycosylation reactions to furnish nucleosides of interest directly from free nucleobases. The current primary bottleneck for the efficient application of these enzymes for synthetic purposes is the low water-solubility of many nucleosides and nucleobases, restricting the substrate loading to the low millimolar range.^[12] Increased substrate solubility can be achieved through the use of harsh reaction conditions (base, heat, cosolvent) and, consequently, thermostable nucleoside phosphorylases have attracted particular interest due to their stability and activity under these conditions.^[1,2,4] Recent work from our group has demonstrated that some of these enzymes can be employed reliably at temperatures of up to 70 °C and over a broad pH range up to at least pH 9, which creates an exceptionally large working space and allows adjustments of the reaction conditions to suit the substrate(s).^[7,13,14] Further benefits of these thermostable enzymes, including their long shelf life and easy purification via heat treatment of crude extracts, make these catalysts attractive for various applications.

The pyrimidine nucleoside phosphorylase from *Thermus thermophilus* (*TtPyNP*, Scheme 1) has been reported to be active at up to 100 °C in aqueous media and to display some activity in

reaction mixtures containing high concentrations of organic solvents like DMSO and DMF.^[15] Therefore, we hypothesized that such a hyperthermostable enzyme would withstand harsh conditions such as near-boiling cosolvent-heavy media and enable greatly increased substrate loading compared to commonly performed nucleoside transglycosylations.^[8,9,16] This prompted us to investigate *TtPyNP* in more detail for applications in nucleoside synthesis and probe the limits of its tolerance to harsh conditions. In this communication, we report that *TtPyNP* is active and stable over a vast working space regarding temperature, pH and cosolvents and accepts a range of substituted pyrimidine nucleosides. In the course of our work we were surprised to discover that *TtPyNP* is inhibited by nucleobases even at low concentrations, which is atypical for pyrimidine nucleoside phosphorylases. Hence, *TtPyNP* is a suboptimal candidate for industrial applications where high substrate loading is a prerequisite.



Scheme 1. Phosphorolysis of pyrimidine nucleosides catalyzed e.g. by *Thermus thermophilus* pyrimidine nucleoside phosphorylase (*TtPyNP*, PDB 2dsj).

Following heterologous expression of the enzyme in *Escherichia coli* and purification via heat treatment and affinity chromatography, we explored the working space of *TtPyNP* using the phosphorolysis of uridine (**1a**) as a model reaction (Figure 1A). Since this reaction is under tight thermodynamic control ($K = 0.2$ at 60 °C and pH 9),^[7] we applied an excess of phosphate in these experiments to drive the reaction in the phosphorolysis direction. *TtPyNP* displayed phosphorolytic activity from pH 4 to 10 (Figure 1B), with a clear preference for acidic conditions as the observed rate constants k_{obs} differed by more than a factor of five between pH 4 and 10. This observation is somewhat counterintuitive since i) pentose-1-phosphates are prone to hydrolysis under acidic con-

COMMUNICATION

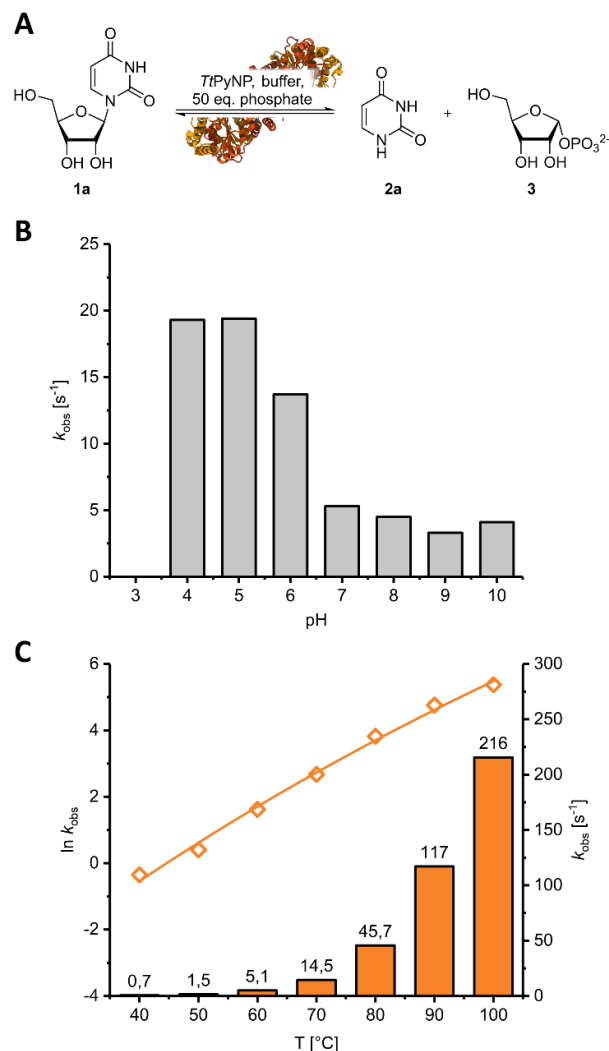


Figure 1. Working space of *TtPyNP*. The phosphorolysis of uridine (**1a**, **A**) was employed to investigate the pH-dependence (**B**) and the temperature-dependence (**C**) of the phosphorolytic activity as quantified by the observed rate constant k_{obs} . To assay across the pH space, reactions were performed with 1 mM **1a**, 50 mM potassium phosphate, 2 or 8 $\mu\text{g mL}^{-1}$ *TtPyNP* at 60 °C in a buffer mix consisting of 5 mM citrate, 10 mM MOPS and 20 mM glycine (all final concentration; adjusted to the respective pH value at 25 °C, not equated for ionic strength) in a final volume of 500 μL . To assay across the temperature space, reactions were carried out with 1 mM **1a**, 50 mM potassium phosphate and 0.06–20 $\mu\text{g mL}^{-1}$ *TtPyNP* in 50 mM glycine/NaOH buffer at pH 9 and the indicated temperature. Data shown represent the average of two experiments. Error bars are too small to see and were omitted for clarity. Fit results for **C** are available from the Supporting Information. Please see the Supporting Information for more experimental details and the externally hosted Supporting Information for raw data and calculations.^[20]

ditions,^[2,17] ii) an intracellular pH in the range of 7 would suggest a preference for neutral conditions and iii) other pyrimidine nucleoside phosphorylases are inactive at pH values below 6.^[18] In accordance with previous reports,^[13,15] *TtPyNP* was active at temperatures of up to 100 °C (Figure 1C), with the temperature-dependence of k_{obs} (in contrast to previous reports)^[15] following the trends predicted by conventional transition state theory as described by the Eyring equation.^[19] These results indicated that

the working space of *TtPyNP* covers most of the pH and temperature range accessible in water and, given the activity of the enzyme, we anticipated that its overall performance would only be limited by its stability under the applied reaction conditions.

Next, we turned our attention to the activity of *TtPyNP* in the presence of organic cosolvents. Previous work with this enzyme indicated that some activity is retained in mixtures containing 50% (v/v) DMSO or DMF.^[15] These two solvents fall into the short list of common organic solvents that meet the prerequisites to be considered as cosolvents for high-temperature biocatalytic reactions involving nucleosides: i) a boiling point > 100 °C, ii) water-miscibility^[21] and iii) resistance to hydrolysis. These prerequisites readily disqualify commonly used alcohols such as methanol, ethanol or isopropanol,^[22] as well as aromatics, ethers, hydrocarbons and esters. Considering that DMF is toxic, highly harmful to the environment^[23] and rather detrimental to the activity of *TtPyNP* (Figure S1), we selected DMSO and ethylene glycol as promising cosolvents and interrogated *TtPyNP*'s activity at different concentrations of these solvents, again employing the phosphorolysis of **1a** as a model reaction. *TtPyNP* displayed activity at up to 60% (v/v) DMSO and 80% (v/v) ethylene glycol, with more cosolvent being tolerated at 80 °C than at 90 °C (Figure

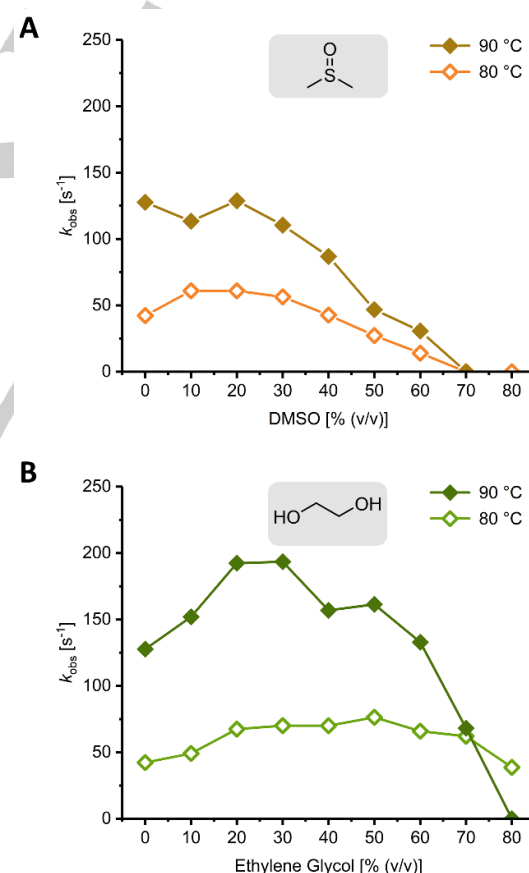


Figure 2. Phosphorolytic activity of *TtPyNP* in the presence of the organic cosolvents dimethyl sulfoxide (DMSO, **A**) and ethylene glycol (**B**). Reactions were run with 1 mM **1a**, 20 mM potassium phosphate and 0.12 or 0.40 $\mu\text{g mL}^{-1}$ *TtPyNP* in 20 mM glycine/NaOH buffer pH 9 containing the indicated amount of cosolvent at the indicated temperature. Data shown represent the average of two experiments. Error bars are too small to see and were omitted for clarity. Please see the Supporting Information for more experimental details and the externally hosted Supporting Information for raw data and calculations.^[20]

COMMUNICATION

2A and B). Interestingly, moderate amounts of either cosolvent (i.e. 20–40% (v/v)) promoted higher activities than observed in purely aqueous solution, presumably due to decreased enzymatic flexibility and a higher affinity for both substrates in a slightly less polar environment.^[24,25]

Having established the activity of *Tt*PyNP at high temperatures and with considerable amounts of cosolvent, we were interested in the half-life and total turnovers of the enzyme to evaluate if these harsh conditions were feasible for any reactions that exceeded the short reaction times of activity assays. To determine the half-life $t_{1/2}$ and predicted total turnover number (pTTN) of *Tt*PyNP, we incubated the enzyme in buffered solution with phosphate, determined its residual activity after various incubation times and approximated the incubation time-dependent decrease in activity as a first-order exponential decay. Despite its remarkable activity at 100 °C and pH 9 in purely aqueous solution (Figure 1B), the half-life of *Tt*PyNP under these conditions was only 2.2 min, corresponding to a pTTN of only around 28,000 (Table 1, entry 1). At 90 °C and 80 °C, we found half-lives of 100 min and more than 19 h, respectively, with the pTTNs increasing accordingly to well above 10^6 , despite the lower turnover rates at these temperatures (Table 1, entries 2 and 3). These experiments demonstrated that denaturation-driven loss of activity proceeds rapidly near the boiling point of water. However, slightly lower temperatures facilitated increased stability and enzymatic activity, as reflected by the predicted total turnovers. As transformations at 80–90 °C appeared feasible from a stability standpoint, we then assessed the stability of *Tt*PyNP in the presence of DMSO and ethylene glycol, using the same experimental set-up. Although both solvents permitted excellent activity of *Tt*PyNP at 90 °C, the half-life of the enzyme did not surpass 30 min at 40% (v/v) of either solvent at this temperature, reflected by pTTNs below 200,000 (Figure 3A and B). Nonetheless, a modest decrease in temperature to 80 °C resulted in much higher half-lives and pTTNs. For example, *Tt*PyNP had a half-life of 4.4 h at 80 °C and 60% (v/v) ethylene glycol, corresponding to around 1,500,000 predicted total turnovers (Figure 3B). Even DMSO was tolerated reasonably well, with *Tt*PyNP achieving a pTTN of 3,100,000 at 80 °C and 30% (v/v) DMSO (Figure 3A). Taken together, these data demonstrate that *Tt*PyNP performs favorably at up to 80 °C in media with up to around 50% (v/v) of DMSO or ethylene glycol.

Table 1. Activity and stability of *Tt*PyNP in aqueous solution.

Temperature [°C]	k_{obs} [s ⁻¹] ^[a]	$t_{1/2}$ [min] ^[b]	pTTN [10 ⁶] ^[c]
100	215.6	2.2 min	0.028
90	117.1	100.2 min	1.296
80	45.7	19.5 h	15.139

[a] Determined as initial rate with **1a** at pH 9 and the respective temperature as shown in Figure 1C. [b] Determined from incubation experiments from the incubation time-dependent decay of enzymatic activity (initial rate) at pH 9 and the respective temperature (please see the externally hosted Supporting Information for all raw and calculated data).^[20] The activity assay was performed at 60 °C to ensure enzyme stability during the assay. [c] Determined via multiplication of k_{obs} and the mean catalyst lifetime τ as detailed in the Supporting Information.

Next, we probed the substrate scope of this enzyme by subjecting a series of substituted pyrimidine nucleosides to phosphorolysis. Previous work had demonstrated that **1a**, its 2'-deoxy analogue **1b** and thymidine (**1d**) are converted by *Tt*PyNP to obtain the corresponding sugar phosphate and nucleobase.^[13,15] Our results corroborate and extend these reports by showing that substitutions in the 5-position at the nucleobase, such as aliphatic residues or halogens, are generally well tolerated without any loss of activity compared to the native substrates **1a** and **1d** (Scheme 2). Comparable or slightly higher levels of activity were obtained with 2'-deoxy nucleosides, which agrees well with the broad substrate spectrum typically observed for non-specific pyrimidine nucleoside phosphorylases.^[7–9] Given all the above results, *Tt*PyNP indeed seemed useful as a catalyst

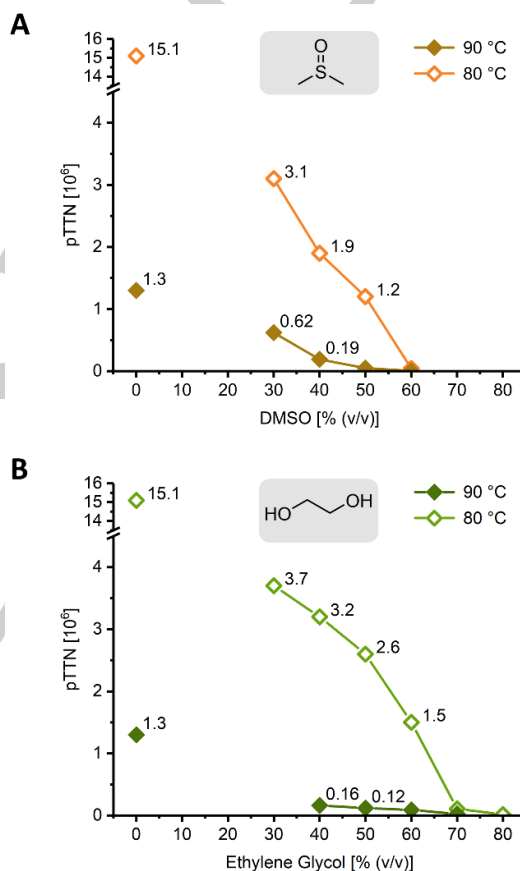
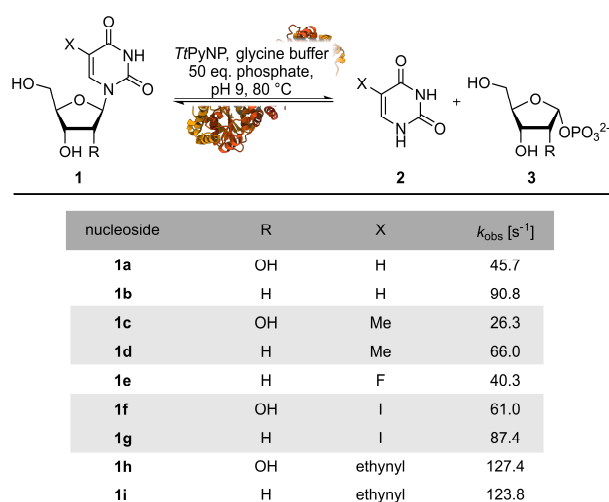


Figure 3. Performance of *Tt*PyNP assessed by the predicted total turnover number (pTTN) of the substrate **1a** in hot cosolvent-heavy reaction mixtures. The half-life of *Tt*PyNP was determined by incubating the enzyme at concentrations of 8.4–12.5 $\mu\text{g mL}^{-1}$ in 20 mM potassium phosphate and 20 mM glycine/NaOH buffer pH 9 and the indicated concentrations of DMSO (A) or ethylene glycol (B) at the indicated temperatures in a total volume of 220 μL in a PCR tube and measuring the residual activity through phosphorolysis of the model substrate **1a** at timely intervals (assay conditions of 1 mM **1a**, 20 mM potassium phosphate and 2.5–3.75 $\mu\text{g mL}^{-1}$ *Tt*PyNP in 20 mM glycine buffer pH 9 at 60 °C). Fitting of the incubation time-dependent decrease in activity as a first-order exponential decay yielded the half-life under the respective conditions, which was used to calculate pTTN via the initial rate constant under these conditions (Figure 2A and B). Please see the externally hosted Supporting Information for all raw and calculated data as well as tabulated half-lives and predicted total turnover numbers.^[20]



for the (reversible) phosphorolysis of various pyrimidine nucleosides as it displays a reasonably broad substrate scope and remarkable stability under harsh conditions including high temperature and cosolvent content.

However, despite *TiPyNP*'s excellent activity and stability, its use as a biocatalyst in synthetic applications is limited due to an apparent inhibition by nucleobases. We discovered this phenomenon when we attempted to determine the Michaelis-Menten constant K_M for the substrate **1a** using concentrations of up to 50 mM (Figure S2). Previous work had reported K_M values in the range of 0.2–1.0 mM at 80 °C and pH 7 (for **1a** and **1d** in phosphate buffer)^[13,15] which compares well with other pyrimidine nucleoside phosphorylases.^[26–28] However, our data at 40 °C and pH 9 suggested a strong inhibition behavior which did not appear to resemble any Michaelis-Menten-type kinetics (Figure S2). Follow-up experiments with **1a** at 80 °C and pH 7 revealed that, indeed, *TiPyNP* appeared to follow Michaelis-Menten-like kinetics for nucleoside concentrations up to 1–2 mM (under saturating phosphate concentrations for which typical Michaelis-Menten behavior was observed; Figure S4). In contrast, the observed rate constants of phosphorolysis at higher nucleoside concentrations suggested a possible substrate inhibition by nucleosides with an apparent inhibitory constant K_i within the same order of magnitude as K_M . However, the non-linearity of the conversion over time at higher substrate concentrations under quasi-steady state conditions (Figure S5) provided some evidence that *TiPyNP* might instead be inhibited by one of the products. Indeed, non-zero initial concentrations of the nucleobase **2a** caused a drastic decrease of the k_{obs} of phosphorolysis, while the sugar phosphate **3** had no effect (Figure 4A). Due to this strong inhibition of *TiPyNP* by **2a**, we were unable to determine the K_i from Michaelis-Menten plots of the phosphorolysis reaction. Therefore, we attempted to approximate the K_i by measuring the K_M for **2a** in the reverse reaction (glycosylation with **3**). However, instead of saturation-

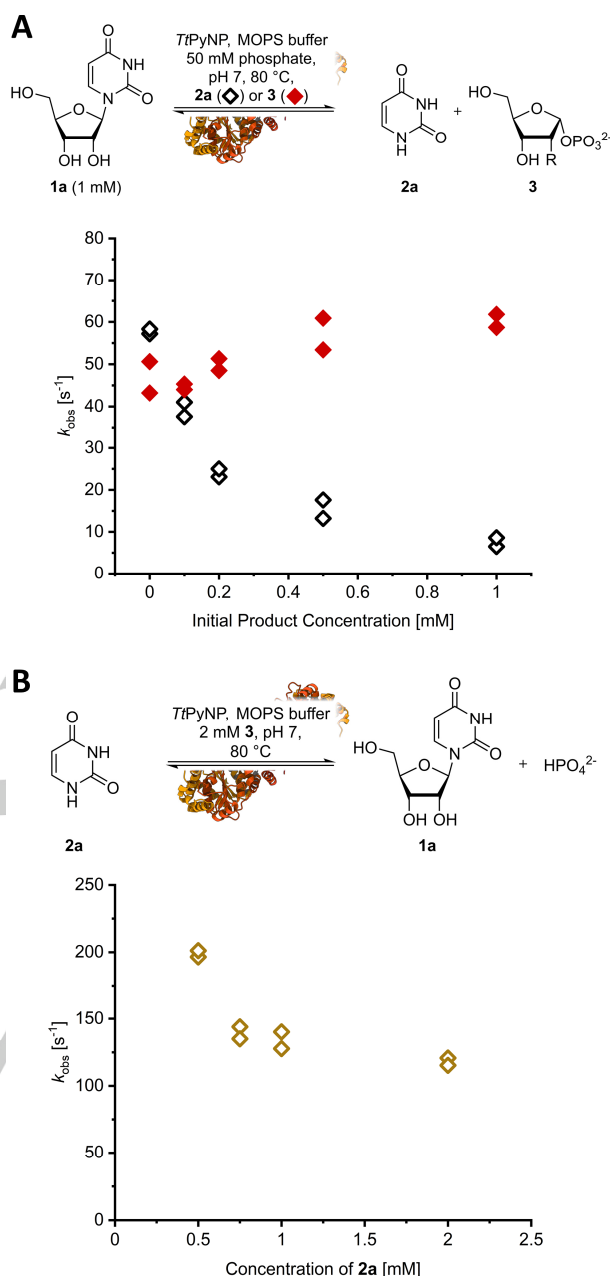


Figure 4. Inhibition of *TiPyNP* by substrates and products. *TiPyNP* is inhibited in the phosphorolysis direction by increasing concentrations of the nucleobase **2a**, but not by the sugar phosphate **3** (A). The reverse reaction is also inhibited by increasing concentrations of **2a** (B). Reactions in A were carried out with 1 mM **1a**, 50 mM potassium phosphate and 0.33 $\mu\text{g mL}^{-1}$ *TiPyNP* in 50 mM MOPS/NaOH buffer pH 7 at 80 °C with the indicated concentration of either product (**2a** or **3**) in a total volume of 200 μL . Reactions in B were performed with 2 mM **3** and 0.17 $\mu\text{g mL}^{-1}$ *TiPyNP* in 50 mM MOPS/NaOH buffer pH 7 at 80 °C with the indicated concentration of **2a** in a total volume of 200 μL . For each condition, reactions were carried out in duplicates and all data points are shown. Raw data and calculations are freely available from an external online repository.^[20]

type kinetics we only observed a significant decrease of the k_{obs} of glycosylation with increasing concentrations of **2a**, indicating that this nucleobase also inhibits its own glycosylation (Figure 4B).

To exclude any of our assay conditions causing these effects, we determined the K_M for **1a** of the corresponding enzyme from *Geobacillus thermoglucosidasius* (GtPyNP) and observed classic Michaelis-Menten behavior with no evidence of inhibition up to 50 mM **1a** in agreement with the available literature (Figure S3).^[13] Interestingly, similar inhibition effects of TtPyNP were also observed, to varying degrees, with the nucleosides **1d** and **1f** (Figure S6), revealing that inhibition of this enzyme by nucleobases is not limited to **2a**. Together, these results present evidence that TtPyNP is inhibited by nucleobases through a yet unknown mechanism. The reason(s) for this apparent product inhibition (or substrate inhibition, depending on the direction) are unclear to date as TtPyNP shares high structural^[29] and sequence identity (see Figure 1 in ^[13]) to other thymidine and pyrimidine nucleoside phosphorylases concerning the active site residues and overall protein structure. Although substrate inhibition is known for uridine phosphorylases,^[28,30] this is, to the best of our knowledge, the first reported example of a pyrimidine nucleoside phosphorylase being competitively substrate/product-inhibited. However, we doubt that this inhibition of TtPyNP holds any physiological significance, as the intracellular concentrations of nucleosides and their bases are typically in the low micromolar range, which is more than two orders of magnitude lower than the concentrations necessary to effect significant inhibition of TtPyNP. In any case, this clearly makes TtPyNP a rather suboptimal candidate for preparative purposes. In order to achieve satisfactory product titers, substrate concentrations of at least 100 mM typically need to be applied.^[12,31,32] Our characterization revealed that TtPyNP is severely inhibited by nucleobases at concentrations upwards of 0.5 mM, which limits its reactivity both in the phosphorolysis and glycosylation direction and renders its performance in potential industrial applications subpar.

In conclusion, we characterized the hyperthermostable pyrimidine nucleoside phosphorylase from *Thermus thermophilus* and revealed its exceptional working space, broad substrate scope as well as excellent stability and tolerance to organic cosolvents. However, its inhibition by nucleobases even at low concentrations discourages its use in synthetic applications. These observations make TtPyNP an outlier among pyrimidine nucleoside phosphorylases, displaying unmatched stability and a rare example of substrate/product inhibition.

Experimental Section

Enzymatic reactions were prepared from stock solutions of nucleoside, potassium phosphate and buffer and started via the addition of enzyme. Reaction conditions were applied as stated in the figure captions and the Supporting Information. Reaction monitoring was performed as described previously.^[7,33,34] Typically, samples of 50 μ L were withdrawn from reaction mixtures containing 1 mM UV-active compounds and pipetted into 450 μ L 100 mM aqueous NaOH to stop the reaction. To record the UV spectra of these alkaline samples, 200 μ L of the quenched samples were transferred to a UV/Vis-transparent 96-well plate (UV star, GreinerBioOne, Kremsmünster, Austria) and UV absorption spectra were recorded from 250 to 350 nm in steps of 1 nm with a high-throughput plate reader (BioTek Instruments, Winooski, USA). The obtained experimental UV spectra were then deconvoluted via spectral unmixing using suitable reference spectra of the nucleoside and nucleobase to derive the respective degree of conversion. All raw data presented in this report, along

with metadata and calculations are freely available from an external online repository.^[20] Likewise, reference spectra and software for spectral unmixing are available from the same repository^[35,36] and described in previous works.^[33,34]

Acknowledgements

The authors thank Kerstin Heinecke (TU Berlin) for proofreading and critical comments.

Keywords: nucleoside • nucleoside phosphorylase • thermostable • cosolvent • enzyme

- [1] H. Yehia, S. Kamel, K. Paulick, A. Wagner, P. Neubauer, *Curr. Pharm. Des.* **2017**, *23*, 6913–6935.
- [2] S. Kamel, M. Weiß, H. F. T. Klare, I. A. Mikhailopulo, P. Neubauer, A. Wagner, *Mol. Catal.* **2018**, *458*, 52–59.
- [3] M. Rabuffetti, T. Bavaro, R. Sempoli, G. Cattaneo, M. Massone, F. C. Morelli, G. Speranza, D. Ubiali, *Catalysts* **2019**, *9*, 355.
- [4] S. Kamel, H. Yehia, P. Neubauer, A. Wagner, in *Enzym. Chem. Synth. Nucleic Acid Deriv.*, **2019**, 1–28.
- [5] R. T. Giessmann, N. Krausch, F. Kaspar, N. M. Cruz Bournazou, A. Wagner, P. Neubauer, M. Gimpel, *Processes* **2019**, *7*, 380.
- [6] F. Kaspar, R. T. Giessmann, K. F. Hellendahl, P. Neubauer, A. Wagner, M. Gimpel, *ChemBioChem* **2020**, *21*, 1428–1432.
- [7] F. Kaspar, R. T. Giessmann, P. Neubauer, A. Wagner, M. Gimpel, *Adv. Synth. Catal.* **2020**, *362*, 867–876.
- [8] M. S. Drenichev, C. S. Alexeev, N. N. Kurochkin, S. N. Mikhailov, *Adv. Synth. Catal.* **2018**, *360*, 305–312.
- [9] C. S. Alexeev, M. S. Drenichev, E. O. Dorinova, R. S. Esipov, I. V. Kulikova, S. N. Mikhailov, *Biochim. Biophys. Acta - Proteins Proteomics* **2020**, *1868*, 140292.
- [10] X. Zhou, K. Szeker, B. Janocha, T. Böhme, D. Albrecht, I. A. Mikhailopulo, P. Neubauer, *FEBS J.* **2013**, *280*, 1475–1490.
- [11] I. Serra, T. Bavaro, D. A. Cecchini, S. Daly, A. M. Albertini, M. Terreni, D. Ubiali, *J. Mol. Catal. B Enzym.* **2013**, *95*, 16–22.
- [12] F. Kaspar, M. R. L. Stone, P. Neubauer, A. Kurreck, *ChemRxiv* **2020**, DOI 10.26434/chemrxiv.12753413.v1
- [13] K. Szeker, X. Zhou, T. Schwab, A. Casanueva, D. Cowan, I. A. Mikhailopulo, P. Neubauer, *J. Mol. Catal. B Enzym.* **2012**, *84*, 27–34.
- [14] K. F. Hellendahl, F. Kaspar, X. Zhou, Z. Huang, P. Neubauer, A. Wagner, **2020**, in preparation.
- [15] M. Almendros, J. Berenguer, J.-V. Sinisterra, *Appl. Environ. Microbiol.* **2012**, *78*, 3128–3135.
- [16] H. Yehia, S. Westarp, V. Röhrs, F. Kaspar, T. R. Giessmann, F. T. H. Klare, K. Paulick, P. Neubauer, J. Kurreck, A. Wagner, *Molecules* **2020**, *25*, 934.
- [17] R. T. Giessmann, F. Kaspar, P. Neubauer, A. Kurreck, M. Gimpel in preparation, preliminary dataset available at DOI 10.5281/zenodo.3572070.
- [18] N. Hori, M. Watanabe, Y. Yamazaki, Y. Mikami, *Agric. Biol. Chem.* **1990**, *54*, 763–768.
- [19] H. Eyring, *J. Chem. Phys.* **1935**, *3*, 107–115.
- [20] F. Kaspar, **2020**, DOI 10.5281/zenodo.4284188.
- [21] Biphasic systems involving hydrophobic solvents are not an option as nucleosides are virtually insoluble in all apolar solvents.
- [22] Even at lower temperatures, small alcohols are unfavorable cosolvents as they work excellently as quenching agents for nucleoside phosphorylases.
- [23] C. M. Alder, J. D. Hayler, R. K. Henderson, A. M. Redman, L. Shukla, L. E. Shuster, H. F. Sneddon, *Green Chem.* **2016**, *18*, 3879–3890.
- [24] H. J. Wiggers, J. Chaleski, A. Zottis, G. Oliva, A. D. Andricopulo, C. A. Montanari, *Anal. Biochem.* **2007**, *370*, 107–114.
- [25] S. Roy, B. Jana, B. Bagchi, *J. Chem. Phys.* **2012**, *136*, 115103.

- [26] D. F. Visser, F. Hennessy, J. Rashamuse, B. Plutschke, D. Brady, *J. Mol. Catal. B Enzym.* **2011**, *68*, 279–285.
- [27] P. P. Saunders, B. A. Wilson, G. F. Saunders, *J. Biol. Chem.* **1969**, *244*, 3691–3697.
- [28] T. A. Krenitsky, *Biochim. Biophys. Acta - Enzymol.* **1976**, *429*, 352–358.
- [29] K. Shimizu, N. Kunishima, **2006**, DOI 10.2210/pdb2DSJ/pdb.
- [30] R. G. Silva, V. L. Schramm, *Biochemistry* **2011**, *50*, 9158–9166.
- [31] Y. Ni, D. Holtmann, F. Hollmann, *ChemCatChem* **2014**, *6*, 930–943.
- [32] R. A. Sheldon, D. Brady, *ChemSusChem* **2019**, *12*, 2859–2881.
- [33] F. Kaspar, R. T. Giessmann, N. Krausch, P. Neubauer, A. Wagner, M. Gimpel, *Methods Protoc.* **2019**, *2*, 60.
- [34] F. Kaspar, R. T. Giessmann, S. Westarp, K. F. Hellendahl, N. Krausch, I. Thiele, M. C. Walczak, P. Neubauer, A. Wagner, *ChemBioChem* **2020**, *21*, 2604.
- [35] R. T. Giessmann, N. Krausch, **2019**, DOI 10.5281/zenodo.3243376.
- [36] R. T. Giessmann, F. Kaspar, **2019**, DOI 10.5281/zenodo.3333469.